Cyprus University of Technology

Faculty of Geotechnical Sciences and Environmental Management

Doctoral Dissertation

Development of biochar-based biocatalysts for fermentative bioethanol overproduction via whole-cell immobilization

Maria Kyriakou

Limassol, May 2024

CYPRUS UNIVERSITY OF TECHNOLOGY

FACULTY OF GEOTECHNICAL SCIENCES AND ENVIRONMENTAL MANAGEMENT

DEPARTMENT OF CHEMICAL ENGINEERING

Doctoral Dissertation

DEVELOPMENT OF BIOCHAR-BASED BIOCATALYSTS FOR FERMENTATIVE BIOETHANOL OVERPRODUCTION VIA WHOLE-CELL IMMOBILIZATION

Maria Kyriakou

Limassol, May 2024

Approval Form

Doctoral Dissertation

DEVELOPMENT OF BIOCHAR-BASED BIOCATALYSTS FOR FERMENTATIVE BIOETHANOL OVERPRODUCTION VIA WHOLE-CELL IMMOBILIZATION

Presented by

Maria Kyriakou

Supervisor: Dr. Michalis Koutinas, Associate Professor

Signature _____

Member of the committee: Dr. Chrysoula Drouza, Associate Professor

Signature _____

Member of the committee: Dr. Theofania Tsironi, Assistant Professor

Signature _____

Cyprus University of Technology

Limassol, May 2024

Copyrights

Acknowledgements

First and foremost, I would like to express my deepest appreciation to my supervisor Dr. Michalis Koutinas for the continuous support, patience, and guidance he provided during my PhD.

Many thanks to all my fellow lab mates for the moral and practise support all this time as well as the under-graduate students we worked together.

Last but not least, I would like to thank my husband for his patient and emotional support. Special thanks to Constantinos Charilaou.

ABSTRACT

Biofuels have received a lot of attention as an important source of renewable energy, with numerous economic impacts but current biofuel production is based on food crops (first generation biofuels) that compete with agricultural lands and biodiverse landscapes. Bioethanol is considered a feasible, sustainable and enduring energy source. In comparison to traditional liquid transportation fuels, the consumption of biofuels results in zero sulfur emissions and significantly reduces the production of particles and hazardous pollutants. Although bioethanol production is considered as one of the most promising alternatives to the use of petroleum-based fuels, bioethanol fermentations are impacted by substrate and product inhibition decreasing process productivity.

The proposed technology exploring the development of biochar-based biocatalysts (BBB), successfully enhanced the efficiency of alcoholic fermentations. Olive kernels, vineyard prunings, sewage sludge and seagrass residues were applied as biowaste for biochar production through pyrolysis at two different temperatures (250 °C and 500 °C), while a commercial type of non-biomass derived char also employed for benchmarking purposes. Three major yeasts were immobilised on materials exhibiting the highest surface areas and applied in repeated batch fermentations using Valencia orange peel hydrolyzates as feedstock. The biocatalysts developed using *Sacharomyces cerevisiae* and *Kluyveromyces marxianus* immobilised on vineyard prunings-based biochar exhibited exceptional ethanol productivities. However, *Pichia kudriavzevii* KVMP10 was not efficient following immobilization on biochar. Immobilised biocatalysts using pistachio-nut shells, peanut shells and corks were also employed in bioethanol fermentations and biochar derived from pistachio shells employing *S. cerevisiae* was employed in fermentations using citrus peel waste hydrolysate, exhibiting 30.8 g L^{-1} ethanol concentration at the elevated temperature of 41 ºC, while free cells achieved significantly lower concentration (13.4 g L^{-1}). The protective role of using biochar as immobilization carrier against multiple stresses encountered by *S. cerevisiae* was confirmed by assessing transcription from important metabolic routes involved in the molecular mechanisms triggered during inhibitory bioprocess conditions. Immobilised cells exhibited higher bioethanol titre (39 g L^{-1}) and productivity (7.72

g L^{-1} h^{-1}) at elevated temperatures compared with the suspended culture that yielded 34 g L^{-1} and 1.99 g L^{-1} h^{-1} respectively. mRNA expression levels of *HSP104*, *HSF1* and *TPS*, confirmed the protective role of BBB against heat stress. Transcription from *MSN2*/*MSN4* indicated the protective role of cell attachment on the biomaterial against stimulation of the heat shock response route and oxidative stress. Additionally, monitoring transcription of *HSP12* and *HSP104* demonstrated the beneficial use of the proposed technology. Proline accumulation during osmotic stress further supported the elevated bioethanol productivity achieved by the immobilised system. Non-biological char materials were used in the current study as support materials employing *S. cerevisiae* in bioethanol fermentations improving the bioprocess performance at elevated temperatures and different dilution rates. Bioethanol production and glucose consumption using immobilised cells of *S. cerevisiae* on unscreened char was monitored in continuous experiments conducted at 37, 39 and 41 °C. The immobilised system demonstrated stable biofuel production at higher dilution rates as opposed to the conventional system where biomass washout occurred in lower dilution rates. Maximum net bioethanol concentration as well as productivity were significantly via the use of extreme temperature conditions, while the immobilised biosystem assisted the buffering capacity protecting cells and improving the performance of the bioprocess under elevated temperatures and increased dilution rates.

Keywords: Biochar, Bioethanol, Immobilised biocatalysts, *S. cerevisiae*, Char, Stress tolerance.

TABLE OF CONTENTS

LIST OF TABLES

LIST OF FIGURES

cells immobilised on SGRB; iii)  : cells immobilised on NBC; iv) 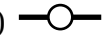 : freely suspended cells.

Figure 3.1.5B: Evaluation of *S. cerevisiae* immobilised biocatalysts for ethanol production. Symbols correspond to sugar's concentration in fermentations conducted at 37 ^{o}C employing: i) 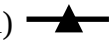 : cells immobilised on VPB; ii)  : cells immobilised on SGRB; iii)  : cells immobilised on NBC; iv) 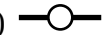 : freely suspended cells.

Figure 3.1.6A: Evaluation of *K. marxianus* immobilised biocatalysts for ethanol production. Symbols correspond to bioethanol concentration in fermentations conducted at 42 ^{o}C employing: i)  : cells immobilised on VPB; ii)  : cells immobilised on SGRB; iii)  : cells immobilised on NBC; iv) 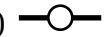 : freely suspended cells.

Figure 3.1.6B: Evaluation of *K. marxianus* immobilised biocatalysts for ethanol production. Symbols correspond to sugar's concentration in fermentations conducted at 42 ^{o}C employing: i)  : cells immobilised on VPB; ii)  : cells immobilised on SGRB; iii)  : cells immobilised on NBC; iv) 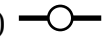 : freely suspended cells.

Figure 3.1.7A: Evaluation of *P. kudriavzevii* immobilised biocatalysts for ethanol production. Symbols correspond to bioethanol concentration in fermentations conducted at 42 ^{o}C employing: i)  : cells immobilised on VPB; ii)  : cells immobilised on SGRB; iii)  : cells immobilised on NBC; iv) 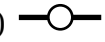 : freely suspended cells.

Figure 3.1.7B: Evaluation of *P. kudriavzevii* immobilised biocatalysts for ethanol production. Symbols correspond to sugar's concentration in fermentations conducted at 42 ^{o}C employing: i)  : cells immobilised on VPB; ii)  : cells immobilised on SGRB; iii)  : cells immobilised on NBC; iv) 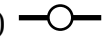 : freely suspended cells.

Figure 3.2.1A: X-ray diffraction pattern of raw materials (CR, PV and AH).

Figure 3.2.1B: X-ray diffraction pattern of biochars produced (CRB, PVB and AHB).

Figure 3.2.3: SEM images of biochar specimens. The samples analyzed comprised: (A) PVB, (B) AHB and (C) CRB, at 3000× magnification.

Figure 3.2.4: SEM images of developed immobilised biocatalysts. (A) PVB, (B) AHB and (C) CRB, at 3000× magnification.

Figure 3.2.5A: Evaluation of biochar's adsorption capacity for bioethanol concentrations. Bars correspond to the concentration of ethanol during the experiments. Dark, medium and light colour groups correspond to measurements conducted at 0, 20 and 60 min respectively.

Figure 3.2.5B: Evaluation of biochar's adsorption capacity for sugar concentrations. Bars correspond to the concentration of sugars during the experiments. Dark, medium and light colour groups correspond to measurements conducted at 0, 20 and 60 min respectively.

Figure 3.2.6: Evaluation of different particle size of PVBC in bioethanol production during a batch alcoholic fermentation. Symbols correspond to: (i) PVB sieved to > 1-2 mm; (ii) PVB sieved to < 1 mm; (iii) unscreened PVB; (iv) freely suspended cells of *S. cerevisiae*.

Figure 3.2.7A: Application of BBBs in repeated batch bioethanol fermentations. Evolution of bioethanol concentration achieved at 37 ^{o}C using *S. cerevisiae*: (i) immobilised on PVBC; (ii) immobilised on AHBC; (iii) immobilised on CRBC; (iv) freely suspended cells.

Figure 3.2.7B: Application of BBBs in repeated batch bioethanol fermentations. Evolution of sugars concentration achieved at 37 ^{o}C using *S. cerevisiae*: (i) immobilised on PVBC; (ii) immobilised on AHBC; (iii) immobilised on CRBC; (iv) freely suspended cells.

Figure 3.2.8A: Evaluation of BBB performance in elevated temperatures during repeated batch alcoholic fermentations. Bioethanol concentration employing: (i) cells immobilised on PVB at 37 ^{o}C; (ii) cells immobilised on PVB at 39 ^{o}C; (iii) cells immobilised on PVB at 41 ^{o}C; (iv) freely suspended cells at 37 ^{o}C; (v) freely suspended cells at 39 ^{o}C; (vi) freely suspended cells at 41 ^{o}C.

Figure 3.2.8B: Evaluation of BBB performance in elevated temperatures during repeated batch alcoholic fermentations. Total sugars conversion employing: (i)  cells immobilised on PVB at 37 ^{o}C; (ii)  cells immobilised on PVB at 39 ^{o}C; (iii)  cells immobilised on PVB at 41 ^{o}C; (iv)  freely suspended cells at 37 ^{o}C; (v)  freely suspended cells at 39 ^{o}C; (vi)  freely suspended cells at 41 ^{o}C.

Figure 3.2.9A: Evaluation of *S. cerevisiae* immobilised biocatalyst employing PVB at the elevated temperature of 41 ^{o}C, for bioethanol production using CPW hydrolyzate. Symbols correspond to ethanol concentration in fermentations conducted at 41 ^{o}C, employing (i)  immobilised cells; (ii)  freely suspended cells.

Figure 3.2.9B: Evaluation of *S. cerevisiae* immobilised biocatalyst employing PVB at the elevated temperature of 41 ^{o}C, for bioethanol production using CPW hydrolyzate. Symbols correspond to sugars conversion in fermentations conducted at 41 ^{o}C, employing (i)  immobilised cells; (ii)  freely suspended cells.

Figure 3.3.1A: Bioethanol production achieved at 30 and 39 ^{o}C using immobilised and freely suspended cells of *S. cerevisiae*. Symbols represent: (i)  immobilised cells at 30 ^{o}C; (ii)  immobilised cells at 39 ^{o}C; (iii)  freely suspended cells at 30 ^{o}C; (iv)  freely suspended cells at 39 ^{o}C.

Figure 3.3.1B: Glucose consumption achieved at 30 and 39 ^{o}C using immobilised and freely suspended cells of *S. cerevisiae*. Symbols represent: (i)  immobilised cells at 30 ^{o}C; (ii)  immobilised cells at 39 ^{o}C; (iii)  freely suspended cells at 30 ^{o}C; (iv)  freely suspended cells at 39 ^{o}C.

Figure 3.3.2A: Relative expression level of *HSP104* gene induced by heat shock in fermentations conducted at 30 and 39 ^{o}C. Light, medium and dark colour groups correspond to measurements conducted at 0, 0.5 and 4 h respectively.

Figure 3.3.2B: Relative expression level of *HSF1* gene induced by heat shock in fermentations conducted at 30 and 39 ^{o}C. Light, medium and dark colour groups correspond to measurements conducted at 0, 0.5 and 4 h respectively.

Figure 3.3.2C: Relative expression level of *TPS* gene induced by heat shock in fermentations conducted at 30 and 39 ^{o}C. Light, medium and dark colour groups correspond to measurements conducted at 0, 0.5 and 4 h respectively.

Figure 3.3.2D: Relative expression level of *MSN2* gene induced by oxidative stress during the fermentations conducted at 30 and 39 ^{o}C. Light, medium and dark colour groups correspond to measurements conducted at 0, 0.5 and 4 h respectively.

Figure 3.3.2E: Relative expression level of *MSN4* gene induced by oxidative stress during the fermentations conducted at 30 and 39 ^{o}C. Light, medium and dark colour groups correspond to measurements conducted at 0, 0.5 and 4 h respectively.

Figure 3.3.3A: Bioethanol production achieved at 30 ^{o}C using immobilised and suspended cells of *S. cerevisiae*. Symbols correspond to: (i) immobilised cells exposed to 90 g L^{-1} of bioethanol, (ii) immobilised cells exposed to 70 g L^{-1} of bioethanol, (iii) immobilised cells exposed to 0 g L^{-1} of bioethanol, (iv) suspended cells exposed to 90 g L^{-1} of bioethanol, (v) suspended cells exposed to 70 g L^{-1} of bioethanol, (vi) suspended cells exposed to 0 g L^{-1} of bioethanol.

Figure 3.3.3B: Glucose consumption achieved at 30 ^{o}C using immobilised and suspended cells of *S. cerevisiae*. Symbols correspond to: (i) immobilised cells exposed to 90 g L^{-1} of bioethanol, (ii) immobilised cells exposed to 70 g L^{-1} of bioethanol, (iii) immobilised cells exposed to 0 g L^{-1} of bioethanol, (iv) suspended cells exposed to 90 g L^{-1} of bioethanol, (v) suspended cells exposed to 70 g L^{-1} of bioethanol, (vi) suspended cells exposed to 0 g L^{-1} of bioethanol.

Figure 3.3.4A: Relative expression level of *HSP12* gene induced by ethanol stress during each fermentation conducted. Bars marked as "Control" refer to experiments conducted using 0 g L^{-1} initial bioethanol content, while "Stress" denotes application of 90 g L^{-1} initial bioethanol concentration. Light, medium and dark colour groups correspond to measurements conducted at 0, 1 and 3 h respectively.

Figure 3.3.4B: Relative expression level of *HSP104* gene induced by ethanol stress during each fermentation conducted. Bars marked as "Control" refer to experiments conducted using 0 g L^{-1} initial bioethanol content, while "Stress" denotes

application of 90 g L^{-1} initial bioethanol concentration. Light, medium and dark colour groups correspond to measurements conducted at 0, 1 and 3 h respectively.

Figure 3.3.5A: Bioethanol production achieved under exposure of immobilised and suspended cells of *S. cerevisiae* to 1 M NaCl. Symbols correspond to: (i)  immobilised cells and (ii)  suspended cells.

Figure 3.3.5B: Glucose consumption achieved under exposure of immobilised and suspended cells of *S. cerevisiae* to 1 M NaCl. Symbols correspond to: (i)  immobilised cells and (ii)  suspended cells.

Figure 3.3.6: Accumulation of intracellular proline in bioethanol fermentations conducted employing suspended and immobilised cells of *S. cerevisiae*. Light, medium and dark colour groups correspond to measurements conducted at 0, 6 and 12 h respectively.

Figure 3.4.1A: Bioethanol production achieved at 37 ^{o}C using immobilised and suspended cells of *S. cerevisiae*. Symbols correspond to *S. cerevisiae*: (i)  immobilised cells on UNC, (ii)  immobilised cells on PLC, (iii)  immobilised cells on PWC, (iv)  freely suspended cells.

Figure 3.4.1B: Glucose' consumption achieved at 37 ^{o}C using immobilised and suspended cells of *S. cerevisiae*. Symbols correspond to *S. cerevisiae*: (i)  immobilised cells on UNC, (ii)  immobilised cells on PLC, (iii)  immobilised cells on PWC, (iv)  freely suspended cells.

Figure 3.4.2A: Bioethanol production achieved at 39 ^{o}C using immobilised and suspended cells of *S. cerevisiae*. Symbols correspond to *S. cerevisiae*: (i)  immobilised cells on UNC, (ii)  immobilised cells on PLC, (iii)  freely suspended cells.

Figure 3.4.2B: Glucose consumption achieved at 39 ^{o}C using immobilised and suspended cells of *S. cerevisiae*. Symbols correspond to *S. cerevisiae*: (i)  immobilised cells on UNC, (ii)  immobilised cells on PLC, (iii)  freely suspended cells.

Figure 3.4.3A: Bioethanol production achieved at 41 ^{o}C using immobilised and suspended cells of *S. cerevisiae*. Symbols correspond to *S. cerevisiae*: (i) 

immobilised cells on UNC, (ii)  immobilised cells on PLC, (iii)  freely suspended cells.

Figure 3.4.3B: Glucose consumption achieved at 41 ^{o}C using immobilised and suspended cells of *S. cerevisiae*. Symbols correspond to *S. cerevisiae*: (i)  immobilised cells on UNC, (ii)  immobilised cells on PLC, (iii)  freely suspended cells.

Figure 3.4.4A: Bioethanol production and glucose consumption achieved at 37 ^{o}C using freely suspended cells of *S. cerevisiae* in a continuous bioreactor under different dilution rates (0.09, 0.13 and 0.17 h^{-1}). Symbols correspond to: (i)  bioethanol concentration, (ii)  glucose concentration.

Figure 3.4.4B: pH and biomass production achieved at 37 ^{o}C using freely suspended cells of *S. cerevisiae* in a continuous bioreactor under different dilution rates (0.09, 0.13 and 0.17 h^{-1}). Symbols correspond to: (i)  pH value, (ii)  biomass concentration.

Figure 3.4.4C: Dilution rates applied during bioethanol fermentation experiments using free cells of *S. cerevisiae.*

Figure 3.4.4D: Bioethanol production and glucose consumption achieved at 37 ^{o}C using freely suspended cells of *S. cerevisiae* in a continuous bioreactor under different dilution rates (0.09, 0.13, 0.17 and 0.20 h^{-1}). Symbols correspond to: (i)  bioethanol concentration, (ii)  glucose concentration.

Figure 3.4.4E: pH monitored during fermentation conducted at 37 ^{o}C using immobilised cells of *S. cerevisiae* in a continuous bioreactor under different dilution rates (0.09, 0.13, 0.17 and 0.20 h^{-1}).

Figure 3.4.4F: Dilution rates applied during bioethanol fermentation experiments using immobilised cells of *S. cerevisiae.*

Figure 3.4.4G: Bioethanol and glucose concentration achieved at 39 ^{o}C and 41 ^{o}C using freely suspended cells of *S. cerevisiae* in a continuous bioreactor under different dilution rates (0.13 and 0.17 h^{-1}). Symbols correspond to: (i)  bioethanol concentration, (ii)  glucose concentration.

Figure 3.4.4H: pH value and biomass concentration achieved at 37 ºC and 41 ºC using freely suspended cells of *S. cerevisiae* in a continuous bioreactor under different dilution rates (0.13 and 0.17 h^{-1}). Symbols correspond to: (i) pH value, (ii) biomass concentration.

Figure 3.4.4I: Bioethanol and glucose concentration achieved at 39 ºC and 41 ºC using immobilised cells of *S. cerevisiae* in a continuous bioreactor under different dilution rates (0.17 and 0.20 h^{-1}). Symbols correspond to: (i) bioethanol concentration, (ii) glucose concentration.

Figure 3.4.4J: pH value monitored during fermentation conducted at 39 and 41 ºC using immobilised cells of *S. cerevisiae* in a continuous bioreactor under different dilution rates (0.17 and 0.20 h^{-1}).

LIST OF ABBREVIATIONS AND MICROORGANISMS

Abbreviations

AH:	*Arachis hypogaea*
AHBC:	*Arachis hypogaea* biochar
BBB:	Biochar-based biocatalysts
BET:	Brunauer-Emmett-Teller
CPW:	Citrus peel waste
CR:	Corks
CRBC:	Corks biochar
D:	Dilution rate
DNS:	3,5-dinitrosalicylic acid
EDS:	Energy-dispersive X-ray spectroscopy
SEM:	Scanning Electron Microscope
ESR:	Environmental stress response
GC:	Gas Chromatography
GPD:	glycerol-3-phosphate dehydrogenase
HMF:	5-hydroxymethylfurfural
HPLC:	High Pressure Liquid Chromatography
HSE:	Heat shock element
HSF1:	Heat shock factor 1
HSF2:	Heat shock factor 2
HSF3:	Heat shock factor 3
HSF4:	Heat shock factor 4
HSP:	Heat shock proteins

HSR:	Heat shock response
NBC:	Non-biological char
OK:	Olive kernels
OKB:	Olive kernels biochar
PLC:	Pellet char
PV:	*Pistachia vera*
PVBC:	*Pistachia vera* biochar
PWB:	Powder char
ROS:	Reactive oxygen species
SGR:	Seagrass residues
SGRB:	Seagrass biochar
SS:	Sewage sludge
SSB:	Sewage sludge biochar
UNC:	Unscreened char
VP:	Vineyard prunings
XRD:	X-ray diffraction

Microorganisms

Saccharomyces cerevisiae	*S. cerevisiae*
Kluyveromyces marxianus	*K. marxianus*
Pichia kudriavzevii	*P. kudriavzevii*

1 Introduction

1.1 Biofuel as a renewable energy source

In recent years, increased fuel utilization, global warming, fossil fuel depletion, and high fuel prices, have forced energy-consuming countries to turn their attention to alternative energy sources [Jayakumar et al., 2023]. The provision of energy relies primarily on fossil fuels, with around 5.8 × 1011 GJ consumed globally in 2016, of which 81% was derived from coal, petroleum, and natural gas [IEA, 2017]. Thus, biofuels have received significant attention as an important source of renewable energy, with numerous economic impacts [Hasan et al., 2023]. Thus far, biomass represents the only renewable energy source for the production of solid, liquid, or gaseous biofuels capable to supply 14% of global energy demands [Jayakumar et al., 2022]. Current biofuel production is based on food crops (first generation biofuels) that compete with agricultural lands and biodiverse landscapes. Furthermore, biofuel production has been linked to several other environmental pressures that may, directly and indirectly, impact biodiversity and the provision of ecosystem services [Correa et al., 2019]. The impacts of biofuels on biodiversity and ecosystem services, however, depend on the type of biofuel production system and other factors associated with its cultivation and production [Immerzeel et al., 2014]. Biofuels are divided into four classes based on the feedstocks applied (first, second, third, and fourth generation) (Figure 1.1).

First generation biofuels are synthesized from raw materials used as foodstuffs, which compete with agricultural and biodiverse lands [Elshout et al., 2019; Jayakumar et al., 2022]. The agricultural production and the biorefinery plant comprise the two main stages of a system producing first generation biofuels where the crop is totally used for the production of energy and therefore constitutes the main input of the biorefinery where biomass is converted into biofuel [Saladini et al., 2016]. The three main types of first generation biofuels used commercially are biodiesel, bioethanol and biogas, which have been produced in large quantities worldwide so far [Javed et al., 2019]. Biomass used for first generation biofuel production includes oilseeds such as corn, sugarcane, wheat, soy, rapeseed and sunflower. Given that the aforementioned materials are considered competitors for

food increasing its price, while requiring large areas of agricultural land for production, they are not extensively used for current production of biofuels [Vassilev et al., 2010;Pushparaj et al., 2022].

Second generation biomass (lignocellulosic biomass, organic residues) does not present the problems of food-derived feedstocks playing an important role in reducing greenhouse gas emissions comprising truly carbon neutral or even carbon negative approaches for biofuel production in terms of CO_2 released [Dailami et al., 2022]. Second generation biomass is comprised mostly of plant cell walls, of which typically 75% is composed of polysaccharides [Pauly and Keegstra, 2008]. The average composition of lignocellulosic biomass is 43% cellulose, 29% hemicellulose, 21% lignin, 2% extractives and 1% ash [Latif et al., 2018]. Cellulose represents the main component of lignocellulosic biomass constituting glucose monomers, connected in a strong crystalline structure insoluble in many organic solvents as well as water. Hemicellulose constitutes a heteropolymer composed of different pentose and hexose sugars as well as uronic acids (xylose, arabinose, mannose, galactose) with 50–200 units [Sharma et al., 2020]. Based on the raw material applied the structure and composition of hemicellulose varies [Chen, 2014]. For example, the main content of agricultural biomass and hardwood hemicellulose is xylan, while glucomannan is the main content of softwood [Bajpai, 2016]. The third-largest component, lignin, is a heteropolymer of phenyl propionic alcohol units (coumaryl alcohol, sinapyl alcohol and coniferyl alcohol) linked together by carbon–carbon (C–C) which is responsible for the stability of plant cell walls and resistance to pathogen infections [Sharma et al., 2020]. Enzymatic or microbial delignification is difficult to occur due to the derivatives formed from lignin that act as toxic compounds for microorganisms and reduce the activity of hydrolytic enzymes [Bajpai, 2016]. Numerous pre-treatment methods are used for the removal of lignin from lignocellulosic biomass constituting cellulose and hemicellulose accessible for hydrolytic enzymes [Zabed et al., 2017]. Although, lignocellulosic biomass is abundantly available and a significant alternative feedstock for bioethanol production, it is also considered as a food competitor due to the use of agricultural land for its production [Ramesh et al., 2022;Liu et al.,

2023]. Thus, second generation bioethanol represents only 3% of the worldwide bioethanol production [Sharma et al. 2020].

The production of third-generation biofuels, also known as algal biofuels, refers to the utilization of algae as feedstock [Chaos-Hernandez et al., 2023]. Macroalgae (multicellular) and microalgae (single celled) are the main groups used for biofuel production based on their high photosynthetic efficiency, high biomass production and faster growth rate as compared to other energy-producing plants such as rapeseed and soybean. As opposed to other plant materials employed for fuel production, algae are efficient in terms of reducing greenhouse gases and consuming less water [Kamyab et al., 2013;Rezania et al., 2021]. Microalgae can accumulate large amounts of lipids, proteins and carbohydrates. Thus, different biofuels (e.g., biodiesel, bioethanol, biohydrogen) and other value-added products can be obtained from algal biomass processing and thermochemical transformation [Robak and Balcerek, 2018;Deshmukh et al., 2019]. The use of algal biomass is eco-friendly, demands less area for cultivation and it is rich in oil contents constituting a valuable feedstock for biofuel production [Shah et al., 2018].

Fourth generation biofuel is produced from genetically modified algae using synthetic biology to construct microorganisms with unusually high levels of CO_2 absorbance characteristics. Genetically modifyied organisms-based biofuel, biofuels decomposed at high temperatures and artificial photosynthesis reactions currently comprise the three main technologies holding the potential to be proposed as the fourth generation of biofuels [Shokravi et al., 2022]. Although several studies have focused on fourth generation biofuels, they mainly deal with metabolic engineering and genetic modification of algal strains to enhance the oil content and biomass yield rather than circular bioeconomy applications [Aamer Mehmood et al., 2021].

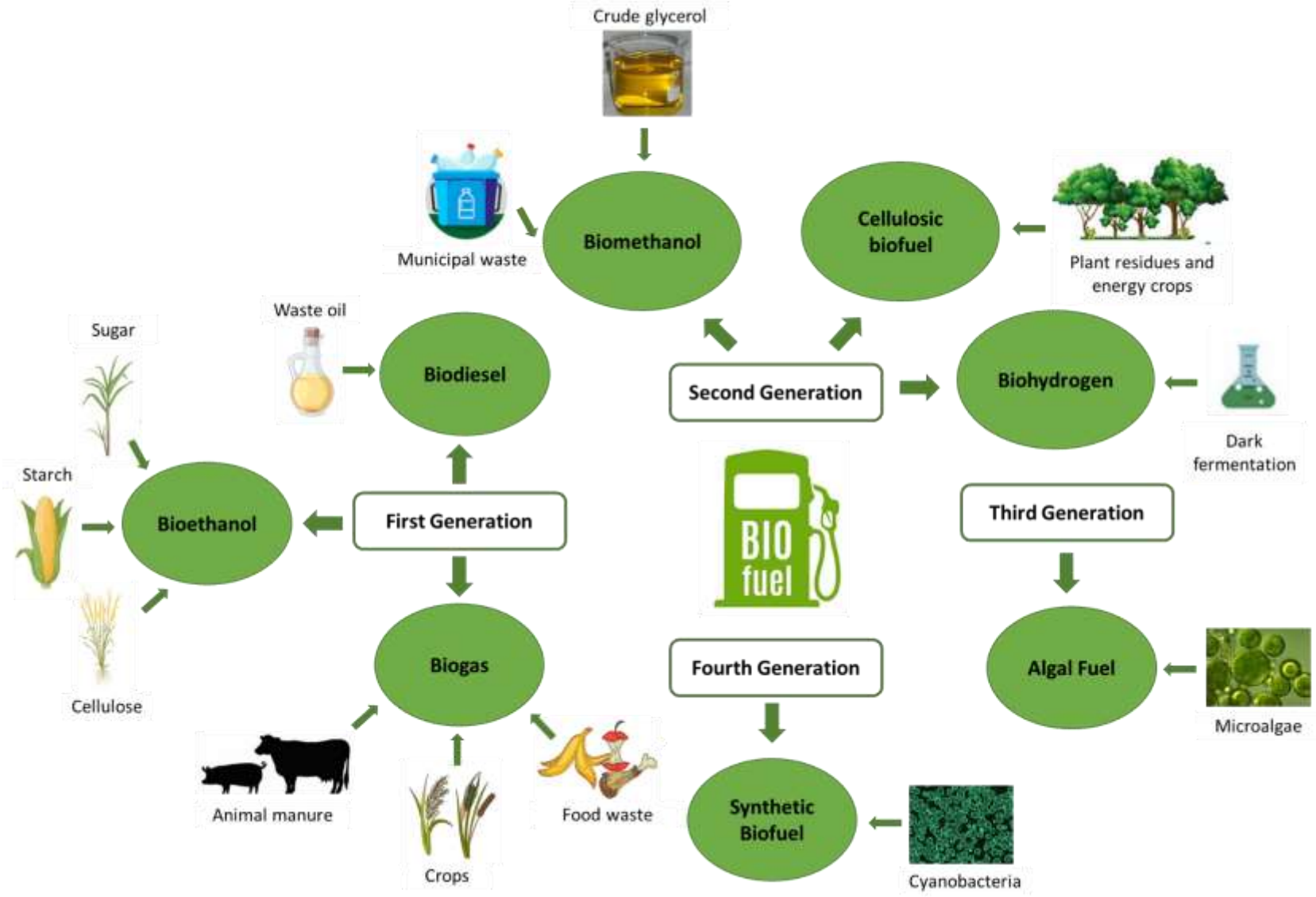

Figure 1.1: Schematic representation of the different types and generations of biofuel.

1.2 Production of bioethanol

Aiming to ensure long-term sustainability and economic feasibility, it is crucial to prioritize the development of cost-effective methods for bioethanol production in order to compete with petroleum fuels [Sims et al., 2010]. In comparison to traditional liquid transportation fuels, the consumption of biofuels results in zero sulfur emissions and significant reduction in the production of particles and hazardous pollutants. Bioethanol incorporated the same structure as its petroleum equivalent and it can be applied in a mixture with gasoline to enhance the combustion process.

Bioethanol is generated through fermentation of sugars derived from various biomass sources, while corn, sugar beet, and sugarcane are commonly utilized as the main substrates for its production [Achinas and Euverink, 2016]. Moreover, abundant agricultural waste, such as lignocellulosic materials, have emerged as a sustainable solution to mitigate the fuel versus food dilemma. The increasing cost of petroleum and the adverse environmental effects caused by fossil fuels serve as strong motivations to explore the use of lignocellulosic materials aiming to fulfill our energy needs [Selvakumar et al., 2022]. Lignocellulosic biomass is the most abundantly available raw, bio-renewable and biodegradable material present in earth [Yousuf et al., 2019]. It is composed of cellulose (carbohydrate homopolymer) hemicellulose (carbohydrate heteropolymer), and lignin (aromatic alcohols) respectively [Zoghlami and Paës, 2019]. Exploiting lignocellulosic biomass for bioethanol production presents a promising approach to effectively utilize agricultural waste. However, it is necessary to pretreat the lignocellulosic materials applied in order to break down the resistant lignin structures present in biomass-based feedstocks [Periyasamy et al., 2022].

The utilization of lignocellulosic waste obtained from forestry, agriculture, and industry presents several advantages in terms of reducing the cost of bioethanol production. Moreover, the aforementioned residues comprise promising substrates for bioethanol production due to their sustainable nature. The process involves hydrolyzing lignocellulosic waste to convert the polysaccharides contained into sugars, which are then fermented under suitable conditions. In the simultaneous

saccharification and fermentation process, yeast cells efficiently convert biomass-derived sugars into bioethanol, eliminating enzyme inhibition and reducing production costs. The final bioethanol concentration achieved is significantly influenced by key operating parameters such as solid biomass concentration, enzyme concentration, temperature and yeast concentration throughout the simultaneous saccharification and fermentation (SSF) process [Periyasamy et al., 2023].

Numerous fermentative microorganisms can produce bioethanol including yeasts, fungi and a number of Gram-negative and positive bacteria. Among them, *S. cerevisiae*, known as baker's or brewer's yeast, and *Zygomonas mobilis* (*Z. mobilis*) include high ethanol titers, often approaching the theoretical maximum using glucose as substrate [Fan et al., 2023;Xia et al., 2019]. However, the main limitation of *S. cerevisiae* is its relatively low tolerance to ethanol concentration and its compatibility with only selected mono- and disaccharides [Tikka et al., 2013]. Bacteria of the genera *Lactobacillus* and *Clostridium* as well as yeast of the *Candida* and *Pachysolen* genera have been also reported as efficient bioethanol producers [Soleimani et al., 2017;Selim et al., 2018]. Moreover, *K. marxianus* constitutes a thermotolerant yeast capable of producing bioethanol [Flores et al., 2013], while *Pichia* species including *kudriavzevii* and *stipites* have been used to produce bioethanol [Hoppert et al., 2022;Cesar Guimaraes et al., 2023]. Additionally, *Metchnikowia cibodasensis Y34* [Chaudhary et al., 2021] and *Spathaspora passalidarum* [Farias and MaugeriFilho, 2021] have been previously used in bioethanol production.

1.2.1 Bioethanol production by *S. cerevisiae*

Saccharomyces cerevisiae is widely used for production of various biofuels, biochemicals, and natural products, particularly bioethanol [Qi et al., 2023]. As a well-known, generally recognized as a safe (GRAS) model microorganism, *S. cerevisiae* is widely used due to its excellent operational convenience and high fermentation efficiency [Wang et al., 2023]. This yeast has been used for thousands of years for the production of food and beverages [Mohd Azhar et al., 2017], while it is currently widely used for the production of biofuels. However, the yeast can convert only hexose sugars such as glucose and is not able to co-ferment glucose and xylose for bioethanol production [Ho and Chang, 1989].

Four stages exist in the production of lignocellulosic-based ethanol: pretreatment, hydrolysis, fermentation and distillation. In the fermentation process, *S. cerevisiae* converts sugars into ethanol via the glycolysis pathway. Although a high ethanol yield can be obtained, other by-products, including glycerol, certain acids and lipids can be also produced in the fermentation process [Tian et al., 2023]. In recent years, significant progress has been made in genetic and enzymatic technologies, leading to improvements in the various stages of ethanol production. These advancements have also expanded the capacity of *S. cerevisiae* to ferment different sugars simultaneously [Parapouli et al., 2020]. Although numerous fungal and recombinant bacteria species capable of fermenting xylose sugar exist, not all of them possess the capacity to adapt to fermentation-process conditions. Additionally, some of these species only yield low amounts of bioethanol. Further refinements are still needed to enhance their tolerance to bioethanol and productivity [Cunha et al., 2019].

1.2.2 Bioethanol production by *K. marxianus*

The thermo-tolerant yeast *Kluyveromyces marxianus* has been proposed as a solution to address part of the challenges faced in bioethanol production [Watanabe et al., 2019]. This strain possesses several advantages and characteristics that constitute it suitable for commercial fermentation processes. These include the capacity to efficiently assimilate sugars, rapid growth with a generation time of around 70 min, tolerance to temperatures up to 52 °C, metabolic versatility and the capacity to ferment both hexoses and pentoses [Diniz et al., 2014]. Since *K. marxianus* holds the ability to growth up to 52 °C, it was therefore chosen as the working strain in SSF processes [Wu et al., 2016].

K. marxianus, as a lactose-fermenting yeast with useful physiological features, has been extensively used in cheese whey fermentations. More specifically, final bioethanol concentrations between 6.4 and 14.0 g L^{-1} have been reported for whey fermentations carried out using different *K. marxianus* strains [Ozmihci and Kargi, 2007]. The potential of *K. marxianus* for bioethanol production using whey permeate media was confirmed by Saini et al., (2017). *K. marxianus* MTCC1389 produced 51.8 g L^{-1} of bioethanol utilizing 150 g L^{-1} of lactose at 37 °C. Moreover, it has also been reported that cells of *K. marxianus* retain the ability to hydrolyze lactose in entrapped forms, constituting the strain suitable for application in continuous and semi-continuous fermentations [Panesar, 2007]. Recent studies including fermentation of electro-activated whey, electro-activated whey permeate and electro-activated lactose using *K. marxianus* ATCC 64884 demonstrated production of various volatile aroma compounds such as ethanol, 2-phenylethanol and isoamyl alcohol with valued organoleptic properties [Karim and Aider, 2022]. Additionally, Tinôco et al. (2021) demonstrated the production of 17.83 g L^{-1} of ethanol using *K. marxianus* which was achieved under fermentation conditions that included initial glucose concentration of 34.2 g L^{-1} obtained from sweet sorghum bagasse and fermentation temperature of 42 °C.

1.2.3 Bioethanol production by *P. kudriavzevii*

The production of bioethanol is currently dominated by *S. cerevisiae*. However, the potential of non-conventional yeasts could be often exploited as given that other yeast species could provide unique properties that *S. cerevisiae* does not possess [Chamnipa et al., 2017]. *Pichia kudriavzevii* constitutes an emerging yeast that is useful based on favourable characteristics that include thermotolerance and tolerance to multiple stresses such as resistace to 5-hydroxymethylfurfural (HMF), acetic acid, and low pH conditions [Ndubuisi et al., 2018]. *Pichia stipitis*, has been studied for fermenting C6 and C5 sugars including the fermentation of xylose to ethanol demonstrating high bioethanol yields [Song et al., 2019]. *Z. mobilis* and *P. stipites* have been additionally used in mixed cultures for efficient bioethanol production [Wirawan et al., 2020].

Previous studies have shown that several yeast species isolated from natural habitats could be classified as industrial-thermotolerant yeasts. *P. kudriavzevii* KVMP10 isolated from soil located beneath apple trees, demonstrated significant technological advantages for the production of sustainable bioenergy, such as utilization of both hexoses (glucose, sucrose, fructose and galactose) and pentoses (xylose) at high temperatures, exemplifying its great potential for application in orange peel based biorefineries for ethanol production. More specifically, the yeast was capable of producing 54 g L^{-1} of ethanol at the elevated temperature of at 42 °C [Koutinas et al., 2016]. Moreover, *P. kudriavzevii* could produce 33.9 g L^{-1} ethanol from kinnow peel in 12 h using a laboratory fermenter at the elevated temperature of at 40 °C [Sandhu et al., 2012]. Furthermore, *P. kudriavzevii* constitutes an osmotolerant yeast as confirmed by the capacity of *P. kudriavzevii* ITV-S42 to ferment 200 g L^{-1} of initial glucose concentration [Diaz-Nava et al., 2017]. Ethanol production was also achieved using *P. kudriavzevii* HOP-01 from alkali- and ozone-treated cotton stalks producing 19.8 g L^{-1} and 11.0 g L^{-1} of ethanol respectively [Kaur et al., 2012].

1.2.4 Bioethanol production by *Zymomonas mobilis*

Zymomonas mobilis constitutes a natural ethanologen with holding various desirable characteristics, constituting the strain as an industrial microbial biocatalyst for commercial production of desirable bioproducts [Wang et al., 2018]. Among the physiological features of *Z. mobilis*, the microorganism includes bioethanol tolerance up to 16% (v/v), as well as the capacity to produce bioethanol across a broad pH range (3.5–7.5, especially low pH). Moreover, *Z. mobilis* does not require controlled aeration during bioethanol fermentation, which leads to reduced production cost [Yang et al., 2016]. The strain is highly susceptible to phenolic aldehydes, and less susceptible to the corresponding alcohols and acids derivatives. However, previous studies have shown that *Z. mobilis* Z198 demonstrated significantly improved conversion of the most toxic phenolic aldehyde by 6.3-fold and cellulosic ethanol production by 21.6% [Yan et al., 2021]. Compared to the workhorse yeast *S. cerevisiae, Z. mobilis* can produce bioethanol three to five times faster per cell and at higher productivity [Palamae et al., 2020].

1.2.5 Bioethanol production via cell immobilization

Bioethanol finds extensive applications in the chemical, pharmaceutical, and food industries, serving as a valuable resource for raw materials, solvents and fuel. The annual production of industrial ethanol constitutes approximately four million tons, 80% of which is produced by fermentation [Zafar and Owais, 2006]. Although bioethanol production is considered as one of the most promising alternatives for petroleum-based fuels, ethanol fermentations are impacted by substrate and product inhibition decreasing process productivity. Immobilised biocatalysts could assist yeasts in the presence of inhibitors performing stable and elevated biofuel production [Kirdponpattara and Phisalaphong, 2013]. More specifically, immobilization has been implemented in both repeated batch and continuous ethanol fermentations aiming to enhance ethanol productivity, elevate cell density, maintain the stability of cellular activity and protect cells against inhibitors [Mojović et al, 2010].

Cell immobilization holds numerous advantages over traditional freely suspended cell cultures that could reduce the overall cost of the system [Moia et al, 2024]. These advantages include better cell stability and resistance to mechanical stress, increased cell biomass, nutritional supplementation without the need to harvest cells and reduced risk of cell contamination [Sagir and Alipour, 2021]. Numerous methods have been reported for cell immobilization including magnetic immobilization using nanoparticles coating with molecules supporting cellular adhesion, such as fibronectin, micro-patterning of growth surfaces or embedding cells into hydrogel for bio-printing, such as alginate or alginate di-aldehyde-gelatin or methacrylated gelation [Ritter et al, 2020]. A multitude of whole cell immobilization methods exist based on the physical mechanism causing immobilization including cells attached to a surface, mechanical containment behind a barrier, adsorption on a surface, entrapment of cells within a porous material, electrostatic binding on a surface and aggregation. (Figure 1.2).

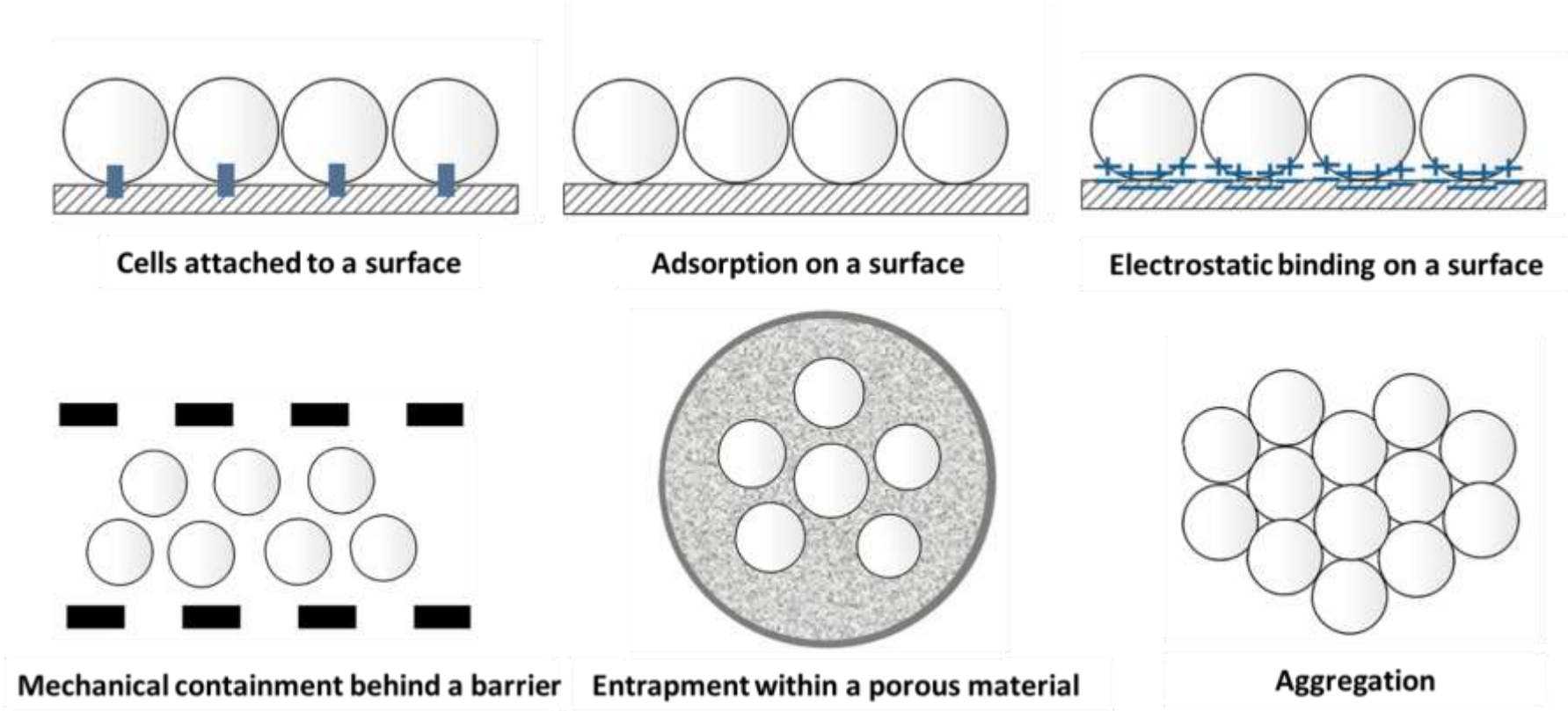

Figure 1.2: Whole cell immobilization methods.

Porous gel matrices, such as calcium alginate, have been widely used for the entrapment of cells and to obtained high biomass loading for fermentation [Ritter et al, 2020]. Support materials such as gels, porous cellulose, natural sponge, agarose and carrageenan have been previously investigated for cell immobilization in fermentations conducted for bioethanol production [Karagoz et al, 2019]. During bioethanol fermentations, the presence of substrate or product inhibition over extended periods can decrease the activity of yeast cells, leading to reduced ethanol production. However, utilizing immobilised cell systems with suitable carriers can enhance the ability of yeast cells to withstand inhibitors or unfavourable conditions compared to free cell systems. This, in turn, results in higher and more consistent ethanol productivity [Phisalaphong et al., 2007].

Different immobilization approaches have been applied in bioethanol fermentation systems including i) entrapment of cells, ii) adsorption, iii) biofilm formation, and iv) self-aggregation [Zhao and Xia, 2010;Mongkolkajit et al., 2011; Mathew et al., 2013;Xu et al., 2005]. The entrapment of cells using alginate gel beads is a commonly used technique for immobilizing living cells, especially in smaller scale laboratory settings because of its simple application and maintenance of high cell viability and activity [Verbelen et al., 2006]. Alginate was also used to immobilize *S. cerevisiae* YPH499 to produce ethanol from hydrolysate of *Chlamydomonas mexicana,* while chitosan beads with calcium alginate feedstock were used to immobilize *S. cerevisiae* for ethanol production using glucose and sucrose [El-Dalatony et al., 2016;Duarte et al., 2013]. However, the process is limited by unstable performance due to poor mechanical properties of the carrier, rapid degradation and its dense structure, limiting application in large scale production in industrial fermentation processes. Moreover, during fermentation the formation of carbon dioxide influences alginate gel beads via expantion, which causes rapid disruption on the bead [Nguyen et al., 2009]. Although the chemical and physical properties of alginate gel beads could be improved by blending with polymers such as polyvinyl alcohol and polyethylene oxide there is still need to identify novel eco-friendly and cost-effective carriers with rigid structure improving the stability of ethanol bioprocesses [Çaykara et al., 2005; Inal and Yigitoglu, 2011].

S. cerevisiae demonstrated effective immobilization on mineral Kissiris via attachment of yeast cells producing 115 g L^{-1} d^{-1} of bioethanol, while no reduction in ethanol productivity and yield was observed for up to 29 repeated batch fermentations [Kana et al., 1989]. The yeast was also immobilised on orange peel pieces for use in alcoholic fermentation and fermented food applications using various carbohydrate substrates (glucose, molasses, raisin extracts) resulting in high ethanol productivities and operational stability of the biocatalyst [Plessas et al., 2006]. Immobilised cells of *S. cerevisiae* AC14 (a recombinant yeast that secretes 7 hydrolytic enzymes) were also applied in a consolidated bioprocess that achieved 100% of biomass hydrolysis and consumption of the substrate offered in a heterogeneous system [Ramos et al., 2023]. High ethanol yield of over 90% was obtained using *S. cerevisiae* immobilised on electrospun Pluronic F127 demethacrylate, producing higher ethanol titer as compared to free cells [Herkommerova et al., 2018]. Given that the immobilization system enhances cell stability, it could be reused for several cycles in a repeated-batch fermentation [El-Dalatony et al., 2016].

Immobilised *K. marxianus* was also used in repeated batch fermentations for bioethanol production demonstrating that both ethanol production as well as productivity were improved and remained constant for at least 8 cycles [Chen et al., 2024]. *K. marxianus* DMKU 3-1042 and *S. cerevisiae* M30 were previously studied for their capacity to improve production and stability of ethanol fermentation. The effectiveness of the immobilised system was confirmed given that the high temperature tolerance was achieved upon coculture immobilization [Eiadpum et al., 2012].

1.3 Biochar: properties, production and application

1.3.1 Biochar production and properties

Biochar is a solid, high carbon material obtained by the heating of biomass feedstocks in the absence or limitation of an oxidizing agent in a controlled process [Wang et al., 2023]. This organic material is produced from lignocellulosic biomass at temperatures ranging between 300 ^{o}C - 700 ^{o}C [Wijitkosum and Sriburi, 2023]. Previous studies reported that biochar could be produced from various types of lignocellulosic biomass feedstock, including both wooden and non-wooden materials such as agricultural waste and residues, sewage sludge, animal manure, as well as wood and woodchips [Ippolito et al., 2020; Wang et al., 2018].

The biomass used for the production of biochar is pyrolyzed, gasified, or hydrothermally carbonized in an oxygen-limited environment [Olugbenga et al., 2024] (Figure 1.3). Slow pyrolysis, thermochemical decomposition under oxygen-limited conditions, has been identified as an efficient process for biochar production, forming a stable carbonaceous and homogeneous structure in high yield [Huang et al., 2021]. The biochar's response to pyrolysis temperature varies between different feedstocks due to the different biopolymers entailed and the distinct chemical composition of each feedstock type [Li et al., 2016]. For example, animal-based feedstocks constitute mainly animal protein such as gelatin, collagen, and polysaccharides (cellulose, starch and carbohydrates), while plant-based biomass commonly consists of cellulose, hemicellulose and lignin with a definite structure [Singh and Cowie, 2010;Bordoloi et al., 2008]. Kloss et al. (2012) and Chen et al. (2016) reported that various biochar feedstocks produced under the same pyrolysis conditions incorporated different properties.

Fast pyrolysis is generally considered as an efficient and feasible method to convert biomass into bio-oil. In fast pyrolysis biomass is rapidly heated to a temperature of about 500 ^{o}C with a short reaction time [Aghbashlo et al., 2019]. According to Brown et al. (2011), the main differences between slow and fast pyrolysis comprise the heating rates and maximum reaction temperatures. Slow pyrolysis heating rates comprise typically between 5 - 20 ^{o}C min^{-1}, while fast pyrolysis can achieve rates exceeding 1000 ^{o}C min^{-1}. Moreover, fast pyrolysis can

be performed in a short time while slow pyrolysis requires several minutes or even hours which affects the properties of the final product. The biochar's residence time in the reactor becomes another important factor since it influences both primary and secondary reactions [Abdullah et al., 2023]. Higher pyrolysis temperatures produced biochar with higher carbon content, lower volatile matter and oxygen composition, as well as higher ash content [Ronsse et al., 2012]. Islam et al. (2019) used banana peel and orange peel in the slow pyrolysis experiment at a heating rate of 10 ^{o}C min^{-1} to produce biochar as an adsorbent for the treatment of palm oil mill effluent. In previous studies multiple applications of biochar produced from slow pyrolysis have been reported [Suman and Gautam, 2017;Rawat et al., 2019].

Biochar possesses diverse physical and chemical properties constituting a versatile material for various applications. Chemically, biochar mainly comprises carbon, with small amounts of oxygen, hydrogen, nitrogen and other elements derived from the biomass feedstock [Barbhuiya et al., 2024]. The elemental composition of biochar affects reactivity, nutrient content and sorption properties. Functional groups such as hydroxyl, carboxyl and phenolic groups that could occur on the biochar's surface can enhance nutrient retention and facilitate chemical reactions in the environment. Depending on pyrolysis conditions and each feedstock type biochar's properties include varying surface area, pH, cation exchange capacity and bulk density. More specifically, Yuan et al. (2015) investigated the effect of pyrolysis temperature on biochar derived from sewage sludge properties, highlighting the significant impact of temperature on surface area, porosity, and nutrient content. Thus, the properties of the material constitute important parameters for further application as soil amendment, in water filtration, carbon sequestration and its use as a catalyst or adsorbent in various industries [Adeniyi et al., 2024].

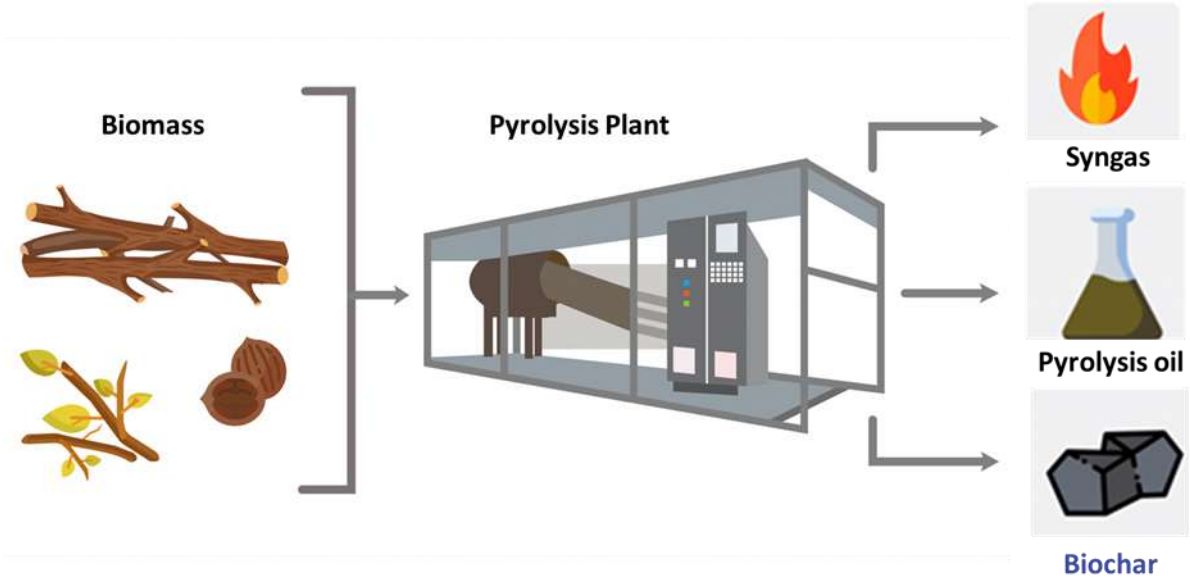

Figure 1.3: Production of syngas, pyrolysis oil and biochar via pyrolysis.

1.3.2 Applications of biochar

The development of carbonaceous materials such as biochar has triggered a hot spot in materials that could serve as a vital platform for energy storage and conversion [Mishra and Mohanty, 2023]. Biochar has gained considerable attraction due to several physicochemical characteristics, such as porosity and surface functionality. Thus, biochar has been extensively used in environmental management applications enhancing environmental restoration, while reducing the environmental impact of polluted areas [Uday et al., 2022]. Biochar has been used as soil amendment improving plant development, decreasing soil erosion and increasing soil's fertility, enhancing the soil's water holding capacity, the availability of nutrients, as well as soil quality. As a soil supplementary material, biochar increases microbial activity in agricultural settings, while its porosity improves nutrient cycling and provides a favorable niche for important soil organisms [Manikandan et al., 2023]. Recent studies have also demonstrated the efficient use of biochar in hydroponic systems upon used as growth medium [Zou et al., 2023]. Moreover, biochar can assist in climate change mitigation through carbon sequestration [Agyekum and Nutakor, 2024].

Based on a number of favourable properties, biochar has been successfully employed in environmental remediation constituting an advanced green sorbent for soil and water organic/inorganic decontamination [Demirbas and Arin, 2002]. Adding biochar to soil and soilless media enables suppressing plant diseases caused by both foliar and soilborne pathogens [Frenkel et al., 2017]. Biochar-elicited suppression of diseases caused by foliar fungal pathogens is clearly related to activation of plant system-wide defenses, given that biochar is spatially distant from the site of pathogen attack. [Jaiswal et al., 2018]. The material demonstrated effective immobilization of heavy metals, minimizing in situ the bioavailability of inorganic and organic contaminants to earthworms, microbes, and plants [Uchimiya et al., 2011], whereas its use in anaerobic digestion is known to enhance methane production, alleviating toxicity inhibition and improving the stability of anaerobic digestion processes [Nie et al., 2024]. More specifically, the presence of biochar in a batch digester can neutralize the pH to alleviate the acid inhibition effect on methanogens, while providing large surface areas for microorganisms to attach and

selectively enrich functional microbes such as syntrophic bacteria and methanogens (e.g., *Methanosarcina* and *Methanosaeta*), leading to faster CH_4 generation [Lu et al., 2016]. Moreover, as a carbonaceous material biochar can promote interspecies electron transfer between syntrophic bacteria and methanogens owing to its conductivity, which is a critically important characteristic influencing the performance of biochar energy storage devices due to its impacts on energy efficiency and power density [Pan et al., 2019;Gabhi et al., 2024].

Based on the carbon rich content and unique physicochemical properties, biochar has emerged as a viable candidate for applications in batteries and supercapacitors, while its use in environmental clean-up applications including water purification and air filtration has been previously explored [Manikandan et al., 2023].

1.3.3 Biochar as a support material for immobilization

Cell immobilization on biochar constitutes a promising approach to achieve high concentration and stability of microbial cells for several applications [Schommer et al., 2023]. Biochar stands out as a promising carrier for cell immobilization due to exceptional properties that include specific surface area and porosity as well as the presence of several functional groups [Deng et al., 2022]. The immobilization of microorganisms on such material can effectively address the issue of saturated adsorption and release of pollutants, which improves the reusability of biochar [Shen et al., 2018]. Numerous enzymes have been immobilised on biochar mainly using the material as adsorbent [Table 1.3]. As opposed to enzyme immobilization, cell immobilization is advantageous due to the elimination of expensive downstream steps including enzyme separation and purification [Mehrotra et al., 2021].

Zhao et al. (2020), demonstrated that the immobilization of *Pseudomonas citronellolis* on biochar improved the efficiency of phenol removal, which was increased up to 99% with the addition of biochar. This can be attributed to the fact that biochar acted as shelter to support the bacterium against the inhibitory effect of the pollutant resisting against extreme bioprocess conditions. Additionally, *Pseudomonas putida* was immobilised on coconut fiber-derived biochar using the adsorption method and covalent binding aiming to enhance paraquat removal from contaminated water [Ha et al., 2021]. *Bacillus subtilis*, *Bacillus cereus* and *Citrobacter* sp. were successfully immobilised on biochar and applied to cadmium and lead-contaminated soil resulting in numerous benefits for the soil including increased organic matter, enhanced cation exchange capacity, elevated enzymatic activity, and improved microecosystem within the rhizosphere of plants. [Schommer et al., 2023].

Immobilised cells of *K. marxianus* and *Debaryomyces hansenii* on biochar derived from wood feedstock were also used in whey fermentation producing value-added biomolecules. Yeast immobilization resulted in increased cell density and 2-phenylethanol production [Castillo et al., 2022].

Table 1.3: Different types of biochar used as support for enzyme immobilization immobilised in different applications.

Biochar source	Enzyme	Immobilization method	Application	Reference
Oat husk	Lipase	Adsorption	Hydrolysis of p-NPP (p-nirophenol palmitate)	Cea et al., 2010
Pinewood	Laccase	Adsorption	Removal of carbamazepine	Naghdi et al., 2017
Pinewood, Pig mannure, Almond shell	Laccase	Covalent binding	Degradation of diclofenac	Lonappan et al., 2018
Pinewood, Pig mannure, Almond shell	Laccase	Adsorption	Degradation of diclofenac	Lonappan et al., 2018
Guava seeds	Lipase	Adsorption	Hydrolysis of olive oil.	Almeida et al., 2017
Wood (Maple and Spruce) biochar	Laccase	Adsorption	Degradation of 4-hydroxy-3,5-dichlorobiphenyl	Li et al., 2018
Pupunha palm	Pepsin	Adsorption/Covalent binding	Casein hydrolysis	Santos et al., 2019
Oat hull biochar	Lipase	Adsorption	Hydrolysis of p-NPP (p-nirophenol palmitate)	Gonzalez et al., 2013

1.4 Non-biological char from car tire waste

The annual production of waste tires has significantly risen due to the rapid growth of the automobile and transportation sectors [Bockstal et al., 2019]. The current estimation suggests that the annual production of tires exceeds 3 billion, and it is anticipated that the market demand will continue to grow at a rate of over 4% [Policella et al., 2019]. As a result, a substantial number of end-of-life waste tires is expected to be inevitably generated, necessitating the implementation of waste management, treatment and disposal measures [Oboirien and North, 2017]. Stockpiling and improper disposal of waste tires causes problems to the environment through providing sites for vermin or breeding grounds for insects and the potential for fire hazard of large tire dumps [Gao et al., 2022].

Recycling the tires as rubber and rubber particles, their use as rubber flooring for sports fields and playgrounds as well as the application of waste tires in civil engineering applications comprise examples of the recovery options available [Presti, 2013;Li et al., 2010; Karthikeyan et al., 2012]. Moreover, the waste management method often applied for waste tires comprises landfill disposal [Simic and Dabic-Ostojic, 2017]. However, for the preferred method for the disposal of waste tires constitutes the recovery of energy via thermal treatment. The three technologies employed for waste tire thermal valorization comprise pyrolysis, combustion and gasification [Pastor et al., 2014].

Gasification of tires constitutes a process in which air, oxygen or steam react with tires in an endothermic reaction to produce mainly syngas (CO and H_2), while other byproducts comprise CO_2, light hydrocarbons and char [Leung and Wang, 2003]. Various studies have focused on the gasification of tires for the production of syngas [Donatelli et al., 2010], as well as the production of hydrogen, activated carbon and carbon nanotubes [Molino et al., 2013;Portofino et al., 2011]. Pyrolysis constitutes a promising method for recycling and energy recovery in the field of waste tire treatment, which could meet the three principles of solid waste treatment: reduction, resource recovery and mitigation of pollutants [Gao et al., 2022]. In comparison with other treatment methods such as, combustion, retread, and landfilling, pyrolysis has been widely studied given that it results in reduced

secondary pollution and the potential for generation of products that includes higher economic value [Hoor and Rowe, 2012]. The transformation of waste tires to fuels allows reduced use of conventional fossil fuels. Therefore, waste tire pyrolysis has been demonstrated as a feasible method to indirectly reduce greenhouse gas emissions [Yaqoob et al., 2021]. Over time, pyrolysis has advanced and reached a level of maturity given that it is considered as a fast and efficient technology to address the environmental burden caused by waste tires. The steel, rubber, carbon black, additives and other materials contained in waste tires could be recovered and nearby no waste by-products could be generated from the pyrolysis process [Wang et al., 2020]. Pyrolysis oil constitutes the primary product obtained from waste tire pyrolysis, when conducted under mild conditions. However, the direct use of pyrolysis oil as fuel oil is limited due to its high sulfur content and composition [Farzad et al., 2021].

The solid carbon residue, also known as char, comprises the carbonaceous material remaining following degradation of rubber during the waste tire pyrolysis process and it can be modified or activated by chemical and thermal treatment [Doja et al., 2022]. Through the activation process, the surface area of carbon is increased during heating in the presence of activating agents [Koreňová et al., 2008]. Shredded waste tires from various sources (cars, trucks and bikes) can be pyrolyzed in an inert atmosphere at a broad range of temperatures (400 ^{o}C to 1000 ^{o}C) yielding char that can be used directly as fuel [Li et al., 2005]. However, various studies have applied higher temperatures (> 600 ^{o}C) during pyrolysis to remove volatiles and alter the pore structure of tire char [Koreňová et al., 2008].

1.5 Response and tolerance of yeast to environmental stresses during bioethanol fermentation

All types of organisms, either individual cells or multi-cellular organisms, have the ability to respond in changes of environmental conditions. The response and adaptation mechanisms against stress are highly complex, while research on stress responses, specifically gene and protein expression analyses, can easily turn into a journey through almost all aspects of cell biology [Hohmann and Mager, 2003]. Yeasts, while living freely in nature, face a range of variations in their environment as well as acting and adaptation mechanisms, which are essential for survival upon exposure to environmental stresses. Temperature, pressure, radiation, water, presence of certain ions, toxic agents, pH and nutrients availability comprise the main environmental stresses experienced by yeast cells. Growth under harsh conditions requires maintenance of the internal system. Thus, when the environmental conditions change abruptly, the cell must rapidly adjust its internal milieu to that required for growth at the new conditions [Saini et al., 2018]. The identification of differentially expressed genes in response to environmental stress offers insights into the roles of the transcriptome in the regulation of physiological responses [Xu et al., 2016].

The presence of an Environmental Stress Response was proposed for *S. cerevisiae* in 1990's [Brown et al., 2020]. According to the current state of knowledge *S. cerevisiae* faces two important environmental challenges: heat and oxidative stress [Sumanu et al., 2023]. Although *S. cerevisiae* is highly ethanol tolerant, high ethanol concentrations inhibit cell growth and viability, limiting fermentation productivity and ethanol yield constituting high ethanol concentrations another environmental stress for the yeast's survival [Galeote et al., 2001].

1.5.1 Heat shock response

Ethanol production at elevated temperatures requires high potential thermotolerant ethanol-producing yeast strains. Fermentation at high temperature is a key requirement for effective bioethanol production in tropical countries where average daytime temperatures are usually high throughout the year [Limtong et al., 2007]. The advantages of fermentation at high temperatures are not only an increased rate of fermentation but also a decreased risk of contamination by mesophilic microorganisms, such as *Williopsis* sp., *Candida* sp., *Zygosaccharomyces* sp. Moreover, high temperature alcoholic fermentations can reduce the cost of the cooling system and enable potential use of simultaneous saccharification and fermentation (SSF) when coupled with a continuous stripping system for ethanol recovery [Qi et al., 2023; Xiao et al., 2018]. Utilization of a highly thermotolerant yeast strain is a key to success in ethanol production at high temperatures [Kiran et al., 2000; Limtong et al., 2007]. There are also several reports in the literature relevant to ethanol production at high temperatures using the thermotolerant yeast *K. marxianus* [Yuan et al., 2011].

The most fundamental stress experienced by a yeast cell comprises ambient temperature. *S. cerevisiae* exhibits optimal growth at temperatures between 25 – 30 ^{o}C. At temperatures higher than 36 – 37 ^{o}C, yeast cells activate a transcriptional program termed as the heat shock response (HSR) and alter several components of their physiology including membrane composition and carbohydrate flux. In eukaryotes the heat shock transcription factor is a protein family and constitutes the primary modulator of the HSR. In *S. cerevisiae* there is also a second transcription factor represented by the *MSN2* and *MSN4* genes that contribute to the heat shock response. The *MSN2/4* regulor includes oxidative stress as well as metabolic and other cytoprotective genes, and it is characterized as environmental stress response (ESR) [Morano et al., 2012].

Under stressful conditions, such as heat, ethanol or osmotic stress, several stress-responsive genes including those encoding for the heat shock proteins (HSPs), enzymes involved in protein degradation, such as ubiquitin ligase, and proteins involved in trehalose and glycogen metabolism in yeast have been reported

to be stimulated [Auesukaree et al., 2012; Lertwattanasakul et al., 2015]. HSPs play a key role as molecular chaperones by either stabilizing new proteins to ensure correct folding or refolding of proteins to the proper conformation, or degrading misfolded proteins which are damaged by stress conditions. HSPs also assist transport proteins across membranes within the cell [Walter and Buchner,2002; Borges and Ramos, 2005]. Trehalose, which is one of the compatible solutes synthesized during adverse environmental conditions, has been reported to protect the cell by replacing water at the surface of macromolecules, thus holding proteins and membranes in their native conformation [Purvis et al., 2005;Li et al., 2009]. Glycogen, which is a reserve carbohydrate in *S. cerevisiae*, has also been reported to be involved in tolerance towards several stresses [Parrou et al., 1997;Unnikrishnan et al., 2003]. More specifically, glycogen, whose synthesis genes are regulated by MSN2/MSN4, has been demonstrated to accumulate following heat shock. However, the role of glycogen in response to heat shock is poorly documented [Wilson et al., 2010].

Heat shock factor 1 (HSF1) primarily regulates HSR in *S. cerevisiae*, while heat shock factor 2 (HSF2) is involved in developmental gene expression. Although the roles of heat shock factor 3 (HSF3) and heat shock factor 4 (HSF4) are less well understood, evidence suggests that the specific factors could functionally interact with HSF1 to modulate gene expression [Akerfelt et al., 2010]. *S. cerevisiae* HSF1 unusually includes an amino-terminal extension of 150 amino acids that acts as a second potent transcriptional activation domain [Sorger, 1990]. HSF1 recognizes a pentameric heat shock element (HSE) defined as repeating units of the sequence nGAAn (Sorger and Pelham 1987). Early investigations defined the HSE as a triple inverted repeat, consistent with the fact that HSF1 binds DNA as a trimer [Sorger and Pelham 1987]. Although a number of genes responsible for the prevention of protein denaturation in yeast cells have been reported, the molecular mechanism

conferring thermotolerance during ethanol fermentation at high temperatures is not yet fully understood.

1.5.2 Ethanol stress response

Ethanol as the main product of fermentation constitutes a primary factor inhibiting the bioprocess [Li et al., 2019]. High ethanol concentration is considered as a common stress on yeast growth during fermentation [Stanley et al., 2010; Mukherjee et al., 2017], resulting in different cellular responses related to changes in membrane fluidity, protein misfolding and chromatin condensation [Ma and Liu, 2010]. The mitochondrial membrane comprises the main target of ethanol, which causes uncoupling of the electron transport chain from the ATPase as well as increase of reactive oxygen species [Zhao et al., 2017]. More specifically, reactive oxygen species induced by ethanol occur mainly due to the high ethanol level on the mitochondrial iron-sulfur cluster assembly system. Thus, constructing an intergraded cell wall can realize physical separation between the endomembrane system and extracellular ethanol [Perez-Gallardo et al., 2013]. High ethanol levels also destroy the integrity of the membrane, damage cell wall, ribosomes and endoplasmic reticulum, perturb protein conformation and disrupt ion homeostasis [Ma and Liu, 2010]. Moreover, typical effects of ethanol stress also include the disruption of cellular proteins and disruption of RNA and protein synthesis [Hu et al., 2006].

Although *S. cerevisiae* is resistant to specific ethanol levels, variations occur among different yeast strains and their resistance to ethanol [Carrasco et al., 2001]. Previous studies have demonstrated that the concentration of ethanol in excess of 9% v/v can affect the growth of *S. cerevisiae* cells [Fujita et al., 2004]. In response to ethanol stress, *S. cerevisiae* regulates several metabolic pathways including signal transduction and protein folding. [Ranganathan et al., 2016]. Several highly expressed cell wall-related genes were previously tested for enhancing ethanol tolerance, encoding HSP150, SPI1, SSD1, SED1 and TIP1 [Zhao et al., 2017]. Although the molecular mechanism of *S. cerevisiae* tolerance to ethanol stress is not yet fully understood, Li et al., (2019) investigated the global mechanism of *S. cerevisiae* Sc131 in response to ethanol stress at transcriptomic and proteomic levels. Among 937 differentially expressed genes and 457 differentially expressed proteins it has been demonstrated that the presence of 10% ethanol can induce filamentous growth and sexual reproduction, whereas mitochondria and

endoplasmic reticulum comprise important organelles assisting the cell to resist ethanol stress. Ethanol stress can induce heat shock proteins (HSP) that appear to be similar to those induced by heat shock [Piper, 1996]. Yeast cells exposed to ethanol synthesize a range of HSPs, including HSP104, HSP82, HSP70, HSP26, HSP30 and HSP12, but only HSP104 and HSP12 have been shown to physiologically influence yeast tolerance to ethanol [Stanley et al., 2010]. More specifically, HSP104 acts as a remodeling agent in the disaggregation of denaturated proteins [Glover and Lindquist 1998], while HSP12 constitutes a membrane-associated protein that can protect liposomal membrane integrity against desiccation and ethanol [Sales et al. 2000].

Ethanol stress (10%, v/v) as well as heat shock can block the export of bulk poly (A)+ mRNA. However, the differences and/or similarity between heat shock and ethanol stress in the mechanisms of mRNA export still remain to be clarified. It has been reported that both heat shock and ethanol stress induce an almost identical response in yeast such as changes in membrane lipid composition, plasma membrane H+-ATPase activity and vacuolar morphology [Izawa et al., 2008]. Several genes encoding trehalose biosynthesis and amino acid pathways, fatty acid and ergosterol have been also identified involving ethanol tolerance [Ma et al., 2010].

1.5.3 Oxidative stress response

Oxidative stress constitutes another severe stress inhibiting *S. cerevisiae* during fermentation and occurs as a result of an imbalance between generation and elimination of reactive oxygen species (ROS) that could be naturally generated during respiration or oxidation of nutrients to obtain energy [de Fatima Alves et al., 2023]. Accumulation of ROS during the fermentation process could be also linked to the formation of toxic by-products resulting from lignocellulose pretreatment, such as furfurals [van der Pol et al., 2014]. ROS pose significant damage to almost all cell components, including DNA, lipids, and proteins, as well as cellular redox balance [Zhao et al., 2014]. Thus, improving the tolerance of *S. cerevisiae* chassis to ROS could potentially result in more efficient bioproduction, offer elimination of conditioning steps operations for yeast tolerance and therefore reduce the cost of the process in industrial-scale ethanol production.

1.5.4 Osmotic stress response

During industrial processes, *S. cerevisiae* is exposed to different stress factors, including high osmolarity, high sulfite dosages, nutrient depletion, acid stress and limited oxygen [Betlej et al., 2020]. Osmotic pressure constitutes a major environmental stress factor experienced by yeast, which quickly increases the osmotic potential within the cell, resulting from the outflow of water and decreases in cell volume and turgor [Zhuang et al., 2017]. It is well established that yeast cells accumulate glycerol and trehalose under high osmotic pressure conditions to avoid lethal damage [Hirasawa et al., 2009]. More specifically, *S. cerevisiae* produces glycerol via a two-step reduction of dihydroxyacetone phosphate by glycerol-3-phosphate dehydrogenase (GPD) and glycerol-3-phosphatasedihydroxyacetone phosphate by glycerol-3-phosphate dehydrogenase (GPD) and glycerol-3-phosphatase [Waterhouse et al., 2016]. Thus, glycerol regulates intracellular NADH/NAD+ ratio, acting as an osmoregulator resulting in the prevention of cells from freezing via action as an anti-freezing agent [Shirvanyan et al., 2023].

1.6 Aim of current work

The objective of this doctoral research was the development of an advanced renewable and low-cost support material for whole cell immobilization in a major industrial bioprocess. This technological aim was pursued through the production of various types of biochar derived from thermal decomposition of lignocellulosic biomass in the absence of oxygen, which were subsequently used for cell immobilization aiming to produce bioethanol using different yeasts. Thus, the development of an efficient bioprocess was targeted by evaluating the applicability of biochar to enhance bioethanol production through immobilization of microbial producers, while evaluating different important properties of the system proposed.

1.6.1 Objectives

The main specific objectives of the current study towards the development of BBB for fermentative bioethanol production were as follows:

- Biochar production from various feedstocks in two different pyrolysis conditions and characterization of the materials generated aiming to assess their potential use as support carriers.
- Repeated batch fermentations using free and supported cells of various fermentative yeasts to evaluate the immobilised biocatalysts developed in terms of bioethanol production and reusability.
- Assessment of immobilised biocatalyst performance under high temperature alcoholic fermentations aiming to address several technological challenges of bioethanol manufacture.
- Optimization of the BBB technology via testing of several materials for the production of biochar, while bioethanol fermentations using BBB were conducted employing hydrolysates generated via a citrus peel waste biorefinery at elevated temperatures.
- The potential stress protective role of BBB was evaluated employing *S. cerevisiae* in bioethanol fermentations under various harsh bioprocess conditions including heat, ethanol, oxidative and osmotic stress, while monitoring transcription from a wide range of genes via RT-qPCR.
- The development of non-biological char-based biocatalysts for the production of bioethanol and their use in lab-scale bioreactor experiments via testing the effect of different operating modes.

2 Research Methodology

2.1 Development of BBB from different biowaste for enhancement of alcoholic fermentations

2.1.1 Biochar production from different feedstocks

According to the International Biochar Initiative (IBI), biochar should be produced through use of waste-derived biomass [Gonzalez et al., 2012]. Thus, biochar was produced utilizing four different types of locally available biomass feedstocks comprising olive kernels (OK, *Olea europaea*, obtained from Pettemerides Olive Oil Mill Ltd, Limassol, Cyprus), vineyard prunings (VP, *Vitis vinifera*, obtained from Dafermou Winery, Larnaca, Cyprus), sewage sludge (SS, Sewerage Board of Limassol – Amathus (SBLA), Moni, Cyprus) and seagrass residues (SGR, *Posidonia oceanica*, collected from a local beach). The biochar specimens derived from OK, VP, SS and SGR will be denoted hereafter as OKB, VPB, SSB and SGRB. Upon collection, all biomass samples were stored in air tight plastic bags until application in pyrolysis. Conventional pyrolysis was performed in a furnace under controlled conditions through the supply of nitrogen gas. The temperature of the furnace was increased at a rate of 10 °C min^{-1}, while 250 °C and 500 °C (for 30 and 3 min respectively) were employed as pyrolysis temperatures. Moreover, char samples of non-biological origin (NBC) were also obtained from CBp Cyprus Ltd (Limassol, Cyprus), producing char and activated carbon from recycled car tires, and it was compared to the renewable materials selected. The production of NBC comprised a continuous pyrolysis process, using a temperature of approximately 500 °C and 1 h residence time in the reactor.

Biochar was additionally produced employing three different types of biowaste that included pistachio shells (*Pistachia vera*, PV), peanut shells (*Arachis hypogaea*, AH) and corks (CR, obtained from Dafermou Winery, Larnaca, Cyprus). Pyrolysis was conducted at 500 ^{o}C as previously described and biochar produced from PV, AH and CR will be denoted hereafter as PVB, AHB and CRB (Figure 2.1).

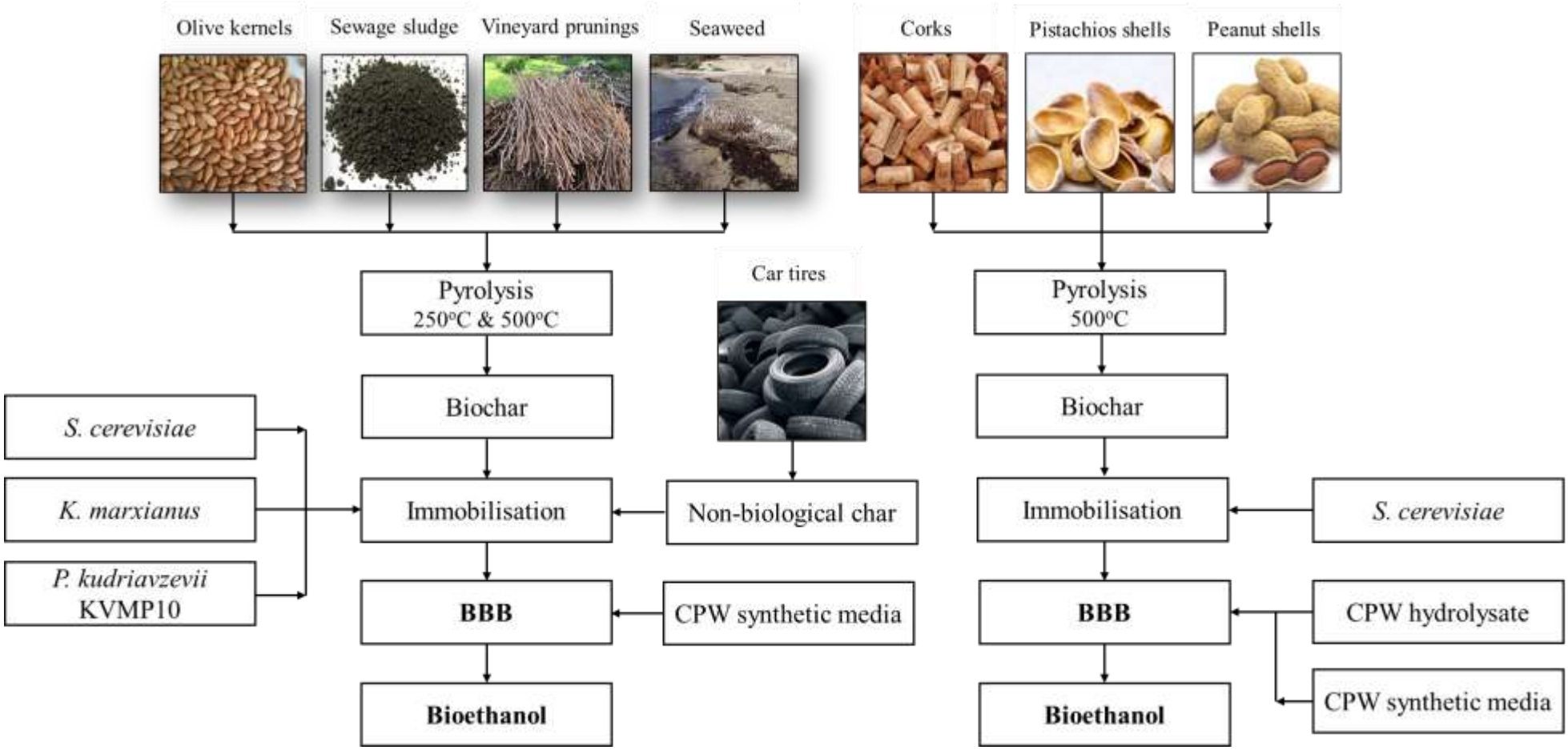

Figure 2.1: Process flow sheet for the production of bioethanol via biochar and immobilised biocatalysts development.

2.1.2 Microorganisms and culture conditions of freely suspended cells

S. cerevisiae and *K. marxianus* were obtained from the Leibniz Institute DSMZ-German Collection of Microorganisms and Cell Cultures (Braunschweig, Germany), while *P. kudriavzevii* KVMP10 was previously isolated as a thermotolerant ethanologenic yeast within our research group [Koutinas et al., 2015]. Fermentations for ethanol production were conducted with each strain using liquid media simulating a Valencia orange peel waste hydrolyzate, which was prepared in 50 mmol L^{-1} citrate buffer at pH 4.8 and consisted of (g L^{-1}): yeast extract 10, peptone 20, fructose 33.2, galactose 8.6, glucose 57.4, and sucrose 1.4 [Wilkins et al., 2007]. The microorganisms were maintained at −80 °C in glycerol stock cultures and prior to the experiment *S. cerevisiae* and *P. kudriavzevii* KVMP10 were cultured in liquid medium consisting of (g L^{-1}): yeast extract 10, peptone 20 and glucose 50. *K. marxianus* was pre-grown in media containing (g L^{-1}): yeast extract 3, malt extract 3, peptone 5 and glucose 50. The inoculums were incubated at 30 °C in an orbital shaker stirred at 100 rpm for 24 h. All chemicals were obtained from Sigma- Aldrich Company Ltd (Dorset, UK) and were of ANALAR grade.

Bioethanol fermentations were conducted in batch mode using 100 mL serum bottles, which were tightly sealed with screw caps and contained 90 mL of fermentation media and 10 mL of inoculum. Serum bottles were incubated in a water bath at a temperature according to the specifications of each experiment and reciprocal shaking at 100 rpm. All fermentations were performed in triplicate, while two samples were analyzed for each replicate constituting analyses of 6 samples at each time point.

2.1.3 Immobilization of microorganisms for repeated bioethanol fermentations

Biocatalysts were prepared through immobilization of *S. cerevisiae, K. marxianus* and *P. kudriavzevii* KVMP10 on biochars derived from VP and SGR, as well as NBC. Each yeast strain was initially pre-grown in liquid medium as described in Section 2.1.3, while grown cells were collected through centrifugation

for inoculum preparation. An amount of 2 g wet pressed yeast cells was suspended in 250 mL of fermentation media and 20 g of the support material was added. The flasks were allowed to ferment the orange peel waste hydrolyzate overnight, using 37 °C for *S. cerevisiae* and 42 °C for *K. marxianus* and *P. kudriavzevii* KVMP10. The supernatant was decanted and the biocatalyst was washed twice with 125 mL of fermentation media prior application to bioethanol production experiments. VPB, SGRB and NBC were used as support materials for bioethanol production.

The preparation of BBB using biochars produced using PVB, AHB and CRB was conducted via the immobilisation of *S. cerevisiae*. The strain was pre-grown in liquid medium as described in Section 2.1.3, while bioethanol production was performed employing two different hydrolyzates: i) synthetic fermentation media simulating a hydrolyzate obtained from Valencia orange peel waste as described in Section 2.1.3, as well as ii) the hydrolyzate obtained from CPW biorefinery. The corresponding hydrolyzate was fermented overnight at 37 ^{o}C, then the supernatant was decanted and the BBBs developed, comprising the biochar-based carrier and the cells attached on its surface, were rinsed with 125 mL of fermentation media twice and subsequently applied to ethanol fermentation trials.

Control experiments employing unsupported cells of the yeast were also conducted in batch mode using the hydrolyzate specified in each experiment. Duplicate cultures were prepared and 6 samples were analyzed at each time point. All chemicals used were purchased from Sigma-Aldrich Company Ltd (Dorset, UK) and were of ANALAR grade.

2.1.4 Adsorption capacity of biochar for ethanol and sugars

The efficiency of biochar to adsorb the ethanol produced was assessed through addition of 8 g PVBC in 100 mL solutions that contained 10, 20, 40, 60 and 80 g L^{-1} of the specific alcohol. The mixtures were incubated at 37 ^{o}C and 100 rpm stirring for 60 min. The same procedure was followed for determination of biochar's capacity to adsorb the sugars contained in the Valencia orange peel waste hydrolysate (see Section 2.1.3) via preparation of solutions that contained 20, 40, 60, 80 and 100 g L^{-1} of sugars.

2.1.5 Impact of biochar's particle sizes on cellular immobilization and fermentation performance

Three different biochar particle sizes were tested in fermentations to assess whether the specific property of the material affected biocatalyst performance. Biochar derived from PV was processed using a laboratory blender and passed through sieves of 1 and 2 mm (Waring Commercial, Texas, USA) obtaining three fractions incorporating different particle size. The biocatalyst was subsequently prepared using each particle fraction, which was applied separately in ethanol fermentations.

2.1.6 Repeated bioethanol fermentations at different temperatures

Bioethanol production using the immobilised biocatalysts developed was evaluated employing different temperatures. Thus, unsupported and BBB (prepared using PVB) cultures were conducted as described in Section 2.1.4. Immobilised and unsupported cells were subsequently applied for ethanol production in fermentations incubated at 37, 39 and 41 ^{o}C. Moreover, the culture incubated at 41 ^{o}C was applied in six repeated batch experiments to assess the recyclability of the biocatalyst. Recovery of the immobilised biocatalysts following completion of fermentation was conducted through filtration. Thus, the liquid media was removed at the end of each batch retaining only the support material with the yeast cells attached on its surface. The recovered biocatalyst (in the form of wet solids) was rinsed with fermentation media twice and reused in a subsequent ethanol fermentation via addition of fresh CPW hydrolysate.

2.1.7 Bioethanol production from CPW hydrolyzates

S. cerevisiae immobilised on PVBC was employed to assess the effectiveness of the developed BBB in enhancing ethanol production during repeated batch fermentations of citrus peel waste (CPW) hydrolyzates produced through a biorefinery (Figure 2.2). Preparation of the immobilised biocatalyst was conducted at 37 ^{o}C as described in Section 2.1.4, while the repeated batch experiments were performed using CPW hydrolyzates produced through the current biorefinery at 41 ^{o}C.

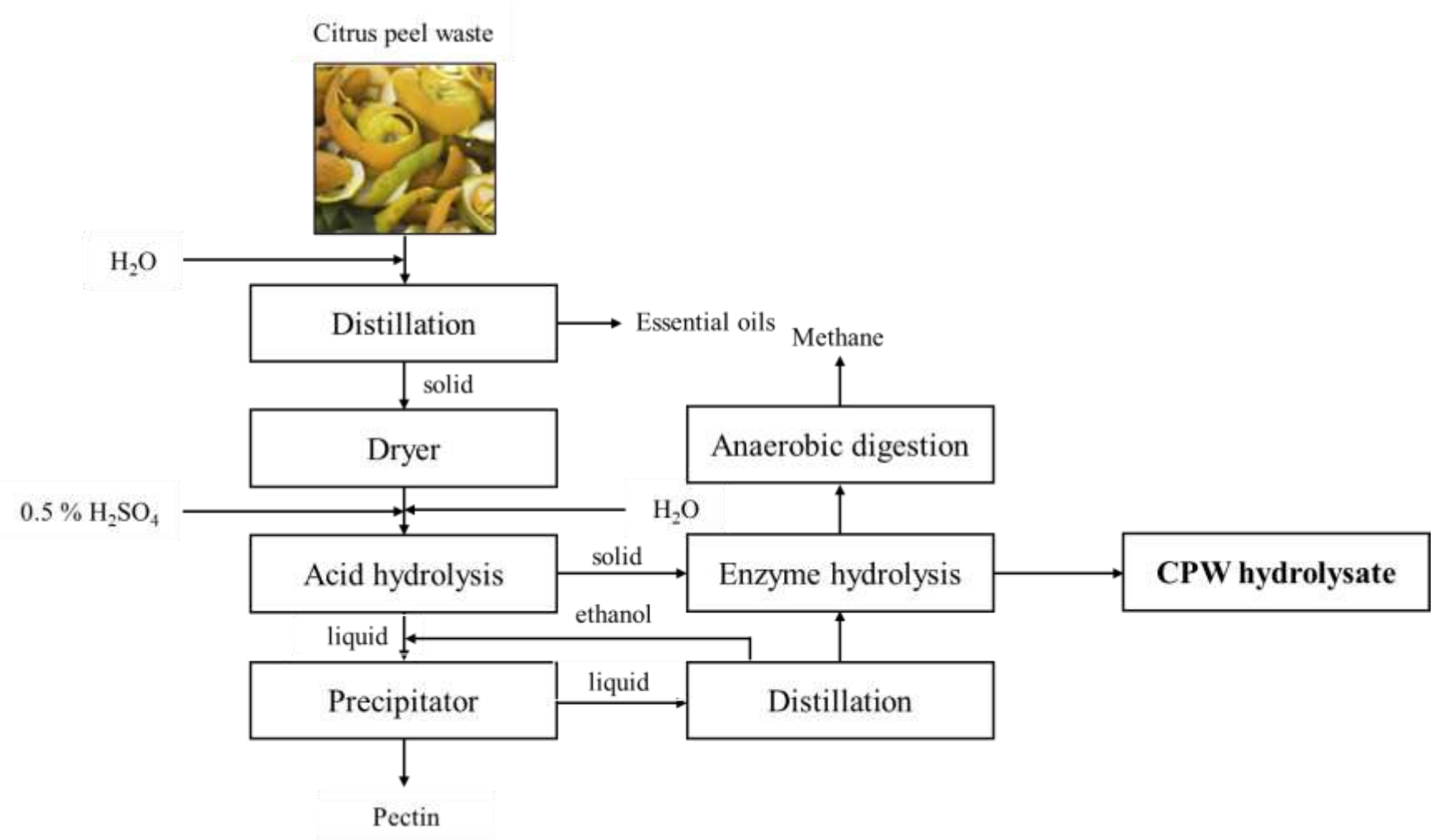

Figure 2.2: Process flow sheet for the CPW biorefinery.

2.1.8 Bioethanol fermentations under stress conditions

Bioethanol fermentation experiments employing freely suspended and supported cells of *S. cerevisiae* were conducted at 30 ºC and 39 ºC to assess the effectiveness of the developed BBB in enhancing ethanol production during heat and oxidative stress. *S. cerevisiae* was pregrown as described in Section 2.1.3 and the immobilised biocatalyst was prepared as described in Section 2.1.4. Supported and unsupported cells of *S. cerevisiae* were additionally exposed to 70 and 90 g L^{-1} of initial bioethanol concentration in fermentation media consisting (g L^{-1}): glucose 70, peptone 20 and yeast extract 10, aiming to assess the potential use of BBB in enhancing the process under ethanol stress. Moreover, the potential stress protective role of BBB to high osmolarity was assessed in experiments conducted by addition of 1 M NaCl to the biomedium.

2.1.9 Repeated bioethanol fermentations of *S. cerevisiae* immobilised on char derived from car tires

Char samples of non-biological origin (NBC) were obtained from CBp Cyprus Ltd (Limassol, Cyprus), producing char and activated carbon from recycled car tires. Powder char (PWC), pellet char (PLC) and unscreened char (UNC) were used as support materials and the respective biocatalysts were prepared through immobilization of *S. cerevisiae* (see Section 2.1.4), which was initially pre-grown in liquid medium as described in Section 2.1.3. Two repeated batch fermentations were conducted at the elevated temperatures of 37, 39 and 41 ºC to evaluate the capacity of the developed biocatalysts in enhancing bioethanol production as compared to the conventional system using fermentation media consisting (g L^{-1}): glucose 70, peptone 20 and yeast extract 10.

2.1.10 Continuous bioethanol fermentations of *S. cerevisiae* in a lab scale bioreactor

Continuous fermentations were conducted in a bioreactor (Minifor, Labda, Brno, Czech Republic) with working volume of 0.3 L (0.45 L total volume) using

freely suspended and immobilised cells of *S. cerevisiae* on UNC. The bioreactor vessel as well as the biomedium were sterilized at 121 ºC for 15 min and the pH-value was controlled at 4.8 in all experiments conducted. The temperature of fermentations was controlled at 37, 39 and 41 ºC, depending on the requirements of each experiment, while the biomedium was not agitated. The feedstock used in continuous experiments consisted of (g L^{-1}): glucose 70, peptone 20, and yeast extract 10. The flow rates and the respective dilution rates used in each experiment are shown in Table 2.1. for free and immobilised cells.

Table 2.1: Dilution rate and flow rate applied during continuous bioethanol fermentations using freely suspended and immobilised cells of *S. cerevisiae*.

Experiment	**Dilution rate [h^{-1}]**	**Flow rate [mL h^{-1}]**
D_1	0.09	27
D_2	0.13	39
D_3	0.17	51
D_4	0.20	60

2.2 Analyses

2.2.1 Characterization of biochar properties

An overview of the structural, physical and chemical characteristics of the biochars prepared in the present study was attempted, aiming to assess their potential use for development of new products and support materials. Thus, the specific surface area of the materials evaluated was determined by N_2 adsorption at 77 K (Brunauer-Emmett-Teller, BET method) and using a multi-point Micromeritics Gemini V System. Samples were pretreated prior to the experiment in a flowing-gas degassing unit for the removal of adsorbed contaminants. Degassing conditions included flowing N_2 gas at 180 °C (453 K) for 12 h [Valanidou et al., 2011].

X-ray diffraction (XRD) was used to probe the crystalline phases within biochar samples. All measurements were performed in a Rigaku Ultima IV diffractometer equipped with a Cu tube and operated at 40 kV voltage and 40 mA current. The system was equipped with a multilayer mirror for parallel X-ray beam geometry and the selected wavelength was the Cu Ka (0.15419 nm). Sample patterns were collected in Bragg-Brentano scanning mode over the 20° − 70° 2-theta range, in a sample holder without rotation [Panagiotou et al., 2018].

The microstructural details of the samples were investigated using a Quanta 200 (FEI, Hillsboro, Oregon, USA) Scanning Electron Microscope (SEM) in various accelerating voltages. All samples were sputter coated with a thin layer of gold (few nm) prior to imaging such as to increase sample's conductivity and prevent surface charging complications. Energy-dispersive X-ray spectroscopy analysis (EDS) was also conducted along with imaging providing information about the elemental composition of the biochars prepared.

2.2.2 Determination of sugars concentration

Depending on the requirements of each experiment two methods (HPLC and DNS) were applied for the determination of sugars concentration. Culture samples were withdrawn aseptically, centrifuged at 13000g for 10 min and filtered using 0.2 μm syringe filters. The concentration of glucose in culture samples was

assessed via the colorimetric method of 3,5-dinitrosalicylic acid (DNS) as described by Miller [Miller, 1959] as well as using High Pressure Liquid Chromatography (HPLC). A Shimadzu Nexera 40 system (Shimadzu, UK) equipped with a Shimadzu RID-20A detector, a Shimadzu SIL-40 C auto sampler and RHM column oven was used. The column was eluted isocratically at a rate of 0.5 mL min^{-1} employing an organic analysis column (Rezex RHM-Monosaccharide H+ (8%) column, Phenomenex, USA) with deionised water at 40 ^{o}C and 10 mL injection volume.

2.2.3 Determination of bioethanol concentration

Bioethanol content was analyzed through Gas Chromatography. A Shimadzu GC-2014 (Shimadzu, Milton Keynes, UK) using a flame ionization detector and a 30 m long Zebron ZB-5 capillary column (Phenomenex, Macclesfield, UK) with 0.25 mm internal diameter was employed. The mobile phase applied was nitrogen, while the stationary phase of the column was 5% phenyl and 95% dimethylpolysiloxane. Ethanol was extracted into hexane by vortexing 1 mL of the filtered sample with 2 mL of the solvent for 1 min. About 1 μL of the extract was injected and the temperature of the column was kept constant at 40 °C for 2.5 min followed by an increase of 30 °C min^{-1} up to 160 °C, while it was maintained at 160 °C for an additional 5 min [Koutinas et al., 2015]. Ethanol concentration was calculated interpolating from a previously established calibration curve and the coefficient of variation for 3 samples was 1.22% at a concentration level of 60 g L^{-1}.

2.2.4 Isolation of total RNA, cDNA synthesis and real-time RT-qPCR

RT-qPCR analysis was performed to determine the mRNA expression level of *HSF1*, *HSP104*, *TPS*, *MSN2*, *MSN4* and *HSP12* genes during *S. cerevisiae* fermentations. Depending on cell density, 1–1.5 mL samples were collected for each time point and centrifuged at 8000 rpm for 10 min at 4 ^{o}C. The cell pellet harvested was soaked in liquid nitrogen and subsequently stored at -80 ^{o}C. Total RNA isolation and cDNA synthesis were performed as previously described [Koutinas et al., 2010]. cDNA synthesis and RT-qPCR were performed using a

SensoQuest labcycler (SensoQuest GmbH, Gottingen, Germany) and qTower3G real-time PCR (Analytik Jena, Jena, Germany) respectively. The primer pairs of each gene analysed are displayed in Table 2.2 (additional data). Triplicate experiments were conducted and two samples were analysed for each replicate comprising analysis of 6 samples in each time point. The 18 S rRNA gene (*RDN18*) was used as housekeeping gene and its expression was employed to normalise the cycle threshold (CT) values of all genes tested (Eqs. 1–3), where CT corresponds to the CT values of *HSF1*, *HSP104*, *TPS*, *HSP12*, *MSN2* and *MSN4* respectively (the relative mRNA expression of each gene was assessed separately), while CT,ref indicates the CT value obtained for *RDN18*. The sample obtained at 0 h of each experiment, was used as calibrator in Eq. 2 to normalize the ΔCT,gene value of each gene at all timepoints assessed. The normalised level of each gene's mRNA expression (NEgene) was calculated using Eq. 3.

$$\Delta C_{T,gene} = C_{T,\,gene} - C_{T,ref} \quad (1)$$

$$\Delta\Delta C_{\,T,gene} = \Delta C_{\,T,gene} - \Delta C_{\,T,gene\,(calibrator)} \quad (2)$$

$$NE_{gene} = 2^{-\Delta\Delta CT,\,gene} \quad (3)$$

2.2.5 Determination of intracellular proline concentration

Aiming to determine the intracellular proline content, 1.5 mL of both immobilised and suspended cells were harvested by centrifugation, washed twice with distilled water and homogenised using 3% aqueous sulphosalicylic acid. The residue was removed by centrifugation at 12000g for 10 min 1 mL of the homogenised material reacted with 1 mL acid-ninhydrin and 1 mL glacial acetic acid in a test tube for 1 h at 100 ^{o}C, while terminating the reaction in an ice bath. The reaction mixture was extracted using 2 mL toluene and maintained at room temperature for 30 min until separation of the two phases was achieved. The chromophore-containing toluene was warmed to room temperature and the optical density was determined at 520 nm using toluene as blank. Proline concentration was determined employing a previously developed standard curve using D-proline [Bates, et al., 1973; Hamid et al., 2003].

2.2.6 Statistical analysis of mRNA expression data

The objective of statistical analysis was to elucidate the relative mRNA expression profile of all genes tested under various stresses. Thus, one-way analysis of variance (ANOVA) was conducted and $p < 0.05$ was defined as acceptable level of significance.

3 Results and Discussion

3.1 Preliminary study of biochar-based biocatalysts for bioethanol production

3.1.1 Biochar production and characterization of immobilization carriers

Pyrolysis process conditions strongly affect the yield, morphology and physicochemical properties of biochar produced [Castilla-Caballero et al., 2023]. Thus, the properties of each specimen tested was determined through XRD, BET surface area, SEM and EDS to evaluate the potential of each biochar-based material for application as carrier for cellular immobilization.

3.1.1.1 XRD analysis of biochar produced

The XRD spectra of NBC and biochars produced at 250 °C and 500 °C from OK, VP, SGR and SS are depicted on Fig. 3.1.1-3.1.2. The XRD patterns of both seagrass samples (Fig. 3.1.1), SGRB250 and SGRB500, demonstrate distinct peaks located at the major crystalline phase present at 27.3°, 31.7°, 45.4°, 56.5° and 66.2°. All aforementioned peaks correspond to halite (NaCl) and remain relatively unchanged independent of the pyrolysis temperature applied. Nevertheless, the XRD patterns of SSB exhibit only a single sharp peak located at 29.4°, which has been assigned to the main and strongest peak (1 0 4) of calcite ($CaCO_3$). Although calcite and quartz are considered as the two major components of sewage sludge [Karamalidis et al., 2008], the latter was not detected in our specimens.

Figure 3.1.2 summarizes the XRD patterns of OKB, VPB and NBC. The XRD spectra of NBC presented peaks from silicon (Si) at 28.4°, 47.3° and 56.1°, as well as calcite ($CaCO_3$) crystallites located at 29.4°, 36.0°, 39.4° and 43.1° respectively. Moreover, the broad “hump” observed between 20° and 30°, centered approximately at 26°, has been assigned to weak diffraction from an amorphous carbon network which is commonly observed in organic samples subject to pyrolysis.

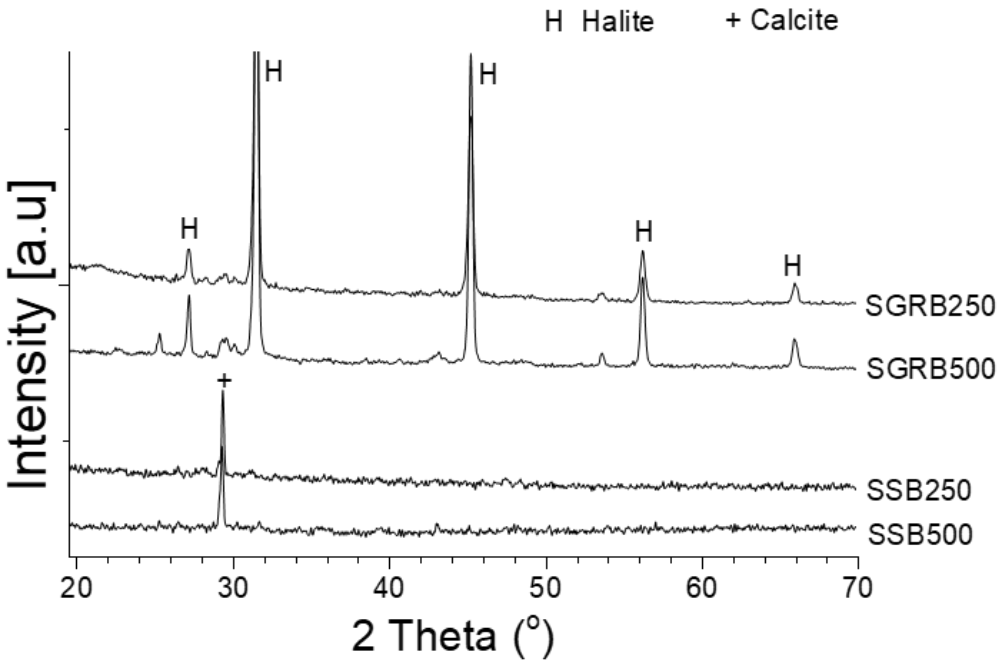

Figure 3.1.1: X-ray diffraction pattern of the biochars produced at 250 °C and 500 °C through the use of SGR and SS.

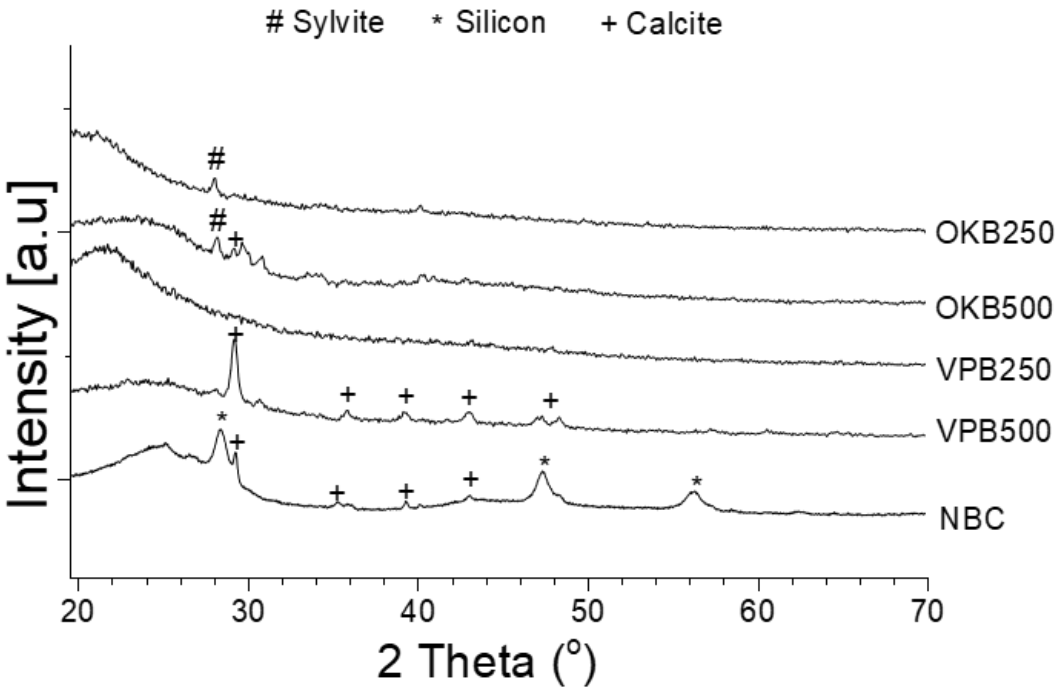

Figure 3.1.2: X-ray diffraction pattern of the biochars produced at 250 °C and 500 °C through the use of OK, VP and NBC.

Sylvite (KCl) was detected in OKB samples produced at both temperatures by the faint peak located at 28.3°. However, although the OKB500 sample (pyrolyzed at higher temperature) exhibited additional peaks, due to poor signal to noise (S/R) ratio and/or small crystallite sizes definitive identification could not be obtained. Both OKB samples exhibited a broad peak between 20° and 30°, centered at approximately 22° for the low temperature sample (OKB250) due to the presence of cellulose, while regarding OKB500 the peak was shifted towards 25-28° resembling a peak from amorphous carbon network [Zhu et al., 2017]. Similar XRD patterns have been previously observed for biochar samples obtained from other renewable feedstocks, such as the formation of calcite in biochar produced from eucalyptus [Singh et al., 2010]. Moreover, the analysis of biochar specimens derived from straws of canola at 300 °C, 500 °C and 700 °C demonstrated that although only sylvite was produced at 300 °C, the increase of pyrolysis temperature resulted in calcite generation [Yuan et al., 2011].

Apart from the broad cellulose peak, the presence of any crystalline phases was not observed in the XRD spectra of VPB250. However, the increase of pyrolysis temperature to 500 °C resulted in crystallization of the calcite phase. Furthermore, the amorphous peak of cellulose was shrunk and shifted towards higher angles demonstrating the conversion to amorphous carbon. The significant crystallization process of the specific sample at 500 °C is expected to increase the specific surface area, since crystallization increases density and subsequent shrinkage can generate cracks and porous within the material. The crystalline mineral phases detected in the biochar samples tested could serve as important factors affecting cell immobilization and culture performance. Calcite crystals provide a safe microenvironment against stressful or hazardous conditions in encapsulated microalgae cultures [Kim et al., 2018] and facilitate flocculation of microalgae enabling easy recovery of the biomass produced following culture completion [Vandamme et al., 2015]. Moreover, immobilization of enzymes on silicon surfaces with high porosity enables significant applications such as decontamination, microbial fuel cells, microreactor healthcare and biological sensing [Létant et al., 2004], demonstrating the potential favorable effect of the

specific crystalline phases when employed as constituents of microbial carriers in ethanol fermentations.

3.1.1.2 BET specific surface area

The effect of pyrolysis temperature on the BET specific surface area of the biochar samples produced is shown in Table 3.1.A. The increase of pyrolysis temperature between 250 °C and 500 °C resulted in increase of the BET specific surface area. All biochars processed at 250 °C exhibited low surface area values. Nevertheless, when pyrolysis was conducted at 500 °C, significant differences between the BET surface areas of the samples were observed. The materials produced from VP and SGR achieved the highest specific surface area that reached 41.7 and 5.3 $m^2 g^{-1}$ respectively, while the BET values of OKB and SSB remained at lower levels (1.5 and 1.4 $m^2 g^{-1}$ respectively). Although NBC demonstrated the highest specific surface area (73 $m^2 g^{-1}$), the aforementioned material constitutes a commercial product incorporating different processing conditions (e.g. pyrolysis temperature, heating rate), and thus, it was applied in the present study for comparison against the renewable feedstocks tested.

Pyrolysis studies of biomass-based feedstocks have previously demonstrated that the resulting surface area of biochar can be low. However, although biochars produced from safflower seed press cake at temperatures between 400 and 600 °C exhibited BET values lower than 4.2 $m^2 g^{-1}$ [Angın, 2003], the specific surface area of VPB at 500 °C was substantially higher. The type of feedstock constitutes an additional important factor demonstrated by the high BET values (376–401 $m^2 g^{-1}$) obtained for hickory wood, bagasse and bamboo at 600 °C [Sun et al., 2014], while optimization of pyrolysis conditions is also crucial considering that the specific surface areas were 30 times higher compared to the values achieved at 450 °C using the same raw materials. Moreover, there is a strong relationship between pyrolysis temperature and the biochar's surface area, which is known to increase at elevated pyrolysis temperatures [Ok et al., 2014]. Thus, similarly to the findings of the present work the specific surface area of biochar produced from SS was enhanced with an increase in pyrolysis temperature from 350 °C to 650 °C, while the porosity can be also improved in higher pyrolysis temperatures [Jindarom et al., 2007].

Table 3.1A: Specific surface area and elemental composition of biochars derived from different feedstocks at 250 °C and 500 °C.

Sample	Temperature (°C)	Specific surface area ($m^2 g^{-1}$)	C (%)	O (%)	Ca (%)	Cl (%)	Si (%)
OKB	250	0.15	61.72	21.42	1.14	0.30	-
	500	1.5	65.73	20.02	2.23	0.64	0.23
VPB	250	0.5	69.62	24.65	3.04	-	-
	500	41.7	71.65	21.59	1.24	-	-
SSB	250	0.7	33.11	34.38	6.30	-	3.48
	500	1.4	55.78	23.47	3.76	-	1.73
SGRB	250	1.9	60.52	24.07	0.61	3.90	0.18
	500	5.3	60.97	22.86	0.6	5.14	-
NBC	-	73.0	88.0	3.16	0.32	0.12	1.26

3.1.1.3 SEM and EDS analyses

The microstructural features of each specimen were evaluated through SEM imaging, while EDS was applied to determine the elemental composition of biochars produced. Observations confirmed the presence of significant differences among the biochar samples produced at each temperature. The morphology of OKB, SGRB and VPB produced at 500 °C (Figure 3.1.3E–G) included formation of smooth surface and porosity. However, the aforementioned biochar samples produced at 250 °C did not demonstrate porosity (Figure 3.1.3A–C), while SSB remained non-porous at both temperatures applied (Figure 3.1.3D and H). Moreover, similarly to the renewable carbonaceous materials formed at 250 °C, no porosity was observed for the commercial NBC tested (data not shown). Thus, SEM analysis confirmed the significant increase of specific surface area which occurs at elevated temperatures for some of the biochars produced (e.g. VPB) highlighting their potential for application in cellular immobilization.

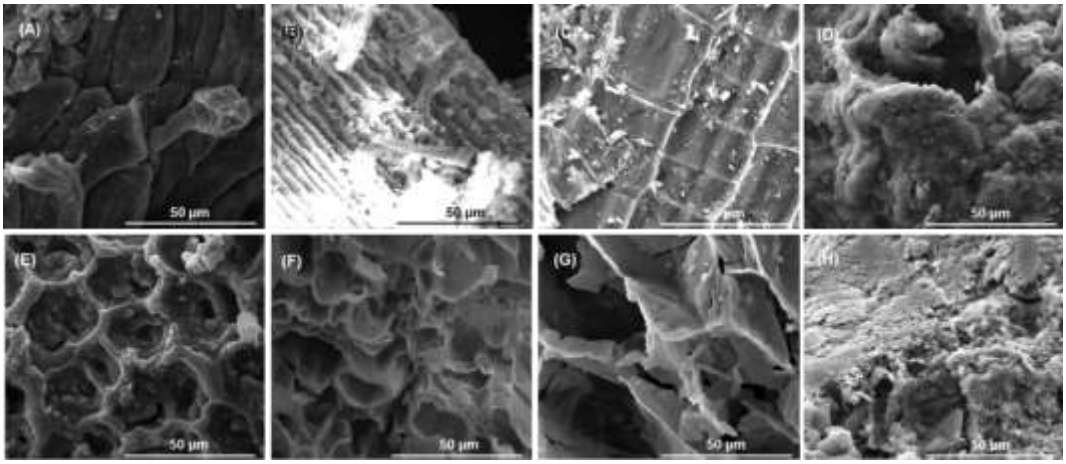

Figure 3.1.3: SEM images of biochar specimens at 3000× magnification. The materials produced using 250 °C comprised: (A) OKB, (B) SGRB, (C) VPB, and (D) SSB. The products formed at 500 °C included: (E) OKB, (F) SGRB, (G) VPB, and (H) SSB.

The elemental EDS analysis of the biochars formed at different pyrolysis temperatures are shown on Table 3.1A. An increase in temperature from 250 °C to 500 °C enhanced the carbon content and reduced that of oxygen in all biochars tested. Thus, increased pyrolysis temperature resulted in more carbonaceous materials, which has been previously demonstrated for other agricultural residues [Fu et al., 2011]. The material exhibiting the highest increase in carbon content was SSB containing 55.8% of carbon at 500 °C, while at the lower temperature carbon remained at 33.1%. Moreover, the specific material exhibited a more pronounced shift in oxygen content, which was reduced from 34.4% to 23.5% between 250 °C and 500 °C respectively. The content of other elements such as calcium, chloride and silicon was also monitored (Table 3.1A) demonstrating that SGRB comprised elevated chloride quantities (5.1% at 500 °C), which could potentially affect the efficiency of the material for biocatalyst development. Overall, the elemental composition of the biochars formed was similar to that of biochar generated from other biomass-based feedstocks including orange peel [Chen and Chen, 2009] and pinewood sawdust [Amutio et al., 2012].

3.1.2 Bioethanol production using freely suspended cells of *S. cerevisiae, K. marxianus* and *P. kudriavzevii*

S. cerevisiae constitutes an industrial workhorse strain for bioethanol production using a wide range of sugar-rich feedstocks [Grellet et al., 2022], while *K. marxianus* is an important bioethanol producer demonstrating elevated growth rate, ability to consume a wide range of sugars and thermotolerance [Tavares et al., 2019]. The latter characteristic, which ensures lower contamination risk and reduced requirements for cooling to maintain fermentation temperature between 25 and 35 °C, is also exhibited by *P. kudriavzevii* KVMP10, a yeast isolated from our research group holding the capacity for elevated bioethanol production from citrus peel hydrolyzates [Koutinas et al., 2015]. Thus, the capacity of these yeasts for bioethanol production at high rates was evaluated through immobilization on biochar. Bioethanol fermentations of the three selected yeasts were initially conducted applying freely suspended cells at two different temperatures (37 and 42 °C) in an attempt to determine suitable fermentation conditions using the media simulating Valencia orange peel hydrolyzate. *S. cerevisiae* produced 51 g L^{-1} of ethanol at 37 °C and 42 g L^{-1} at 42 °C following 40 and 64 h of incubation respectively. The elevated temperature of 42 °C enhanced ethanol production from *K. marxianus* which yielded 46 g L^{-1}, while *P. kudriavzevii* produced 45 g L^{-1}. However, the use of 37 °C reduced biofuel formation from *K. marxianus* and *P. kudriavzevii* producing 39 g L^{-1} and 24 g L^{-1} of ethanol respectively.

The production of ethanol observed was similar to previous studies employing the specific strains in fermentations of citrus peel hydrolyzates [Koutinas et al., 2015]. Thus, the preliminary fermentations conducted using freely suspended yeast cells demonstrate that biofuel production was enhanced at 37 °C in *S. cerevisiae* fermentations, while *K. marxianus* and *P. kudriavzevii* KVMP10 performed elevated ethanol formation at 42 °C. Thus, the capacity of each strain for the development of immobilised biocatalysts was tested at the aforementioned conditions maximizing ethanol formation.

3.1.3 Development and evaluation of immobilised biocatalysts for ethanol production

3.1.3.1 Immobilization of yeasts on selected carriers

Specific surface area constitutes a major factor for the development of immobilised biocatalysts, considering that elevated surface area would enhance the formation of porous structures within biochar, thus controlling the material's capacity for adsorption of nutrients and cell attachment [Sun et al., 2014]. VPB and SGRB produced at 500 °C, as well as NBC, demonstrated the highest specific surface area values holding significant potential for effective immobilization of *S. cerevisiae*, *K. marxianus* and *P. kudriavzevii* KVMP10 for optimal bioethanol production. Therefore, biocatalyst development was evaluated employing the selected materials summarized above. The electron micrographs obtained from fermentations of the three yeast strains following immobilization on each material are depicted on Figure 3.1.4. The results confirmed that the yeasts adhered densely and homogenously to the surface of each carrier, as a result of either physical adsorption by electrostatic forces or due to natural cell entrapment into the porous or covalent binding between the membrane and the support. Moreover, apart from the SEM images presented, effective immobilization was further established by the ability of biocatalysts (following thorough washing to remove free cells) to perform efficiently in repeated batch fermentations as discussed below.

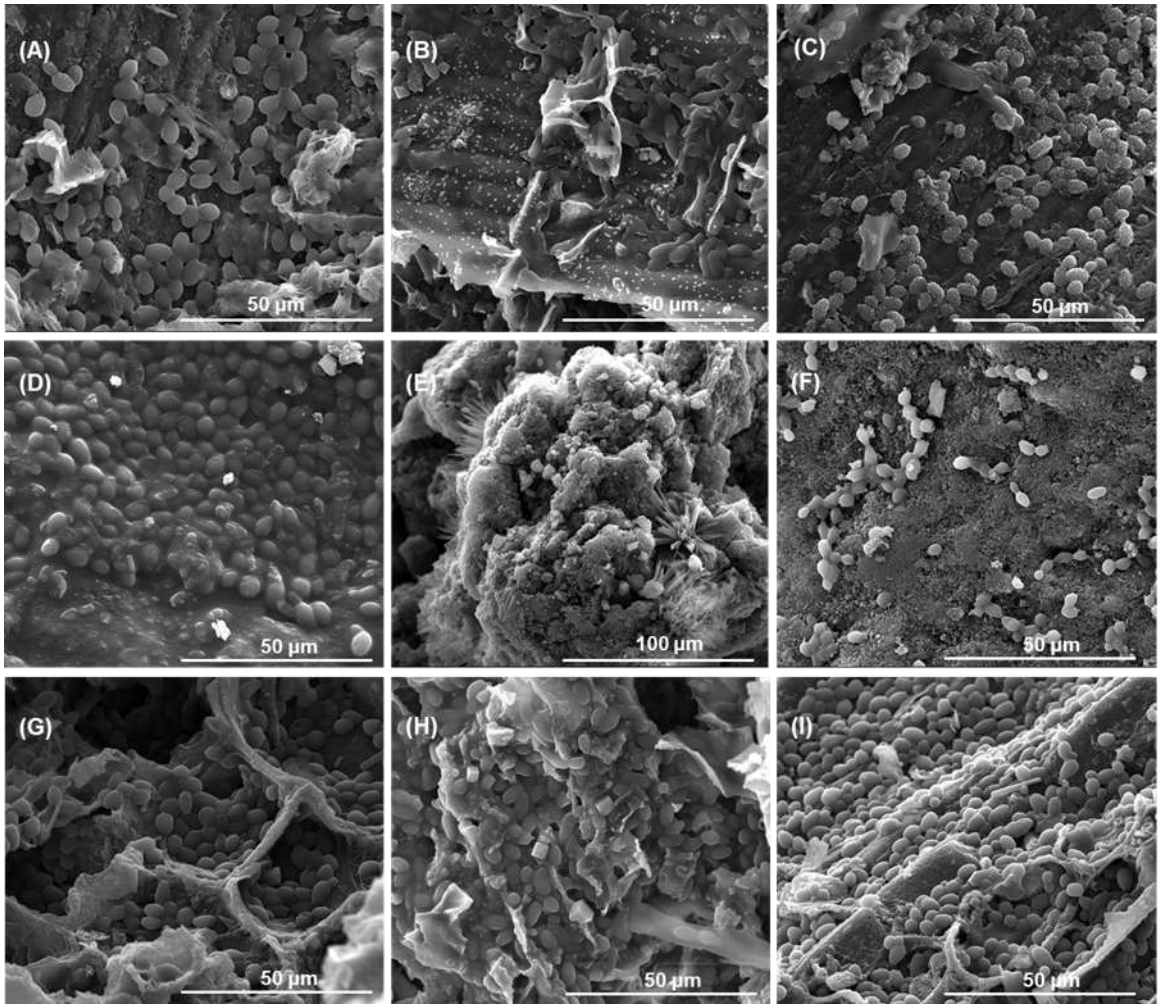

Figure 3.1.4: SEM images of immobilised biocatalysts at 3000× magnification. A) *S. cerevisiae*, B) *P. kudriavzevii* KVMP10, and C) *K. marxianus* cells following immobilization on SGRB obtained at 500 ^{o}C. D) *S. cerevisiae*, E) *P. kudriavzevii* KVMP10, and F) *K. marxianus* immobilised on NBC. G) *S. cerevisiae*, H) *P. kudriavzevii* KVMP10, and I) *K. marxianus* immobilised on VPB obtained at 500 ^{o}C.

3.1.3.2 Repeated batch fermentations of S. cerevisiae for ethanol production

S. cerevisiae immobilised on VPB, SGRB and NBC was employed in two repeated batch fermentations to evaluate the capacity of the developed biocatalysts for enhancing the production of ethanol as compared to freely suspended cells (Figure 3.1.5A-B). During the first batch, the developed *S. cerevisiae*-based biocatalysts employing VPB and NBC achieved faster kinetics as compared to free cells and those immobilised on SGRB. Nevertheless, recycling of the biocatalysts in a subsequent batch demonstrated that cells immobilised on VPB exhibited the highest productivity generating net production of 72 g L^{-1} within 10 h of fermentation, while the NBC-based biocatalyst also promoted net ethanol production reaching 60 g L^{-1} over the same period. The maximum net ethanol concentrations formed using cells immobilised on SGRB and the suspended culture remained at lower levels reaching 48 g L^{-1} and 53 g L^{-1} respectively. Moreover, although cells immobilised on VPB exhibited significantly higher ethanol production over the first 10 h of the second batch experiment, as compared to suspended cells, the consumption of sugars was similar in both fermentations. Thus, higher substrate quantities were potentially utilized by immobilised cells for product formation rather than yeast growth as opposed to the suspended culture. The results presented demonstrate that the VPB-based biocatalyst produced 36% more ethanol compared to the conventional process, serving as an efficient cell carrier that elevates substantially the production of the biofuel, while enabling easy recycling of yeast cells in subsequent batch experiments and improvement of biocatalytic efficiency.

S. cerevisiae constitutes the most widely used yeast for industrial ethanol production based on a number of favorable characteristics which include among others osmotolerant, inexpensive, high ethanol production, low generation of by-products as well as toleration of elevated ethanol and sugar concentration [Grellet et al., 2022]. Thus, numerous studies have previously investigated immobilization of the yeast to other support materials through application of different immobilization techniques [Santos et al., 2018]. *S. cerevisiae* produced 50 g L^{-1} of ethanol from 120 g L^{-1} of glucose in an immobilised cell reactor using calcium alginate as a support [Fu et al., 2011]. The same carrier was employed for ethanol

generation from non-sterilized beet molasses demonstrating maximum production of 53 g L^{-1} through fermentation of 250 g L^{-1} of sugars [Roukas, 1996]. Moreover, Yu et al [2007], reported ethanol production of 96.7 g L^{-1} from 200 g L^{-1} of sugars with the use of *S. cerevisiae* immobilised on natural sorghum bagasse. The results obtained here demonstrate that bioethanol produced from orange peel hydrolyzates through fermentations of *S. cerevisiae* immobilised on biochar-based materials could serve as a future sustainable fuel.

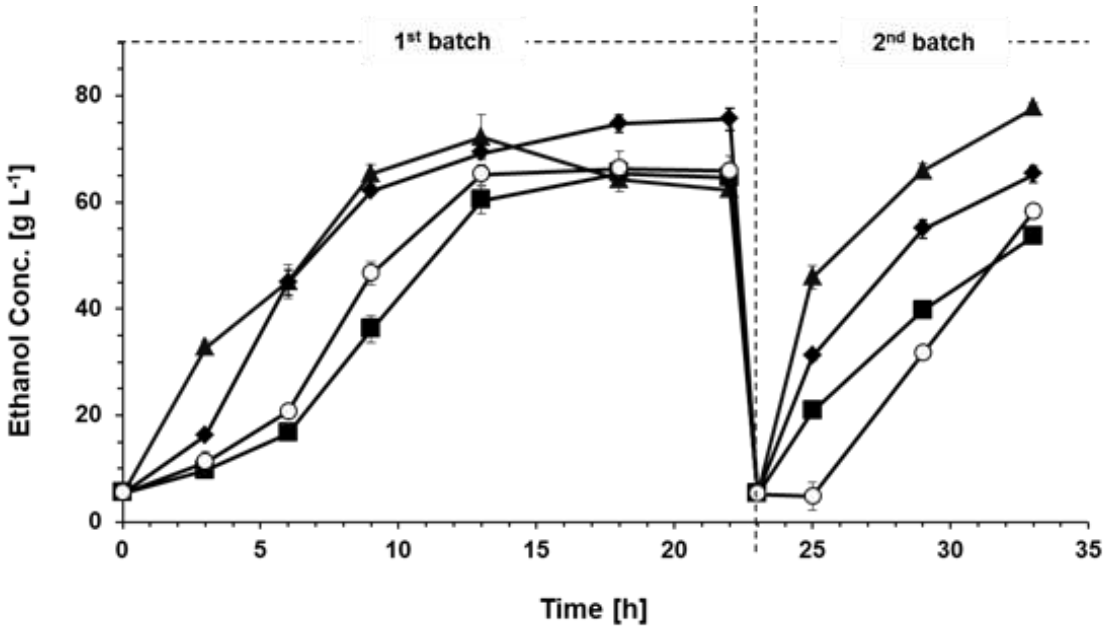

Figure 3.1.5A: Evaluation of *S. cerevisiae* immobilised biocatalysts for ethanol production. Symbols correspond to ethanol concentration in fermentations conducted at 37 ^{o}C employing: i) ▲ : cells immobilised on VPB; ii) ■ : cells immobilised on SGRB; iii) ◆ : cells immobilised on NBC; iv) ○ : freely suspended cells.

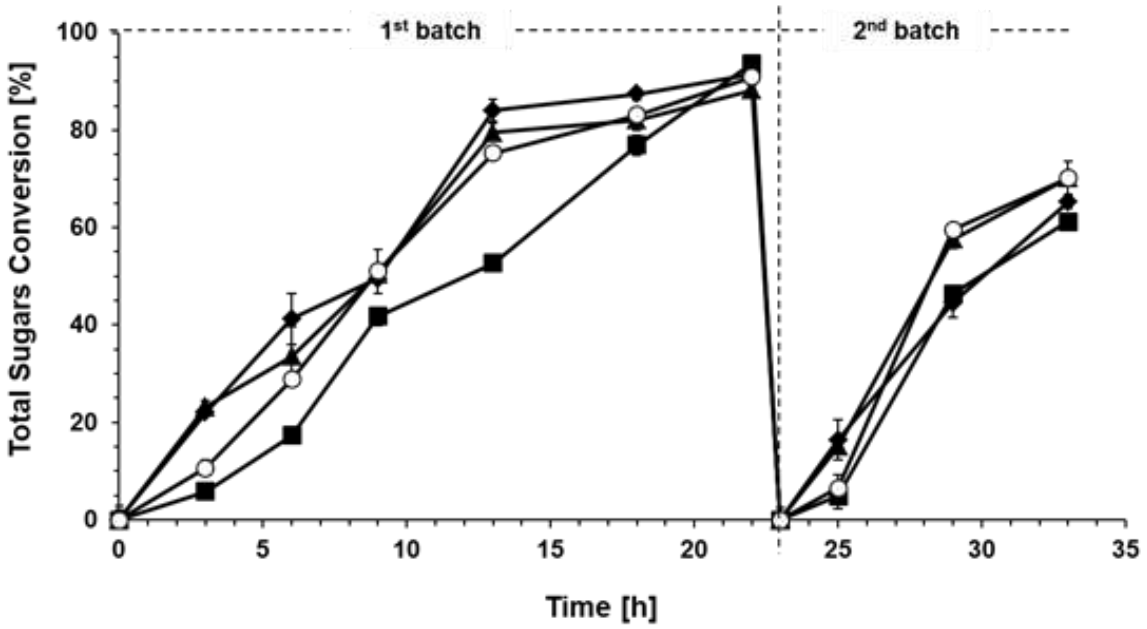

Figure 3.1.5B: Evaluation of *S. cerevisiae* immobilised biocatalysts for ethanol production. Symbols correspond to sugar's concentration in fermentations conducted at 37 ºC employing: i) ▲ : cells immobilised on VPB; ii) ■ : cells immobilised on SGRB; iii) ◆ : cells immobilised on NBC; iv) ○ : freely suspended cells.

3.1.3.3 Repeated batch fermentations of K. marxianus for ethanol production

K. marxianus exhibits thermotolerant properties, low repression by glucose as well as the capacity to utilize hemicellulolytic hydrolyzates [Dhiman et al., 2017]. Based on these technological advantages a series of investigations have been conducted for ethanol production applying *K. marxianus* usually through supplementation of lactose, while delignified cellulose [Kourkoutas et al., 2002] and sodium alginate [Guo et al., 2010] constitute examples of carriers successfully used for bioprocess improvement. Herein, the yeast was immobilised on VPB, SGRB and NBC for production of the biofuel from citrus peel hydrolyzates in two repeated batch experiments, while a suspended culture was also conducted for comparison purposes (Figure 3.1.6A and B).

During the first batch the performance of VPB- and SGRB-based biocatalysts were not evidently different as compared to suspended cells, both with respect to biofuel production and sugars consumption. However, *K. marxianus* immobilised on VPB significantly enhanced net ethanol production, which reached 73 g L^{-1} (52% higher compared to free cells) following 10 h of fermentation in the repeated batch experiment. Although the NBC-based biocatalyst generated net production of 56 g L^{-1} as compared to the 48 g L^{-1} formed by freely suspended cells at 10 h, the kinetics of the two experiments were not significantly different in the second batch. Net biofuel production using cells attached to SGRB remained at 43 g L^{-1}, demonstrating that similarly to the use of VPB for *S. cerevisiae* immobilization the specific biochar-based carrier could be efficiently applied for the development of advanced biocatalysts employing *K. marxianus*.

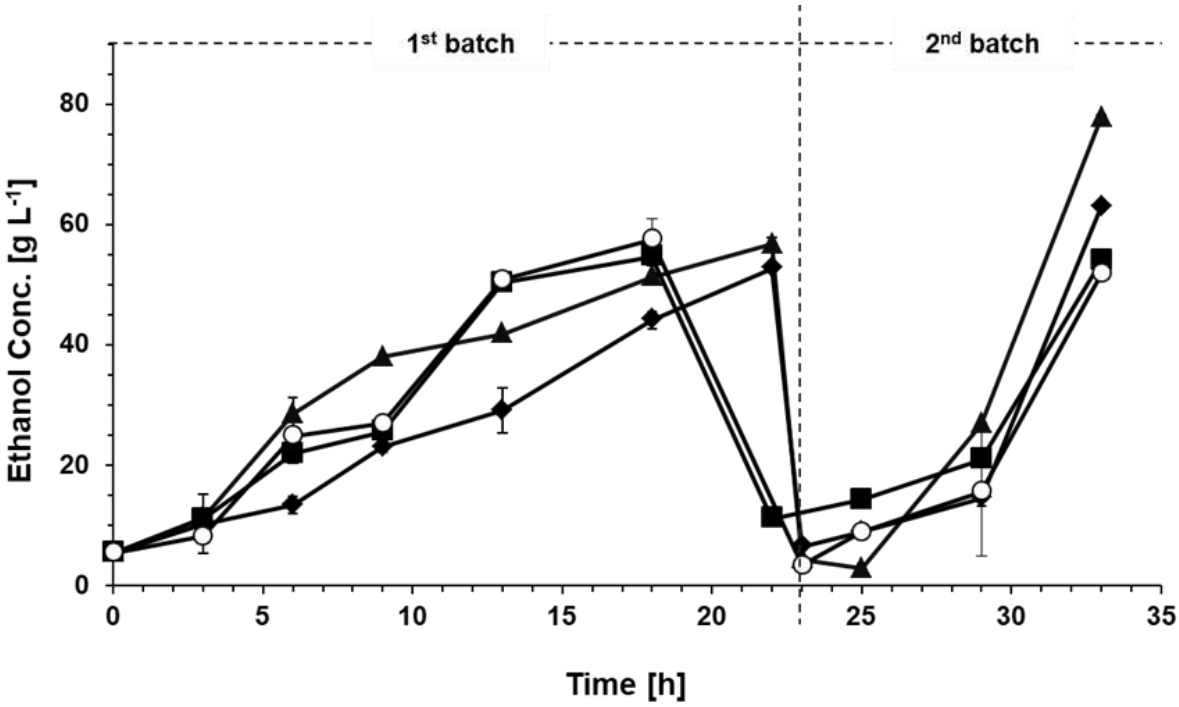

Figure 3.1.6A: Evaluation of *K. marxianus* immobilised biocatalysts for ethanol production. Symbols correspond to ethanol concentration in fermentations conducted at 42 ^{o}C employing: i) ▲ : cells immobilised on VPB; ii) ■ : cells immobilised on SGRB; iii) ◆ : cells immobilised on NBC; iv) ○ : freely suspended cells.

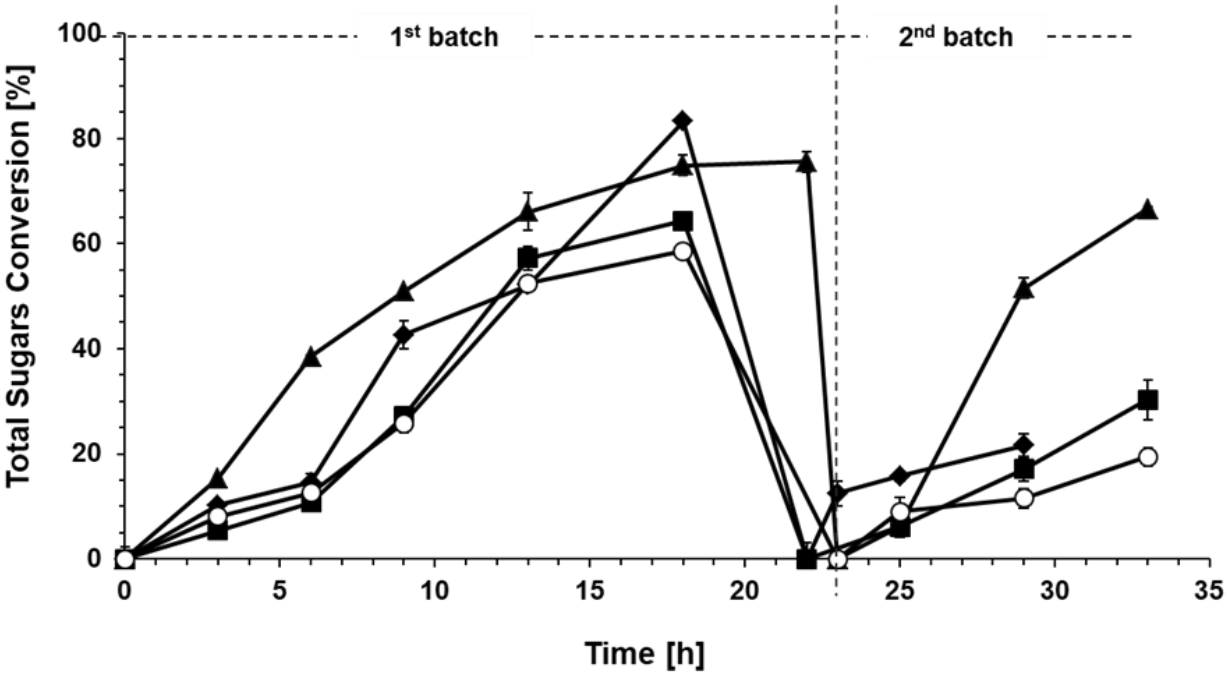

Figure 3.1.6B: Evaluation of *K. marxianus* immobilised biocatalysts for ethanol production. Symbols correspond to sugar's concentration in fermentations conducted at 42 ^{o}C employing: i) ▲ : cells immobilised on VPB; ii) ■ : cells immobilised on SGRB; iii) ◆ : cells immobilised on NBC; iv) ○ : freely suspended cells.

3.1.3.4 Repeated batch fermentations of P. kudriavzevii for ethanol production

P. kudriavzevii exhibits multiple types of tolerance against extreme conditions during alcoholic fermentation, including tolerance towards elevated temperatures and acidic conditions [Nieto-Sarabia et al., 2022;Seong et al., 2017]. Thus, *P. kudriavzevii* KVMP10 was applied as a third technologically important yeast in alcoholic fermentations of orange peel hydrolyzates employing immobilised cells on NBC, VPB and SGRB, as well as suspended cultures in repeated batch experiments (Figure 3.1.7A-B). Nevertheless, the developed immobilised biocatalysts could not enhance ethanol formation as compared to free cells demonstrating that not all yeast strains could be efficient in the bioprocess proposed. Similarly to the present work, immobilised cells of *S. cerevisiae* and *P. kudriavzevii* into poly(vinyl alcohol) hydrogel lens-shaped particles have been previously compared for their capacity to increase bioethanol generation from waste paper, demonstrating that *S. cerevisiae* was better in biofuel production maintaining higher levels of metabolic activity in repeated batch experiments [Zichová et al., 2017]. The reduced performance of *P. kudriavzevii* observed in the present work could be potentially attributed to various alterations that may occur in the physiology of immobilised cells as well as restricted mass transfer and reduced water activity, comprising significant stresses that cells often need to overcome during attachment on different carriers [Verbelen et al., 2006].

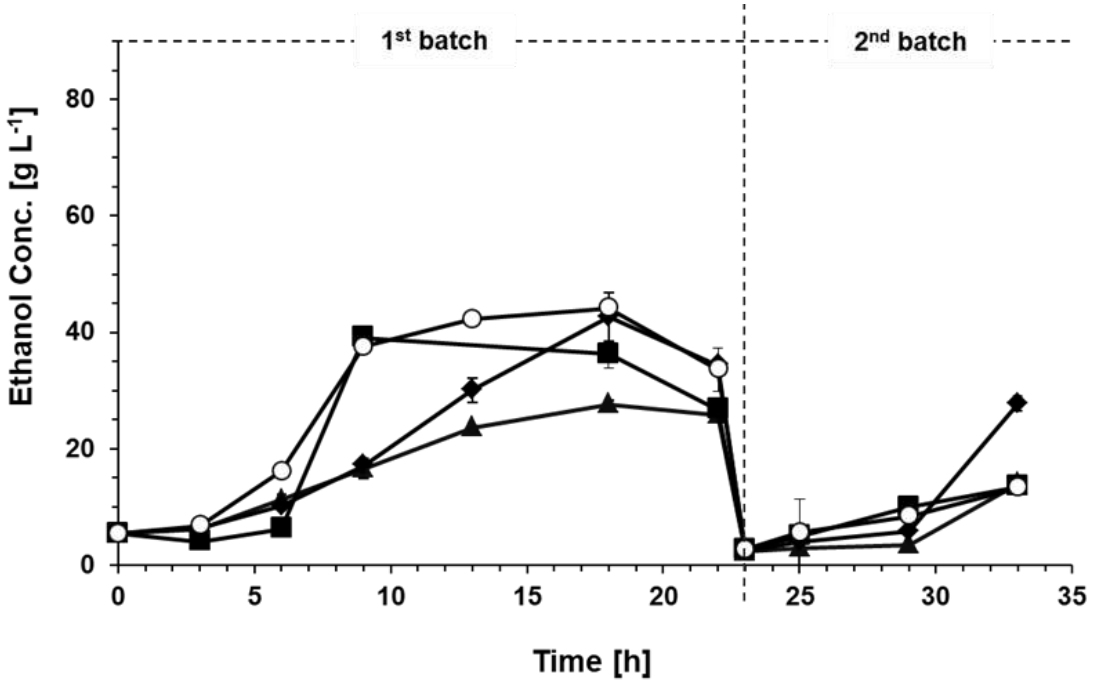

Figure 3.1.7A: Evaluation of *P. kudriavzevii* immobilised biocatalysts for ethanol production. Symbols correspond to ethanol concentration in fermentations conducted at 42 ^{o}C employing: i) —▲— : cells immobilised on VPB; ii) —■— : cells immobilised on SGRB; iii) —◆— : cells immobilised on NBC; iv) —○— : freely suspended cells.

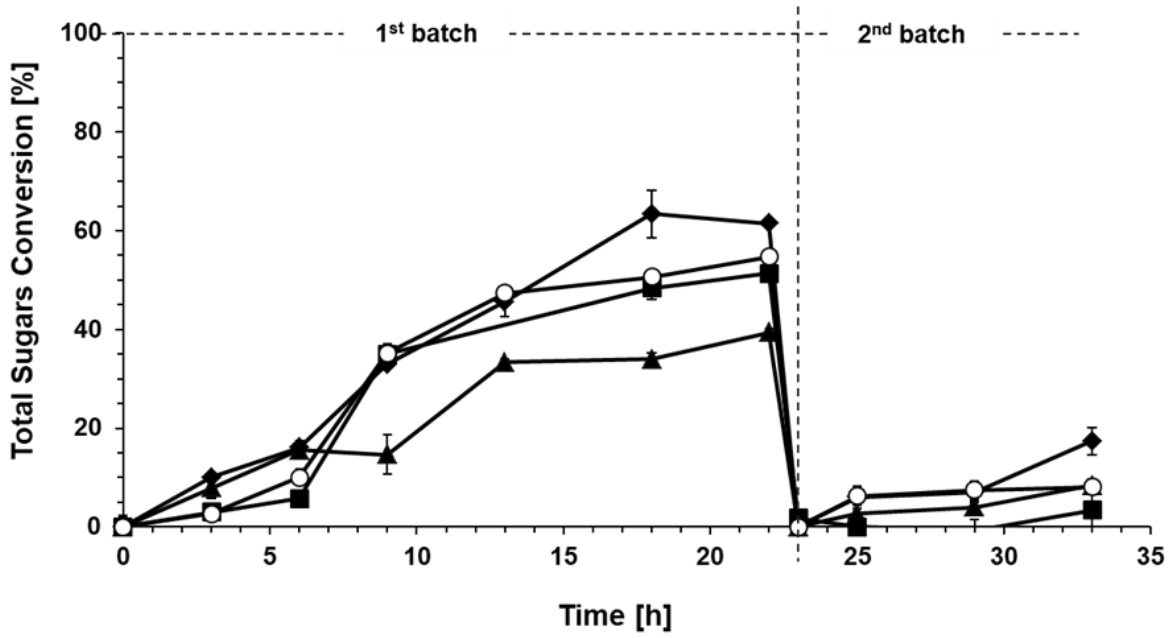

Figure 3.1.7B: Evaluation of *P. kudriavzevii* immobilised biocatalysts for ethanol production. Symbols correspond to sugar's concentration in fermentations conducted at 42 ^{o}C employing: i) —▲— : cells immobilised on VPB; ii) —■— : cells immobilised on SGRB; iii) —◆— : cells immobilised on NBC; iv) —○— : freely suspended cells.

3.1.4 Critical aspects for the use of biochar in biofuel production

Traditional alcoholic fermentation systems utilize suspended cells in batch bioreactor operation. However, continuous ethanol fermentations provide, among other advantages, elevated conversion and fermentation rates as well as environmental merits. Immobilization of yeasts on different carriers offer recycling of the biocatalyst in continuous systems enabling high cell densities, enhanced productivity, improved stability of cells and economic benefits [Zichová et al., 2017]. Biochar has been previously investigated in industrial biotechnology for cell and enzyme immobilization due to its affordability, high porosity, presence of functional groups on its surface, thermal stability and large surface area [Kaur et al., 2021;Jenjaiwit et al., 2021]. The use of enzyme immobilised on biochar has been a potential approach for the removal of contaminants. Pine wood, pig manure and almond shell biochar have been demonstrated as excellent sorption material for immobilization of crude laccase towards diclofenac degradation [Lonappan et al., 2018]. Additionally, lipase immobilised on biochar impregnated with calcite enhanced the yield of fatty acid methyl esters and increased the reusability leading to efficient production of biodiesel [Almeida et al., 2020]. However, most investigations have focused on the use of biochar as microbial or enzyme support to tackle environmental stresses and cell washout as well as improve contaminant removal efficiency [Pandey et al., 2020]. The biocatalyst proposed, constitutes the first attempt to our knowledge for whole-cell immobilization in industrial biotechnology for the enhancement of bioethanol production. *S. cerevisiae* immobilised on VPB exhibited the highest ethanol production as compared to the rest of the microorganisms tested, while the results obtained via the VPB-based biocatalyst using *K. marxianus* were also promising. Thus, considering the major industrial significance of *S. cerevisiae* and the applicability of *K. marxianus* as a lactose fermenting yeast [Verbelen et al., 2006] the technology proposed could offer an advanced technological solution to sustainable manufacturing of the biofuel.

The efficiency of different immobilised biocatalysts employing *S. cerevisiae* in bioethanol production is compared in Table 3.1.4. The productivity of ethanol achieved with the use of *S. cerevisiae* immobilised on NBC and VPB reached 6.0 g L^{-1} h^{-1} and 7.2 g L^{-1} h^{-1} respectively constituting substantially higher

values compared to other carriers employed using similar feedstocks. Moreover, although initial sugar concentration was lower compared to other studies, substantially high ethanol concentrations were achieved (ranging between 60 and 72 g L^{-1} for *S. cerevisiae* and *K. marxianus*) demonstrating the beneficial use of the novel approach. The literature studies presented on Table 3.1.4. incorporated fermentation temperatures that ranged between 30 and 33 °C. Thus, the elevated temperatures applied in the current work (37 °C and 42 °C for *S. cerevisiae* and *K. marxianus* respectively) constitute another advantage of the bioprocess enabling the reduction of operational costs due to decreased energy use for cooling and lower contamination risk. Although *K. marxianus* constitutes a promising yeast for efficient ethanol production at elevated temperatures (between 38 and 45 °C) [Sene et al., 2023], the strain includes lower tolerance in ethanol concentrations as compared to *S. cerevisiae*, which limits the production of the biofuel leading to high energy demand in the fuel-ethanol production plant [Li et al., 2018]. Moreover, the prospect of yeast reusability enabled through immobilization of cells on biochar could significantly enhance the overall economics as well as the whole process offering new prospects for instrumentation and control [Mulko et al., 2016]. Herein, high concentrations of ethanol were produced by *K. marxianus* cells immobilised on VPB (net ethanol production reached 73 g L^{-1}) and increased biofuel productivities were achieved at the second batch following the recycling of yeast cells. The specific results indicate that the technology proposed could be attractive for conducting high temperature fermentations and to test the stability of long-term bioprocess operation by biomass recycling of two major yeast strains. Therefore, future research is required towards the aforementioned directions.

The specific surface area of VPB (41.7 m^2 g^{-1}) was significantly higher than that of SGRB (5.3 m^2 g^{-1}) potentially enhancing yeast immobilization. However, although NBC involved higher specific surface area (73 m^2 g^{-1}), VPB was more efficient as cell carrier exemplifying that other parameters of the material could potentially affect the metabolic properties of the yeast. As previously stated in Section 3.1.2, the specific surface area of biochar is usually low and thus, different approaches have been proposed for biochar modification to improve the specific parameter including addition of magnesium and carbon activation [Li et al., 2017].

Although activated carbon has been extensively applied as immobilization carrier for different applications, the cost related to carbon activation elevates the overall investment [Bailey et al., 1999]. Nevertheless, the specific surface area of VPB was relatively high compared to other biochar materials, while activation was not employed in an attempt to reduce the cost required for biocatalyst development.

Strategies for mitigating global warming employ carbon sequestration, which includes forestation and reforestation, innovative technologies (such as underground geological and ocean CO_2 fixation) and use of carbonaceous materials for long term carbon storage [Yusuf and Ibrahim, 2023]. Moreover, biochar constitutes a common renewable solid biofuel [Awogbemi and Von Kallon, 2023], while bioethanol from biomass (e.g. sugars, starch, lignocellulosics and algae) plays a crucial role as a supplement/substitute for petroleum fuels [Ok et al., 2016]. Thus, the use of biochar as a low-cost cell carrier in ethanol fermentations could upgrade biofuel production processes offering more stable performance [Zhang et al., 2016] and biomass recycling [Dhiman et al., 2017], while eliminating yeast inhibition [Kirdponpattara and Phisalaphong, 2013]. Considering that biochar is generated from biowaste, the current approach employing the material to enhance the productivity of ethanol bioprocesses enables integration of thermal and biological methods targeting the manufacture of commodities with increased added-value, lowering the environmental impact of industrial production [Martínez et al., 2018]. Moreover, even though thermal methods often involve increased energy demand, no additional fuel is required for pyrolysis exhibiting energy self-efficiency [Cong et al., 2018]. Therefore, the combination of biofuel production with pyrolysis is expected to enhance energy gains constituting a highly novel approach for biowaste reduction [Khosla et al., 2017]. Thus far, efforts to combine pyrolysis and fermentations have been attempted mainly in biorefineries using the thermal method either for biomass pretreatment or for the refinement of biorefinery residues [Luque et al., 2014]. The application of biochar as immobilization carrier for microbial cells constitutes a novel use of this stable by-product generated from biowaste.

The redox properties of biochar have been shown to promote biological activity and the formation of biofilms acting as significant electron acceptors or

donors [Prévoteau et al., 2016]. However, the addition of external electron acceptors in alcoholic fermentations is known to substantially boost enzymatic activity [Dimarogona et al., 2012] and ethanol yield, which was increased from 0.62 mol ethanol/mol xylose to 1.35 mol ethanol/mol xylose following acetoin addition, doubling at the same time the specific ATP production without any increase in *S. cerevisiae* biomass content [Wahlbom and Hahn–Hägerdal, 2002]. Thus, a potential cause for the elevated ethanol productivity achieved in the present study could be attributed to the quantity and type of electron accepting and donating units within biochar.

Table 3.1B: Bioethanol production with the use of immobilised yeast cells.

Yeast strain	Feedstock	Method	Carrier	Ethanol conc. [g L^{-1}]	Ethanol productivity [g L^{-1} h^{-1}]	Specific surface area [m^2 g^{-1}]	Reference
S. cerevisiae	Sugar molasses	Cross-linking and covalent binding	Alginate-based MCM-41 mesoporous zeolite composite	78.6	6.55	-	Zheng et al., 2012
S. cerevisiae M30	Cane molasses	Cross-linking	Bacterial cellulose-alginate sponge	92	1.92	-	Kirdponpattara et al., 2013
Mutant baker's yeast 3013	Glucose and sucrose	Adsorption	Sorghum bagasse	92.7	5.72	3.0-5.0 [Yan et al., 2018]	Mohd Azhar et al., 2017
S. cerevisiae MTCC 174	Sugarcane bagasse	Adsorption	Sugarcane bagasse	15.4	0.43	3.0-12.7 [Sharma et al., 1994]	Singh et al., 2013
S. cerevisiae M30	Blackstrap molasses	Adsorption	Thin-shell silk cocoon	80.6	1.85	-	Rattanapan et al., 2011
S. cerevisiae DTN	Sugar beet thick juice	Adsorption	Sugar beet pulp	52.3	1.09	3.0-16.5 [Sharma et al., 1994]	Vučurović et al., 2012
S. cerevisiae NP 01	Sorghum juice	Adsorption	Sweet sorghum stalks	98.5	1.37	3.0-5.0 [Yan et al., 2018]	Ariyajaroenwong et al., 2012
S. cerevisiae CTCRI	Mahula flower	Entrapment	Calcium alginate	25.8	0.27	-	Behera et al., 2010

S. cerevisiae var. *ellipsoideus*	Corn meal	Entrapment	Calcium alginate	88.9	2.34	-	Behera et al., 2010
S. cerevisiae T0936	Wheat straw	Entrapment	Calcium alginate	37.1	0.38	-	Ishola et al., 2015
S. cerevisiae	Glucose	Cross-linking and covalent binding	Mineral Kissiris	48	3.06	2.2 [Kana et al., 1989]	Mohd Azhar et al., 2017
S. cerevisiae	Molasses	Cross-linking and covalent binding	Orange peel	58.9	4.17	0.4 [Kratchanova et al., 2004]	Plessas et al., 2007
S. cerevisiae	Orange peel waste hydrolysate	Cross-linking and covalent binding	NBC	60	6.0	73.0	Current study
S. cerevisiae	Orange peel waste hydrolysate	Cross-linking and covalent binding	VPB	72	7.2	41.7	Current study
K. marxianus	Orange peel waste hydrolysate	Cross-linking and covalent binding	NBC	56	5.6	73.0	Current study
K. marxianus	Orange peel waste hydrolysate	Cross-linking and covalent binding	VPB	73	7.3	41.7	Current study

3.2 Bioethanol overproduction via whole-cell immobilization at elevated temperatures: Application in a citrus peel waste biorefinery

3.2.1 Biochar production and characterization of immobilization carriers

Following the development of BBB, the optimization of the developed biocatalysts was investigated using different promising feedstocks for the production of the support material that are expected to contribute distinctive physicochemical properties including increased specific surface area, the presence of a range of surface functional groups and rich pore structure.

3.2.1.1 XRD analysis of biochar

The XRD patterns of all materials, acquired before and after pyrolysis at 500 °C, are presented in Figure 3.2.1A-B. PV and AH showed a broad peak centered at ~21° 2theta and a weaker one at ~15°, that can be assigned to the crystalline planes (101) and (200) of cellulose. Beyond that no other major crystalline phases were detected apart from a small quantity of NaCl (Halite) in PV.

Following application of pyrolysis, only AHB demonstrated clear diffraction peaks which are assigned to $CaCO_3$ (Calcite) and KCl (Sylvite). The process of pyrolysis (Figure 3.2.1B) eliminates both peaks (at 15° and 21°) for samples PVB and AHB and a new broader one appears at 2θ = 23 - 24°, characteristics consistent with the amorphization and gradual decomposition of cellulose with temperature. As reported in the literature [Liang et al., 2018] the initial semicrystalline cellulose goes through a densification stage and hydrogen bond removal until 325 °C where the main stage of pyrolysis occurs. At this stage all ordered structures of cellulose disappear. At temperature values higher than 350 °C, aromatic carbons form and the broad peak at 2θ = 23 - 24°can be assigned to their stacking. Similar XRD patterns have been detected in carbonaceous materials obtained from other biomass-based feedstocks, including the presence of calcite in biochars formed from vineyard prunings and eucalyptus [Chapter 3.1;Singh et al., 2010]. Moreover, the presence of the distinct sharp peak of crystalline cellulose was

also observed in biochar produced from switch grass [Kumar et al., 2011]. The absence of the crystal cellulosic structure in the biochars tested confirmed that cellulose mainly decomposed in the specific samples forming amorphous components.

CR also demonstrates a peak around 21° 2theta (Figure 3.2.1A) which relates to a natural biopolyester, regularly found in the cell walls of plants and abundant in cork oak (particularly the *Quercus suber* species), called suberin. The crystal structure of suberin is quite complex and usually its pattern is reported in the literature after depolymerization [Sousa et al., 2016]. Following pyrolysis, the CRB sample continues to exhibit a broad peak, with a minor reduction in FWHM and a shift towards lower diffraction angles, around $2\theta = 20°$ (Figure 3.2.1B). These changes indicate that pyrolysis at 500 °C did not significantly affect the crystalline structure of cork samples, consistent with the relative stability of suberin at high temperatures.

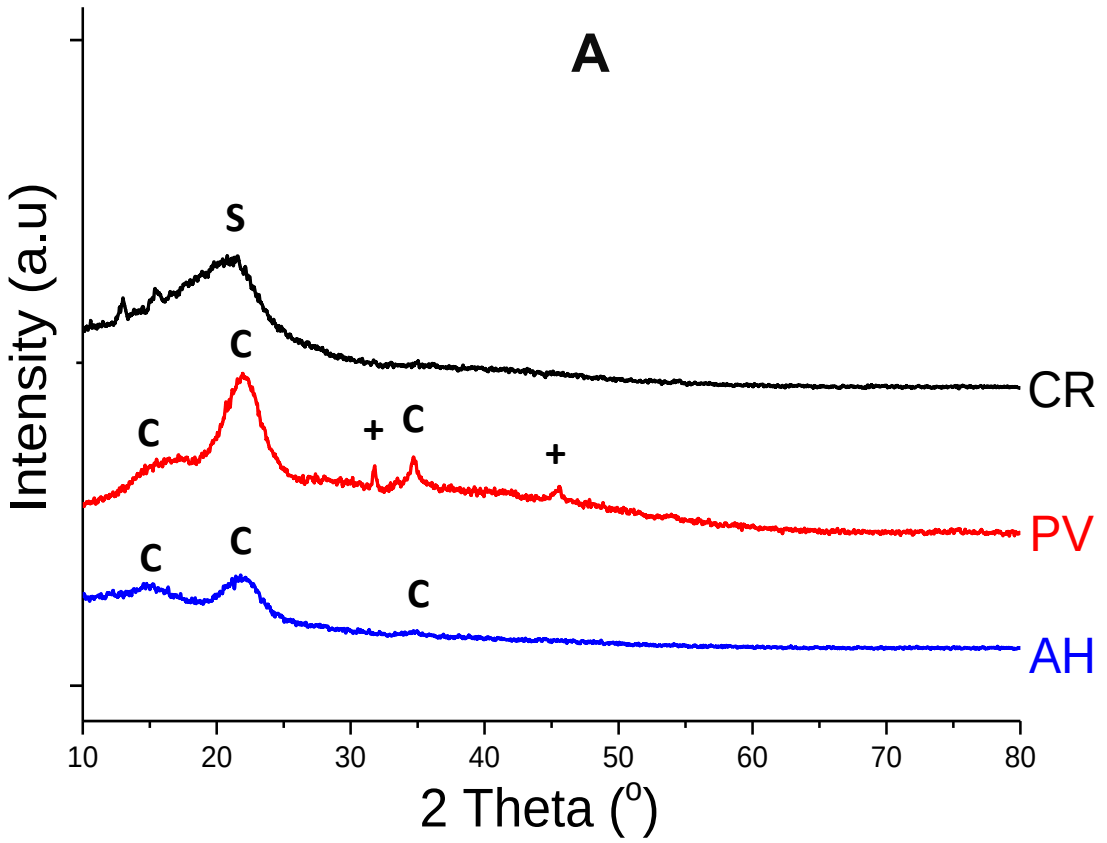

C cellulose; + Halite (NaCl); S Suberin; # Sylvite (KCl); * Calcite ($CaCO_3$)

Figure 3.2.1A: X-ray diffraction pattern of raw materials (CR, PV and AH).

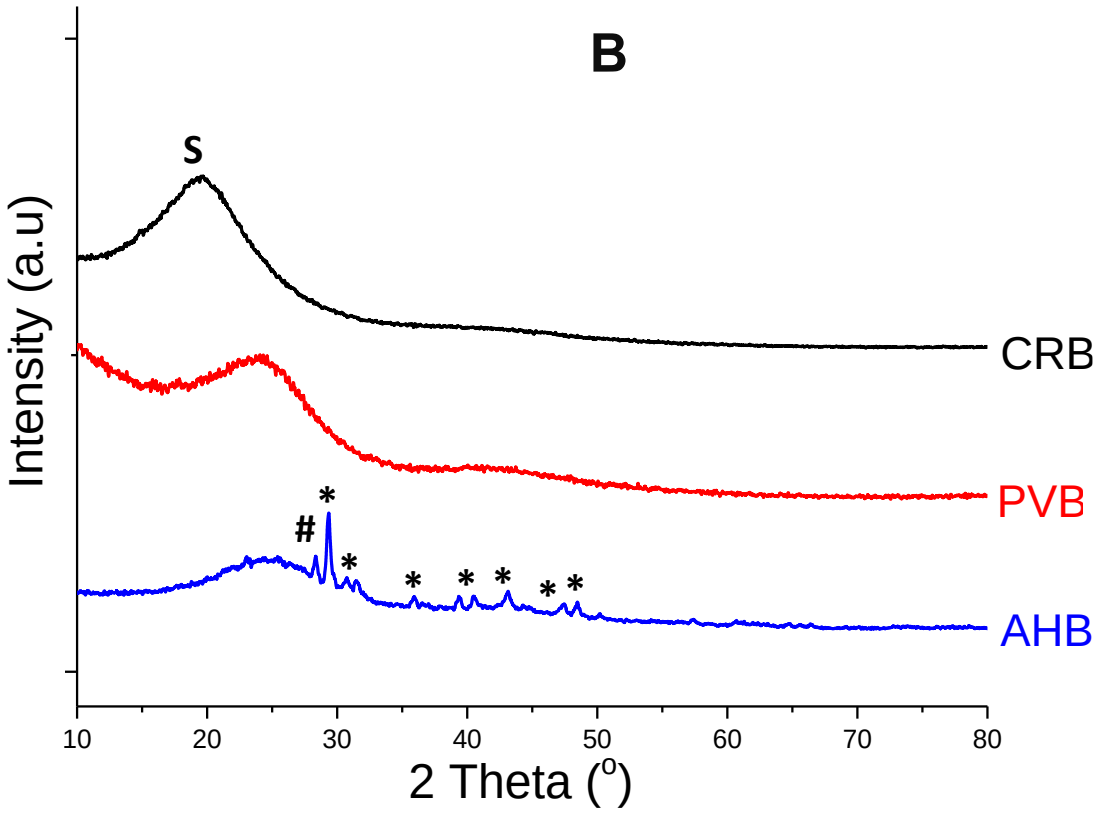

C cellulose; + Halite (NaCl); S Suberin; # Sylvite (KCl); * Calcite ($CaCO_3$)

Figure 3.2.1B: X-ray diffraction pattern of biochars produced (CRB, PVB and AHB).

3.2.1.2 EDS and SEM analyses of biochar

Different morphological and microstructural properties of the various biochar materials produced were evaluated using SEM. SEM images of PVB, AHB and CRB specimens are shown in Figure 3.2.2A-C respectively demonstrating a relatively open structure with pores, but with significant differences among them. The morphology of PVB (Figure 3.2.2A) constitutes a relatively dense network of interconnected porous with no apparent orientation between them, while from the cross section shown the pore diameters range between 1 and 10 mm. Although AHB (Figure 3.2.2B) incorporates similar microstructural characteristics to PVB, its porous are aligned to each other forming a parallel tubing system. In contrast to the aforementioned samples, CRB (Figure 3.2.2C) presents a very low density microstructure, with large pore opening and very thin pore walls. The diameter of pores ranges between 10 and 50 mm and the thin walls of the material comprise folds, crevasses and alcoves which could serve as a promising matrix for cell adhesion.

EDS was conducted to decipher the composition of biochar specimens in different elements, which is presented in Table 3.2. Due to the pyrolysis process and the increased temperature applied, carbonaceous materials with reduced oxygen content were formed. The material exhibiting the highest carbon content was PVB containing 83.2% of carbon, while oxygen remained at 14.0%. AHB and CRB demonstrated similar composition to PVB in terms of carbon and oxygen. Moreover, the content of other elements monitored included calcium, chloride, sodium, magnesium, sulfur, potassium and nickel exhibiting that AHB contained a larger amount of trace elements.

Various studies have focused on analysis of the physicochemical properties of biochar demonstrating favorable physical and chemical characteristics including elevated specific surface area as well as porosity [Lou et al., 2019]. Results presented, confirmed the formation of smooth and porous surface of biochars was produced from different biological feedstocks using the same temperature of pyrolysis, while the overall composition of the products formed included lower oxygen and higher carbon contents. Moreover, biochars derived from rice straw, sawdust and eggshell incorporated high porosity as well as lower carbon content as

compared to the materials tested here, which were produced under the same pyrolysis conditions [Xu et al., 2019]. However, the carbonaceous specimens formed using soybean and peanut shell demonstrated similar elemental composition to PVB, AHB and CRB [Ahmad et al., 2012].

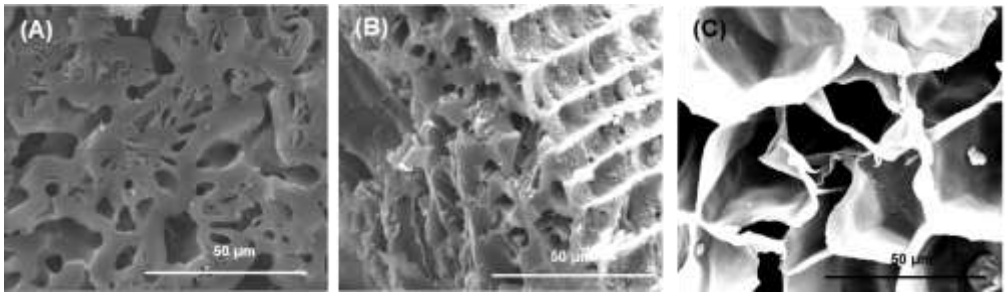

Figure 3.2.3: SEM images of biochar specimens. The samples analyzed comprised: (A) PVB, (B) AHB and (C) CRB, at 3000× magnification.

Table 3.2: Elemental composition of PVB, AHB and CRB.

Sample	C (%)	O (%)	Ca (%)	Cl (%)	Na (%)	Mg (%)	K (%)
PVB	83.17	13.97	0.36	-	-	-	0.66
AHB	80.58	12.95	-	0.43	0.57	0.51	2.25
CRB	78.57	13.21	-	-	-	0.33	-

3.2.2 *Saccharomyces cerevisiae* immobilization on biochar-based support materials

Biocatalyst development was evaluated employing PVB, AHB and CRB. All carbonaceous materials formed demonstrated porosity, constituting an important parameter for effective immobilization of the yeast to enhance ethanol production. The porous structure of the biochars produced was composed of two levels: (a) the nanoscale level (<100 nm) and (b) the micrometer level (1-100 mm). The micrometer level connected porosity achieved is of great importance for cell immobilization providing additional surface area accessible to the yeast, which possesses characteristic dimensions in the order of ~1 mm. The dimensions of cells are depicted on the electron micrographs derived from the BBBs applied in alcoholic fermentations shown on Figure 3.2.4. The images demonstrate that *S. cerevisiae* was attached and entrapped to the surface and porous of PVB, AHB and CRB, potentially due to physical adsorption or covalent bonding formed among the carrier and the cell membrane. Thus, apart from the results obtained through SEM, the efficient attachment of *S. cerevisiae* to each support as well as the capacity of the developed BBBs to enhance ethanol production was confirmed in fermentations as presented below.

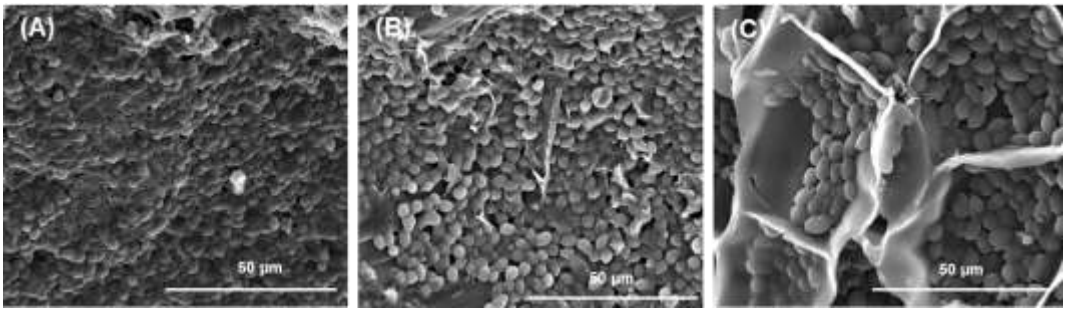

Figure 3.2.4: SEM images of developed immobilised biocatalysts. (A) PVB, (B) AHB and (C) CRB, at 3000× magnification.

3.2.3 Assessment of different parameters affecting the performance of BBB

Various critical parameters that potentially impact the performance of BBBs were explored aiming to enhance the performance of the bioprocess proposed. Thus, the adsorption capacity of the support material for the substrate and the product as well as particle size, temperature and efficiency of biomass recycling were tested during fermentations to advance ethanol production towards sustainable manufacturing.

3.2.3.1 Adsorption capacity of biochar for ethanol and sugars

The effect of PVB in product and substrate adsorption was tested at ethanol and sugar concentrations that ranged between 10 and 80 g L^{-1} and 20-100 g L^{-1} respectively (Figure 3.2.5A-B). The ethanol adsorption capacity of PVB increased significantly by increasing the dosage of the specific biofuel reaching a maximum of 0.17 g g^{-1}, while in concentrations higher than 60 g L^{-1} biochar was saturated and ethanol was not further adsorbed. A similar trend was monitored in the presence of sugars where the maximum adsorption capacity reached 0.16 g g^{-1} using 40 g L^{-1} of sugars. Thus, the capacity of biochar to adsorb significant contents of ethanol and substrate demonstrates that the carbonaceous material could substantially impact alcoholic fermentations affecting nutrients availability and product release, while providing a rich microenvironment potentially influencing the metabolic behavior of immobilised cells.

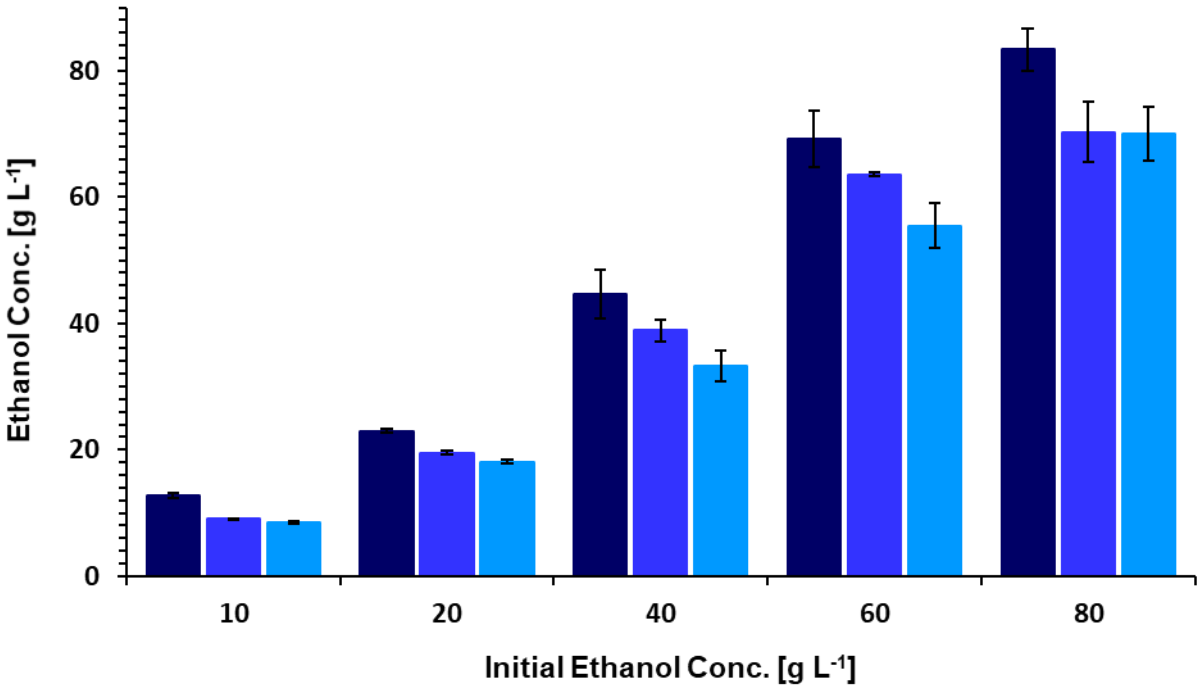

Figure 3.2.5A: Evaluation of biochar's adsorption capacity for ethanol concentrations. Bars correspond to the concentration of ethanol during the experiments. Dark, medium and light colour groups correspond to measurements conducted at 0, 20 and 60 min respectively.

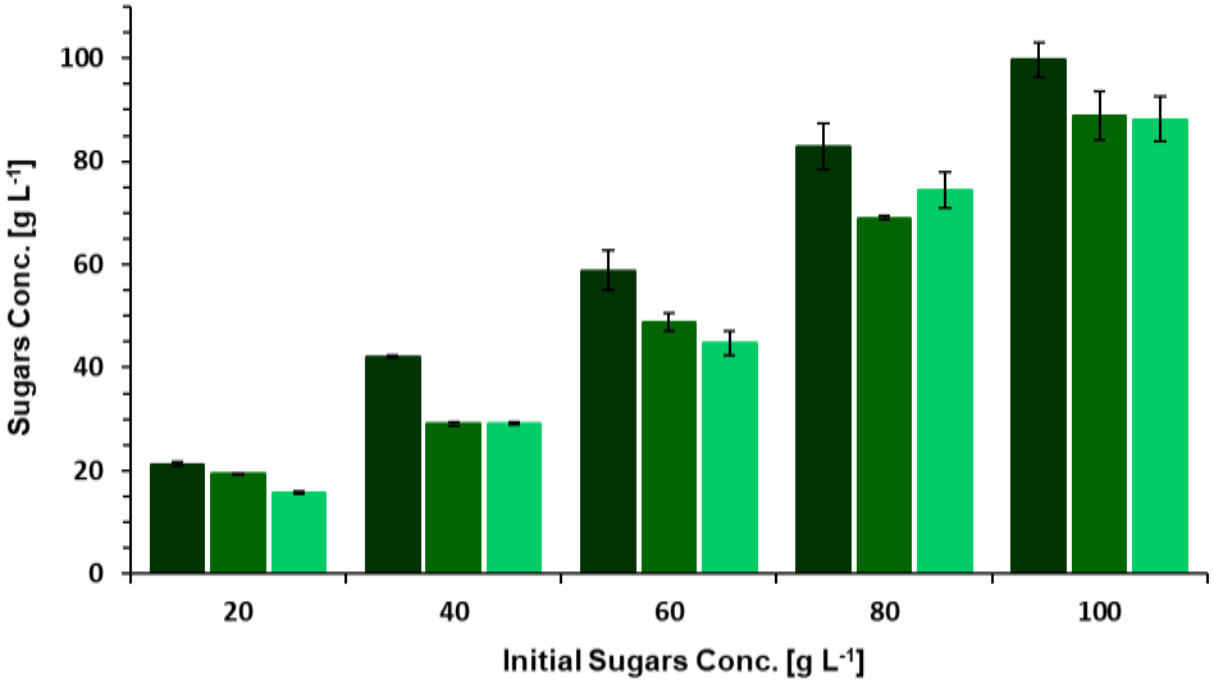

Figure 3.2.5B: Evaluation of biochar's adsorption capacity for sugars concentrations. Bars correspond to the concentration of sugars during the experiments. Dark, medium and light colour groups correspond to measurements conducted at 0, 20 and 60 min respectively.

3.2.3.2 Effect of biochars particle size on cell immobilization and fermentation performance

The performance of the biosystem with the use of different BBB particle sizes was investigated. The immobilised biocatalyst developed using biochar particle sizes of <1 mm and 1-2 mm substantially reduced ethanol production as compared to unsupported cells and unscreened biochar (Figure 3.2.6). Thus, although the diameter of the material constitutes a key factor affecting the adsorption capacity of biochar, the lower sizes employed did not enhance the bioprocess as expected potentially due to loss of the biochar's microstructure and insufficient cell attachment which could be significantly influenced by the grinding process used for size reduction. Various studies reported substantial enhancement of adsorption by different materials that employed low particle sizes. Panagiotou et al. [2018] applied calcinated waste eggshells sieved to diameters lower than 1 mm achieving substantially higher P removal efficiency as opposed to the use of bigger particles. Moreover, the use of scallop shells with diameters lower than 1 mm exhibited over 80% of P removal demonstrating the effectiveness of low particle sizes in improving the sorption phenomena in the process [Yeom and Jung, 2009]. Based on the results obtained, all subsequent experiments were conducted using unscreened biochar that comprised of the following particle size distribution: 2-3 mm 69%, 1-2 mm 25% and less than 1 mm 6%.

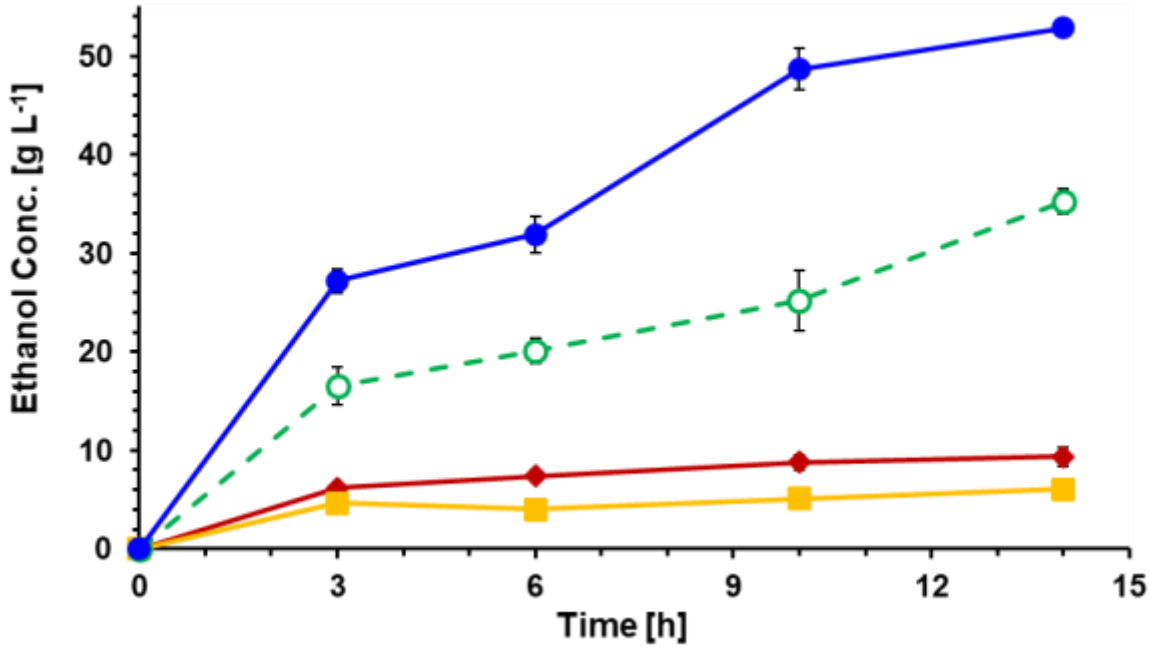

Figure 3.2.6: Evaluation of different particle size of PVBC in ethanol production during a batch alcoholic fermentation. Symbols correspond to: (i) PVB sieved to > 1-2 mm; (ii) PVB sieved to < 1 mm; (iii) unscreened PVB; (iv) freely suspended cells of *S. cerevisiae*.

3.2.4 Repeated batch ethanol fermentations with the use of different BBBs

S. cerevisiae immobilised biocatalysts produced using on PVB, AHB and CRB were applied in three repeated batch experiments to assess the efficiency of different BBBs in enhancement of ethanol generation as opposed to the use of unsupported cultures (Figure 3.2.7A-B). The biocatalysts applying PVB and AHB exhibited faster kinetics as opposed to yeasts immobilised on CRB and the unsupported culture over the first batch. However, re-use of biocatalysts in the following two batches performed confirmed that cells immobilised on PVB were more efficient achieving 63 g L^{-1} net ethanol concentration in the third experiment, which corresponded to 7.8 g L^{-1} h^{-1} productivity. Moreover, the CRB-based biocatalyst achieved 51 g L^{-1} net ethanol concentration towards the end of the third batch and 3.9 g L^{-1} h^{-1} productivity. The performance of unsupported cells was gradually reduced during the repeated batch fermentations exhibiting maximum ethanol concentration of 54 g L^{-1} and 3.8 g L^{-1} h^{-1} productivity, constituting the least efficient option between the experiments conducted. The patterns of sugars' conversion during the experiments was similar to ethanol production. The results obtained confirm that all BBBs enabled easy recirculation of cells enhancing ethanol production as compared to the conventional process, while the PVB-based biocatalyst was the most efficient technological option.

S. cerevisiae constitutes a major cell factory for application in biorefineries [Hong and Nielsen, 2012], which is broadly used in industrial ethanol manufacture based on a number of unique properties incorporating rapid growth rate, sufficient tolerance to environmental stresses, elevated ethanol production and efficient glucose repression [Bai et al., 2008]. In an attempt to improve ethanol production by the specific yeast various studies have focused on immobilizing the strain to various supports. However, although different materials have been employed for *S. cerevisiae* immobilization, such as calcium or alumina alginate gels, bioprocess performance was unstable due to poor mechanical properties of the aforementioned carriers [Mongkolkajit et al., 2011]. Nuanpeng et al. (2018) reported 84.5 g L^{-1} ethanol generation using *S. cerevisiae* DBKKUY-53 immobilised on alginate-loofah that reached significantly lower productivity (1.37 g L^{-1} h^{-1}) as compared to the use of BBBs developed here [Nuanpeng et al., 2018]. However, although

immobilised *S. cerevisiae* cells on chitosan-covered calcium alginate generated ethanol concentrations ranging between 30.7 and 33.5 g L^{-1}, following completion of 8 repeated batch fermentations of 10 h duration rupture of the beads occurred constituting the biocatalyst inappropriate for re-use [Duarte et al., 2013].

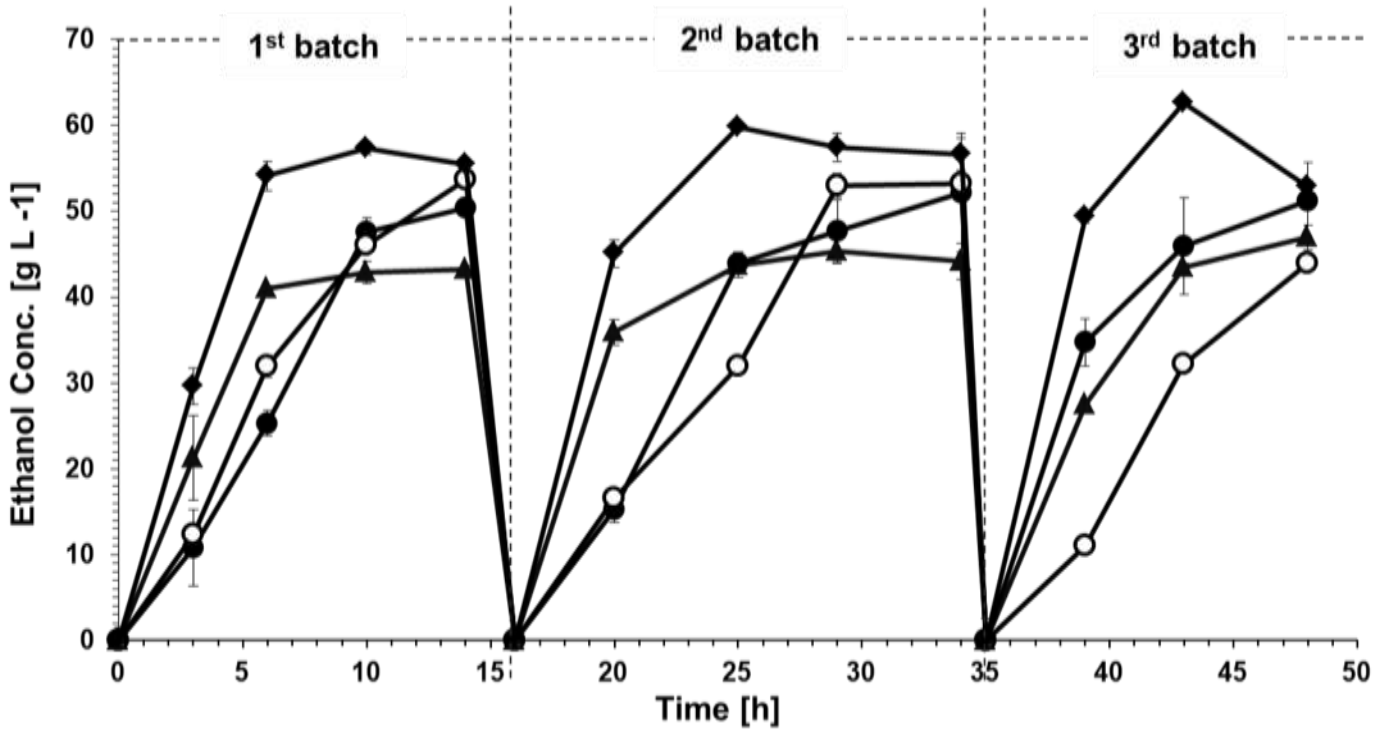

Figure 3.2.7A: Application of BBBs in repeated batch ethanol fermentations. Evolution of ethanol concentration achieved at 37 ºC using *S. cerevisiae*: (i) ◆ immobilised on PVB; (ii) ▲ immobilised on AHB; (iii) ● immobilised on CRB; (iv) ○ freely suspended cells.

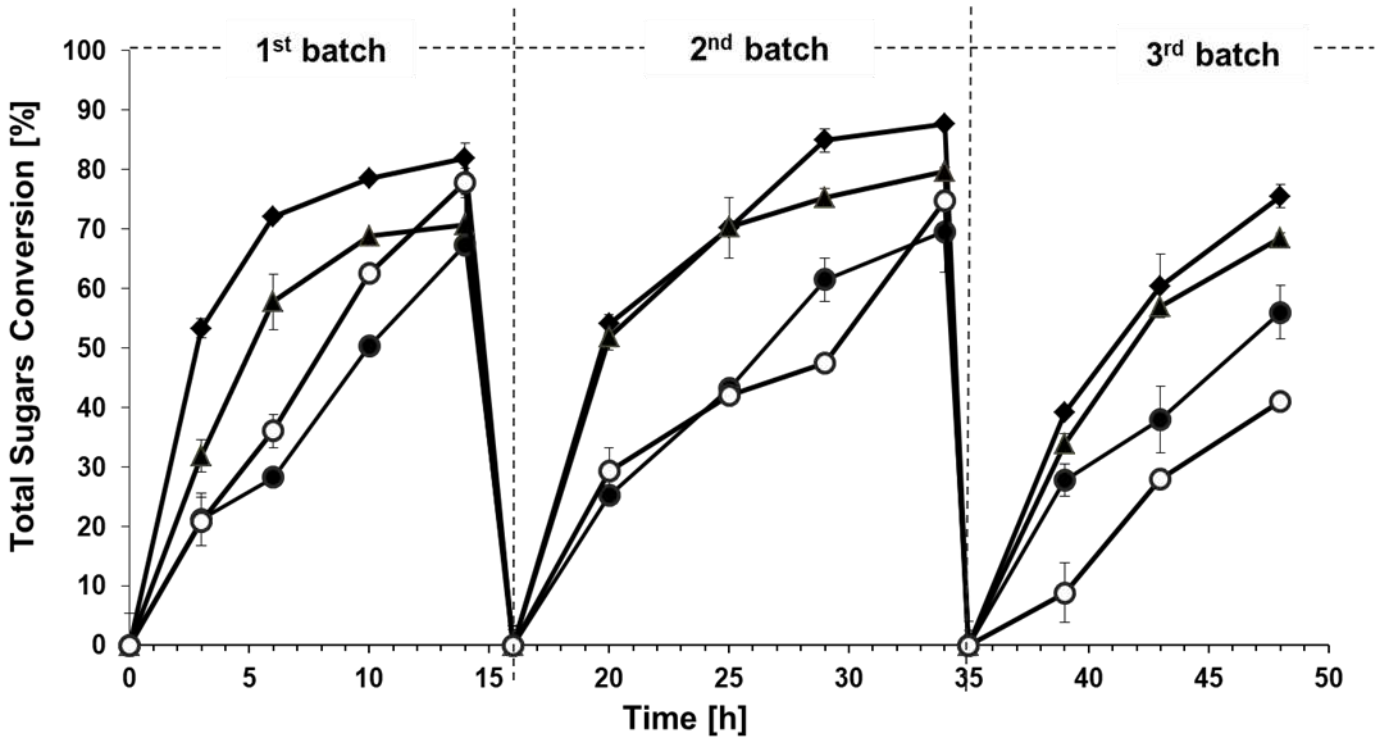

Figure 3.2.7B: Application of BBBs in repeated batch ethanol fermentations. Evolution of sugars concentration achieved at 37 ºC using *S. cerevisiae*: (i) ◆ immobilised on PVB; (ii) ▲ immobilised on AHB; (iii) ● immobilised on CRB; (iv) ○ freely suspended cells.

3.2.5 BBB bioethanol fermentations in elevated temperatures during repeated batch experiments

S. cerevisiae immobilised on PVB was applied in three repeated batch cultures to assess the efficiency in ethanol production from the yeast at elevated temperatures that ranged between 37 and 41 ^{o}C (Figure 3.2.8A-B). Overall, all immobilised biocatalysts performed faster ethanol production kinetics as opposed to the respective unsupported cultures conducted at each temperature. Moreover, the experiments maintained at 37 and 39 ^{o}C produced higher ethanol contents than those performed at 41 ^{o}C including both fermentations that employed immobilised and freely unsupported cells. Thus, the maximum ethanol concentrations obtained using the BBB system comprised 67.8 g L^{-1} at 37 ^{o}C and 64 g L^{-1} at 39 ^{o}C.

Temperature tolerance constitutes an important trait of the strains applied in alcoholic fermentations, while the performance of *S. cerevisiae* in ethanol production is reduced at temperatures higher than 37 ^{o}C [Patsalou et al., 2019;Koutinas et al., 2016]. Thus, the performance of the strain at the highest temperature tested (41 ^{o}C) was evaluated in 6 repeated batch fermentations to assess the effect of biochar to sustain the bioprocess at higher temperatures. Recycling of BBB in sequential batch fermentations confirmed that yeast cells attached to biochar demonstrated significantly faster kinetics at 41 ^{o}C. The productivity of ethanol ranged between 5.1 and 5.7 g L^{-1} h^{-1} in the last three batches performed using the BBB system, which was substantially higher as opposed to the value exhibited by unsupported cells that reached 3.3-3.7 g L^{-1} h^{-1}. Moreover, product formation in all batches conducted at 41 ^{o}C was stable exhibiting 51.6 g L^{-1} maximum ethanol concentration, while that of the corresponding free cell cultures reached a maximum value of 32.4 g L^{-1}. The data obtained demonstrate that the use of BBB enabled increased ethanol production potentially protecting yeasts cells against major yeast environmental stresses (e.g. high temperature). Thus, cells immobilised on PVB produced 59% more ethanol as compared to the conventional process at 41 ^{o}C, holding the capacity for application as an efficient carrier that significantly improves alcoholic fermentations allowing easy recycling of the biocatalyst in subsequent batch fermentations.

The literature on high temperature alcoholic fermentations shows a variety of approaches on the beneficial use of thermotolerant yeasts [Banat et al., 1998, Choudhary et al., 2016]. Eiadpum et al. [2012] reported that *S. cerevisiae* M30 was substantially more effective in ethanol production by blackstrap molasses conducted at 37 ^{o}C generating up to 80 g L^{-1} of ethanol, while the increase of fermentation temperature to 40 and 45 ^{o}C imposed a negative impact reducing the concentration achieved to 40 and 3 g L^{-1} respectively. Furthermore, although the initial concentration of sugar's employed was higher as compared to the present work, ethanol concentration using *S. cerevisiae* M30 immobilised on an alginate loofa matrix reached 43 g L^{-1} at 40 ^{o}C, which was lower than the 51.6 g L^{-1} achieved with the use of BBB at 41 ^{o}C demonstrating the beneficial use of biochar as an efficient support material. In an attempt to achieve cost-effective fuel-grade ethanol from biowaste, the importance of applying thermotolerant yeast strains including *K. marxianus* and *P. kudriavzevii* has been shown [Koutinas et al., 2016]. Moreover, the use of microorganisms fermenting at higher temperatures is also known to enable simultaneous saccharification and fermentation commonly conducted at 40-50 ^{o}C [Sivarathnakumar et al., 2019]. However, although *K. marxianus* was employed for ethanol production from sugar cane juice at 40 and 45 ^{o}C, lower productivities were achieved (0.96-1.51 g L^{-1} h^{-1}) as compared to the use of BBB (4.22-5.48 g L^{-1} h^{-1}) at 41 ^{o}C enabling application of the mesophilic yeast *S. cerevisiae* at higher temperatures [Limtong et al., 2007].

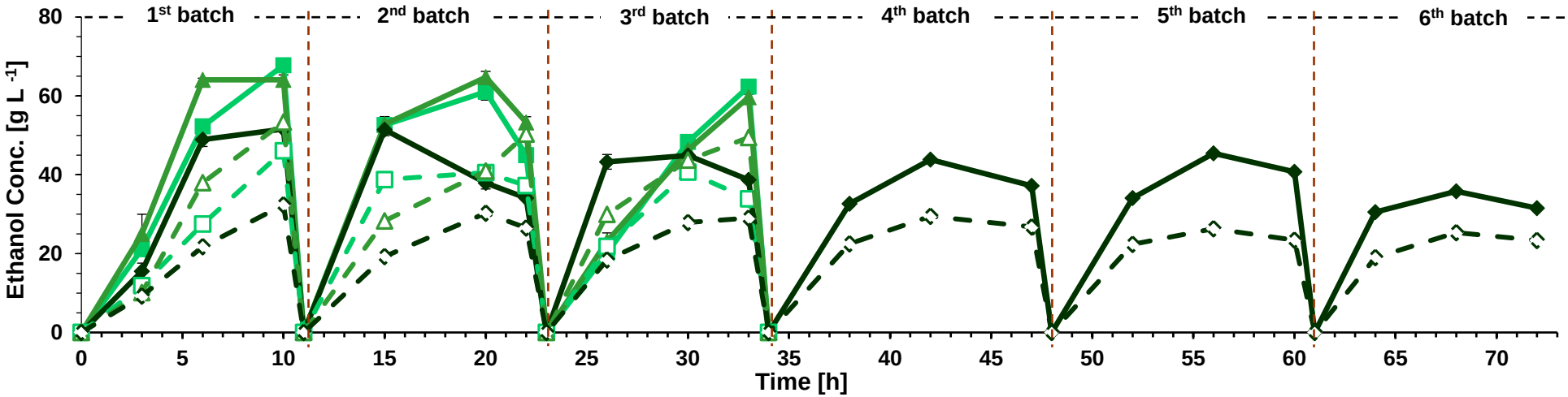

Figure 3.2.8A: Evaluation of BBB performance in elevated temperatures during repeated batch alcoholic fermentations. Ethanol concentration employing: (i) cells immobilised on PVB at 37 ^{o}C; (ii) cells immobilised on PVB at 39 ^{o}C; (iii) cells immobilised on PVB at 41 ^{o}C; (iv) freely suspended cells at 37 ^{o}C; (v) freely suspended cells at 39 ^{o}C; (vi) freely suspended cells at 41 ^{o}C.

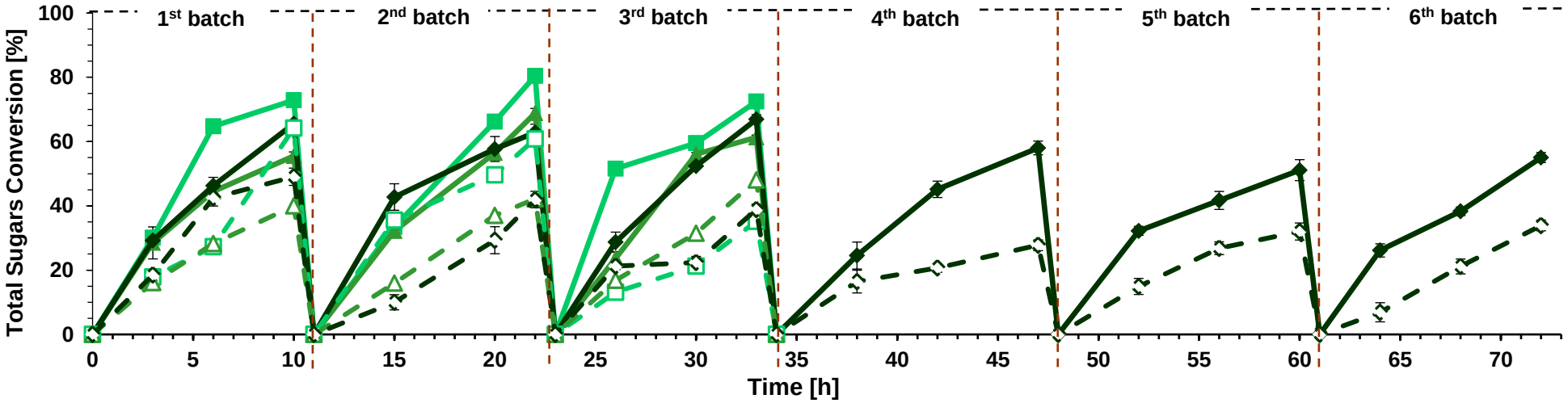

Figure 3.2.8B: Evaluation of BBB performance in elevated temperatures during repeated batch alcoholic fermentations. Total sugars conversion employing: (i) cells immobilised on PVB at 37 ^{o}C; (ii) cells immobilised on PVB at 39 ^{o}C; (iii) cells immobilised on PVB at 41 ^{o}C; (iv) freely suspended cells at 37 ^{o}C; (v) freely suspended cells at 39 ^{o}C; (vi) freely suspended cells at 41 ^{o}C.

3.2.6 Enhancement of ethanol production in a citrus peel waste biorefinery with the use of BBB

Following assessment of BBBs' application under different fermentation conditions employing media simulating a Valencia orange peel hydrolyzate, the effect of the developed biocatalyst was tested in the CPW hydrolyzate produced via the biorefinery. Thus, given that synthetic hydrolyzates contain only the main nutrients incorporated in the feedstock, excluding other molecules that could be released during preprocessing (e.g. inhibitors, such as hydroxymethylfurfural [Sweygers et al., 2018], and micronutrients), the performance of the immobilised system as compared to unsupported cultures was further evaluated using the hydrolyzate of the biorefinery proposed here under similar conditions. Following extraction of essential oils and pectin as well as application of enzyme hydrolysis, free cells and *S. cerevisiae* immobilised on PVB were employed in two repeated batch fermentations conducted at 41 ^{o}C (Figure 3.2.9A-B).

During the first batch, the developed BBB generated 30.8 g L^{-1} net ethanol concentration within 9 h, which was substantially higher as compared to free unsupported cells that reached 13.4 g L^{-1}. The same performance was also exhibited during the second batch, were the maximum ethanol concentration formed included 33 g L^{-1} for the BBB system and 12 g L^{-1} using unsupported cells. Therefore, the use of the immobilised biocatalyst strongly enhanced biosystem performance at an elevated temperature as opposed to the conventional process. Based on this technological advantage, substantially increased ethanol formation could be achieved in the CPW biorefinery with the use of BBBs offering an advanced solution to tackle major limitations of the bioprocess. Previous studies have shown that unsupported cultures of *S. cerevisiae* and *K. marxianus* produced 40 and 37 g L^{-1} of ethanol respectively at 37 ^{o}C in fermentations of a solution modeling Valencia orange peel waste hydrolyzate [Wilkins et al., 2007]. Moreover, *S. cerevisiae* produced 38.6 g L^{-1} of ethanol using a CPW hydrolysate [Pourbafrani et al., 2010], while *S. cerevisiae* KCTC 7906 cells immobilised in sodium alginate generated ethanol concentrations ranging between 14.4 and 29.5 g L^{-1} through fruit waste and CPW fermentations [Choi et al., 2015]. Thus, the enhanced ethanol

production achieved here at 41 ^{o}C demonstrates that employing the BBB system in fuel-grade ethanol production could potentially increase energy savings via reduction of cooling costs, increased fermentation and saccharification rates, lower ethanol distillation costs and reduced contamination risk.

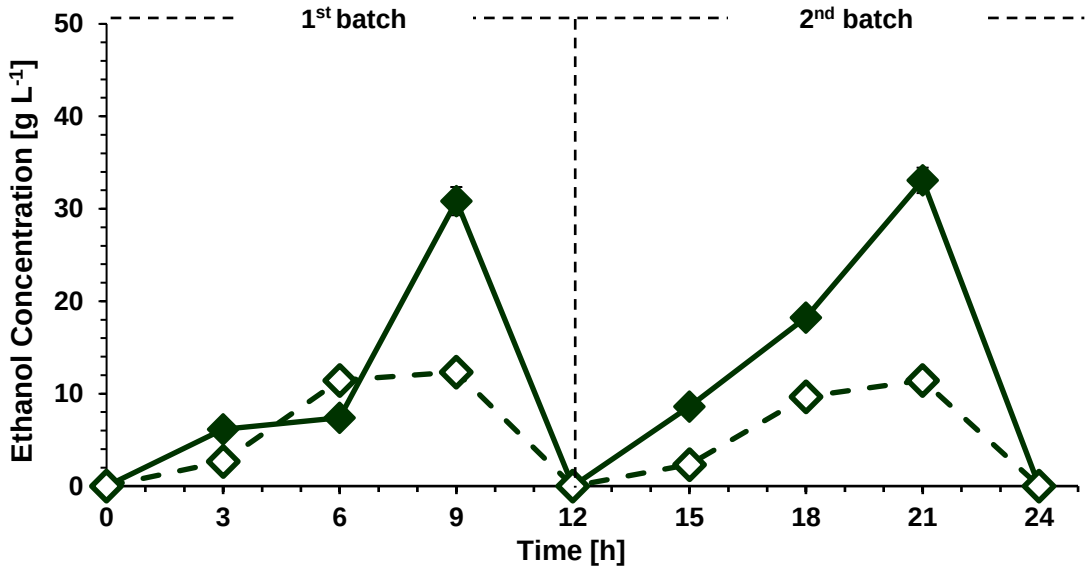

Figure 3.2.9A: Evaluation of *S. cerevisiae* immobilised biocatalyst employing PVB at the elevated temperature of 41 ^{o}C, for ethanol production using CPW hydrolyzate. Symbols correspond to ethanol concentration in fermentations conducted at 41 ^{o}C, employing (i) —●— immobilised cells; (ii) —○— freely suspended cells.

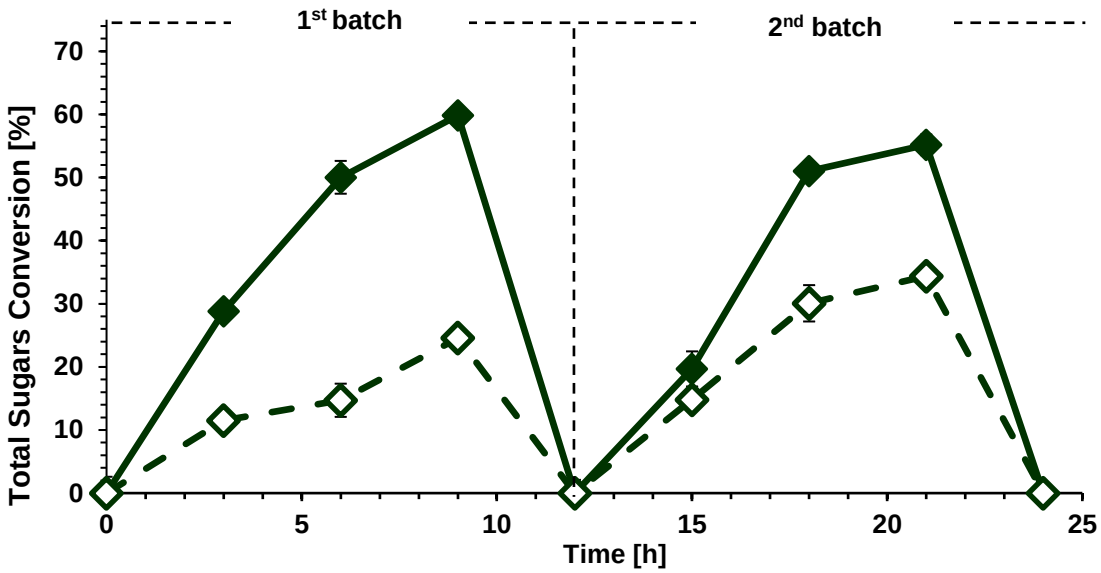

Figure 3.2.9B: Evaluation of *S. cerevisiae* immobilised biocatalyst employing PVB at the elevated temperature of 41 ^{o}C, for ethanol production using CPW hydrolyzate. Symbols correspond to sugars conversion in fermentations conducted at 41 ^{o}C, employing (i) —●— immobilised cells; (ii) —○— freely suspended cells.

3.3 Improvement of stress multi-tolerance and bioethanol production by *S. cerevisiae* immobilised on biochar

3.3.1 *S. cerevisiae* bioethanol fermentations under heat shock and oxidative stress

S. cerevisiae faces two important environmental challenges, namely heat shock and oxidative stress. Heat shock constitutes the most fundamental stress condition experienced by *S. cerevisiae* cells, which exhibit optimal growth between 25 and 30 ^{o}C. However, at higher temperatures than 36 ^{o}C yeast cells activate a protective transcriptional program termed the heat shock response and alter various components of their physiology, including membrane composition and carbohydrate flux [Morano et al., 2012]. Moreover, oxidative stress constitutes one of the main metabolic burdens causing cell death via accumulation of intracellular reactive oxygen species. The modulation of energy metabolism, from fermentation to respiration, imposes great influence on lipid stability to oxidation, especially during biomass propagation [Rakin et al., 2009]. Therefore, based on the above rationale the efficiency of biochar to protect *S. cerevisiae* against various environmental stresses faced during the industrial bioethanol production process was assessed through exposure of both immobilised and suspended cells to heat, oxidative, ethanol and osmotic stress conditions during bioethanol fermentation experiments.

3.3.1.1 Bioethanol fermentations under elevated temperatures

S. cerevisiae immobilised on biochar produced using pistachios shells was applied in bioethanol fermentations conducted at 30 and 39 ^{o}C. The efficiency of the developed biocatalyst in enhancing the performance of the bioprocess at elevated temperatures was determined as opposed to the use of freely suspended cells (Figure 3.3.1A-B). The BBB system demonstrated faster kinetics as well as higher bioethanol production as opposed to freely suspended cells at both temperatures employed. The maximum net bioethanol concentration achieved by immobilised cells at 30 ^{o}C was 41 g L^{-1} following 12 h of fermentation reaching productivity of 3.44 g L^{-1} h^{-1}. However, the suspended culture performed lower

concentration levels for the biofuel that reached 35 g L^{-1} over the same period and productivity of 2.94 g L^{-1} h^{-1}. The significant potential of the immobilised biocatalyst for application at elevated temperatures was confirmed at the culture conducted at 39 ^{o}C. The use of BBB at 39 ^{o}C demonstrated bioethanol concentration of 39 g L^{-1} following 12 h of incubation, while the control experiment yielded 34 g L^{-1} over the same period. Faster bioprocess kinetics were obtained using BBB exhibiting productivity of 7.72 g L^{-1} h^{-1} following 4 h of incubation, which was substantially higher as opposed to freely suspended cells that achieved 1.99 g L^{-1} h^{-1} over the same period.

Bioethanol production by immobilised cells of *S. cerevisiae* on different support materials (e.g. sodium alginate, γ-alumina, polyvinyl alcohol) have previously demonstrated the beneficial use of immobilised biocatalysts that confer increased ethanol tolerance and productivity as well as lower substrate inhibition [Rakin et al., 2009; Galanakis et al., 2012]. The production of bioethanol at elevated temperatures using BBB has been previously investigated employing the specific strain in fermentations of citrus peel waste hydrolysates performing stable and elevated biofuel production as opposed to the conventional bioprocess at 42 ^{o}C [Section 3.1 and 3.2]. Thus, the capacity of the BBB technology to enhance bioprocess performance at elevated temperatures was further assessed in the experiments conducted via monitoring of expression from the metabolic route triggering the heat shock response of the yeast.

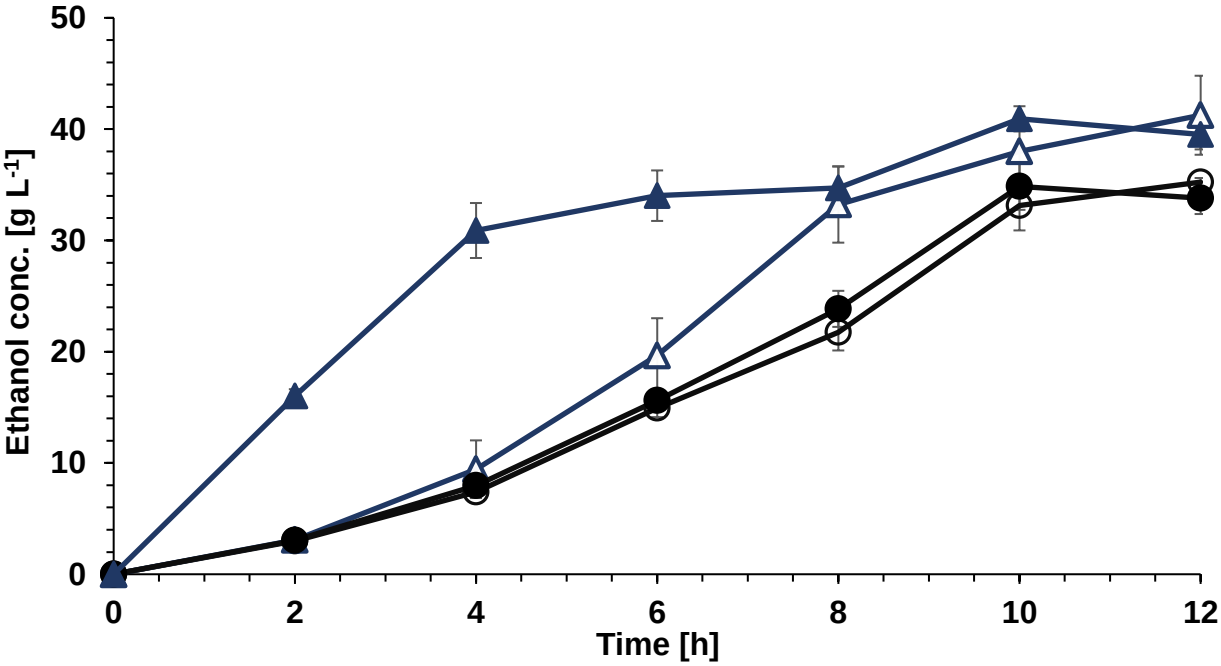

Figure 3.3.1A: Bioethanol production achieved at 30 and 39 ºC using immobilised and freely suspended cells of *S. cerevisiae*. Symbols represent: (i) immobilised cells at 30 ºC; (ii) immobilised cells at 39 ºC; (iii) freely suspended cells at 30 ºC; (iv) freely suspended cells at 39 ºC.

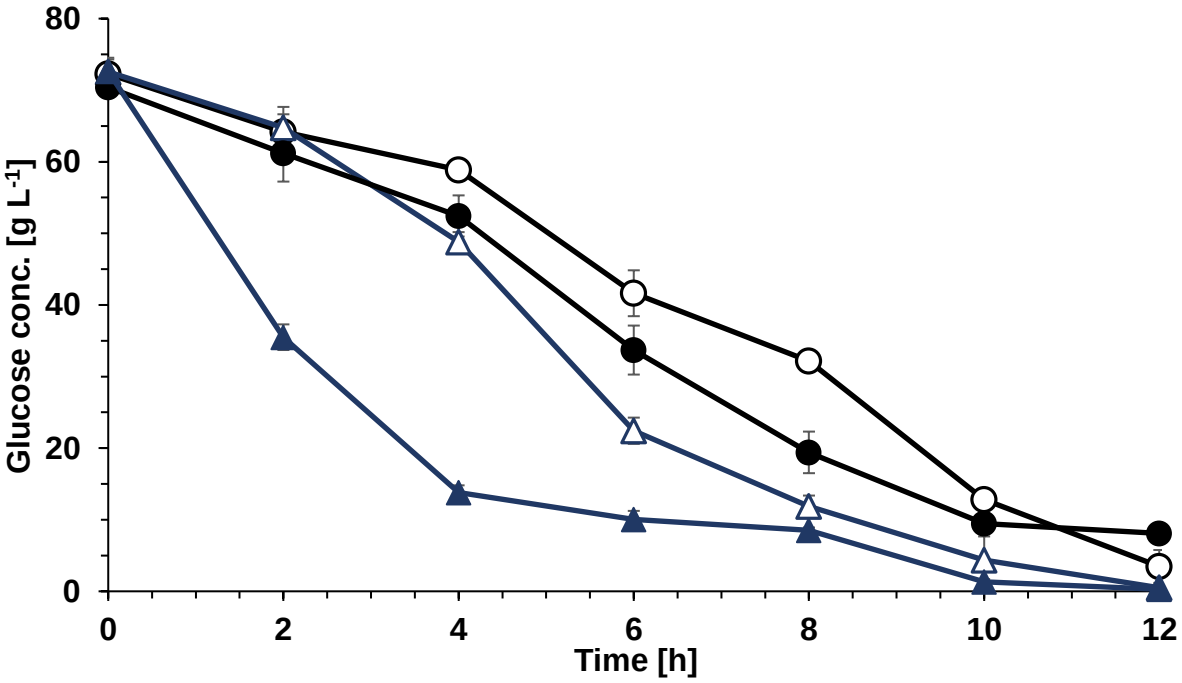

Figure 3.3.1B: Glucose consumption achieved at 30 and 39 ^{o}C using immobilised and freely suspended cells of *S. cerevisiae*. Symbols represent: (i) immobilised cells at 30 ^{o}C; (ii) immobilised cells at 39 ^{o}C; (iii) freely suspended cells at 30 ^{o}C; (iv) freely suspended cells at 39 ^{o}C.

3.3.1.2 Relative expression of genes involved in heat shock and oxidative stress response of *S. cerevisiae*

Sustainable ethanol production at elevated temperatures requires highly thermotolerant ethanol-producing yeast strains [Saini et al., 2018]. HSPs serve as molecular chaperones by either stabilizing new proteins to ensure correct folding or refolding to the proper conformation or degrading misfolded proteins which have been damaged by stress conditions. Moreover, HSPs participate in protein transportation across membranes within the cell [Borges and Ramos, 2005], while major players in heat hock response comprise heat shock factor 1 (HSF1) as well as MSN2/MSN4 also known as oxidative stress-responsive genes [Morano et al., 2012; Davidson et al., 1996].

Transcription of *HSP104*, *HSF1* and *TPS* was monitored in the aforementioned experiments to determine heat shock activation in each case. The heat shock protein *HSP104*, which is responsible to stabilize unfolded proteins and prevent aggregation, constitutes a chaperone which plays a critical rule in induced thermotolerance [Morano et al., 2012]. Moreover, trehalose is considered as a chemical chaperone for protein folding holding properties similar to the chaperone *HSP104*, while its biosynthesis is controlled by trehalose-6-phosphate synthase encoded by *TPS* [Simola et al., 2000]. In *S. cerevisiae*, upon induction of *TPS*, the level of the disaccharide trehalose increases rapidly during heat shock, along with the induction of HSPs [Hottiger et al., 1987], stabilising the structures and enzymatic activities of proteins against thermal denaturation and preventing the aggregation of misfolded proteins [Hottiger et al., 1994]. Trehalose serves as positive regulator of *HSF1* activity, which suggests protein protective function at the initial stages of heat shock prior complete induction of HSPs.

The relative expression levels of *HSP104*, *HSF1* and *TPS* were determined using real-time RT-qPCR during the bioethanol fermentations conducted at 30 and 39 ^{o}C using both the BBB system as well as freely suspended cells (Figure 3.3.2A-C). The relative expression of *HSP104* in the suspended culture conducted at 30 ^{o}C was not significantly different over the time points assessed ($p > 0.05$). At the elevated temperature of 39 ^{o}C, the mRNA expression level of *HSP104* exhibited 2.15-fold increase compared with 0 h. The activity of *HSP104* reached maximum

expression following 4 h of fermentation, demonstrating that heat stress was stimulated upon exposure of cells at higher temperatures ($p < 0.05$). However, significant differences were observed over time employing BBB in the bioethanol fermentation conducted at 30 ^{o}C, where *HSP104* expression was down-regulated following 4 h of fermentation as opposed to the expression observed at 0 h ($p < 0.05$). Moreover, 0.5-fold increase in the relative mRNA expression of *HSP104* was monitored employing immobilised cells exposed to heat stress over the same period ($p > 0.05$). Thus, significantly lower increase of *HSP104* expression levels occurred at 39 ^{o}C with the use of cells immobilised on biochar as opposed to the suspended culture of *S. cerevisiae*. A similar pattern was additionally observed for the transcriptional kinetics of *HSF1* during the experiments. Although the relative mRNA expression of *HSF1* in free cells remained stable over time at 30 ^{o}C, the raise of temperature to 39 ^{o}C resulted in significant induction ($p < 0.05$) of transcript levels which was 3-fold higher at 4 h compared with the beginning of the experiment. However, the gene was not activated at 30 ^{o}C using cells immobilised on biochar ($p > 0.05$).

Application of the immobilised biocatalyst did not exhibit significant differences in transcription of *HSF1* over time in both temperatures assessed. Moreover, the relative mRNA expression of *TPS* confirmed the buffering effect of BBB against heat shock. Free cells performed 3.8-fold increase of *TPS* transcription at 39 ^{o}C ($p < 0.05$), while no stimulation of the heat shock response pathway was observed during fermentations conducted at 30 ^{o}C. The corresponding activation of the gene demonstrated 1.05- and 2.6-fold increase in immobilised cells following 4 h of cultivation at 30 and 39 ^{o}C respectively. Overall, the relative expression levels of all genes monitored under conditions triggering the heat shock route in suspended cells exhibited significantly lower values in immobilised cultures demonstrating that the heat shock response pathway was not stimulated following attachment of the yeast on the biomaterial.

Although elevated temperature represents the primary insult during heat shock, one of the major secondary effects taking place during heat stress involves the production of reactive oxygen species [Halliwell, 2006]. Oxidative stress is expressed by the *MSN2*/*MSN4* system, which was additionally monitored here as

illustrated in Figure 3.3.2D-E. Monitoring transcription levels of both genes indicated that oxidative stress was not expressed using the BBB technology. Specifically, immobilised cells of *S. cerevisiae* on biochar demonstrated 0.5- and 0.3-fold decrease in *MSN2* relative expression at 30 and 39 ^{o}C respectively between 0 and 4 h in each experiment. However, in contrast to the use of biochar, freely suspended cells performed a 2-fold increase in *MSN2* transcription at 39 ^{o}C ($p < 0.05$). Moreover, transcription of *MSN4* confirmed the advanced capacity of the immobilised biocatalyst to dampen the metabolic burden imposed by oxidative stress. Expression levels of *MSN4* showed a 0.2- and 2.7-fold increase ($p < 0.05$) at 30 and 39 ^{o}C, respectively, employing free cells of *S. cerevisiae* between 0 and 4 h of fermentation, while a 0.3- and 1.4-fold increase ($p < 0.05$) in the gene's mRNA levels were observed under the same conditions using the immobilised biocatalyst.

Various studies have previously examined the accumulation of misfolded proteins under exposure of *S. cerevisiae* cells to heat shock. According to Canonero et al., [2022], coordinated regulation of mRNA abundance, translation, localisation, and turnover rates of individual mRNAs were enhanced upon induction of several stress conditions including heat shock. The expression level of genes encoding *HSP26*, *HSP70*, *HSP90*, *HSP104*, pyruvate kinase, trehalose-6-phosphate synthase, neutral trehalase and glycogen synthase were investigated in fermentations conducted at 30 and 40 ^{o}C employing *S. cerevisiae* DBKKU Y-53 and SC90. All the aforementioned genes were highly expressed at 40 ^{o}C compared with 30 ^{o}C [Nuanpeng et al., 2016]. Moreover, *HSP100* and *HSP104* were strongly induced in response to a variety of stressful conditions [Parsell et al., 1994]. Therefore, the reduction of transcription from a series of genes associated with the occurrence of heat shock in *S. cerevisiae* immobilised on biochar demonstrates that the use of the specific material as cell carrier could serve as a technological alternative to strain modification in high temperature bioethanol fermentations.

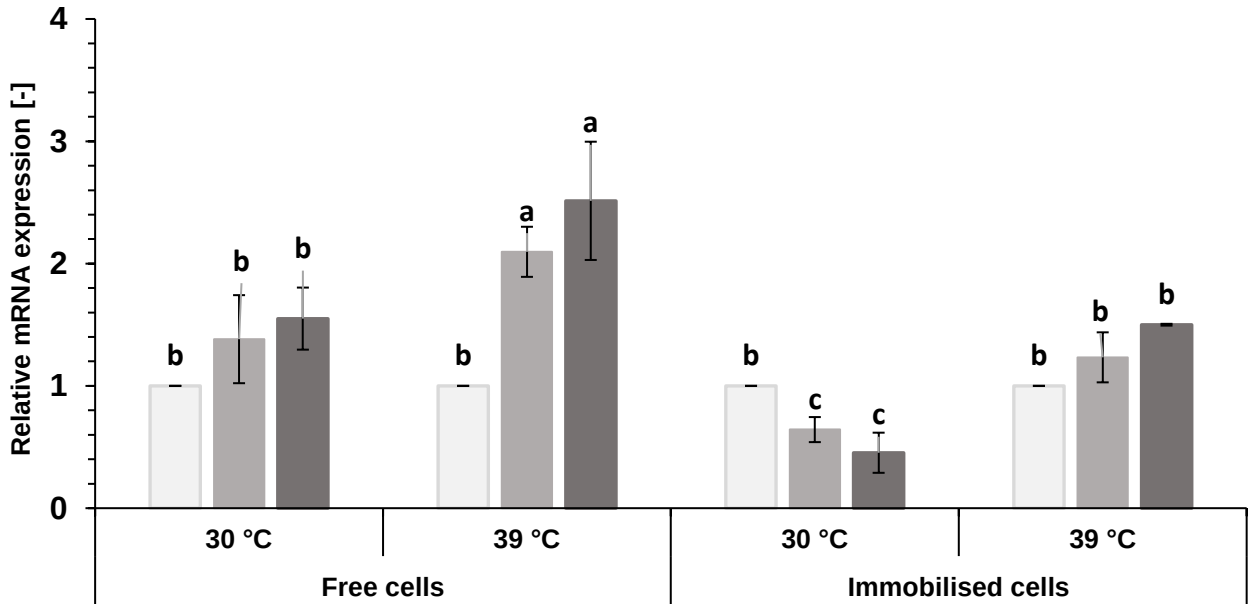

Figure 3.3.2A: Relative expression level of *HSP104* gene induced by heat shock in fermentations conducted at 30 and 39 ºC. Light, medium and dark colour groups correspond to measurements conducted at 0, 0.5 and 4 h respectively.

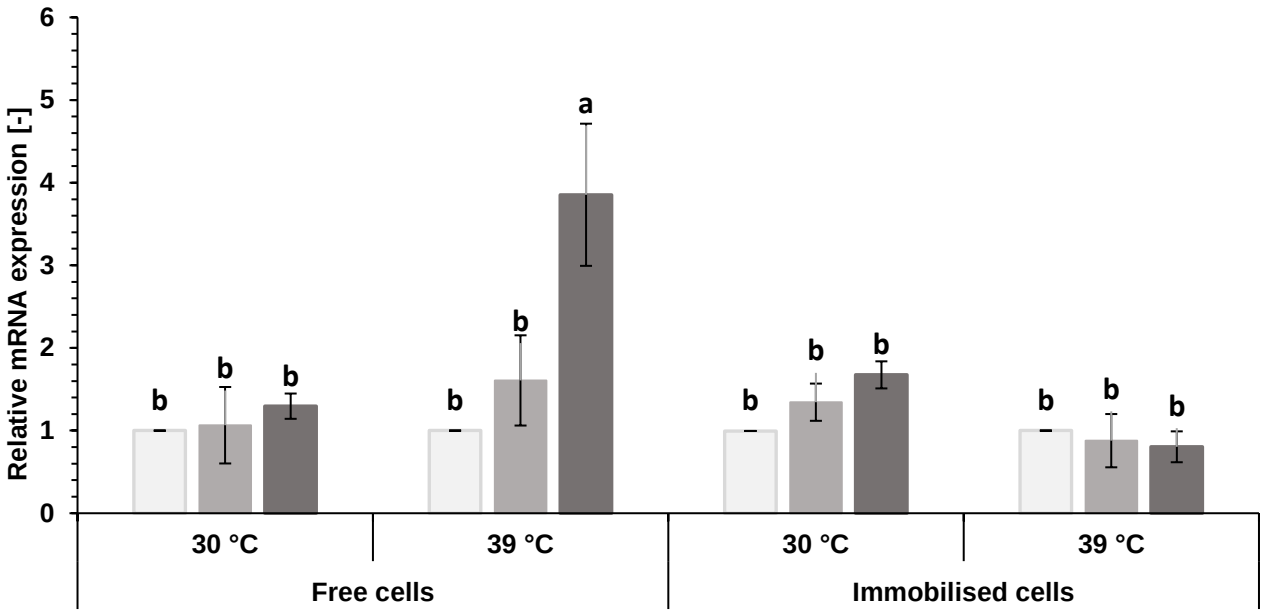

Figure 3.3.2B: Relative expression level of *HSF1* gene induced by heat shock in fermentations conducted at 30 and 39 ºC. Light, medium and dark colour groups correspond to measurements conducted at 0, 0.5 and 4 h respectively.

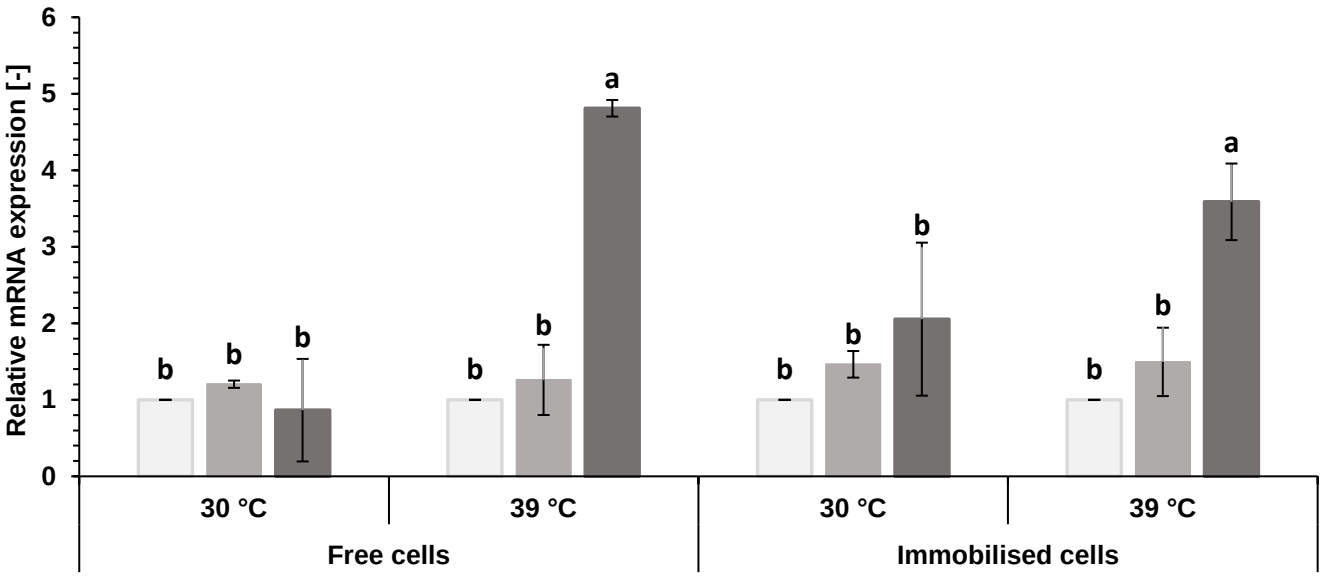

Figure 3.3.2C: Relative expression level of *TPS* gene induced by heat shock in fermentations conducted at 30 and 39 ºC. Light, medium and dark colour groups correspond to measurements conducted at 0, 0.5 and 4 h respectively.

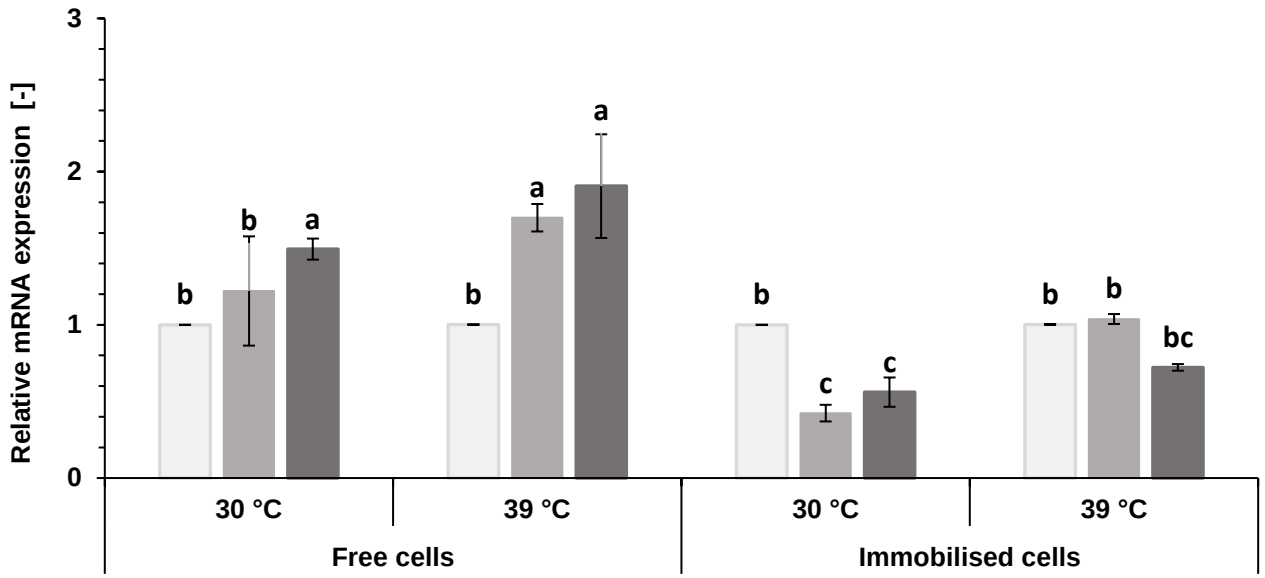

Figure 3.3.2D: Relative expression level of *MSN2* gene induced by oxidative stress during the fermentations conducted at 30 and 39 ^{o}C. Light, medium and dark colour groups correspond to measurements conducted at 0, 0.5 and 4 h respectively.

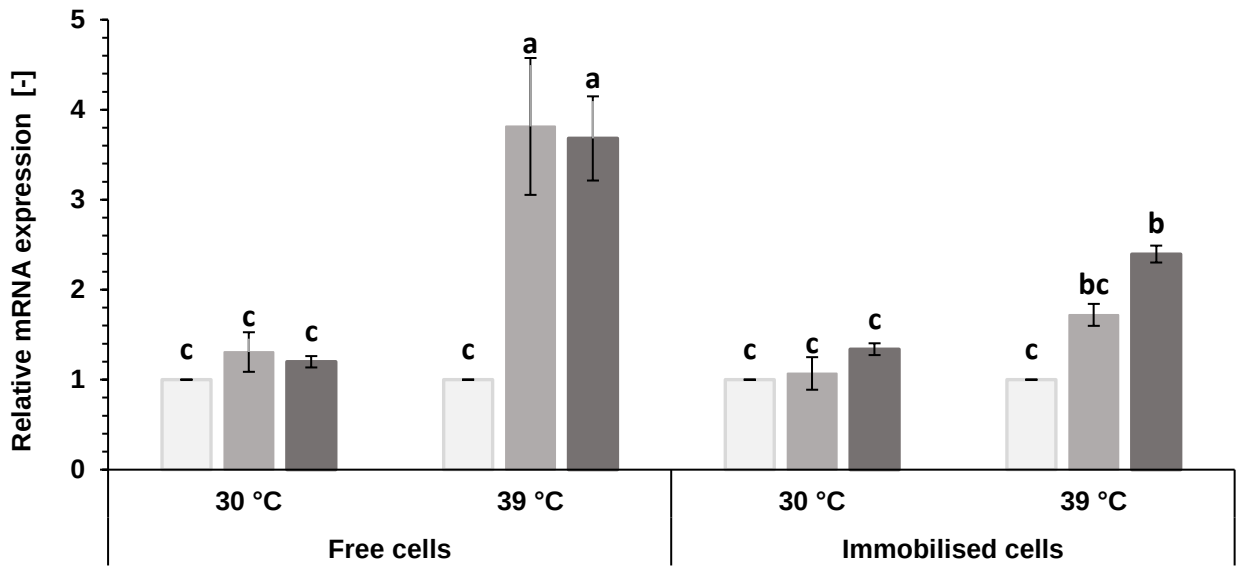

Figure 3.3.2E: Relative expression level of *MSN4* gene induced by oxidative stress during the fermentations conducted at 30 and 39 ºC. Light, medium and dark colour groups correspond to measurements conducted at 0, 0.5 and 4 h respectively.

3.3.2 *S. cerevisiae* bioethanol fermentations under bioethanol stress

3.3.2.1 Biofuel fermentations under inhibitory bioethanol contents

Although *S. cerevisiae* constitutes a superb ethanol producer among numerous fermentative microorganisms, the strain is inhibited by the high bioethanol concentrations required for cost-effective production of the biofuel [Liu et al., 2008]. Thus, accumulation of bioethanol in the biomedium inhibits cell growth and viability, which leads to reduction in production efficiency [Casey and Ingledew,1986;Bai et al., 2004].

Bioethanol manufacture using the immobilised biocatalyst developed as well as freely suspended cells of *S. cerevisiae* were evaluated employing two different initial bioethanol concentrations (70 and 90 g L^{-1}), whereas a control experiment that did not involve bioethanol addition at the beginning of fermentation was also conducted (Figure 3.3.3A-B). All experiments performed using the immobilised biocatalyst exhibited higher bioethanol production during fermentation as compared to the corresponding suspended culture. Immobilised cells exposed to initial biofuel contents of 90 g L^{-1} produced 21 g L^{-1} of bioethanol following 3 h of incubation consuming 40.8 g L^{-1} of glucose, while reaching productivity of 7 g L^{-1} h^{-1}. However, freely suspended cells were completely inhibited by the extreme initial bioethanol concentration failing to consume the carbon source as well as to produce the biofuel, a response that confirmed the protective role of BBB against high bioethanol contents. The immobilization of *S. cerevisiae* on biochar additionally enhanced the performance of cells exposed to 70 g L^{-1} of initial bioethanol content yielding 25 g L^{-1} net production of biofuel consuming 48 g L^{-1} of glucose, as opposed to the suspended culture that generated 17 g L^{-1} of bioethanol over the same period, while decreasing glucose concentration by 32 g L^{-1}. Moreover, the productivity achieved with the use of BBB and free cells reached 2.8 and 1.9 g L^{-1} h^{-1} respectively.

The fermentation experiments conducted without bioethanol addition at the beginning of each culture enhanced the bioprocess performed using the immobilised biocatalyst as compared to suspended cells. However, bioprocess improvement as a result of biochar addition was more prominent in the experiments

performed under inhibitory initial bioethanol contents. Faster bioethanol production kinetics and higher titres of the biofuel were obtained using immobilised cells, that yielded 36 g L^{-1} of bioethanol reaching productivity of 4.0 g L^{-1} h^{-1} as opposed to freely suspended cells that produced 23 g L^{-1} of the biofuel, while the increase in the initial bioethanol content resulted in substantially more profound inhibition of the conventional system compared to the use of BBB.

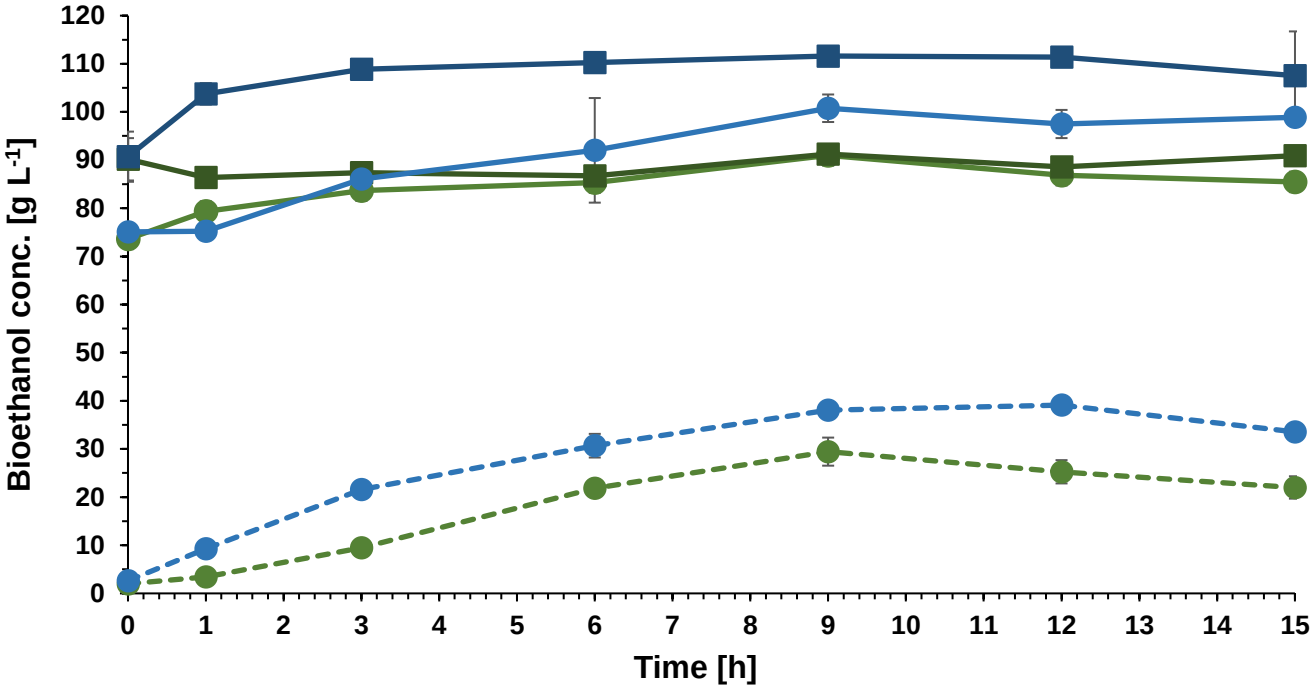

Figure 3.3.3A: Bioethanol production achieved at 30 ^{o}C using immobilised and suspended cells of *S. cerevisiae*. Symbols correspond to: (i) immobilised cells exposed to 90 g L^{-1} of bioethanol, (ii) immobilised cells exposed to 70 g L^{-1} of bioethanol, (iii) immobilised cells exposed to 0 g $L^{-1}$of bioethanol, (iv) suspended cells exposed to 90 g L^{-1} of bioethanol, (v) suspended cells exposed to 70 g L^{-1} of bioethanol, (vi) suspended cells exposed to 0 g L^{-1} of bioethanol.

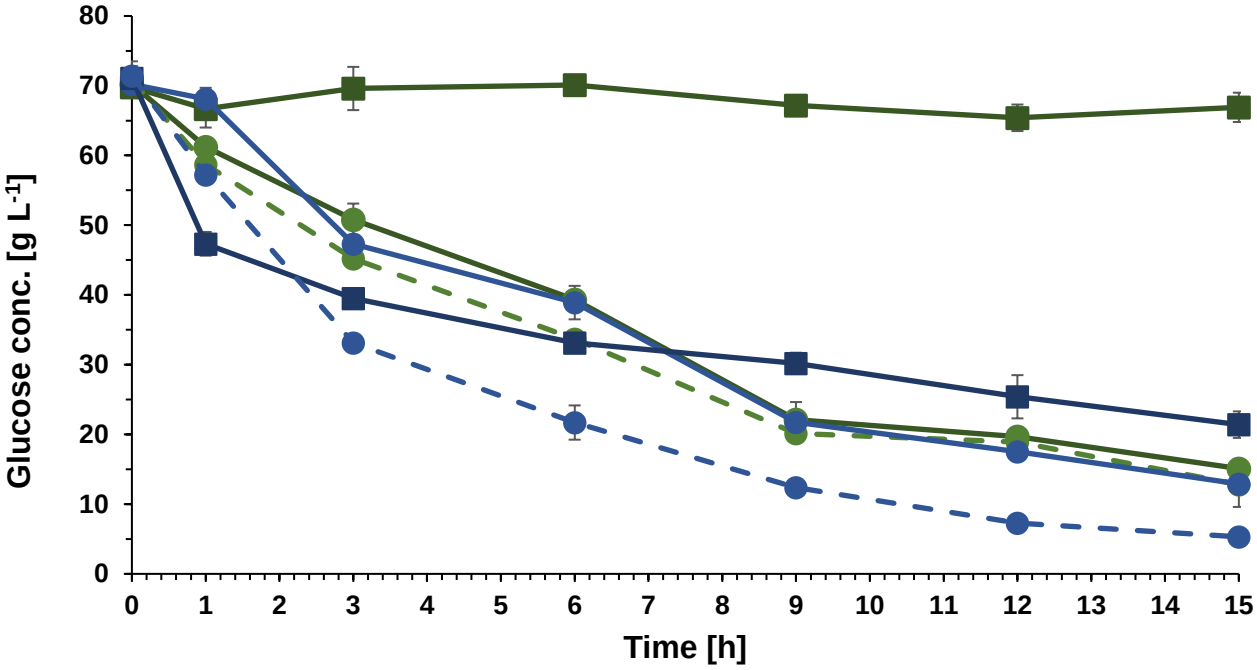

Figure 3.3.3B: Glucose consumption achieved at 30 ^{o}C using immobilised and suspended cells of *S. cerevisiae*. Symbols correspond to: (i) immobilised cells exposed to 90 g L^{-1} of bioethanol, (ii) immobilised cells exposed to 70 g L^{-1} of bioethanol, (iii) immobilised cells exposed to 0 g L^{-1} of bioethanol, (iv) suspended cells exposed to 90 g L^{-1} of bioethanol, (v) suspended cells exposed to 70 g L^{-1} of bioethanol, (vi) suspended cells exposed to 0 g L^{-1} of bioethanol.

3.3.2.2 Relative expression of genes involved in ethanol stress response of *S. cerevisiae*

Ethanol tolerance constitutes an important trait of the strains applied in alcoholic fermentations, which is crucial particularly for *S. cerevisiae*, a strain traditionally employed in alcoholic beverage and bioethanol production [Grbin and Jiranek, 2004]. However, the performance of *S. cerevisiae* can be compromised by the negative impact of bioethanol accumulation on cell vitality during fermentation, limiting the productivity and bioethanol yield of the process [Stanley et al., 2010;Galeote et al., 2001]. Previous studies have demonstrated that the concentration of bioethanol in excess of 9% v/v can affect the growth of *S. cerevisiae* resulting in different cellular effects related to changes in membrane fluidity, protein misfolding and chromatin condensation [Fujita et al., 2004;Ma and Liu, 2010]. Ethanol stress induces heat shock proteins (HSP) that appear to be similar to those induced by heat shock [Piper, 1995]. Although cells synthesise a range of HSPs, including *HSP104*, *HSP82*, *HSP70*, *HSP26*, *HSP30* and *HSP12* upon yeast exposure to bioethanol, only *HSP104* and *HSP12* have been confirmed to physiologically influence yeast tolerance to bioethanol [Stanley et al., 2010].

The relative expression of *HSP12* and *HSP104* was monitored during bioethanol fermentations performed at 30 ^{o}C using both immobilised and freely suspended cells exposed to 90 g L^{-1} initial bioethanol content (Figure 3.3.4A-B). The results presented demonstrate the stress-protective role of BBB against high bioethanol concentrations, given that transcription from both genes monitored was significantly lower as compared to the conventional system. The mRNA expression level of *HSP12* in suspended cells exhibited 0.3- and 1.0-fold increase following 1 and 3 h, respectively, at the control experiment, while 1.5- and 2.8-fold increase ($p < 0.05$) was obtained over the same period respectively, following exposure of cells to 90 g L^{-1} of initial bioethanol content. However, transcription was only increased by 0.5- and 0.8-fold using the immobilised biocatalyst upon exposure to 0 and 90 g L^{-1} of initial bioethanol content following 3 h of fermentation respectively. Lower relative expression levels of the gene encoding *HSP104* were additionally observed using BBB. Although the relative expression level of *HSP104* was slightly increased using free cells of *S. cerevisiae* at the control experiment (0.5- and 0.7-

fold increase at 1 and 3 h respectively), transcription was rapidly up-regulated under exposure of cells to 90 g L^{-1} of initial bioethanol content demonstrating 1.3- and 3.15-fold increase in expression from *HSP104* following 1 and 3 h respectively. Moreover, activation of *HSP104* using immobilised cells of *S. cerevisiae* at both fermentation conditions applied was only increased by 0.9- and 1.0-fold at the control experiment and 0.6- and 0.3-fold under exposure of cells to 90 g L^{-1} initial bioethanol content.

S. cerevisiae ethanol stress response includes the regulation of metabolic pathways, signal transduction and protein folding control [Ding et al., 2010]. Several highly expressed, cell wall-related genes were previously tested for enhancing ethanol tolerance, encoding *HSP150*, *SPI1*, *SSD1*, *SED1* and *TIP1* [Zhao et al., 2017]. Various studies have explored genetic recombination technologies to improve yeast tolerance to ethanol, while the wild type strain is capable of resisting up to 9% v/v [Liu et al., 2023]. Expression of *HSP12* has been confirmed to correlate with various environmental stresses such as heat shock, freezing, desiccation and osmotic stress [Pacheco et al., 2009]. However, quantification of the native HSP12 protein in response to stress has not been performed to date [Leger et al., 2021]. Karreman et al., [2005] demonstrated that fusion protein GFP-Hsp12, regulated by the *HSP12* promoter, was synthesized upon entry of yeast cells to stationary phase as well as salt, osmotic, ethanol and heat stresses. Similarly, *HSP104* has been proposed to act as an ATP-dependent "molecular crowbar" that can pry aggregated proteins apart, permitting other chaperones to gain access to otherwise inaccessible hydrophobic surfaces sequestered in the aggregates, thereby facilitating protein refolding [Lum et al., 2004]. The lower levels of *HSP12* and *HSP104* relative mRNA expression using cell attachment on biochar as compared to freely suspended cells demonstrates the beneficial use of the proposed technology against high ethanol concentrations, improving the tolerance of the wild-type *S. cerevisiae* avoiding genetic modification to gain the specific trait.

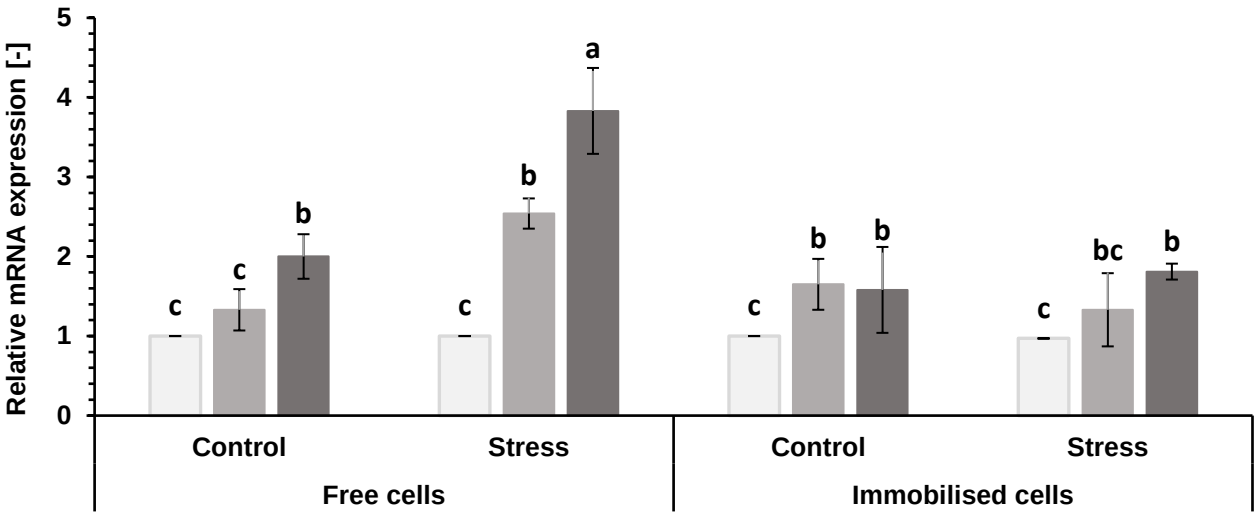

Figure 3.3.4A: Relative expression level of *HSP12* gene induced by ethanol stress during each fermentation conducted. Bars marked as "Control" refer to experiments conducted using 0 g L^{-1} initial bioethanol content, while "Stress" denotes application of 90 g L^{-1} initial bioethanol concentration. Light, medium and dark colour groups correspond to measurements conducted at 0, 1 and 3 h respectively.

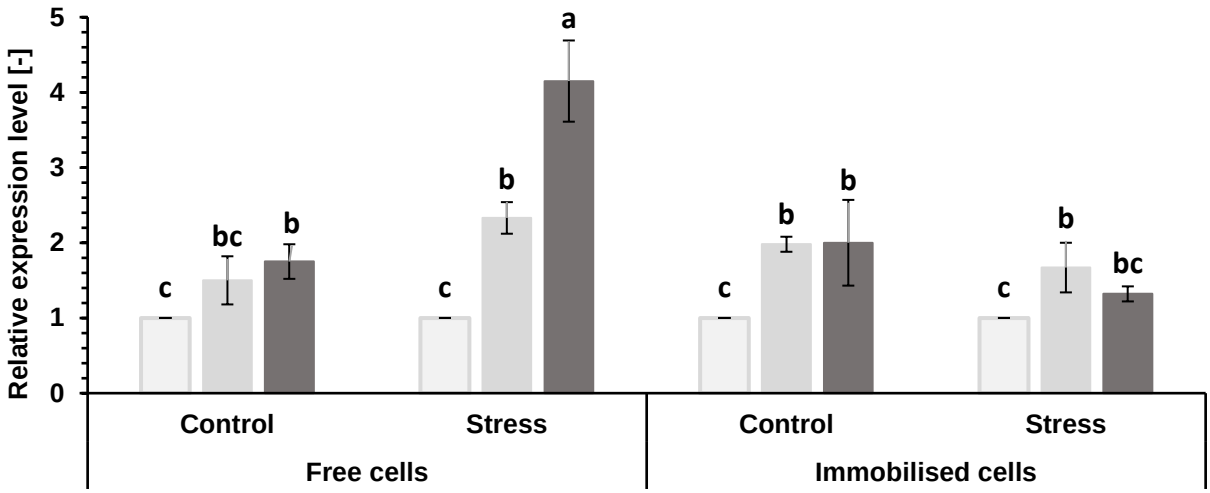

Figure 3.3.4B: Relative expression level of *HSP104* gene induced by ethanol stress during each fermentation conducted. Bars marked as "Control" refer to experiments conducted using 0 g L^{-1} initial bioethanol content, while "Stress" denotes application of 90 g L^{-1} initial bioethanol concentration. Light, medium and dark colour groups correspond to measurements conducted at 0, 1 and 3 h respectively.

3.3.3 *S. cerevisiae* bioethanol fermentations under osmotic stress

3.3.3.1 Biofuel fermentations under osmotic stress

Bioethanol fermentations were conducted via biomedium supplementation with 1 M NaCl, exposing both suspended and immobilised cells to osmotic stress (Figure 3.3.5A-B). The maximum net bioethanol concentration formed in both cultures was not significantly different yielding 27.4 and 28.7 g L^{-1} of bioethanol using free and immobilised cells respectively. However, faster bioethanol production kinetics were observed using *S. cerevisiae* cells immobilised on biochar maximising biofuel concentration at 9 h via consumption of 66.1 g L^{-1} glucose, while suspended cells required 15 h to reach the maximum bioethanol content utilising 61.9 g L^{-1} of glucose. Thus, the productivity achieved with the use of BBB and free cells reached 3.0 and 1.8 g L^{-1} h^{-1} respectively, indicating the osmoprotective function of biochar in the bioprocess.

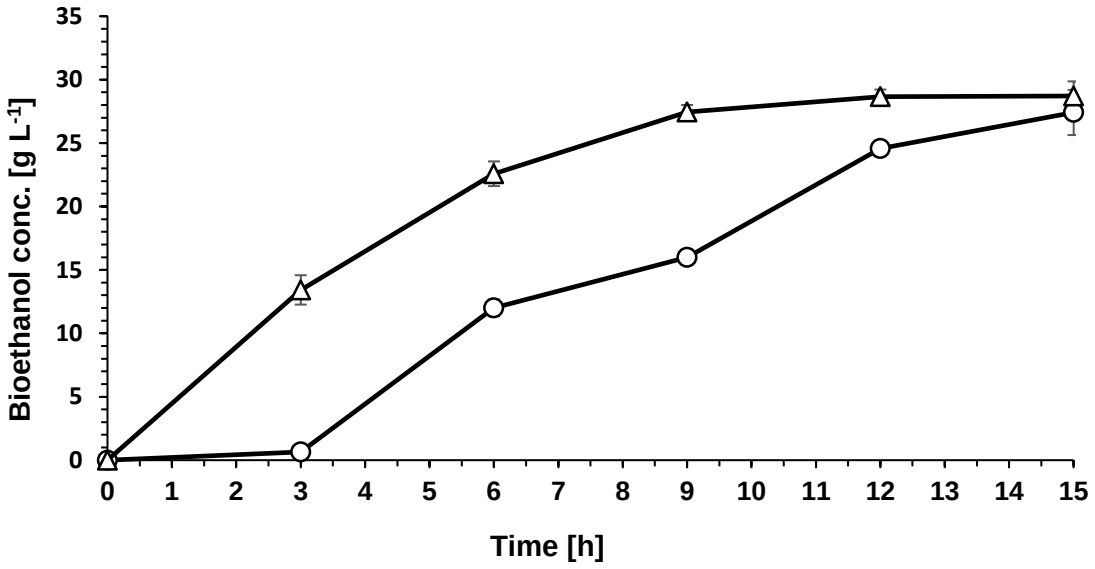

Figure 3.3.5A: Bioethanol production achieved under exposure of immobilised and suspended cells of *S. cerevisiae* to 1 M NaCl. Symbols correspond to: (i) —△— immobilised cells and (ii) —○— suspended cells.

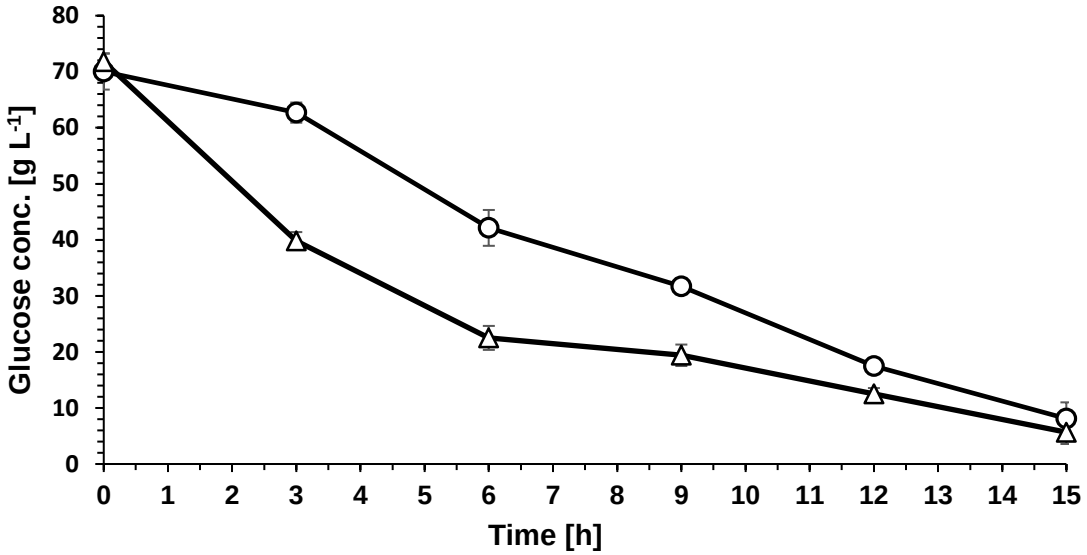

Figure 3.3.5B: Glucose consumption achieved under exposure of immobilised and suspended cells of *S. cerevisiae* to 1 M NaCl. Symbols correspond to: (i) —△— immobilised cells and (ii) —○— suspended cells.

3.3.3.2 Accumulation of intracellular proline in immobilised and suspended cultures of *S. cerevisiae* under osmotic stress

It is well established that the osmotic stress response signalling pathway of *S. cerevisiae* is crucial for the survival of cells under osmotic stress [Thorne et al., 2011]. The mRNA expression levels of *HSP26* as well as the production of proteins related to translation and stress response were increased in *S. cerevisiae* following addition of 1 M NaCl [Hirasawa et al., 2009]. Moreover, batch and fed-batch fermentations of *S. cerevisiae* conducted under high salt and sugar concentration induced osmotic stress that stimulated increased formation of glycerol, acetic acid and acetaldehyde as byproducts [Frohman and de Orduna, 2013], while proline can be accumulated in cells as membrane stabilizer, protein-folding chaperone and reactive oxygen species scavenger during the inhibitory bioprocess condition [Kaul et al., 2008]. Therefore, the intracellular proline content was monitored during the aforementioned bioethanol fermentations conducted under 1 M NaCl, confirming the protective role of biochar against osmotic stress in *S. cerevisiae* (Figure 3.3.6). The concentration of proline in free cells was significantly increased following 12 h of cultivation (2.5 μmol proline g^{-1} wet cell mass), while the BBB-based culture accumulated 1.2 μmol proline g^{-1} wet cell mass intracellularly over the same period. The results suggested that proline levels in suspended cells were at least 2-fold higher as compared to the immobilised system demonstrating that the occurrence of osmotic stress in the conventional process was more profound stimulating enhanced proline accumulation to tackle the inhibition that resulted in reduced bioprocess performance.

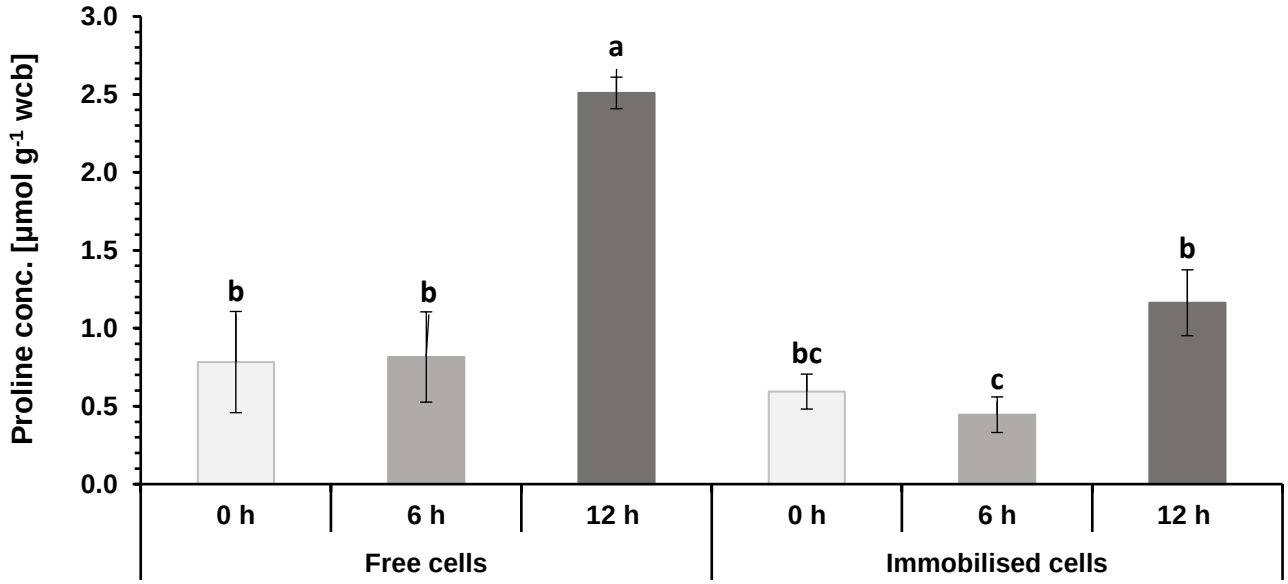

Figure 3.3.6: Accumulation of intracellular proline in bioethanol fermentations conducted employing suspended and immobilised cells of *S. cerevisiae*. Light, medium and dark colour groups correspond to measurements conducted at 0, 6 and 12 h respectively.

3.4 Development of continuous bioethanol fermentation using *S. cerevisiae* immobilised on char derived from car tire waste

3.4.1 Repeated batch fermentations of *S. cerevisiae* for bioethanol production immobilised on different types of tire waste char

Non-biological char obtained from car tire waste was investigated as a potential support material for cell immobilization aiming to enhance bioethanol production though immobilization of *S. cerevisiae*. Due to favorable characteristics previously examined in Chapter 3.1 carbonaceous materials produced from car tire waste could be efficiently used in major industrial bioprocess.

S. cerevisiae immobilised on PWB, PLC and UNC was employed in two repeated batch fermentations at the elevated temperature of 37 ^{o}C to evaluate the capacity of the developed biocatalysts to enhance bioethanol production as compared to the conventional system (Figure 3.4.1A-B). The efficiency of the developed biocatalysts to enhance bioethanol fermentations was determined as opposed to freely suspended cells. During the first batch, the developed biocatalyst employing UNC achieved faster kinetics as well as higher bioethanol concentration compared to free cells and the immobilised PWC and PLC biocatalysts reaching 33.0 g L^{-1} of bioethanol and 3.30 g L^{-1} h^{-1} productivity. Moreover, recycling of all biocatalysts in a subsequent batch fermentation demonstrated that *S. cerevisiae* immobilised on UNC exhibited the highest bioethanol productivity generating net production of 30.6 g L^{-1} within 6 h of fermentation, reaching productivity of 5.10 g L^{-1} h^{-1}. Nevertheless, during the second batch fermentation, the PLC-based biocatalyst and the freely suspended culture produced 25.5 and 26.3 g L^{-1} of bioethanol respectively within 6 h of fermentation. Bioethanol production using *S. cerevisiae* immobilised on PWC was substantially lower as compared to the rest of the experiments conducted. Similarly to bioethanol formation, faster glucose consumption was observed using *S. cerevisiae* immobilised on UNC and PLC biocatalysts compared to cells immobilised on PWC as well as the freely suspended culture at both batch experiments applied (Figure 3.4.1B). The results presented confirmed that the UNC-based biocatalyst generated substantially higher bioethanol contents compared to the conventional process and it could serve as an

efficient support material for the production of biofuels. Moreover, the PLC-based system also performed elevated bioethanol production and its use was proposed for further experiments.

Although several studies have been conducted relevant to different applications of char produced from car tire waste, this is the first effort focusing on the development of such biocatalysts employing the specific material as carrier for the enhancement of biofuel production. The main applications proposed include activated carbon as adsorbents prepared by modifying tire char, rubber reinforcing materials (commercial carbon black), battery materials, catalyst support materials and asphalt additives [Gao et al., 2022].

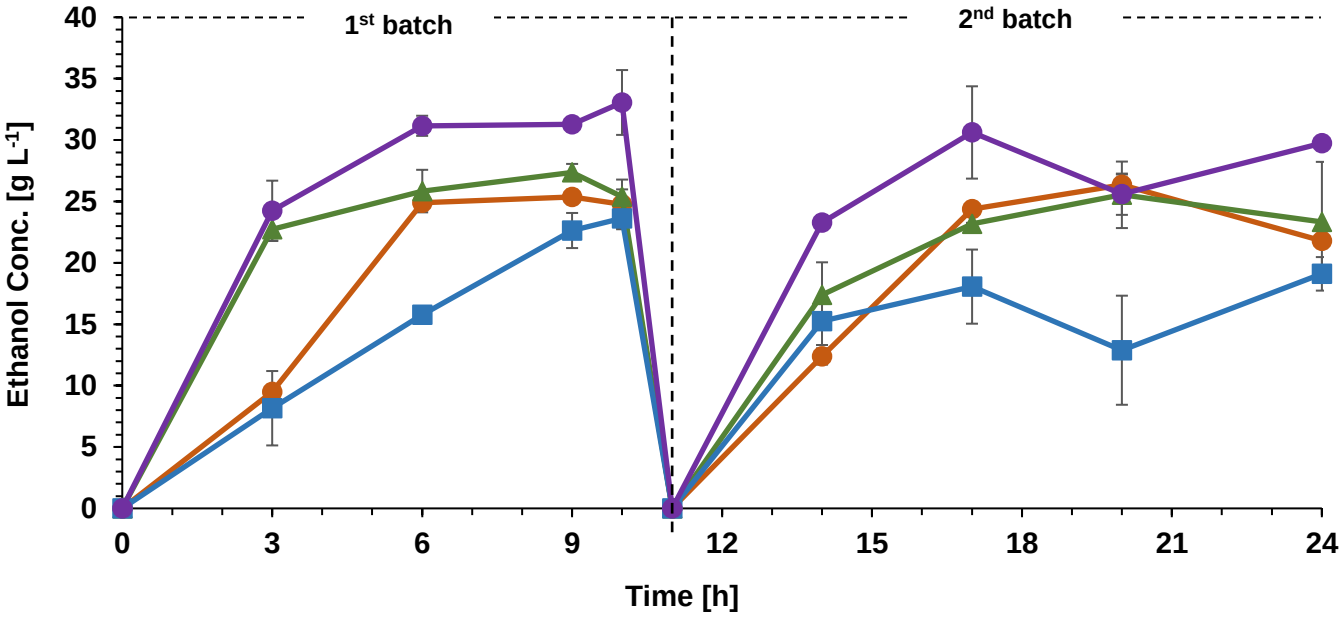

Figure 3.4.1A: Bioethanol production achieved at 37 ^{o}C using immobilised and suspended cells of *S. cerevisiae*. Symbols correspond to *S. cerevisiae*: (i) immobilised cells on UNC, (ii) immobilised cells on PLC, (iii) immobilised cells on PWC, (iv) freely suspended cells.

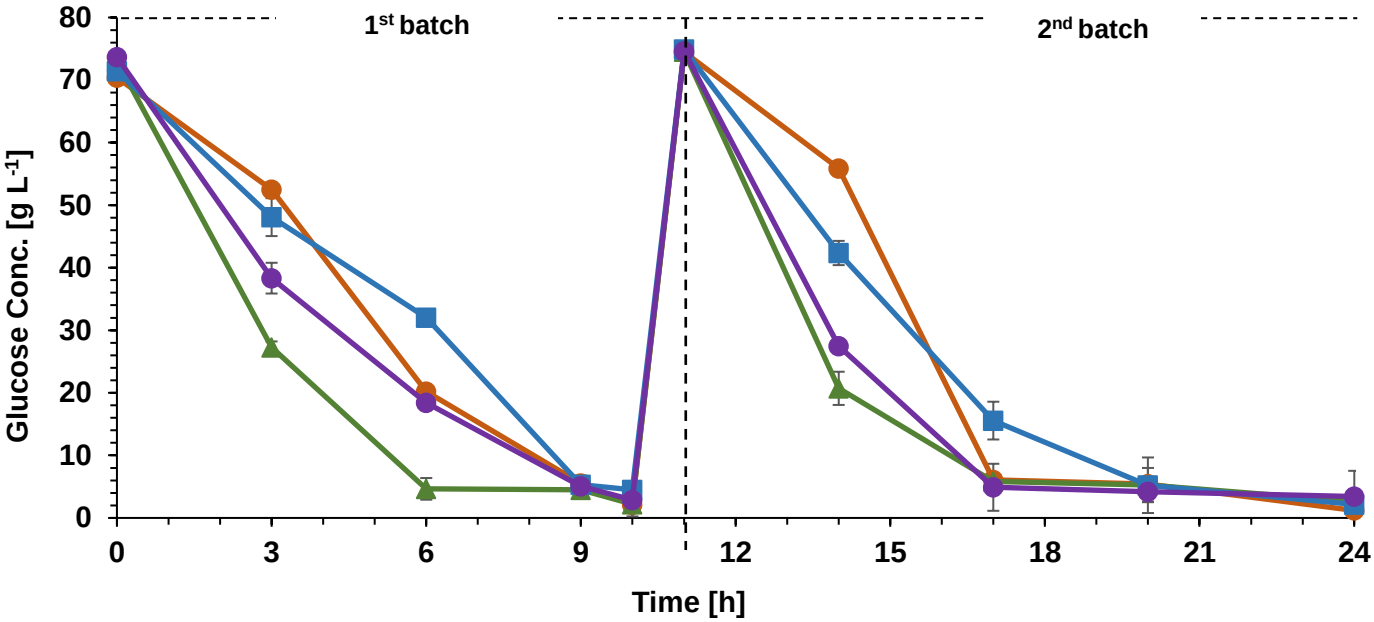

Figure 3.4.1B: Glucose consumption achieved at 37 ^{o}C using immobilised and suspended cells of *S. cerevisiae*. Symbols correspond to *S. cerevisiae*: (i) immobilised cells on UNC, (ii) immobilised cells on PLC, (iii) immobilised cells on PWC, (iv) freely suspended cells.

3.4.2 Repeated batch fermentations of *S. cerevisiae* for ethanol production immobilised on UNC and PLC at the elevated temperature of 39 ºC

S. cerevisiae immobilised on UNC and PLC was applied in six repeated batch fermentations to assess the efficiency of the developed biocatalysts in ethanol production at the elevated temperature of 39 ºC (Figure 3.4.2A-B). Overall, both immobilised biocatalysts performed faster kinetics as well as higher bioethanol production as opposed to the respective freely suspended cells system at all repeated batches performed. More specifically, the maximum net ethanol production during the first batch, achieved by immobilised cells using PLC generated 31.2 g L^{-1} reaching productivity of 4.0 g L^{-1} h^{-1}. Similarly, cells immobilised on UNC produced 30.1 g L^{-1} of bioethanol reaching productivity of 5.0 g L^{-1} h^{-1}, while the freely suspended system produced 25.8 g L^{-1} of bioethanol over the same period (4.3 g L^{-1} h^{-1}). *S. cerevisiae* immobilised on UNC demonstrated faster kinetics during the second batch reaching productivity of 8.0 g L^{-1} h^{-1}, while cells immobilised on PLC and freely suspended cells yielded 4.7 and 3.6 g L^{-1} h^{-1}. During the three last batches of the experiment performed, net bioethanol production as well as productivity was not significantly different among the biocatalysts used. However, the freely suspended culture demonstrated decrease over the experiment in terms of bioethanol production and productivity.

S. cerevisiae immobilised on UNC demonstrated faster kinetics at all batches performed as opposed to unsupported cells. Thus, recycling the biocatalyst in sequential batch fermentations confirmed that yeast cells attached to UNC demonstrated productivity that ranged between 4.0 and 8.0 g L^{-1} h^{-1}, as opposed to freely suspended cells that reached productivity between 3.2 and 4.5 g L^{-1} h^{-1}. The glucose consumption achieved by immobilised cells using both support materials was similar and substrate quantities were utilized faster by immobilised *S. cerevisiae* cells as compared to the suspended culture.

Free and immobilised cells of *S. cerevisiae* in sodium alginate were previously used in four batches for bioethanol production using galactose. The reusability of the immobilised yeast achieved maximum ethanol concentration, while the product concentration and the yeast relative activity were reduced insignificantly during the first and the third cycle demonstrating that the

immobilised yeast was still stable and could be used for the next batch fermentation. However, bioethanol concentration was reduced significantly following the third cycle indicating that the immobilised yeast inside the beads was deactivated [Azhar and Abdulla, 2018]. Seven cycles of repeated batch fermentation using *S. cerevisiae* yeast cells immobilised in alginate beads for bioethanol production were conducted confirming the gradual increase in bioethanol concentration. Immobilised yeast cells enabled repetitive production of ethanol for 7 cycles displaying fermentation efficiency of 79% for five consecutive cycles [El-Dalatony et al., 2016].

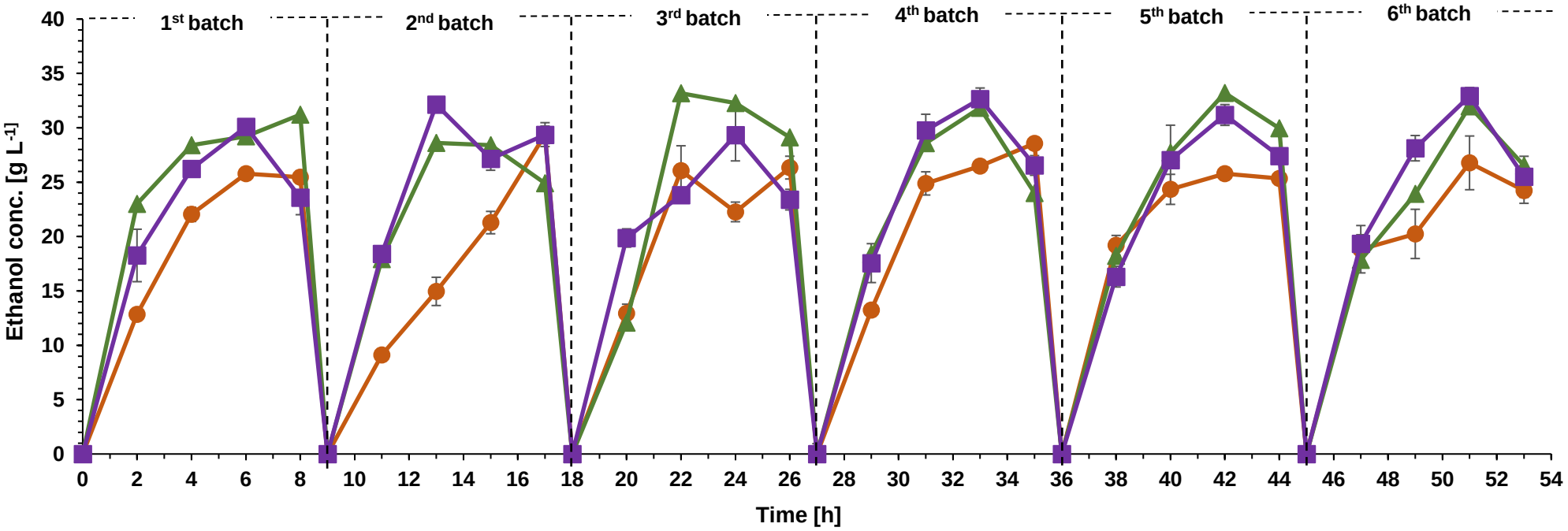

Figure 3.4.2A: Bioethanol production achieved at 39 ^{o}C using immobilised and suspended cells of *S. cerevisiae*. Symbols correspond to *S. cerevisiae*: (i) immobilised cells on UNC, (ii) immobilised cells on PLC, (iii) freely suspended cells.

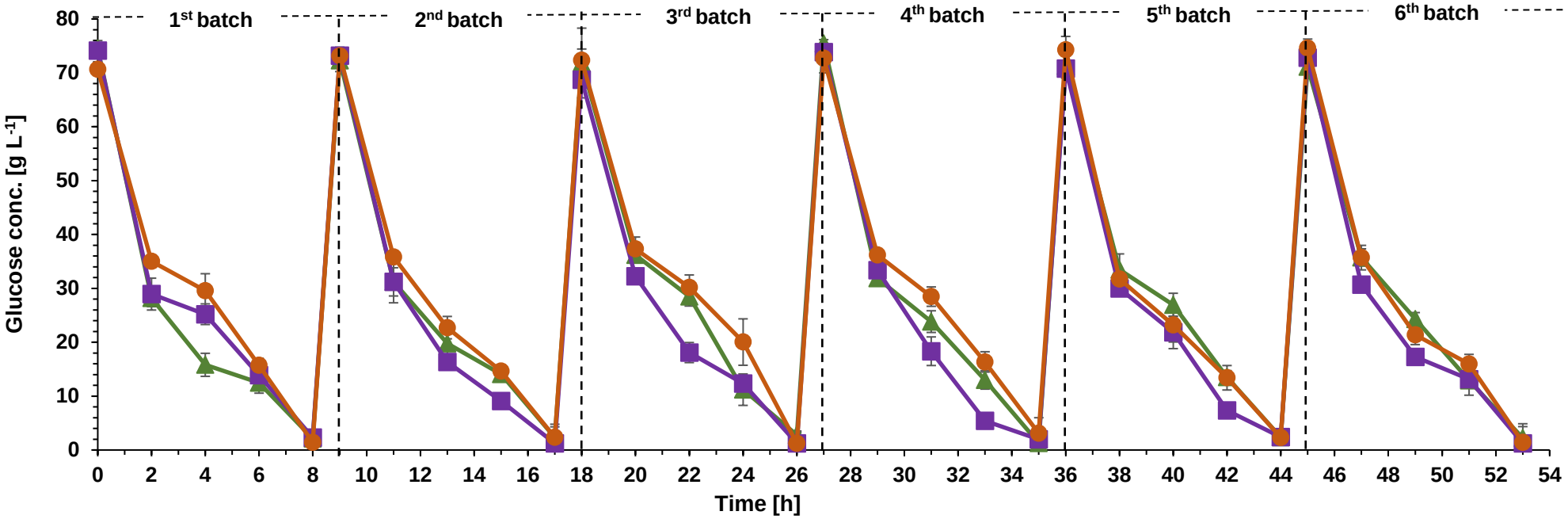

Figure 3.4.2B: Glucose consumption achieved at 39 ^{o}C using immobilised and suspended cells of *S. cerevisiae*. Symbols correspond to *S. cerevisiae*: (i) immobilised cells on UNC, (ii) immobilised cells on PLC, (iii) freely suspended cells.

3.4.3 Repeated batch fermentations of *S. cerevisiae* for ethanol production immobilised on UNC and PLC at the elevated temperature of 41 ºC

The carriers used in the aforementioned experiments as well as free cells of *S. cerevisiae* were employed in six repeated batch fermentations at the elevated temperature of 41 ºC, given that temperature tolerance constitutes an important trait of the strains applied in alcoholic fermentation (Figure 3.4.3A-B). Overall, both immobilised biocatalysts achieved higher bioethanol concentration and productivity at all batches performed. *S. cerevisiae* cells immobilised on UNC achieved maximum net ethanol production at the first five batches generating 34.7 g L^{-1} of the biofuel reaching productivity that ranged between 4.0 g L^{-1} h^{-1} and 8.5 g L^{-1} h^{-1}. During the last batch performed, cells immobilised on UNC demonstrated slight decrease in bioprocess performance. Although cells immobilised on PLC demonstrated lower ethanol production as opposed to the UNC-based system, the productivity was slightly improved during the recycling of the biocatalyst in subsequent experiments demonstrating values that ranged between 3.77 g L^{-1} h^{-1} and 8.77 g L^{-1} h^{-1}. The freely suspended culture exhibited substantially reduced efficiency achieving maximum production 26.2 g L^{-1} of ethanol, which was further decreased to 20.47 g L^{-1} following six repeated batches, while bioethanol productivity ranged between 3.69 g L^{-1} h^{-1} and 5.0 g L^{-1} h^{-1} in all experiments conducted.

Although cells immobilised on UNC exhibited higher ethanol production over the first 5 cycles as compared to those immobilised on PLC, the consumption of sugars was initially similar in both fermentations. Higher substrate quantities were utilized by cells immobilised on UNC during the second and fifth cycle while the consumption of glucose using freely suspended cells of *S. cerevisiae* was significant lower (Figure 3.4.3B). Overall, faster glucose consumption was achieved using both immobilised biocatalysts as opposed the freely suspended cells.

Immobilised coculture of *K. marxianus* and *S. cerevisiae* was performed aiming to improve bioethanol production as well as the stability of bioethanol fermentation at elevated temperatures [Eiadpum et al., 2012]. The results indicated that the cocultivation of the two strains could improve ethanol production at

temperatures ranging between 33 ºC and 45 ºC. Higher temperature tolerance was achieved when the coculture was immobilised resulting in elevated bioethanol concentrations as compared to the suspended culture. The coculture immobilised on thin-shell silk cocoon and fermented at 37 ºC and 40 ºC generated maximal ethanol concentrations of 81.4 and 77.3 g L^{-1} respectively, which were 5.9–8.7% and 16.8–39.0% higher than those of the suspended culture, respectively. Production of bioethanol at elevated temperatures was also assessed using *K. marxianus* IMB3 immobilised in calcium alginate [Gough et al., 1998]. Maximum concentration of bioethanol obtained was 60 g L^{-1} using 140 g L^{-1} sugars from molasses into the system representing 84% of the maximum theoretical yield at the elevated temperature of 45 ºC.

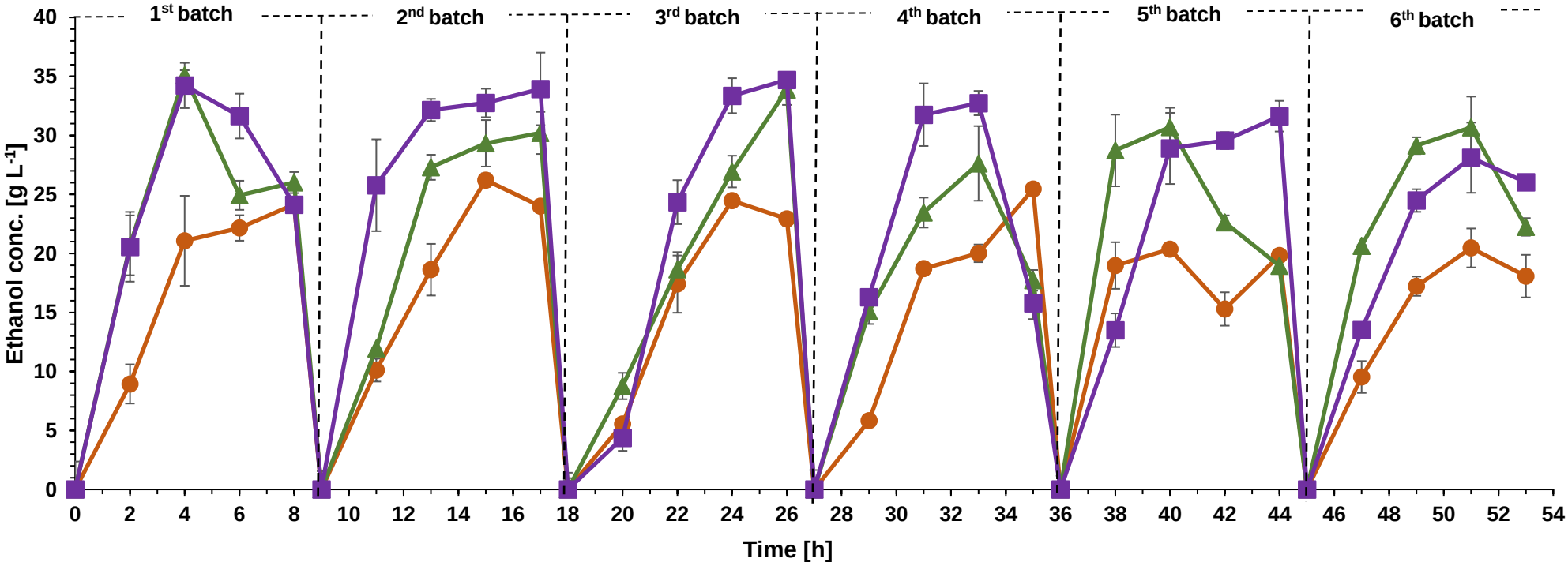

Figure 3.4.3A: Bioethanol production achieved at 41 ^{o}C using immobilised and suspended cells of *S. cerevisiae*. Symbols correspond to *S. cerevisiae*: (i) immobilised cells on UNC, (ii) immobilised cells on PLC, (iii) freely suspended cells.

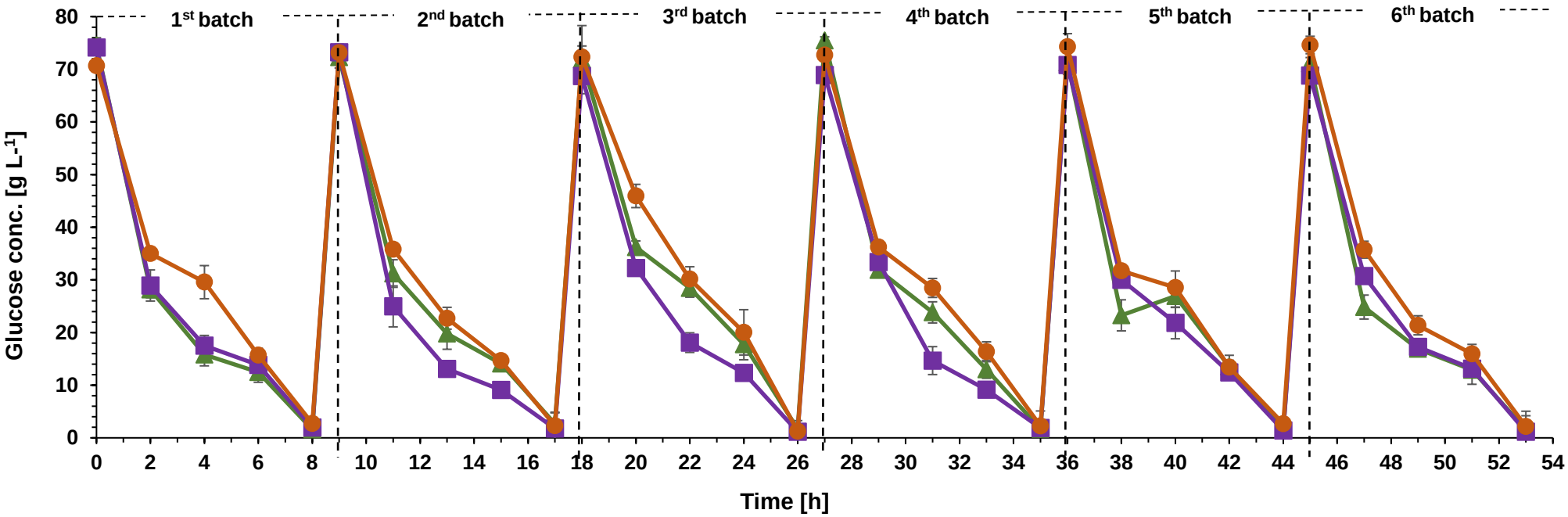

Figure 3.4.3B: Glucose consumption achieved at 41 ^{o}C using immobilised and suspended cells of *S. cerevisiae*. Symbols correspond to *S. cerevisiae*: (i) immobilised cells on UNC, (ii) immobilised cells on PLC, (iii) freely suspended cells.

3.4.4 Continuous bioethanol fermentations in a lab-scale bioreactor using UNC-based biocatalyst at different temperatures and dilution rates

Fermentations at high temperatures offer several advantages, such as energy savings through reduced cooling costs and lower costs during the distillation process for ethanol separation, while reducing the contamination risk [Shahsavarani et al., 2013]. The performance of free and immobilised cells of *S. cerevisiae* were compared in continuous bioethanol fermentations using different dilution rates. Continuous experiments were conducted by feeding 70 g L^{-1} glucose as substrate, while the temperature was set at 37, 39 and 41 ^{o}C as described below.

3.4.4.1 Continuous bioethanol production at 37 ^{o}C using free cells of *S. cerevisiae*

Bioethanol production and sugar consumption achieved by free cells of *S. cerevisiae* at 37 °C for each dilution rate (0.09, 0.13, and 0.17 h^{-1}) assessed are depicted in Figure 3.4.4A. The pH-value monitored as well as the biomass content of free cells are illustrated in Figure 3.4.4B. The continuous fermentation lasted a total of 95 h, evaluating the effect of three different dilution rates as follows: i) 0.09 h^{-1} between 0 – 35 h (D_1), ii) 0.13 h^{-1} (D_2, 35–67 h) and iii) 0.17 h^{-1} (D_3, 67–95 h) (Figure 3.4.4C). The production of bioethanol at D_1 using free cells of *S. cerevisiae* achieved maximum net bioethanol concentration 40.1 g L^{-1} following 21 h of experiment. The steady-state using 0.09 h^{-1} was obtained following 11 h of fermentation, where bioethanol concentration reached 35.0 g L^{-1} ($p > 0.05$). Under steady-state conditions bioethanol productivities achieved ranged between 3.15-3.60 g L^{-1} h^{-1}. During the first 35 h stable bioethanol production was observed and the concentration ranged between 37.5-40.1 g L^{-1} ($p < 0.05$).

When the dilution rate changed and increased at 0.13 h^{-1}, bioethanol production remained stable for the next 30 h with a slight decrease observed at 70 h of experiment were the concentration dropped to 25 g L^{-1}. Bioethanol productivity during fermentation conducted using 0.13 h^{-1} ranged between 3.34-4.47 g L^{-1} h^{-1}. Additionally, glucose concentration increased upon dilution rate

increase which indicates the reduction of the consumption rate. Moreover, *S. cerevisiae* biomass remained stable during fermentation at the first two dilution rates (D_1 and D_2) applied. However, upon dilution rate increase to D_3, biomass was rapidly reduced from 1.92 to 0.82 g L^{-1} (57 % reduction), demonstrating that the increased dilution rate resulted in wash out of cells. Therefore, between 74 – 82 h bioethanol productivity was 4.66 g L^{-1} h^{-1} and it was gradually reduced throughout the fermentation to 2.75 g L^{-1} h^{-1} after 95 h of experiment, while *S. cerevisiae* cells were eventually washed out.

S. cerevisiae is the most widely used yeast for industrial ethanol production based on a number of favorable characteristics that include, among others, resistance to osmotic pressure, high bioethanol production, low by-product formation as well as resistance to high concentrations of ethanol and sugars [Mohd et al., 2017]. Thus, various studies have explored bioethanol production using *S. cerevisiae* employing continuous systems at 37 °C [Wilkins et al., 2007]. *S. cerevisiae* TJ14 demonstrated effective production of bioethanol reaching 45 g L^{-1} through simultaneous saccharification and fermentation of 100 g (w/v) L^{-1} cellulose using continuous flow bioreactors [Shahsavarani et al., 2013]. Continuous bioethanol fermentations with free cells of *S. cerevisiae* NCIM 3095 were carried out in a 20 L bioreactor using two different dilution rates 0.09 h^{-1} and 0.24 h^{-1} employing glucose as the sole carbon source (48.3 g L^{-1}) and fermentation temperature of 32 °C. During first dilution rate (0.09 h^{-1}) maximum concentration of bioethanol (31.5 g L^{-1}) was reached, which was decreased due to continuous separation of bioethanol by microfiltration. Increasing the dilution rate to 0.24 h^{-1} the bioethanol concentration reached 23 g L^{-1} [Saha et al., 2019]. Tan et al. (2015) studied continuous bioethanol fermentation using raw and thick juice of sugar beet which can fermented by *S. cerevisiae* strain KF-7, generating 70.7 g L^{-1} bioethanol concentration and 21.2 g L^{-1} h^{-1} bioethanol productivity by single stage fermentation of raw juice at 0.3 h^{-1} dilution rate. Moreover, bioethanol concentration of 80 g L^{-1} and productivity of 8.8 g L^{-1} h^{-1} were achieved employing a dilution rate of 0.11 h^{-1}. *S. cerevisiae* CHFY0321 was also used to produce bioethanol from cassava pulp in a continuous flow bioreactor at two different flow rates (0.028 $h^{-1}$and 0.031 h^{-1}) achieving final bioethanol concentration of 86.1 g

L^{-1}. Stable biofuel production was achieved at 0.028 h^{-1} that ranged between 85–86 g L^{-1}. However, in an attempt to improve productivity, the increase of dilution rate to 0.031 h^{-1} disturbed stable bioethanol production. However, when the dilution rate reduced to 0.028 h^{-1} the continuous process appeared to reach a near steady state over 5 d [Moon et al., 2012].

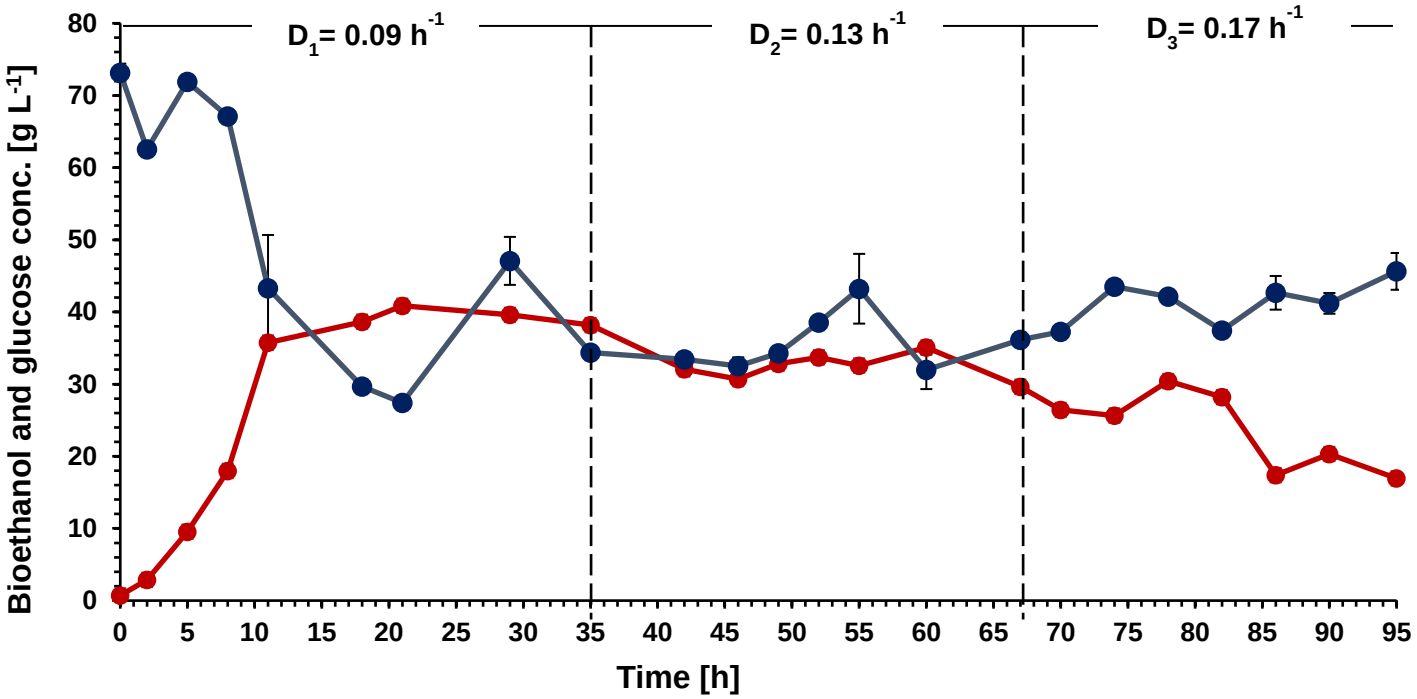

Figure 3.4.4A: Bioethanol production and glucose consumption achieved at 37 ºC using freely suspended cells of *S. cerevisiae* in a continuous bioreactor under different dilution rates (0.09, 0.13 and 0.17 h^{-1}). Symbols correspond to: (i) bioethanol concentration, (ii) glucose concentration.

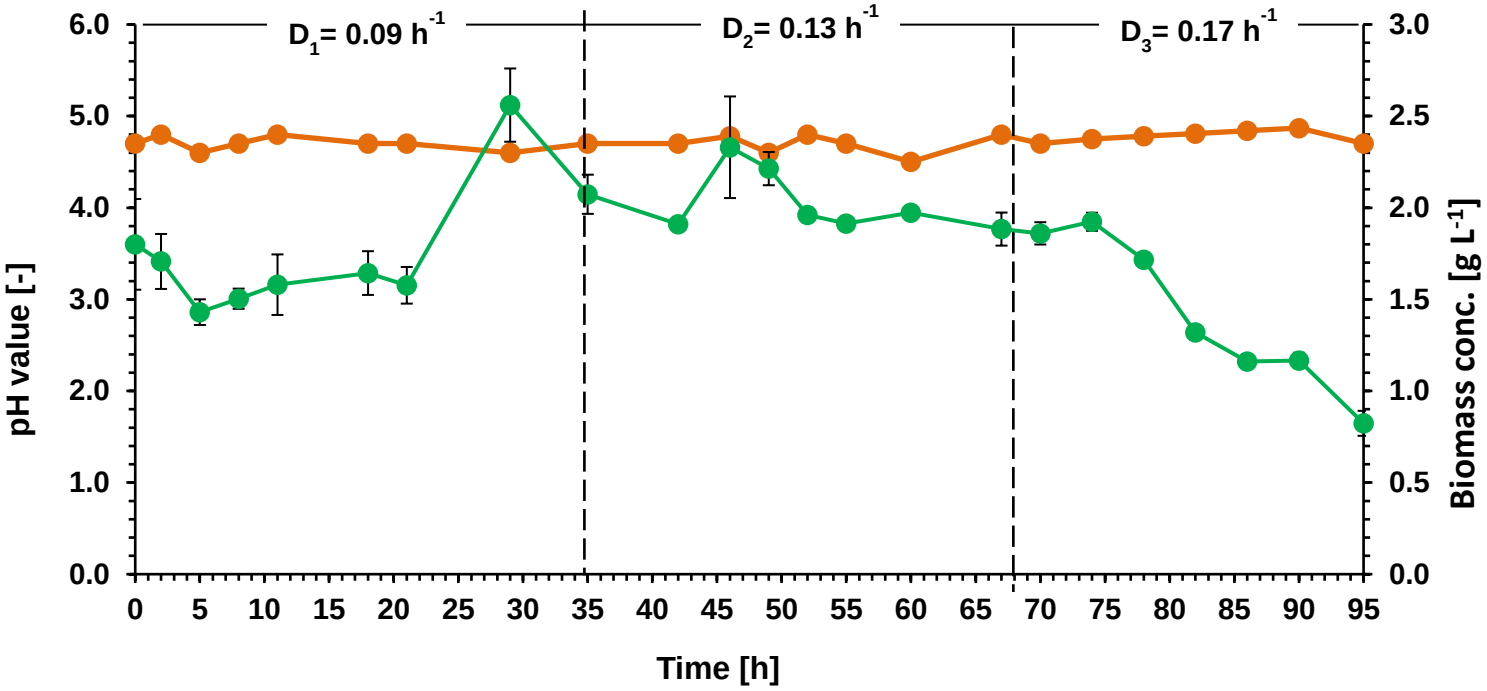

Figure 3.4.4B: pH and biomass production achieved at 37 ºC using freely suspended cells of *S. cerevisiae* in a continuous bioreactor under different dilution rates (0.09, 0.13 and 0.17 h^{-1}). Symbols correspond to: (i) pH value, (ii) biomass concentration.

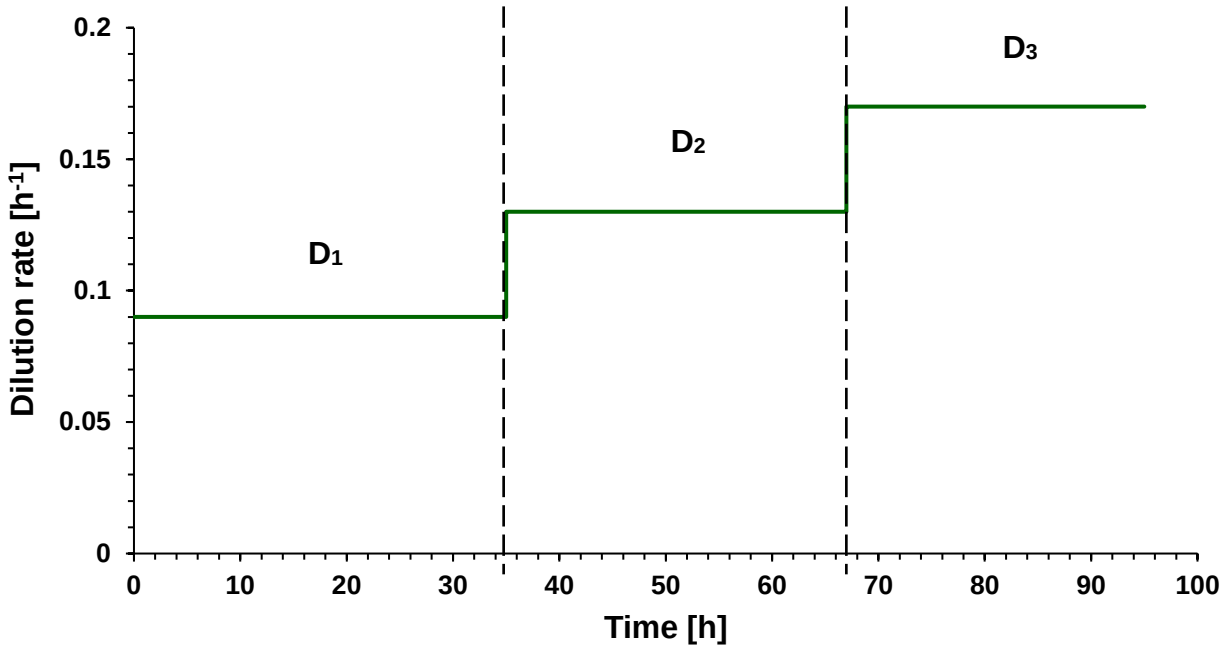

Figure 3.4.4C: Dilution rates applied during bioethanol fermentation experiments using free cells of *S. cerevisiae.*

3.4.4.2 Continuous bioethanol fermentation using immobilised cells of *S. cerevisiae*

Bioethanol production and glucose consumption using immobilised cells of *S. cerevisiae* on UNC was monitored in continuous experiments conducted at 37 °C and dilution rates 0.09, 0.13, 0.17 and 0.20 h^{-1} (Figure 3.4.4D). Additionally, the pH was monitored during the fermentation as depicted in Figure 3.4.4E. The experiment performed using immobilised cells produced 42 g L^{-1} of bioethanol following 8 h of experiment using 0.09 h^{-1} (Figure 3.4.4F) reaching productivity of 3.80 g L^{-1} h^{-1}, which was slightly higher as compared to that obtained using the conventional culture. Thus, the steady state bioethanol concentration established between 11 – 35 h of experiment ranged between 38 – 40 g L^{-1} ($p > 0.05$). Increasing the dilution rate to 0.13 h^{-1} resulted in steady state with bioethanol content of 36 – 38 g L^{-1}, while a slight increase in glucose concentration was also achieved. Further increase of the dilution rate to 0.17 h^{-1} resulted in stable performance of the immobilised system, under conditions that washed cells out of the conventional process. Thus, stable biofuel production occurred using 0.17 h^{-1} exhibiting bioethanol concentration that reached 38 g L^{-1} and bioethanol productivity of 6.61 g L^{-1} h^{-1}, as opposed to the freely suspended culture that demonstrated continuous decrease in bioethanol production. Although the immobilised system protected the process at 0.17 h^{-1}, further increase of the dilution rate to 0.20 h^{-1} resulted in washout. Bioethanol productivity was decreased to 2.9 g L^{-1} h^{-1} while bioethanol concentration was significantly decreased to 14.7 g L^{-1} following 117 h of experiment.

It has been previously demonstrated that fermentations can be significantly improved when a continuous fermentation is combined with cell immobilization [Verbelen et al., 2006]. However, although different cell immobilization approaches have been applied for bioethanol production using *S. cerevisiae*, as well as various methods and media, this is the first study to our knowledge carried out using a carbonaceous material as a support. Ghorbani et al, (2011) explored the production of bioethanol via immobilization of *S. cerevisiae* to sodium alginate beads in continuous flow bioreactors, where sugarcane molasses was used as carbon source. Four different dilutions rates were assessed (0.064, 0.096, 0.144, 0.192 h^{-1})

employing 50, 100 and 150 g L^{-1} of molasses that produced 6.32, 12.55 and 19.15 g L^{-1} of bioethanol respectively, using 0.064 h^{-1}. *S. cerevisiae M30* immobilised on loofah-enhanced alginate was also used for bioethanol production in a continuous fermentation packed bed bioreactor using initial sugar concentrations of 200 – 248 g L^{-1} employing sugarcane molasses. When the initial sugar concentration was at 200 – 220 g L^{-1}, ethanol productivity increased linearly with the dilution rate, from 0.1 to 0.2 h^{-1}, and then remained nearly constant. Employing a dilution rate of 0.2 h^{-1} maximized bioethanol productivity, achieving 11.5 g L^{-1} h^{-1}, while bioethanol concentration reached 57.4 g L^{-1}. Maximum net bioethanol concentration was achieved using a dilution rate of 0.11 h^{-1} that generated 82.1 g L^{-1} of bioethanol content, demonstrating that the concentration of bioethanol decreased with the increase of the dilution rate, similarly to the current study [Bangrak et al., 2011].

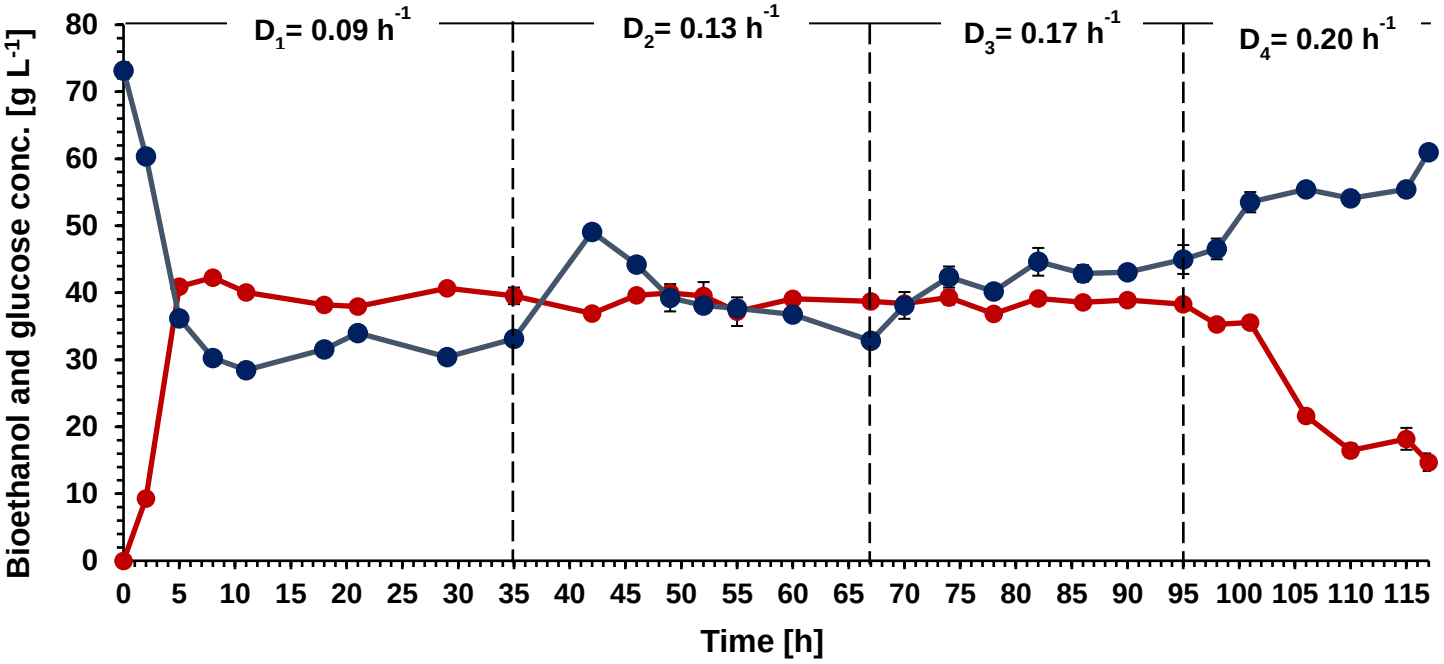

Figure 3.4.4D: Bioethanol production and glucose consumption achieved at 37 ºC using freely suspended cells of *S. cerevisiae* in a continuous bioreactor under different dilution rates (0.09, 0.13, 0.17 and 0.20 h^{-1}). Symbols correspond to: (i) bioethanol concentration, (ii) glucose concentration.

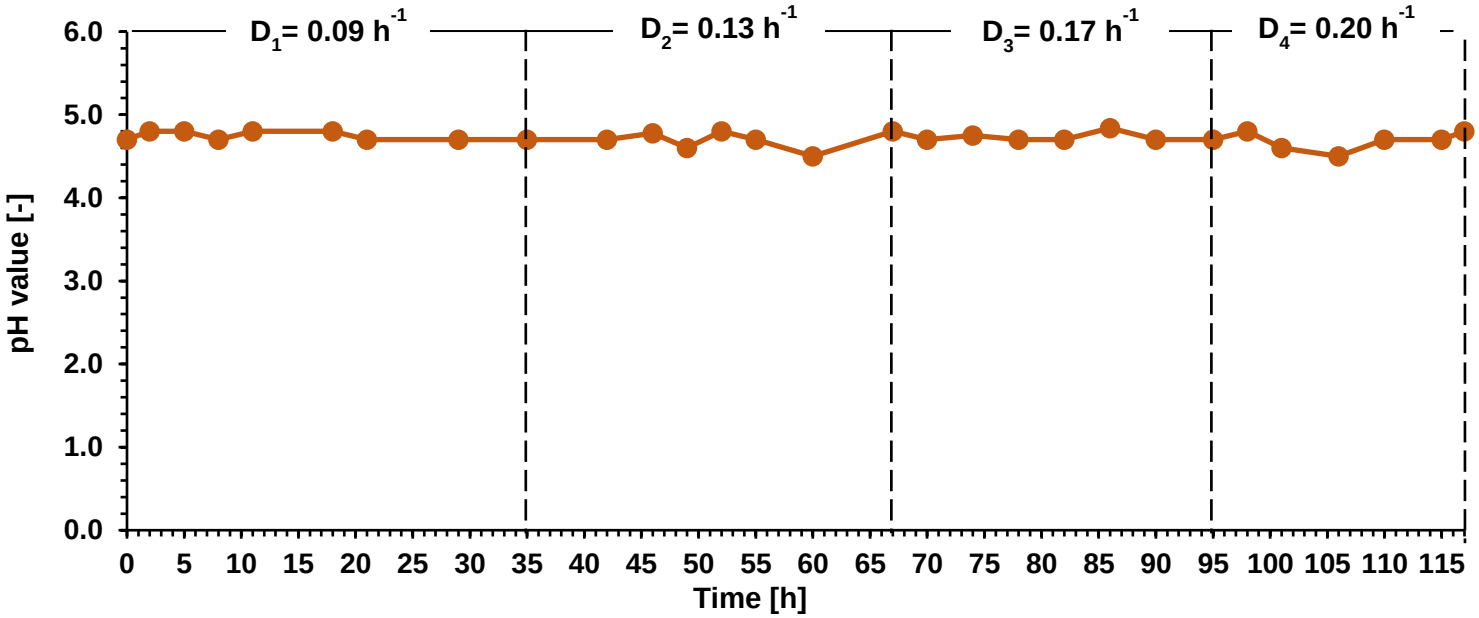

Figure 3.4.4E: pH monitored during fermentation conducted at 37 ^{o}C using immobilised cells of *S. cerevisiae* in a continuous bioreactor under different dilution rates (0.09, 0.13, 0.17 and 0.20 h^{-1}).

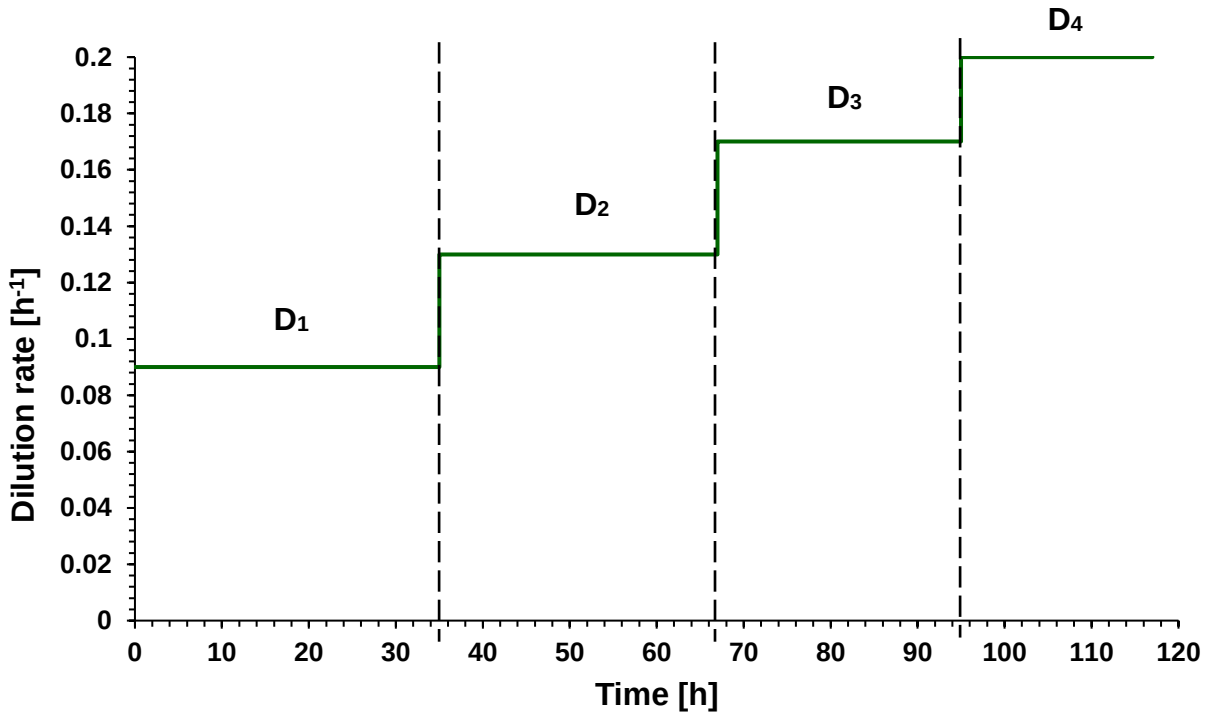

Figure 3.4.4F: Dilution rates applied during bioethanol fermentation experiments using immobilised cells of *S. cerevisiae.*

3.4.4.3 Continuous bioethanol fermentation at the elevated temperatures of 39 and 41 ºC using free cells of *S. cerevisiae*

Freely suspended cells were employed in continuous bioethanol fermentations conducted at inhibitory temperatures for *S. cerevisiae* (39 and 41 ºC) using dilution rates of 0.13 and 0.17 h^{-1} (Figure 3.4.4G). Employing 0.13 h^{-1} resulted in maximum bioethanol concentration of 33 g L^{-1} and productivity of 4.29 g L^{-1} h^{-1} at 25 h. Following establishment of steady state between 40 – 75 h aiming to assess the performance of the bioprocess under extreme temperature conditions, the temperature was increased from 39 to 41 ºC. Bioethanol concentration started decreasing from the initial stages of the temperature increase. Although the bioethanol concentrations were not significantly different upon temperature increase to 41 ºC, the free cells of *S. cerevisiae* were stressed due to the shock condition applied and a decrease in bioethanol content was observed when the temperature was reduced to 39 ºC at 75 h. Thus, bioethanol concentration decreased to 15.6 g L^{-1} upon dilution rate increase to 0.17 h^{-1} and it was gradually decreased to 13.0 g L^{-1} prior wash out. The inhibitory effect of the extreme temperature employed on bioprocess performance was also confirmed by the glucose concentration profile, which was substantially increased following the increase of temperature. Moreover, the biomass content decreased rapidly with the increase of temperature to 41 ºC from 1.57 to 1.35 g L^{-1}, while increasing the dilution rate 0.17 h^{-1} resulted in complete washout of the culture (0.21 g L^{-1}).

Phisalaphong et al., (2006) presented the effects of temperature on the kinetic parameters of ethanol fermentation by the flocculating yeast, *S. cerevisiae* M30, using cane molasses as substrate demonstrating that high temperatures (38 and 42 ºC) resulted in decreased bioethanol production and cell yield.

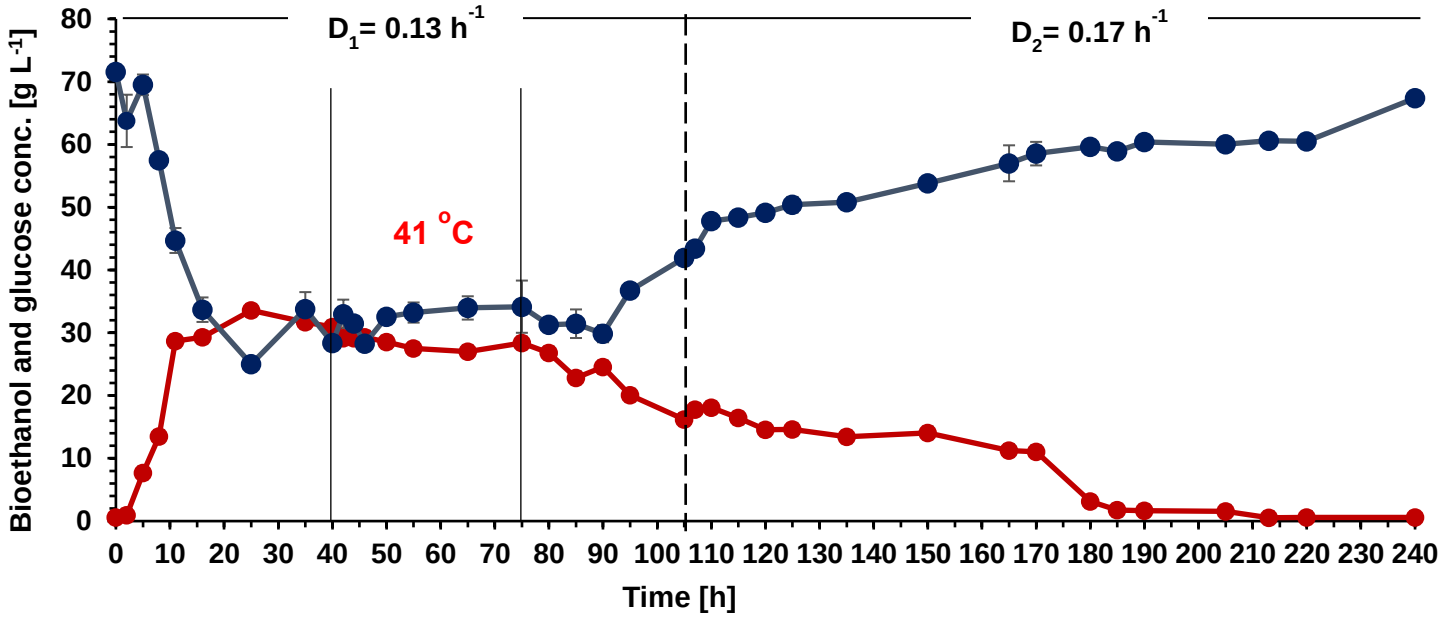

Figure 3.4.4G: Bioethanol and glucose concentration achieved at 39 ºC and 41 ºC using freely suspended cells of *S. cerevisiae* in a continuous bioreactor under different dilution rates (0.13 and 0.17 h^{-1}). Symbols correspond to: (i) bioethanol concentration, (ii) glucose concentration.

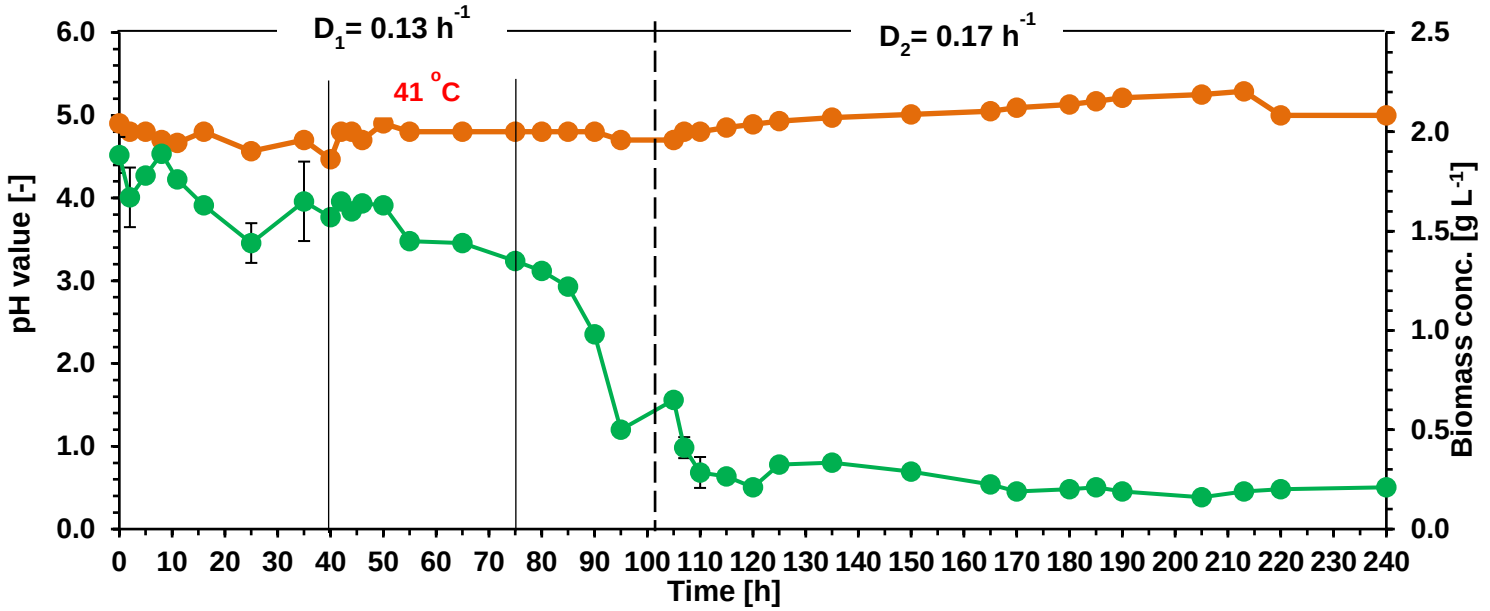

Figure 3.4.4H: pH value and biomass concentration achieved at 37 ºC and 41 ºC using freely suspended cells of *S. cerevisiae* in a continuous bioreactor under different dilution rates (0.13 and 0.17 h^{-1}). Symbols correspond to: (i) pH value, (ii) biomass concentration.

3.4.4.4 Continuous bioethanol fermentation at the elevated temperatures of 39 and 41 ºC using immobilised cells of *S. cerevisiae*

The significant potential of the immobilised biocatalyst to enhance the continuous bioprocess was assessed under conditions that were more extreme as compared to those that resulted in complete failure of the conventional system. Thus, continuous fermentations employing *S. cerevisiae* immobilised on UNC were conducted at the elevated temperatures of 39 and 41 ºC and dilution rates of 0.17 and 0.20 h^{-1} (Figure 3.4.4I).

The total duration of the experiment was 240 h, where the dilution rate was controlled at 0.17 h^{-1} for the first 105 h and at 0.20 h^{-1} thereafter. 29 g L^{-1} of bioethanol concentration was formed in the first 16 h of the experiment reaching productivity of 4.91 g L^{-1} h^{-1} while the maximum net bioethanol concentration achieved was 32 g L^{-1} at 40 h. Following the first 40 h the temperature was increased from 39 to 41 ºC, where the bioethanol production rate remained stable and bioethanol concentrations ranged between 29 – 32 g L^{-1}. Stable bioethanol production was observed until 107 h where the dilution rate was increased to 0.20 h^{-1}, which resulted in washout. The specific effect was confirmed by the glucose concentration monitored that rapidly increased at the initial stages of the dilution rate increase. The production of bioethanol was completely inhibited by the increase of dilution rate. However, the increased temperature, which was applied for a prolonged period (25 h), did not affect bioprocess's performance. Moreover, the immobilised system buffered the inhibitory effect of the extreme temperature under an increased dilution rate (0.17 h^{-1}) as compared to the conventional system demonstrating that the carbonaceous-based biocatalyst can improve a major industrial bioprocess under high temperatures and dilution rates.

S. cerevisiae ATCC 24553, immobilised in k-carrageenan and packed in a tapered glass column reactor for bioethanol production from pineapple cannery waste at 30°C demonstrated 42.8 g L^{-1} at a dilution rate of 1.5 h^{-1} which was 11.5 times higher than those obtained by free cells confirming the significant contribution of the immobilised biocatalyst in bioethanol production enhancement [Nigam, 1999]. The immobilization of *S. cerevisiae* in sodium-alginate beads for

bioethanol production at dilution rates (0.064, 0.096, 0.144 and 0.192 h^{-1}) was assessed by Ghorbani et al., (2011). In the specific system, the maximum bioethanol concentration obtained was 19.2 g L^{-1} and the volumetric productivity 2.39 g L^{-1} h^{-1}.

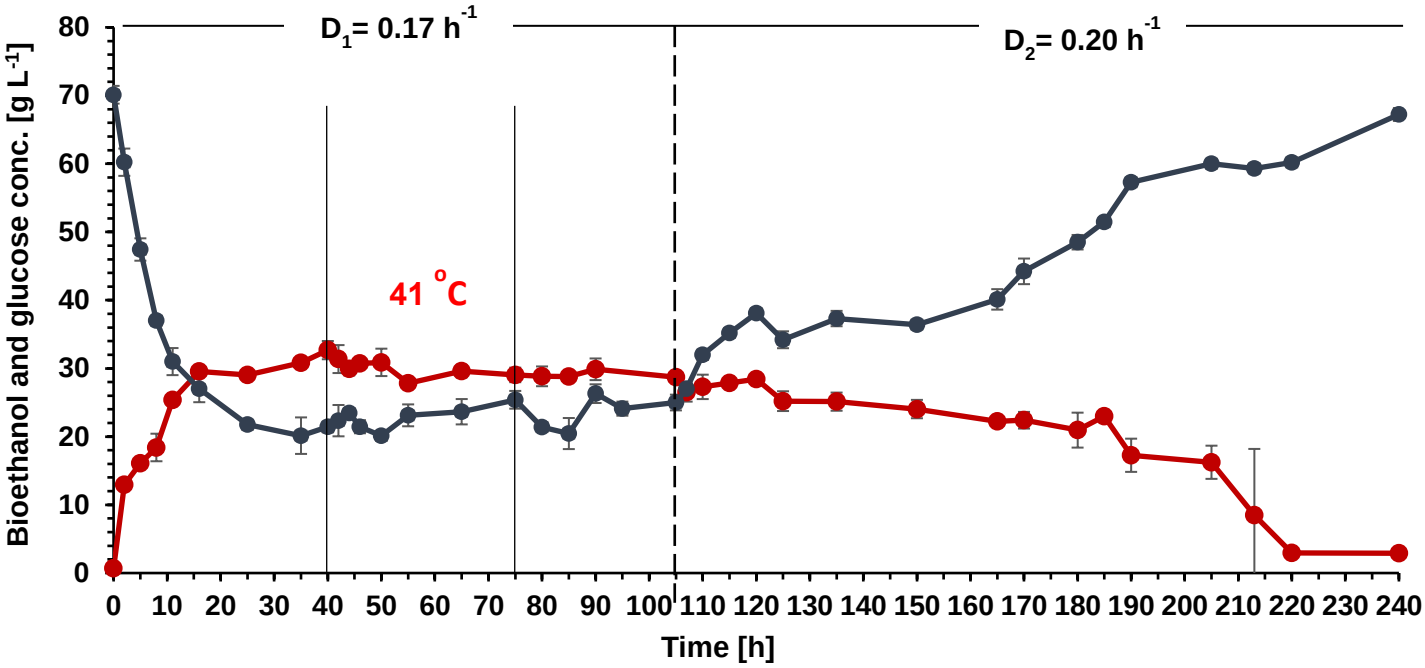

Figure 3.4.4I: Bioethanol and glucose concentration achieved at 39 ºC and 41 ºC using immobilised cells of *S. cerevisiae* in a continuous bioreactor under different dilution rates (0.17 and 0.20 h^{-1}). Symbols correspond to: (i) bioethanol concentration, (ii) glucose concentration.

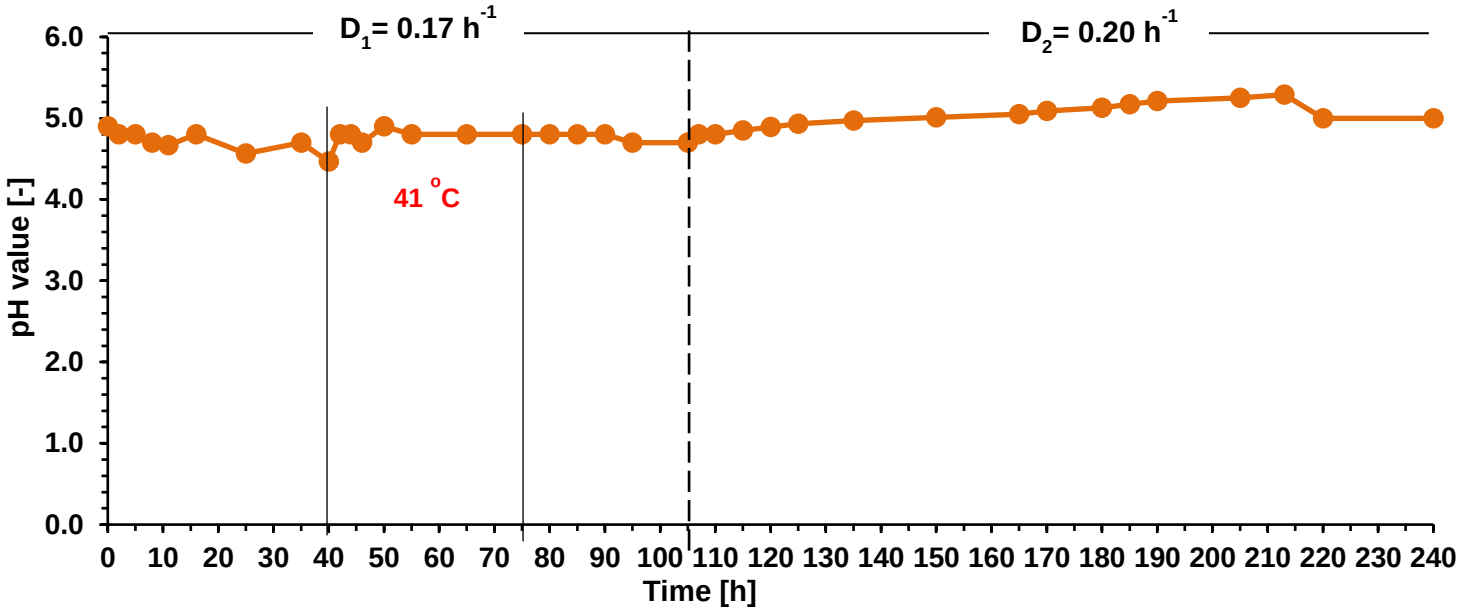

Figure 3.4.4J: pH value monitored during fermentation conducted at 39 and 41 ^{o}C using immobilised cells of *S. cerevisiae* in a continuous bioreactor under different dilution rates (0.17 and 0.20 h^{-1}).

4 PROJECT REVIEW

The research objectives of the current thesis (as presented in section 1.6) have been achieved. The main conclusions derived from the results of the present study are presented below.

4.1 Conclusions

4.1.1 Preliminary study of biochar-based biocatalysts for bioethanol production

This work explored the potential use of biochar as a microbial cell carrier enhancing the efficiency of alcoholic fermentations. Olive kernels, vineyard prunings, sewage sludge and seagrass residues were applied as biowaste for biochar production through pyrolysis at two different temperatures (250 °C and 500 °C), while a commercial type of char derived from car tire waste was also employed for benchmarking purposes. Apart from vineyard prunings pyrolyzed at 250 °C, all other carbonaceous materials presented crystalline phases including halite, calcite, sylvite and/or silicon. Moreover, increase in pyrolysis temperature enhanced biochar's porosity and BET-specific surface area, which reached 41.7 m^2 g^{-1} for VP-based biochar remaining at lower levels (0.15–5.3 m^2 g^{-1}) in other specimens tested. Elemental analysis demonstrated reduction in oxygen and increase in the carbon content of biochars produced at elevated temperatures, while biochar obtained from seagrass included residues of chloride (0.3–5.14%). Three major yeasts were immobilised on materials exhibiting the highest surface areas and applied in repeated batch fermentations using Valencia orange peel hydrolyzates as feedstock. The biocatalysts developed using *S. cerevisiae* and *K. marxianus* immobilised on vineyard prunings-based biochar exhibited exceptional ethanol productivities as compared to the relevant literature, which reached 7.2 g L^{-1} h^{-1} and 7.3 g L^{-1} h^{-1} respectively. Although the aforementioned strains improved biofuel production by 36–52% compared to the conventional process, *P. kudriavzevii* KVMP10 was not efficient following immobilization on biochar. The approach constitutes an innovative method for bioenergy production, demonstrating a novel application of biochar in industrial biotechnology which incorporates

important technological advances such as enhanced biofuel production and biomass recycling.

An innovative technology was developed for the production of renewable energy, which mitigates the environmental effects from food waste disposal and improves the sustainability of energy systems. Specifically, an advanced use of biochar was explored evaluating applicability of the material for immobilization of whole-cells in a major industrial biotechnology process. Vineyard prunings, seagrass residues and sewage sludge were applied in pyrolysis without activation, while process temperature and the type of feedstock strongly affected the physicochemical properties of the biochar produced. The increase in temperature resulted in higher specific surface area and porosity, whereas both crystalline and amorphous structures were formed incorporating varying elemental composition and carbon content. Three major yeast strains were immobilised on vineyard prunings and seagrass residues biochar generated at 500 °C as well as on a non-renewable form of non-biological char to evaluate bioethanol production using a Valencia orange peel hydrolyzate. *S. cerevisiae* and *K. marxianus* demonstrated significant potential for the development of biochar-based biocatalysts yielding elevated biofuel production in repeated batch experiments as compared to the relevant literature.

4.1.2 Enhancing bioproduction and thermotolerance in *Saccharomyces cerevisiae* via cell immobilization on biochar

A novel method for enhancement of bioethanol production and temperature tolerance of *S. cerevisiae* through the development of BBBs was reported. Immobilised BBBs were applied in alcoholic fermentations of hydrolyzates generated via a CPW biorefinery. Pistachio-nut shells, peanut shells and corks were employed for biochar generation via pyrolysis to produce the cell carriers required. All materials were highly carbonaceous with mesopore size structures (1–50 mm), while peanut shells biochar was crystalline incorporating calcite and sylvite. *S. cerevisiae* immobilised on pistachio-nuts biochar grown on a synthetic CPW hydrolysate, exhibited 63 g L^{-1} ethanol concentration and 7.9 g L^{-1} h^{-1} productivity improving substantially biosystem performance as compared to unsupported cultures. Alcoholic fermentations conducted at different elevated temperatures (37–41 ^{o}C) exhibited stable performance of the immobilised system for six repeated batch experiments. Fermentations of the CPW-hydrolyzate formed through the biorefinery at 41 ^{o}C using BBB produced 30.8 g L^{-1} of bioethanol, while free cells achieved significantly lower concentration (13.4 g L^{-1}). The proposed technology confers thermotolerance on *S. cerevisiae,* which buffers the negative impact of high temperatures on cells leading in increased bioethanol production and lower energy demand.

Summing up the results, it can be concluded that the use of BBBs has substantially enhanced fermentative bioethanol production from hydrolyzates generated using the CPW biorefinery, while alleviating important technological constraints and environmental effects of the process. Immobilization of *S. cerevisiae* on biochar enabled applying the workhorse of the current bioethanol industry at high temperature alcoholic fermentations, which could potentially provide multiple advantages such as increased ethanol production, reduction of operating costs, biocatalyst recyclability and low contamination risk.

4.1.3 Improvement of stress multi-tolerance and bioethanol production by *Saccharomyces cerevisiae* immobilised on biochar:

The study determined the protective role of using biochar as immobilization carrier against multiple stresses encountered by *Saccharomyces cerevisiae* assessing transcription from important metabolic routes involved in the molecular mechanisms triggered during inhibitory bioprocess conditions. Immobilised cells exhibited higher bioethanol titre (39 g L^{-1}) and productivity (7.72 g L^{-1} h^{-1}) at elevated temperatures compared with the suspended culture that yielded 34 g L^{-1} and 1.99 g L^{-1} h^{-1} respectively. Fermentation at 39 ^{o}C resulted in 2.15-fold increase of *HSP104* relative mRNA expression in suspended cells, while the gene was induced by 0.5-fold using the immobilised biocatalyst. A similar response occurred for *HSF1* and *TPS* exhibiting 3.0- and 3.8-fold increase using suspended cells as opposed to the application of immobilised cells where transcription of the aforementioned genes was raised by 0.0- and 2.6-fold upon temperature increase respectively. Transcription from *MSN2*/*MSN4* under the aforementioned conditions indicated the protective role of cell attachment on the biomaterial against stimulation of the heat shock response route and oxidative stress. Although fermentations conducted under ethanol stress resulted in failure of the conventional process, immobilised cells produced 21 g L^{-1} bioethanol exhibiting 7 g L^{-1} h^{-1} productivity, while monitoring transcription of *HSP12* and *HSP104* demonstrated the beneficial use of the proposed technology. Proline accumulation during osmotic stress further supported the elevated bioethanol productivity achieved by the immobilised system, which was 74% higher as opposed to the conventional process. The study confirmed that *S. cerevisiae* immobilization on biochar conferred cells with heat tolerance, ethanol tolerance, osmotolerance and improved fermentation capacity. The technology proposed constitutes a sustainable technological alternative to strain modification improving multiple stress-tolerance in bioethanol fermentations.

Immobilization of yeast cells on biochar produced robust performance of *S. cerevisiae*, which demonstrated improved tolerance against heat, ethanol, osmotic and oxidative stress as well as efficient fermentation capacity. Thus, cell attachment on the biomaterial enhanced bioethanol production at high temperatures, yielded

74% higher productivity under osmotic stress and acted as buffer for the bioprocess under elevated ethanol contents that resulted in complete inhibition of the conventional system. Furthermore, monitoring of transcription from *TPS* associated with trehalose accumulation, oxidative stress responsive genes (*MSN2*, *MSN4*) as well as genes encoding HSPs (*HSP104*, *HSP12*) and the heat shock transcription factor (*HSF1*) sustained the protective action of biochar against multiple stresses, hampering bioethanol production by *S. cerevisiae*. The current technology holds significant potential to tackle major challenges associated with the industrial bioprocess, limiting the need for genetic modification of the workhorse strain aimed to confer stress tolerance traits and improved fermentation performance.

4.1.4 Bioethanol overproduction of *S. cerevisiae* immobilised on char derived from car tire waste

The work explored the potential use of non-biological char produced from car tire waste as support material for cell immobilization employed in continuous bioethanol fermentations. PWC, PLC and UNC demonstrated effective immobilization of *S. cerevisiae* as well as enhanced bioethanol overproduction in terms of higher ethanol concentrations, faster kinetics and the potential application of the bioprocess under high temperatures, which is expected to reduce the operational cost. Continuous fermentations conducted using UNC demonstrated that via attachment of the yeast on the biomaterial, higher dilution rates can be used in a continuous alcoholic fermentation achieving stable biofuel production as opposed to the freely suspended cells of *S. cerevisiae* that was affected by both dilution rates and high temperatures limiting bioprocess performance.

4.2 Future work

Following completion of the present Thesis, the topics presented below could be proposed as future work relevant to the use of the immobilised biocatalyst in industrial bioprocesses.

4.2.1 Optimization of immobilised biocatalysts for bioethanol production

The current work proposed biochar-based biocatalyst for bioethanol overproduction utilizing both synthetic media as well as a CPW hydrolysate employing *S. cerevisiae*, which confirmed that the material holds great potential as microbial cell carrier in a major industrial process enabling achievement of multiple technological objectives. Immobilization of *S. cerevisiae*, the industrial workhorse strain, as well as *K. marxianus* applied in bioethanol fermentations, improved biofuel production by 36-52% compared to the conventional process conferring tolerance to yeast stressing factors (e.g. high temperature, bioethanol concentration) that reduce process efficiency.

Cheese whey constitutes an important bioresource for the development of advanced bioethanol production processes and immobilised *K. marxianus* could be employed in fermentations that enable lactose utilization for bioethanol production. Thus, subsequent bioethanol fermentations using both free and immobilised cells of *K. marxianus*, a strain capable for lactose fermentation, could be performed under various technologically important conditions, including elevated temperatures, as well as high substrate, product and inhibitor (e.g. hydroxymethylfurfural) concentrations. Following evaluation of the capacity of the immobilised biocatalysts to buffer the inhibitory effect posed in each case, direct application of cheese whey as fermentation broth could be applied in *K. marxianus* fermentation for ethanol production. Repeated batch as well as continuous fermentations could be performed to determine the production rate of bioethanol using a fully automated lab-scale bioreactor. Biochar could be additionally employed to immobilize hydrolytic enzymes and/or cells aiming to develop simultaneous saccharification and fermentation processes.

Potato waste could be applied as a source of starch for bioethanol production. Prior fermentation the content of starch should be hydrolyzed to produce directly assimilable glucose. Thus, *Aspergillus* strains could be employed to perform amylase and glucoamylase production, employed to hydrolyze starch and produce a glucose-rich feedstock. The hydrolytic microorganism could be employed both in the form of suspended and immobilised cells using biochar. Trials where *Aspergillus* strains and *K. marxianus* immobilised on separate biochar/(nano)biochar particles could be employed while feeding potato waste hydrolysates and cheese whey.

The proposed technology could be improved by the use of (nano)biochar as immobilization carrier aiming to achieve higher surface area, which constitutes a key parameter for cell immobilization. By scaling down biochar to (nano)biochar an advanced material holding multiple potential applications will be prepared, while its physicochemical and textural properties could be evaluated comprising crucial indicators in determining the potential applications. The surface chemistry of the material could be investigated aiming to assess the future potential role of biochar as functional material (e.g. catalyst, adsorbent, electrode material).

4.2.2 Construction of a mathematical model capable of predicting the performance of BBB

Previous research has shown that the development of experimentally validated models of key genetic circuits (comprising groups of cellular elements that interact) could improve prediction of the kinetic properties of a microorganism. In order to predict the kinetics of the microorganism in relation to glucose uptake and consumption as well as bioethanol production, a logic model could be developed with the use of logic gates. In the logic model, interacting molecular components could be described as a combination of logic gates, while Hill functions could be used to construct a dynamic mathematical model for the targeted circuit. Thus, the model could enable predicting transcription from targeted genes involved in glucose metabolism as well as bioethanol production. The mRNA expression levels of *HXK2*, *PDC5* and *ADH1* could be initially monitored using freely suspended cells of *S. cerevisiae*, while transcription from the specific genes could be additionally quantified and predicted in fermentations employing BBB.

REFERENCES

Aamer Mehmood M, Shahid A, Malik S, Wang N, Javed MR, Haider MN, Verma P, Farooq Ashraf MU, Habib N, Syafiuddin A, Boopathy R. Advances in developing metabolically engineered microbial platforms to produce fourth-generation biofuels and high-value biochemicals. Bioresour Technol 2021;337:125510.

Abdullah N, Taib RM, Aziz NSM, Omar MR, Disa NM. Banana pseudo-stem biochar derived from slow and fast pyrolysis process. Heliyon 2023;9:e12940.

Achinas S, Euverink GJW. Consolidated briefing of biochemical ethanol production from lignocellulosic biomass. Electron J Biotechnol 2016;23:44–53.

Adeniyi AG, Iwuozor KO, Emenike EC, Amoloye MA et al. Leaf-based biochar: A review of thermochemical conversion techniques and properties. J Anal Appl Pyrolysis 2024;177:106352.

Aghbashlo M, Tabatabaei M, Nadian MH, Davoodnia V, Soltanian S. Prognostication of lignocellulosic biomass pyrolysis behavior using ANFIS model tuned by PSO algorithm. Fuel 2019;253:189–198.

Agyekum EB, Nutakor C. Recent advancement in biochar production and utilization – A combination of traditional and bibliometric review. Int J Hydrogen Energy 2024;54:1137–1153.

Ahmad M, Lee SS, Dou X, Mohan D, Sung JK, Yang JE, Ok YS. Effects of pyrolysis temperature on soybean stover- and peanut shell-derived biochar properties and TCE adsorption in water. Bioresour Technol 2012;118:536–544.

Åkerfelt M, Morimoto RI, Sistonen L. Heat shock factors: integrators of cell stress, development and lifespan. Nat Rev Mol Cell Biol 2010;11(8): 545–555.

Almeida LC, Barbosa AS, Fricks AT, Freitas LS, Lima AS, Soares CMF. Use of conventional or non-conventional treatments of biochar for lipase immobilization. Process Biochem 2017;61:124–129.

Amutio M, Lopez G, Artexte M, Elordi G, Olazar M, Bilbao J. Influence of temperature on biomass pyrolysis in a conical spouted bed reactor. Resour Conserv Recycl 2012;59:23–31.

Angın D. Effect of pyrolysis temperature and heating rate on biochar obtained from pyrolysis of safflower seed press cake. Bioresour Technol 2013;128:593–7.

Ariyajaroenwong P, Laopaiboon P, Jaisil P, Laopaiboon L. Repeated-batch ethanol production from sweet sorghum juice by *Saccharomyces cerevisiae* immobilized on sweet sorghum stalks. Energies 2012;5:1215–28.

Awogbemi O, Von Kallon DV. Application of biochar derived from crops residues for biofuel production. Fuel Communications 2023;15:100088.

Azhar STM, Abdulla R. Bioethanol production from galactose by immobilized wild-type *Saccharomyces cerevisiae*. ISBAB 2018;14:457–465.

Bai FW, Anderson WA, Moo-Young M. Ethanol fermentation technologies from sugar and starch feedstocks, Biotechnol Adv 2008;26:89–05.

Bai FW, Chen LJ, Zhang Z, Anderson WA, Moo-Young M. Continuous ethanol production and evaluation of yeast cell lysis and viability loss under very high gravity medium conditions. J Biotechnol 2004;110:287–293.

Bailey SE, Olin TJ, Bricka RM, Adrian DD. A review of potentially low-cost sorbents for heavy metals. Wat Res 1999;33:2469–79.

Bajpai P. Pretreatment of Lignocellulosic Biomass for Biofuel Production. 2016. Springer Briefs in Green Chemistry for Sustainability.

Banat IM, Nigam P, Singh D, Marchant R, McHale AP. Review: ethanol production at elevated temperatures and alcohol concentrations: Part I - yeasts in general. World J Microbiol Biotechnol 1998;14:809–821.

Bangrak P, Limtong S, Phisalaphong M. Continuous ethanol production using immobilized yeast cells entrapped in loofareinforced alginate carriers. Braz J Microbiol 2011;42:676–684.

Barbhuiya S, Das BB, Kanavaris F. Biochar-concrete: A comprehensive review of properties, production and sustainability. Case Stud Constr Mater 2024;20:e02859.

Bates LS, Waldren RP, Teare ID. Rapid determination of free proline for water stress studies, Plant Soil 1973;39:205–207.

Behera S, Kar S, Ray RC. Comparative study of bio-ethanol production from mahula (*Madhuca latifolia* L.) flowers by *Saccharomyces cerevisiae* cells immobilized in agar agar and Ca-alginate matrices. Appl Energy 2010;87:96–100.

Betlej G, Bator E, Oklejewicz B, Potocki L, Górka A, Słowik-Borowiec M, Czarny W, Domka W, Kwiatkowska A. Long-Term Adaption to High Osmotic Stress as a Tool for Improving Enological Characteristics in Industrial Wine Yeast. Genes 11 2020;576.

Bockstal L, Berchem T, Schmetz Q, Richel A. Devulcanisation and reclaiming of tires and rubber by physical and chemical processes: A review. J Clean Prod 2019;236:117574.

Bordoloi S, Gadi VK, Hussain R, Sahoo L, Garg A, Sreedeep S, Mei G, Poulsen TG. Infuence of *Eichhornia crassipes* fibre on water retention and cracking of vegetated soils. Géotech Lett 2018;8(2):130–137.

Borges JC, Ramos CH. Protein folding assisted by chaperones. Protein Pept Lett 2005;12:257−261.

Borges JC, Ramos CH. Protein folding assisted by chaperones. Protein Pept Lett 2005;12:257–261.

Brown AJP, Larcombe DE, Pradhan A. Thoughts on the evolution of Core Environmental Responses in yeasts. Gungal Biol Rev 2020;124:475-481.

Brown TR, Wright MM, Brown RC. Estimating profitability of two biochar production scenarios: slow pyrolysis vs fast pyrolysis. Biofuels Bioprod Biorefin 2011;5(1):54–68.

Canonero L, Pautasso C, Galello F, Sigaut L, Pietrasanta L, Arroyo J, Bermúdez-Moretti M, Portela P, Rossi S. Heat stress regulates the expression of TPK1 gene at transcriptional and post-transcriptional levels in *Saccharomyces cerevisiae*. Biochim Biophys Acta Mol Cell Res 2022;1869:119209.

Carrasco P, Querrol A, Del OM. Analysis of the stress resistance of commercial wine yeast strains. Arch Microbiol 2001;175:450-457.

Casey GP, Ingledew WM. Ethanol tolerance in yeasts. Crit Rev Microb 1986;13:219–280.

Castilla-Caballero D, Hernandez-Ramirez A, Vazquez-Rodriguez S, Colina-Marquez J, Machuca-Martínez F et al. Effect of pyrolysis, impregnation, and calcination conditions on the physicochemical properties of TiO2/Biochar composites intended for photocatalytic applications. J Environ Chem Eng 2023;11:110274.

Castillo MV, Brar SK, Arriaga S, Blais JF, Ramirez AA. Effect of passive cell immobilization of co-cultured yeasts on the whey fermentation and alcohols production. J Clean Prod 2022;375:133988.

Caykara T, Demirci S, Eroglu M, Guven O. Poly (ethylene oxide) and its blends with sodium alginate. Polymer 2005;46:10750–10757.

Cea N, Sangaletti N, Gonzalez ME, Navia R. Candida rugose lipase immobilization on biochar derived from agricultural residues. Nat Resour 15.

Cesar Guimaraes CE, Neto FS, de Castro Bizerra V et al. Sustainable bioethanol production from first- and second-generation sugar-based feedstocks: Advanced bibliometric analysis. Bioresour Technol 2023;23:101543.

Chamnipa N, Thanonkeo S, Klanrit P, Thanonkeo P. The potential of the newly isolated thermotolerant yeast *Pichia kudriavzevii* RZ8-1 for high-temperature ethanol production. Braz J Microbiol 2017;49(2):378–391.

Chaos-Hernandez D, Reynel-Avila HE, Bonilla-Petriciolet A, Villalobos-Delgado FJ. Extraction methods of algae oils for the production of third generation biofuels – A review. Chemoshpere 2023;341:139856.

Chaudhary A, Hussain Z, Aihetasham A, El-Sharnouby M, Rehman RA, Khan MAU, Zahra S, Saleem A, Azhar S, Alhazmi A, El Askary A, Sayed S, El Enshasy HA, Hanapi SZ, Qamer S. Pomegranate peels waste hydrolyzate optimization by Response Surface Methodology for Bioethanol production. Saudi J Biol Sci 2021;28:4867–4875.

Chen B, Chen Z. Sorption of naphthalene and 1-naphthol by biochars of orange peels with different pyrolytic temperatures. Chemosphere 2009;76:127–33.

Chen H. Biotechnology of Lignocellulose Theory and Practice. 2014. Springer Dordrecht Heidelberg New York London.

Chen HY, Khumsupan D, Kumar Patel A, Kee PE, Ng HS, Hsu HY, Lin SP, Cheng KC. Immobilization of *Kluyveromyces marxianus* K21 via coaxial electrospinning of PVA and sugarcane bagasse composite for bioethanol production. Appl Energy 2024;356:122405.

Chen XW, Wong JTF, Ng CWW, Wong MH. Feasibility of biochar application on a landfill final cover: A review on balancing ecology and shallow slope stability. Environ Sci Pollut Res 2016;23(8):7111–7125.

Choi IS, Lee YG, Khanal SK, Park BJ, Bae HJ. A low-energy, cost-effective approach to fruit and citrus peel waste processing for bioethanol production. Appl Energy 2015;140:65-74.

Choudhary J, Singh S, Nain L. Theromotolerant fermenting yeasts for simultaneous saccharification fermentation of lignocellulosic biomass. Electron J Biotechnol 2016;21:82–92.

Cong H, Mašek O, Zhao L, Yao Z, Meng H, Hu E, et al. Slow pyrolysis performance and energy balance of corn stover in continuous pyrolysis-based poly-generation system. Energy Fuel 2018;32:3743–50.

Correa DF, Beyer HL, Fargione JE, Hill JD, Possingham HP, Thomas-Hall SR, Schenk PM. Towards the implementation of sustainable biofuel production systems. Renew Sust Energ Rev 2019;107:250–263.

Cunha JT, Soares PO, Romaní A, Thevelein JM, Domingues L. Xylose fermentation efficiency of industrial *Saccharomyces cerevisiae* yeast with separate or combined xylose reductase/xylitol dehydrogenase and xylose isomerase pathways. Biotechnol Biofuels 2019;12:20

Dailami AA, Ahmad I, Kamyab H, Abdullah N, Koji I, Ashokkumar V, Zabara B. Sustainable solid waste management in Yemen: environmental, social aspects, and challenges. Biomass Convers Biorefin 2022;1–27.

de Fatima Alves L, Bortolucci J, Reginatto V, Guazzaroni ME, Mussato SI. Improving *Saccharomyces cerevisiae* acid and oxidative stress resistance using a prokaryotic gene identified by functional metagenomics.

Demirbas A, Arin G. An overview of biomass pyrolysis. Energ Source 2002;24:471–82.

Deng M, Li K, Yan YJ, Huang F, Peng D. Enhanced cadmium removal by growing *Bacillus cereus* RC-1 immobilized on different magnetic biochars through simultaneous adsorption and bioaccumulation. Environ Sci Pollut Res 2022;29:18495–18507.

Deshmukh S, Kumar R, Bala K. Microalgae biodiesel: A review on oil extraction, fatty acid composition, properties and effect on engine performance and emissions. Fuel Process Technol 2019;191:232–247.

Dhiman SS, David A, Braband VW, Hussein A, Salem DR, Sani RK. Improved bioethanol production from corn stover: Role of enzymes, inducers and simultaneous product recovery. Appl Energy 2017;208:1420–9.

Diaz-Nava LE, Montes-Garcia N, Dominguez JM, Aguilar-Uscanga MG. Effect of carbon sources on the growth and ethanol production of native yeast *Pichia kudriavzevii* ITV-S42 isolated from sweet soghum juice. Bioprocess Biosyst Eng 2017;40:1069–1077.

Dimarogona M, Topakas E, Christakopoulos P. Cellulose degradation by oxidative enzymes. Comput Struct Biotechnol J 2012;2:201209015.

Ding J, Huang X, Zhao N, Gao F, Lu Q, Zhang KQ. Response of *Saccharomyces cerevisiae* to ethanol stress involves actions of protein Asr1p. J Microbiol Biotechnol 2010;20:1630–1636.

Diniz RHS, Rodrigues MQRB, Fietto LG, Passos FML, Silveira WB. Optimizing and validating the production of ethanol from cheese whey permeate by *Kluyveromyces marxianus* UFV-3. Biocatal Agric Biotechnol 2014;3(2):111–117.

Doja S, Pillari LK, Bichler L, Processing and activation of tire-derived char: A review. Renew Sust Energ Rev 2022;155:111860.

Donatelli A, Iovane P, Molino A. High energy syngas production by waste tyres steam gasification in a rotary kiln pilot plant. Experimental and numerical investigations. Fuel 2010;89:2721–2728.

Duarte JC, Rodrigues JAR, Moran PJS, Valenca GP, Nunhez J. Effect of immobilized cells in calcium alginate beads in alcoholic fermentation. Amb Express 2013;3:31.

Duarte JC, Rodrigues JAR, Moran PJS, Valença GP, Nunhez JR. Effect of immobilized cells in calcium alginate beads in alcoholic fermentation. AMB Express 2013;3:1–8.

Eiadpum A, Limtong S, Phisalaphong M. High-temperature ethanol fermentation by immobilized coculture of *Kluyveromyces marxianus* and *Saccharomyces cerevisiae*. J Biosci Bioeng 2012;114:325–329.

El-Dalatony MM, Kurade MB, Abou-Shanab RAI, Kim H, Salama ES, Jeon BH. Long-term production of bioethanol in repeated-batch fermentation of microalgal biomass using immobilized *Saccharomyces cerevisiae*. Bioresour Technol 2016;219:98–105.

Elshout PM, van Zelm R, van der Velde M, Steinmann Z, Huijbregts MA. Global relative species loss due to first-generation biofuel production for the transport sector. GCB Bioenergy 2019;11:763–772.

Fan Y, Xia W, Ma C, Huang Y, Li S, Wang X, Qian C, Chen K, Liu D. Recent advances of computational studies on bioethanol to light olefin reactions using zeolite and metal oxide catalysts. Chem Eng Sci 2023;270:118532.

Farias D, Maugeri-Filho F. Sequential fed batch extractive fermentation for enhanced bioethanol production using recycled *Spathaspora passalidarum* and mixed sugar composition. Fuel 2021;288:119673.

Farzad S, Mandegari M, Görgens JF. A novel approach for valorization of waste tires into chemical and fuel (limonene and diesel) through pyrolysis: Process development and techno economic analysis. Fuel Process Technol 2021;224:107006.

Fijita K, Matsuyama A, Kobayashi Y, Iwahashi H. Comprehensive gene expression analysis of the response to straight-chain alcohols in *Saccharomyces cerevisiae* using cDNA Microarray. J Appl Microbiol 2004;97(1):57-67.

Flores JA, Gschaedler A, Amaya-Delgado L, Herrera-López EJ, Arellano M, Arrizon J. Simultaneous saccharification and fermentation of *Agave tequilana* fructans by *Kluyveromyces marxianus* yeasts for bioethanol and tequila production. Bioresour Technol 2013;146:267–273.

Frenkel O, Jaiswal AK, Elad Y, Lew B, Graber ER. The effect of biochar on plant diseases: What should we learn while designing biochar substrates? J Environ Eng Landsc Manag 2017;25(2):105–113.

Frohman CA, de Orduna RM. Cellular viability and kinetics of osmotic stress associated metabolites of *Saccharomyces cerevisiae* during traditional batch and fedbatch alcoholic fermentations at constant sugar concentrations. Int Food Res J 2013;53:551–555.

Fu P, Yi W, Bai X, Li Z, Hu S, Xiang J. Effect of temperature on gas composition and char structural features of pyrolyzed agricultural residues. Bioresour Technol 2011;102:8211–9.

Fujita K, Matsuyama A, Kobayashi Y, Iwahashi H. Comprehensive gene expression analysis of the response to straight-chain alcohols in *Saccharomyces cerevisiae* using cDNA microarray. J Appl Microbiol 2004;97:57–67.

Gabhi R, Tan K, Feng T, Kirk DW, Giorcelli M, Tagliaferro A, Jia CQ. Intrinsic electrical conductivity of monolithic biochar. Biomass & Bioenergy 2024;181:107051.

Galanakis CM, Kordulis C, Kanellaki M, KoutinasAA, Bekatorou A, Lycourghiotis A. Effect of pressure and temperature on alcoholic fermentation by *Saccharomyces cerevisiae* immobilized on γ-alumina pellets. Bioresour Technol 2012;114:492–498.

Galeote VA, Blondin B, Dequin S, Sablayrolles JM. Stress effects of ethanol on fermentation kinetics by stationary-phase cells of *Saccharomyces cerevisiae*. Biotechnol Lett 2001;23:677–681.

Galeote VA, Blondin B, Dequin S, Sablayrolles JM. Stress effects of ethanol on fermentation kinetics by stationary-phase cells of *Saccharomyces cerevisiae*. Biotechnol Lett 2001;23:677–681.

Gao N, Wang F, Quan C, Santamaria L, Lopez G, Williams PT. Tire pyrolysis char: Processes, properties, upgrading and applications. Prog Energ Combust 2022;93:101022.

Ghorbani F, Younesi H, Esmaeili Sari A, Najafpour G. Cane molasses fermentation for continuous ethanol production in an immobilized cells reactor by *Saccharomyces cerevisiae*. Renew Energy 2011;36:503–509.

Glover JR, Lindquist S. Hsp104, Hsp70, and Hsp40: A novel chaperone system that rescues previously aggregated proteins. Cell 1998;94:73–82.

González ME, Cea M, Sangaletti N, González A, Toro C, Diez MC, Moreno N, Querol X, Navia R. Biochar Derived from Agricultural and Forestry Residual Biomass: Characterization and Potential Application for Enzymes Immobilization. J Biobased Mater Bioenergy 2013;7(6):724–732.

Gonzalez ME, Gonzalez A, Toro CA, Cea M, Sepulveda N, Diez MC, et al. Biochar as a renewable matrix for the development of encapsulated and immobilized novel added-value bioproducts. J Biobased Mater Bio 2012;6:1–12.

González-González RB, González LT, Iglesias-González S, González-González E, Martinez-Chapa SO, Madou M, Alvarez MM, Mendoza A. Characterization of chemically activated pyrolytic carbon black derived from waste tires as a candidate for nanomaterial precursor. Nanomaterials 2020;10(11):1–22.

Gough S, Barron N, Zubov AL, Lozinsky VI, McHale AP. Production of ethanol from molasses at 45 °C using *Kluyveromyces marxianus* IMB3 immobilized in calcium alginate gels and poly(vinyl alcohol) cryogel. Bioprocess Eng 1998;19:87–90.

Grbin PR, Jiranek V, ed., YEAST: PRODUCTS AND DISCOVERY, in: Proceedings of the 3rd Australian Conference on Yeast: Products and Discovery. Australia 2004:4–6.

Guo X, Zhou J, Xiao D. Improved ethanol production by mixed immobilized cells of *Kluyveromyces marxianus* and *Saccharomyces cerevisiae* from cheese whey powder solution fermentation. Appl Biochem Biotechnol 2010;160:532–538.

Ha NTH, Toan NC, Kajitvichyanukul P. Enhanced paraquat removal from contaminated water using cell-immobilized biochar. Clean Technol Environ Policy 2021;24:1073–1085.

Halliwell B. Reactive species and antioxidants. Redox biology is a fundamental theme of aerobic life. Plant Physiol 2006;141:312–322.

Hamid A, Khedr A, Abbas MA, Wahid AAA, Quick WP, Abogadallah GM. Proline induces the expression of salt-stress-responsive proteins and may improve the adaptation of Pancratium maritimum L, salt-Stress. J Exp Bot 2003;54:2553–2562.

Hasan M, Abedin MZ, Amin MB, Nekmahmud M, Olah J. Sustainable biofuel economy: A mapping through bibliometric research. J Environ Manage 2023;336:117644.

Herkommerová K, Zemančíková J, Sychrová H, Antošová Z. Immobilization in polyvinyl alcohol hydrogel enhances yeast storage stability and reusability of recombinant laccaseproducing *S. cerevisiae*. Biotechnol Lett 2018;40:405–411.

Hirasawa T, Yamada K, Nagahisa K, Dinh TN, Furusawa C, Katakura Y, Shioya S, Shimizu H. Proteomic analysis of responses to osmotic stress in laboratory and sake-brewing strains of *Saccharomyces cerevisiae*. Process Biochem 2009;44:647–653.

Hirasawa T, Yamada K, Nagahisa K, Dinh TN, Furusawa C, Katakura Y, Shioya S, Shimizu H. Proteomic analysis of responses to osmotic stress in laboratory and sake-brewing strains of *Saccharomyces cerevisiae*. Process Biochem 2009;44:647–653.

Ho NWY, Chang SF. Cloning of yeast xylulokinase gene by complementation of E. coli and yeast mutations. Enzyme Microbiol Technol 1989;11:417–421.

Hohmann S, Mager WH, 2003. Yeasts stress responses, Springer, Verlag Berlin Heidelberg NewYork.

Hong KK, Nielsen J. Metabolic engineering of *Saccharomyces cerevisiae*: a key cell factory platform for future biorefineries. Cell Mol Life Sci 2012;69:2671–2690.

Hoor A, Rowe RK. Application of tire chips to reduce the temperature of secondary geomembranes in municipal solid waste landfills. Waste Manage 2012;32(5):901–911.

Hoppert L, Kolling R, Einfalt D. Investigation of stress tolerance of *Pichia kudriavzevii* for high gravity bioethanol production from steam–exploded wheat straw hydrolysate. Bioresour Technol 2022;364:128079.

Hottiger T, Boller T, Wiemken A. Rapid changes of heat and desiccation tolerance correlated with changes of trehalose content in *Saccharomyces cerevisiae* cells subjected to temperature shifts. FEBS Lett 1987;220:113–115.

Hottiger T, de Virgilio C, Hall MN, Boller T, Wiemken A. The role of trehalose synthesis for the acquisition of thermotolerance in yeast II. Physiological concentrations of trehalose increase the thermal stability of proteins in vitro. Eur J Biochem 1994;219:187–193.

Hu X, Wang M, Tan T, Li J, Yang H, Leach L, Zhang R, Luo Z. Genetic dissection of ethanol tolerance in the budding yeast *Saccharomyces cerevisiae*. Genetic Society of America 2006;175:1479-1487.

Huang H, Reddy NG, Huang X, Chen P, Wang P, Zhang Y, Huang Y, Lin P, Garg A. Effects of pyrolysis temperature, feedstock type and compaction on water retention of biochar amended soil. Sci Rep 2021;11(1):7419.

IEA,2017. Bioenergy. Energy system. Renewables. International Energy Agency.

Immerzeel DJ, Verweij PA, Van Der Hilst F, Faaij APC. Biodiversity impacts of bioenergy crop production: a state-of-the-art review. Glob Change Biol Bioenergy 2014;6:183–209.

Inal M, Yigitoglu M. Production of bioethanol by immobilized *Saccharomyces cerevisiae*. J Chem Technol Biotechnol 2011;86:1548–1554.

Ippolito JA, Cui L, Kammann C, Wrage-Monnig N, Estavillo JM, Fuertes-Mendizabal T, Cayuela ML, Sigua G, Novak J, Spokas K. Feedstock choice,

pyrolysis temperature and type influence biochar characteristics: a comprehensive meta-data analysis review. Biochar 2020;2:421–438.

Ishola MM, Brandberg TT, Taherzadeh MJ. Simultaneous glucose and xylose utilization for improved ethanol production from lignocellulosic biomass through SSFF with encapsulated yeast. Biomass Bioenergy 2015;77:192–9.

Islam M, Halder M, Siddique MAB, Razir SAA, Sikder S, Joardar J.C. Banana peel biochar as alternative source of potassium for plant productivity and sustainable agriculture. Int J Recycl Org Waste Agric 2019;8(1):407–413.

Izawa S, Kita T, Ikeda K, Inoue Y. Heat shock and ethanol stress provoke distinctly different responses in 3′-processing and nuclear export of HSP mRNA in *Saccharomyces cerevisiae*. Biochem J 2008;414(1):111–119.

Jaiswal AK, Frenkel O, Tsechansky L, Elad Y, Graber ER. Immobilization and deactivation of pathogenic enzymes and toxic metabolites by biochar: A possible mechanism involved in soilborne disease suppression. Soil Biol Biochem 2018;121:59–66.

Javed MR, Bilal MJ, Ashraf MUF, Waqar A, Mehmood MA, Saeed M, Nashat N. Microalgae as a Feedstock for Biofuel Production: Current Status and Future Prospects. 2019. In book: Top 5 Contributions in Energy Research and Development: 3rd Edition (pp.1-39) Publisher: Avid Science.

Jayakumar M, Gebeyehu KB, Abo LD, Tadesse AW, Vivekanandan B, Sundramurthy VP, Bacha W, Ashokkumar V, Baskar G. A comprehensive outlook on topical processing methods for biofuel production and its thermal applications: Current advances, sustainability and challenges. Fuel 2023;349:128690.

Jayakumar M, Gebeyehu KB, Selvakumar KV, Parvathy S, Kim W, Karmegam N. Waste Ox bone based heterogeneous catalyst synthesis, characterization, utilization and reaction kinetics of biodiesel generation from *Jatropha curcas* oil. Chemosphere 2022;288:132534.

Jenjaiwit S, Supanchaiyamat N, Hunt AJ, Ngernyen Y, Ratpukdi T, Siripattanakul-Ratpukdi S. Removal of triclocarban from treated wastewater using cell-

immobilized biochar as a sustainable water treatment technology. J Clean Prod 2021;320:128919.

Jindarom C, Meeyoo V, Kitiyanan B, Rirksomboon T, Rangsunvigit P. Surface characterization and dye adsorptive capacities of char obtained from pyrolysis/ gasification of sewage sludge. Chem Eng J 2007;13:239–46.

Kamyab H, Soltani M, Ponraj M, Fadhil MD DIN M, Viony Putri E. A review on microalgae as potential lipid container with wastewater treating functions. J Environ Treat Tech 2013;1(2):76–80.

Kana K, Kanellaki M, Psarianos C, Koutinas A. Ethanol production by *Saccharomyces cerevisiae* immobilized on mineral Kissiris. J Ferment Bioeng 1989;68:144–7.

Kana K, Kanellaki M, Psarianos C, Koutinas AA. Ethanol Production by *Saccharomyces cerevisiae* Immobilized on Mineral Kissiris. J Biosci Bioeng 1989;68(2):144–147.

Karagoz P, Bill RM, Ozkan M. Lignocellulosic ethanol production: Evaluation of new approaches, cell immobilization and reactor configurations. Renew Energy 2019;143:741–752.

Karamalidis KA, Psycharis V, Nicolis I, Pavlidou E, Bénazeth S, Voudrias EA. Characterization of stabilized/solidified refinery oily sludge and incinerated refinery sludge with cement using XRD, SEM and EXAFS. J Environ Sci Heal A 2008;43:1144–56.

Karim A, Aider M. Bioconversion of electro-activated lactose, whey and whey permeate to produce single cell protein, ethanol, aroma volatiles, organic acids and fat by *Kluyveromyces marxianus*. Int Dairy J 2022;129:105334.

Karreman RJ, Brand WF, Lindsey GG. The yeast *Saccharomyces cerevisiae* stress response protein Hsp12p decreases the gel strength of agarose used as a model system for the β-glucan layer of the cell wall. Carbohydr Polym 2005;60:193–198.

Karthikeyan S, Sathiskumar C, Moorthy RS. Effect of process parameters on tire pyrolysis: A review. J Sci Ind Res 2012;71:309–315.

Kaul S, Sharma SS, Mehta IK. Free radical scavenging potential of L-proline: evidence from in vitro assays. J Amino Acids 2008;34:315–320.

Kaur N, Bhardwaj P, Singh G, Arya SK. Applicative Insights on Nascent Role of Biochar Production, Tailoring and Immobilization in Enzyme Industry -A Review. Process Biochem 2021;107:153–163.

Kaur U, Oberoi HS, Bhargav VK, Sharma-Shivappa R, Dhaliwal SS. Ethanol production from alkali- and ozone-treated cotton stalks using thermotolerant *Pichia kudriavzevii* HOP-1. In Crops Prod 2012;37:219–226.

Khosla K, Rathour R, Maurya R, Maheshwari N, Gnansounou E, Larroche C, et al. Biodiesel production from lipid of carbon dioxide sequestrating bacterium and lipase of psychrotolerant *Pseudomonas* sp. ISTPL3 immobilized on biochar. Bioresour Technol 2017;245:743–50.

Kim M, Choi MG, Ra HW, Park SB, Kim Y-J, Lee K. Encapsulation of multiple microalgal cells via a combination of biomimetic mineralization and LbL coating. Materials 2018;11:296.

Kiran SN, Sridhar M, Suresh K, Banat IM, Venkateswar RL. Isolation of thermotolerant, osmotolerant, flocculating Saccharomyces cerevisiae for ethanol production. Bioresour Technol 2000;72:43−46.

Kirdponpattara S, Phisalaphong M. Bacterial cellulose–alginate composite sponge as a yeast cell carrier for ethanol production. Biochem Eng J 2013;77:103–109.

Kirdponpattara S, Phisalaphong M. Bacterial cellulose-alginate composite sponge as a yeast cell carrier for ethanol production. J Biochem Eng 2013;77:103–9.

Kirdponpattara S, Phisalaphong M. Bacterial cellulose-alginate composite sponge as a yeast cell carrier for ethanol production. J Biochem Eng 2013;77:103–9.

Kloss S, Zehetner F, Dellantonio A, Hamid R, Ottner F, Liedtke V, Schwanninger M, Gerzabek MH, Soja G. Characterization of slow pyrolysis biochars: Efects of feedstocks and pyrolysis temperature on biochar properties. J Environ Qual 2012;41(4):990–1000.

Koreňová Z, Haydary J, Annus J, Markoš J, Jelemenský L. Pore structure of pyrolyzed scrap tires. Chem Pap 2008;62(1):86–91.

Kourkoutas Y, Dimitropoulou S, Kanellaki M, Marchant R, Nigam P, Banat IM, et al. High-temperature alcoholic fermentation of whey using *Kluyveromyces marxianus* IMB3 yeast immobilized on delignified cellulosic material. Bioresour Technol 2002;82:177–81.

Koutinas M, Lam M, Kiparissides A, Silva-Rocha R, Godinho M, Livingston AG, Pistikopoulos EN, de Lorenzo V, dos Santos VAPM, Mantalaris A. The regulatory logic of m-xylene biodegradation by *Pseudomonas putida* mt-2 exposed by dynamic modelling of the principal node Ps/Pr of the TOL plasmid. Environ Microbiol 2010;12:1705–1718.

Koutinas M, Patsalou M, Stavrinou S, Vyride I. High temperature alcoholic fermentation of orange peel by the newly isolated thermotolerant *Pichia kudriavzevii* KVMP10. Lett Appl Microbiol 2016;62:75–83.

Koutinas M, Patsalou M, Stavrinou S, Vyrides I. High temperature alcoholic fermentation of orange peel by the newly isolated thermotolerant *Pichia kudriavzevii* KVMP10. Lett Appl Microbiol 2015;62:75–83.

Kratchanova M, Pavlova E, Panchev I. The effect of microwave heating of fresh orange peels on the fruit tissue and quality of extracted pectin. Carbohydr Polym 2004;56:181–5.

Kumar S, Loganathan VA, Gupta RB, Barnett MO. An Assessment of U (VI) removal from groundwater using biochar produced from hydrothermal carbonization. J Environ Manag 2011;92:2504–2512.

Latif A, Harun S, Sajab MS, Markom M. Ammonia-based pretreatment for ligno-cellulosic biomass conversion – an overview. J Eng Sci Technol 2018;13(6):1595–1620.

Leger A, Azouz M, Lecomte S, Dole F, Hocquellet A, Chaignepain S, Cabanne C. PiP2 favors an α-helical structure of non-recombinant Hsp12 of *Saccharomyces cerevisiae*. Protein Expr Purif 2021;181:105830.

Letant SE, Hart BR, Kane SR, Hadi MZ, Shields SJ, Reynolds JG. Enzyme immobilization on porous silicon surfaces. Adv Mater 2004;16:689–93.

Leung DYC, Wang CL. Fluidized-bed gasification of waste tire powders. Fuel Process Techno 2003;84(1-3):175–196.

Li F, Shen K, Long X, Wen J, Xie X, Zeng X, Liang Y, Wei Y, Lin Z, Huang W, Zhong R. Preparation and characterization of biochars from Eichornia crassipes for cadmium removal in aqueous solutions. PLoS One 2016;11(2):e0148132.

Li LL, Ye YR, Pan L, Zhu Y, Zheng SP, Lin Y. The induction of trehalose and glycerol in *Saccharomyces cerevisiae* in response to various stresses. Biochem Biophy Res Commun 2009;387:778−783.

Li N, Qiuyang X, Meihong N, Qingwei P, Huining X. Immobilizing Laccase on Different Species Wood Biochar to Remove the Chlorinated Biphenyl in Wastewater. Sci Rep 2018;8(1):13947.

Li P, Fu X, Li S, Zhang L. Engineering TATA-binding protein Spt15 to improve ethanol tolerance and production in *Kluyveromyces marxianus*. Biotechnol Biofuels 2018;11:207.

Li R, Miao Y, Yuan S, Li Y, Wu Z, Weng P. Integrated transcriptomic and proteomic analysis of the ethanol stress response in *Saccharomyces cerevisiae* Sc131. J Proteomics 2019;203:103377.

Li SQ, Yao Q, Wen SE, Chi Y, Yan JH. Properties of pyrolytic chars and activated carbons derived from pilot-scale pyrolysis of used tires. J Air Waste Manage Assoc 2005;55(9):1315–1326.

Li X, Berger W, Musante C, Mattina MI. Corrigendum to “Characterization of substances released from crumb rubber material used on artificial turf fields”. Chemosphere 2020;80(3):1406–1407.

Li Z, Zhang X, Xiong X, Zhang B, Wang L. Determination of the best conditions for modified biochar immobilized petroleum hydrocarbon degradation microorganism by orthogonal test. J Earth Environ Sci 2017;94:012191.

Liang J, Chen L, Wu S, Liu C, Lei M. Comprehensive insights into cellulose structure evolution: via multi-perspective analysis during a slow pyrolysis process. Sustain Energ Fuels 2018;1855–1862.

Limtong S, Sringiew C, Yongmanitchai W. Production of fuel ethanol at high temperature from sugar cane juice by a newly isolated *Kluyveromyces marxianus*. Bioresour Technol 2007;98(17):3367-3374.

Limtong S, Sringiew C, Yongmanitchai W. Production of fuel ethanol at high temperature from sugar cane juice by a newly isolated *Kluyveromyces marxianus*. Bioresour Technol 2007;98:3367–3374.

Liu J, Zhou F, Abed AM, Le BN, Dai L, Ali HE, Khadimallah MA, Zhang G. Macroalgae as a potential source of biomass for generation of biofuel: Artificial intelligence, challenges, and future insights towards a sustainable environment. Fuel 2023;336:126826.

Liu S, Dai J, Sun Y, Xiu Z, Whang X, Li F, Liu H, Whang L, Li Y, Tong Y. Effects of rice husk on the tolerance of *Saccharomyces cerevisiae* to high temperature and ethanol concentration. Fuel 2023;333:126406.

Liu ZL, Saha BC, Slininger PJ, in: Wall J, Harwood C, Demain A (Eds.). Lignocellulosic biomass conversion to ethanol by *Saccharomyces*. Bioenergy ASM Washington DC 2008;17–36.

Lonappan L, Liu Y, Rouissi T, Brar SK, Verma M, Surampalli RY. Adsorptive immobilization of agro-industrially produced crude laccase on various micro-biochars and degradation of diclofenac. Sci Total Environ 2018;640–641:1251–1258.

Lonappan L, Liu Y, Rouissi T, Pourcel F, Brar SK, Verma M, Surampalli RY. Covalent immobilization of laccase on citric acid functionalized microbiochars derived from different feedstock and removal of diclofenac. J Chem Eng 2018;351:985–994.

Lou L, Huang Q, Lou Y, Lu J, Hu B, Lin Q. Adsorption and degradation in the removal of nonylphenol from water by cells immobilized on biochar. Chemosphere 2019;228:676–684.

Lü, F, Luo C, Shao L, He P. Biochar alleviates combined stress of ammonium and acids by firstly enriching *Methanosaeta* and then *Methanosarcina*. Water Res 2016;90:34–43.

Lum R, Tkach JM, Vierling E, Glover JR. Evidence for an unfolding/threading mechanism for protein disaggregation by *Saccharomyces cerevisiae* Hsp104. J Biol Chem 2004;279:29139–29146.

Luque L, Westerhof R, Rossum GV, Oudenhoven S, Kersten S, Berruti F, et al. Pyrolysis based bio-refinery for the production of bioethanol from demineralized lingo-cellulosic biomass. Bioresour Technol 2014;161:20–8.

Ma M, Liu ZL. Mechanisms of ethanol tolerance in *Saccharomyces cerevisiae*. J Appl Microbiol Biotechnol 2010;87:829-845.

Ma M, Liu ZL. Mechanisms of ethanol tolerance in *Saccharomyces cerevisiae*. J Appl Microbiol Biotechnol 2010;87:829–845.

Manikandan S, Vickram S, Subbaiya R, Karmegam N, Chang SW, Ravindran B, Awasthi MK. Comprehensive review on recent production trends and applications of biochar for greener environment. Bioresour Technol 2023;388:129725.

Martínez EJ, Rosas JG, Sotres A, Moran A, Cara J, Sánchez ME, et al. Codigestion of sludge and citrus peel wastes: Evaluating the effect of biochar addition on microbial communities. Biochem Eng J 2018;137:314–25.

Mathew AK, Crook M, Chaney K, Humphries AC. Comparison of entrapment and biofilm mode of immobilisation for bioethanol production from oilseed rape straw using *Saccharomyces cerevisiae* cells. Biomass Bioenergy 2013;52:1–7.

Mehrotra T, Dev S, Banerjee A, Chatterjee A, Singh R, Aggarwal S. Use of immobilized bacteria for environmental bioremediation: A review. J Environ Chem Eng 2021;9:105920.

Miller GL. Use of dinitrosalicylic acid reagent for determination of reducing Sugar. J Anal Chem 1959;31:426–428.

Mishra RK, Mohanty K. A review of the next-generation biochar production from waste biomass for material applications. Sci Total Environ 2023;167171.

Mohd Azhar SH, Abdulla A, Jambo SA, Marbawi H, Gansau JA, Mohd Faik AA, et al. Yeasts in sustainable bioethanol production: A review. Biochem Biophys Rep 2017;10:52–61.

Moia IC, Kanaropoulou A, Ghanotakis DF, Carlozzi P, Touloupakis E. Photofermentative hydrogen production by immobilized *Rhodopseudomonas* sp. S16-VOGS3 cells in photobioreactors. Energy Reviews 2024;3:100055.

Mojović L, Rakin M, Vukašinović M, Nikolić S, Pejin J, Pejin D. Production of bioethanol by simultaneous saccharification and fermentation of corn meal by immobilized yeast. Chem Eng Trans 2010;21:1333–1338.

Molino A, Erto A, Natale FD, Donatelli A, Iovane P, Musmarra D. Gasification of Granulated Scrap Tires for the Production of Syngas and a Low-Cost Adsorbent for Cd (II) Removal from Wastewaters. Ind Eng Chem Res 2013;52:34:2154–12160.

Mongkolkajit J, Pullsirisombat J, Limtong S, Phisalaphong M. Alumina-doped alginate gel as a cell carrier for ethanol production in a packed-bed bioreactor. Biotechnol Bioproc Eng 2011;16:505–512.

Mongkolkajit J, Pullsirisombat J, Limtong S, Phisalaphong M. Alumina-doped alginate gel as a cell carrier for ethanol production in a packed-bed bioreactor. Biotechnol Bioproc Eng 2011;16:505–512.

Moon SK, Kim SW, Choi GW. Simultaneous saccharification and continuous fermentation of sludge-containing mash for bioethanol production by *Saccharomyces cerevisiae* CHFY0321. J Biotechnol 2012;157:584–589.

Morano KA, Grant CM, Moye-Rowley WS. The response to heat shock and oxidative stress in *Saccharomyces cerevisiae*. Genetics 2012;190:1157−1195.

Mukherjee V, Radecka D, Aerts G, Verstrepen KJ, Lievens B, Thevelein JM. Phenotypic landscape of non-conventional yeast species for different stress tolerance traits desirable in bioethanol fermentation. Biotechnol Biofuels 2017;10:216.

Mulko L, Rivarola CR, Barbero CA, Acevedo DF. Bioethanol production by reusable *Saccharomyces cerevisiae* immobilized in a macroporous monolithic hydrogel matrices. J Biotechnol 2016;233:56–65.

Naghdi M, Taheran M, Brar SK, Kermanshahi-pour A, Verma M, Surampalli RY. Immobilized laccase on oxygen functionalized nanobiochars through mineral acids

treatment for removal of carbamazepine. Sci Total Environ 2017;584–585:393–401.

Ndubuisi IA, Nweze JE, Onoyima NJ, Yoshinori M, Ogbonna JC. Ethanol Production from Cassava Pulp by a Newly Isolated Thermotolerant *Pichia kudriavzevii* LC375240, Energy Power Eng 2018;10:457–474.

Nguyen DN, Ton NMN, Le VVM. Optimization of *Saccharomyces cerevisiae* immobilization in bacterial cellulose by 'adsorption–incubation' method. Int Food Res J 2009;16:59–64.

Nie W, He S, Lin Y, Chen JJ, Yang C. Functional biochar in enhanced anaerobic digestion: Synthesis, performances, and mechanisms. Sci Total Environ 2024;906:167681.

Nieto-Sarabia VL, Ballinas-Cesatti CB, Melgar-Lalanne G, Cristiani-Urbina E, Morales-Barrera L. Isolation, identification, and kinetic and thermodynamic characterization of a *Pichia kudriavzevii* yeast strain capable of fermentation. Food Bioprod Process 2022;131:109–124.

Nigam JN. Continuous ethanol production from pineapple cannery waste using immobilized yeast cells. J Biotech 1999;80:189–193.

Nuanpeng S, Thanonkeo S, Klanrit P, Thanonkeo P. Ethanol production from sweet sorghum by *Saccharomyces cerevisiae* DBKKUY-53 immobilized on alginate-loofah matrices. Braz J Microbiol 2018;49:140–150.

Oboirien BO, North BC. A review of waste tyre gasification. J Environ Chem Eng 2017;5:5169–5178.

Ok SY, Uchimiya S, Chang S, Bolan N. Biochar production, characterization and applications. New York: CRC Press; 2016.

Olugbenga OS, Adeleye PG, Oladipupo SB, Adeleye AT, John KI. Biomass-derived biochar in wastewater treatment- a circular economy approach. Waste Management Bulletin 2024;1(4):1–14.

Ozmihci S, Kargi F. Comparison of yeast strains for batch ethanol fermentation of cheese-whey powder (CWP) solution. Lett Appl Microbiol 2007;44:602–606.

Pacheco A, Pereira C, Almeida MJ, Sousa MJ. Small heat-shock protein Hsp12 contributes to yeast tolerance to freezing stress. Microbiology 2009;155:2021–2028.

Palamae S, Choorit W, Chatsungnoen T, Chisti Y. Simultaneous nitrogen fixation and ethanol production by *Zymomonas mobilis*. J Biotech 2020;314-315:41–52.

Pan J, Ma J, Zhai L, Liu H. Enhanced methane production and syntrophic connection between microorganisms during semi-continuous anaerobic digestion of chicken manure by adding biochar. J Clean Prod 2019;240:118178.

Pandey D, Daverey A, Arunachalam K. Biochar: Production, properties and emerging role as a support for enzyme immobilization. J Clean Prod 2020;255:120267.

Panesar PS. Kinetic analysis of lactose hydrolysis in milk using *Kluyveromyces marxianus* cells immobilized by alginate and agar gel entrapment. International J Dairy Sci 2007;2(2):138–44.

Parapouli M, Vasileiadis A, Afendra AM, Hatziloukas E. *Saccharomyces cerevisiae* and its industrial applications. AIMS Microbiol 2020;6(1):1–31.

Parrou JL, Teste MA, Francois J. Effects of various types of stress on the metabolism of reserve carbohydrates in *Saccharomyces cerevisiae*: Genetic evidence for a stress-induced recycling of glycogen and trehalose. Microbiology 1997;143:1891−1900.

Parsell DA, Kowal AS, Lindquist S. *Saccharomyces cerevisiae* Hsp104 Protein. J Biol Chem 1994;269:4480–4487.

Pastor JM, Garcia LD, Quintana S, Pena J. Glass reinforced concrete panels containing recycled tyres: Evaluation of the acoustic properties of for their use as sound barriers. Constr Build Mater 2014;54:541–549.

Patsalou M, Samanides CG, Protopapa E, Stavrinou S, Vyrides I, Koutinas M. A citrus peel waste biorefinery for ethanol and methane production. Molecules 2019;24:2451.

Pauly M, Keegstra K. Cell-wall carbohydrates and their modification as a resource for biofuels. Plant J 2008;54(4): 559–568.

Perez-Gallardo RV, Briones LS, Diaz-Perez AL, Gultierrez S, Rodriguez-Zavala JS, Campos-Carcia J. Reactive oxygen species production induced by ethanol in *Saccharomyces cerevisiae* increases because of a dysfunctional mitochondrial iron-sulfur cluster assembly system. FEMS Yeast Res 2013;13:804-819.

Periyasamy S, Isabel JB, Kavitha S, Karthik V, Mohamed BA, Gizaw DG, Sivashanmugam P, Aminabhavi TM. Recent advances in consolidated bioprocessing for conversion of lignocellulosic biomass into bioethanol – A review. J Chem Eng 2023;453:139783.

Periyasamy S, Karthik V, Senthil Kumar P, Isabel JB, Temesgen T, Hunegnaw BM, Melese BB, Mohamed BA, Nguyen Vo DV. Chemical, physical and biological methods to convert lignocellulosic waste into value-added products. A review. Environ Chem Lett 2022;20:1129–1152.

Phisalaphong M, Budiraharjo R, Bangrak P, Mongkolkajit J, Limtong S. Alginate–loofa as carrier matrix for ethanol production. J Biosci Bioeng 2007;104:214–217.

Piper P. Induction of heat shock proteins and thermotolerance. Methods Mol Biol 1996;53:313-317.

Piper PW. The heat shock and ethanol stress responses of yeast exhibit extensive similarity and functional overlap. FEMS Microbiol Lett 1995;134:121–127.

Plessas S, Bekatorou A, Koutinas AA, Soupioni M, Banat IM, Marchant R. Use of *Saccharomyces cerevisiae* cells immobilized on orange peel as biocatalyst for alcoholic fermentation. Bioresour Technol 2007;98:860–5.

Plessas S, Bekatorou AA, Koutinas AA, Soupioni M, Banat IM, Marchant R. Use of *Saccharomyces cerevisiae* cells immobilized on orange peel as biocatalyst for alcoholic fermentation. Bioresour Technol 2007;98:860–865.

Policella M, Wang Z, Burra KG, Gupta AK. Characteristics of syngas from pyrolysis and CO_2-assisted gasification of waste tires. Appl Energy 2019;254:113678.

Portofino S, Casu S, Iovane P, Russo A, Martino M, Donatelli A, Galvagno S. Optimizing H2 Production from Waste Tires via Combined Steam Gasification and Catalytic Reforming. Energy Fuels 2011;25:5:2232–2241.

Pourbafrani M, Forgacs G, Horvath IS, Niklasson C, Taherzadeh MJ. Production of biofuels, limonene and pectin from citrus wastes. Bioresour Technol 2010;101:4246-4250.

Presti DL. Recycled Tyre Rubber Modified Bitumens for road asphalt mixtures: A literature review. Constr Build Mater 2013;49:863–881.

Prévoteau A, Ronsse F, Cid I, Boeckx P, Rabaey K. The electron donating capacity of biochar is dramatically underestimated. Sci Rep 2016;6:32870.

Purvis JE, Yomano LP, Ingram LO. Enhanced trehalose production improved growth of *Escherichia coli* under osmotic stress. Appl Environ Microbiol 2005;71:3761−3769.

Pushparaj K, Liu WC, Meyyazhagan A, Orlacchio A, Pappusamy M, Vadivalagan C, Robert AA, Arumugam VA, Kamyab H, KlemeS JJ, Khademi T, Mesbah M, Chelliapan S, Balasubramanian B. Nano- from nature to nurture: A comprehensive review on facets, trends, perspectives and sustainability of nanotechnology in the food sector. Energy 2022;240:122732.

Qi X, Wang Z, Lin Y, Guo Y, Dai Z, Wang Q. Elucidation and engineering of mitochondrial respiratory-related genes for improving bioethanol production at high temperatures in *Saccharomyces cerevisiae*. Engineering Microbiology 2023;100108.

Rakin M, Mojovic L, Nikolic S, Vukasinovic M, Nedovic V. Bioethanol production by immobilized *Sacharomyces cerevisiae* var. ellipsoideus cells. Afr J Adv Biotechnol 2009;8:464–471.

Ramesh P, Selvan VAM, Babu D. Selection of sustainable lignocellulose biomass for second-generation bioethanol production for automobile vehicles using lifecycle indicators through fuzzy hybrid PyMCDM approach. Fuel 2022;322:124240.

Ramos MDN, Sandri JP, Claes A, Carvalho BT, Thevelein JM, Zangirolami TC, Milessi TS. Effective application of immobilized second generation industrial *Saccharomyces cerevisiae* strain on consolidated bioprocessing. N Biotechnol 2023;78:153–161.

Ranganathan S, Bai G, Luybetskaya A, Knapp GS, Peterson MW, Gazdik M, Gomes AL, Galagan JE, Mcdonough KA. Characterization of a cAMP responsive transcription factor, Cmr (Rv1675c), in TB complex mycobacterial reveals overlap with the DosR (DevR) dormancy regulon. Nucleic Acids Res 2015;44(1):134.

Rattanapan A, Limtong S, Phisalaphong M. Ethanol production by repeated batch and continuous fermentations of blackstrap molasses using immobilized yeast cells on thin-shell silk cocoons. Appl Energy 2011;88:4400–4.

Rawat J, Saxena J, Sanwal P. Biochar: a sustainable approach for improving plant growth and soil properties, in: V. Abrol, P. Sharma (Eds.), Biochar – an Imperative Amendment for Soil and the Environment, IntechOpen, 2019.

Rezania S, Kamyab H, Rupani PF, Park J, Nawrot N, Wojciechowska E, Yadav KK, Ghahroud ML, Mohammadi AA, Thirugnana ST, Chelliapan S, Cabral-Pinto MMS. Recent advances on the removal of phosphorus in aquatic plant-based systems. Environ Technol Innov 2021;24:101933.

Ritter P, Bye LJ, Finol-Urdaneta RK, Lesko C, Adams DJ, Friedrich O, Gilbert DF. A method for high-content functional imaging of intracellular calcium responses in gelatin-immobilized non-adherent cells. Exp Cell Res 2020;395:112210.

Robak K, Balcerek M. Review of Second Generation Bioethanol Production from Residual Biomass. Food Technol Biotechnol 2018;56(2):174–187.

Ronsse F, van Hecke S, Dickinson D, Prins W. Production and characterization of slow pyrolysis biochar: influence of feedstock type and pyrolysis conditions. GCB Bioenergy 2013;5(2):104–115.

Roukas T. Ethanol production from non-sterilized beet molasses by free and immobilized *Saccharomyces cerevisiae* cells using fed-batch culture. J Food Eng 1996;27:87–96.

Sagir E, Alipour S. Photofermentative hydrogen production by immobilized photosynthetic bacteria: Current perspectives and challenges. Renew Sust Energ Rev 2021;141:110796.

Saha K, Maharana A, Sikder J, Chakraborty S, Curcio S, Drioli E. Continuous production of bioethanol from sugarcane bagasse and downstream purification using membrane integrated bioreactor. Catal Today 2019;331:68–77.

Saini P, Beniwal A, Kokkiligadda A, Vij S. Response and tolerance of yeast to changing environmental stress during ethanol fermentation. Process Biochem 2018;72.1–12.

Saladini F, Patrizi N, Pulselli FM, Marchettini N, Bastianoni S. Guidelines for emergy evaluation of first, second and third generation biofuels. Renew Sust Energ Rev 2016; 66: 221–227.

Sales K, Brandt W, Rumbak E, Lindsey G. The LEA-like protein HSP 12 in *Saccharomyces cerevisiae* has a plasma membrane location and protects membranes against desiccation and ethanol-induced stress. Biochim Biophys Acta 2000;15;1463(2):267–278.

Sandhu SK, Oberoi HS, Dhaliwal SS, Babbar N, Kaur U, Nanda D, Kumar D. Ethanol production from Kinnow mandarin (*Citrus reticulata*) peels via simultaneous saccharification and fermentation using crude enzyme produced by *Aspergillus oryzae* and the thermotolerant *Pichia kudriavzevii* strain. Ann Microbiol 2012;62:655–666.

Santos E, Rostro-Alanís M, Parra-Saldívar R, Alvarez AJ. A novel method for bioethanol production using immobilized yeast cells in calcium-alginate films and hybrid composite pervaporation membrane. Bioresour Technol 2018;247:165–73.

Santos MPF, Brito MJP, Junior ECS, Bonomo RCF, Veloso CM. Pepsin immobilization on biochar by adsorption and covalent binding, and its application for hydrolysis of bovine casein. J Chem Technol Biotechnol 2019;94(6):1982–1990.

Schommer VA, Vanin AP, Nazari MT, Ferrari V, Dettmer A, Colla LM, Piccin JS. Biochar-immobilized *Bacillus* spp. for heavy metals bioremediation: A review on immobilization techniques, bioremediation mechanisms and effects on soil. Sci Total Environ 2023;881:163385.

Selim KA, El-Ghwas DE, Easa SM, Abdelwahab Hassan MI. Bioethanol a Microbial Biofuel Metabolite; New Insights of Yeasts Metabolic Engineering. Fermentation 2018;4(1):16.

Selvakumar P, Adane AA, Zelalem T, Hunegnaw BM, Karthik V, Kavitha S, Jayakumar M, Karmegam N, Govarthanan M, Kim W. Optimization of binary acids pretreatment of corncob biomass for enhanced recovery of cellulose to produce bioethanol. Fuel 2022;321:124060.

Sene L, Tavares B, das Graças de Almeida Felipe M, dos Santos JC, Pereira FM, Capello Tominc G, Alves da Cunha MA. Ethanol production by *Kluyveromyces marxianus* ATCC 36907: Fermentation features and mathematical modelling. ISBAB 2023;51:102789.

Seong YJ, Lee HJ, Lee JE, Kim S, Lee DY, Kim KH, et al. Physiological and metabolomic analysis of Issatchenkia orientalis MTY1 with multiple tolerance for cellulosic bioethanol production. Biotechnol J 2017;12:1–11.

Shah SH, Raja IA, Rizwan M, Rashid N, Mahmood Q, Shah FA, Pervez A. Potential of microalgal biodiesel production and its sustainability perspectives in Pakistan. Renew Sust Energ Rev 2018;81:76–92.

Shahsavarani H, Hasegawa D, Yokota D, et al. (2013) Enhanced bio-ethanol production from cellulosic materials by semisimultaneous saccharification and fermentation using high temperature resistant *Saccharomyces cerevisiae* TJ14. J Biosci Bioeng 115:20–23.

Sharma B, Larroche C, Dussap CG. Comprehensive assessment of 2G bioethanol production. Bioresour Technol 2020;313:123630.

Sharma DC, Forster CF. A Preliminary examination into the adsorption of hexavalent chromium using low-cost adsorbents. Bioresour Technol 1994;47:257–64.

Shen Y, Zhu W, Li H, Ho SH, Chen J, Xie Y, Shi X. Enhancing cadmium bioremediation by a complex of water-hyacinth derived pellets immobilized with *Chlorella* sp. Bioresour Technol 2018;257:157–163.

Shirvanyan A, Mirzoyan S, Trchounian K. Relationship between proton/ potassium fluxes and central carbon catabolic pathways in different *Saccharomyces cerevisiae* strains under osmotic stress conditions. Process Biochem 2023;133:309–318.

Shokravi H, Heidarrezaei M, Shokravi Z, Ong HC, Lau WJ. Din MFM, Ismail AF. Fourth generation biofuel from genetically modified algal biomass for bioeconomic development. J Biotech 2022;360:23–36.

Simic V, Dabic-Ostojic S. Interval-parameter chance-constrained programming model for uncertainty-based decision making in tire retreading industry. J Clean Prod 2017;167:1490–1498.

Simola M, Hanninen AL, Stranius SM, Makarow M. Trehalose is required for conformational repair of heat-denatured proteins in the yeast endoplasmic reticulum but not for maintenance of membrane traffic functions after severe heat stress. Mol Microbiol 2000;37:42–53.

Sims PE, Mabee W, Saddler N, Taylor M. An overview of second generation biofuel technologies. Bioresour Technol 2010;101:1570–1580.

Singh A, Sharma P, Saran AK, Singh N, Bishnoi NR. Comparative study on ethanol production from pretreated sugarcane bagasse using immobilized *Saccharomyces cerevisiae* on various matrices. Renew Energy 2013;50:488–93.

Singh B, Cowie A. Characterisation and evaluation of biochars for their application as soil amendment. Aust J Soil Res 2010;48:516–525.

Singh B, Pal Singh BP, Cowie AL. Characterisation and evaluation of biochars for their application as a soil amendment. Aust J Soil Res 2010;48:516–25.

Sivarathnakumar S, Jayamuthunagai J, Baskar G, Praveenkumar R, Selvakumari IAE, Bharathiraja B. Bioethanol production from woody stem Prosopis juliflora using thermo tolerant yeast *Kluyveromyces marxianus* and its kinetics studies. Bioresour Technol 2019;293:122060.

Soleimani SS, Adiguzel A, Nadaroglu H. Production of bioethanol by facultative anaerobic bacteria. J Inst Brew 2017;123:402–406.

Song Y, Cho EJ, Park CS, Oh CH, Park BJ, Bae HJ. A strategy for sequential fermentation by *Saccharomyces cerevisiae* and *Pichia stipitis* in bioethanol production from hardwoods. Renew Energy 2019;139:1281–1289.

Sorger PK, Pelham HR. Purification and characterization of a heat-shock element binding protein from yeast. EMBOJ1987;6:3035-3040.

Sorger PK. Yeast heat shock factor contains separable transient and sustained response transcriptional activators. Cell 1990;62:793-805.

Sousa AF, Gardini A, Caetano A, Maria TM, Freire CS, Neto CP, Silvestre AJ, Unravelling the distinct crystallinity and thermal properties of suberin compounds from *Quercus suber* and *Betula pendula* outer barks. Int J Biol Macromol 2016;93:686–694.

Stanley D, Bandara A, Fraser S, Chambers P, Stanley GA. The ethanol stress response and ethanol tolerance of *Saccharomyces cerevisiae*. J Appl Microbiol 2010;109:13-24.

Stanley D, Bandara A, Fraser S, Chambers P, Stanley GA. The ethanol stress response and ethanol tolerance of *Saccharomyces cerevisiae*. J Appl Microbiol 2010;109:13–24.

Suman S, Gautam S. Pyrolysis of coconut husk biomass: Analysis of its biochar properties. Energy Sources, Part A Recovery, Util Environ Eff 2017;39(8):761–767.

Sumanu VO, Byaruhanga C, Bosman AM, Ochai SO, Naidoo V, Oosthuizen MC, Chamunorwa JP. Effects of probiotic (*Saccharomyces cerevisiae*) and ascorbic acid on oxidative gene damage biomarker, heat shock protein 70 and interleukin 10 in broiler chickens exposed to heat stress. Animal Gene 2023;28:200150.

Sun Y, Gao B, Yao Y, Fang J, Zhang M, Zhou Y, et al. Effects of feedstock type, production method, and pyrolysis temperature on biochar and hydrochar properties. Chem Eng J 2014;240:574–8.

Sweygers N, Alewaters N, Dewil R, Appels L. Microwave effects in the dilute acid hydrolysis of cellulose to 5-hydroxymethylfurfural. Sci Rep 2018;8:7719.

Tan L, Sun ZY, Okamoto S, Takaki M, Tang YQ, Morimura S, Kida K. Production of ethanol from raw juice and thick juice of sugar beet by continuous ethanol fermentation with flocculating yeast strain KF-7. Biomass Bioenergy 2015;81:265–272.

Tavares B, de Almeida Felipe MG, dos Santos JC, Pereira FM, Gomes SD, Sene L. An experimental and modeling approach for ethanol production by *Kluyveromyces marxianus* in stirred tank bioreactor using vacuum extraction as a strategy to overcome product inhibition. Renew Energy 2019;131:261–7.

Thorne TW, Ho HL, Huvet M, Haynes K, Stumpf MPH. Prediction of putative protein interactions through evolutionary analysis of osmotic stress response in the model yeast *Saccharomyces cerevisae*. Fungal Genet Biol 2011;48:504–511.

Tian J, Lin Y, Su X, Tan H, Gan C, Ragauskas AJ. Effects of *Saccharomyces cerevisiae* quorum sensing signal molecules on ethanol production in bioethanol fermentation process. Microbiol Res 2023;271:127367.

Tikka C, Osuru HP, Atluri N, Raghavulu PCV, Kumar yellapu N, Mannur IS, Prasad UV, Aluru S, Varma K N, Bhaskar M. Isolation and characterization of ethanol tolerant yeast strains. Bioinformation 2013;9(8):421–425.

Tinôco D, André Genier HL, da Silveira WB. Technology valuation of cellulosic ethanol production by *Kluyveromyces marxianus* CCT 7735 from sweet sorghum bagasse at elevated temperatures. Renew Energ 2021;173:188–196.

Uchimiya M, Chang S, Klasson KT. Screening biochars for heavy metal retention in soil: role of oxygen functional groups. J Hazard Mater 2011;190:432–41.

Uday V, Harikrishnan PS, Deoli K et al. Current trends in production, morphology, and real-world environmental applications of biochar for the promotion of sustainability. Bioresour Technol 2022;359:127467.

Unnikrishnan I, Miller S, Meinke M, LaPorte DC. Multiple Positive and Negative Elements Involved in the Regulation of Expression of GSY1 in *Saccharomyces cerevisiae*. J Biol Chem 2003;278(29):26450−26457.

Valanidou L, Theologides C, Zorpas AA, Savva PG, Costas CN. A novel highly selective and stable Ag/MgO-CeO2-Al2O3 catalyst for the low-temperature ethanol-SCR of NO. Appl Catal B 2011;107:164–76.

van der Pol EC, Bakker RR, Baets P, Eggink G. By-products resulting from lignocellulose pretreatment and their inhibitory effect on fermentations for (bio) chemicals and fuels. Appl Microbiol Biotechnol 2014;98:9579–9593.

Vandamme D, Pohl PI, Beuckels A, Foubert I, Brady PV, Hewson JC, et al. Alkaline flocculation of *Phaeodactylum tricornutum* included by brucite and calcite. Bioresour Technol 2015;196:656–61.

Vassilev SV, Baxter D, Andersen LK, Vassileva CG. An overview of the chemical composition of biomass. Fuel 2010;89:913–933.

Verbelen PJ, De Schutter DP, Delvaux F, Verstrepen KJ, Delvaux FR. Immobilized yeast cell systems for continuous fermentation applications. Biotechnol Lett 2006;28:1515–1525.

Verbelen PJ, De Schutter DP, Delvaux F, Verstrepen KJ, Delvaux FR. Immobilized yeast cell systems for continuous fermentation applications. Biotechnol Lett 2006;28:1515–25.

Vučurović VM, Razmovski RN. Sugar beet pulp as support for *Saccharomyces cerevisiae* immobilization in bioethanol production. Ind Crops Prod 2012;39:128–34.

Wahlbom CF, Hahn-Hägerdal B. Furfural, 5-hydroxymethyl furfural, and acetoin act as external electron acceptors during anaerobic fermentation of xylose in recombinant *Saccharomyces cerevisiae*. Biotechnol Bioeng 2002;78:172–8.

Walter S, Buchner J. Molecular chaperones-cellular machines for protein folding. Angew Chem 2002;41:1098−1113.

Wang D, Lan Y, Chen W, Han X, Liu S, Cao D, Cheng X, Wang Q, Zhan Z, He W. The six-year biochar retention interacted with fertilizer addition alters the soil organic nitrogen supply capacity in bulk and rhizosphere soil. J Environ Manage 2023;338:117757.

Wang F, Gao N, Quan C, Lopez G. Investigation of hot char catalytic role in the pyrolysis of waste tires in a two-step process. J Anal Appl Pyrolysis 2020;146:104770.

Wang S, Zhao F, Yang M, Lin Y, Han S. Metabolic engineering of *Saccharomyces cerevisiae* for the synthesis of valuable chemicals. Crit Rev Biotechnol 2023;

Wang X, He Q, Yang Y, Wang J, Haning K, Hu Y, Wu B, He M, Zhang Y, Bao J, Contreras LM, Yang S. Advances and prospects in metabolic engineering of *Zymomonas mobilis*. Metab Eng 2018;50:57–73.

Watanabe K, Tachibana S, Konishi M. Modeling growth and fermentation inhibition during bioethanol production using component profiles obtained by performing comprehensive targeted and nontargeted analyses. Bioresour Technol 2019;281:260–268.

Waterhouse AL, Sacks GL, Jeffery DW. Understanding Wine Chemistry, Wiley, 2016.

Whang Y, Zhong B, Shafi M, Ma J, Guo J, Wu J, Ye Z, Liu D, Jin H. Effects of biochar on growth, and heavy metals accumulation of moso bamboo (*Phyllostachy pubescens*), soil physical properties, and heavy metals solubility in soil. Chemosphere 2018;219:510–516.

Wijitkosum S, Sriburi T. Aromaticity, polarity, and longevity of biochar derived from disposable bamboo chopsticks waste for environmental application. Heliyon 2023;9:e19831.

Wilkins MR, Suryawati L, Maness NO, Chrz D. Ethanol production by *Saccharomyces cerevisiae* and *Kluyveromyces marxianus* in the presence of orange-peel oil. World J Microbiol Biotechnol 2007;23:1161-1168.

Wilson WA, Roach PJ, Montero M, Fernantez EB, Munoz FJ, Eydallin G, Viale AM, Pozueta-Romero J. Regulation of glycogen metabolism in yeast and bacteria. FEMS Microbiol Rev 2010;34:952–985.

Wirawan F, Cheng CL, Lo YC, Chen CY, Chang JS, Leu SY, Lee DJ. Continuous cellulosic bioethanol co-fermentation by immobilized *Zymomonas mobilis* and suspended *Pichia stipitis* in a two-stage process. Appl Energy 2020;266:114871.

Wu WH, Hung WC, Lo KY, Chen YH, Wan HP, Cheng KC. Bioethanol production from taro waste using thermo-tolerant yeast *Kluyveromyces marxianus* K21. Bioresour Technol 2016;201:27–32.

Xia J, Yang Y, Liu CG, Yang S, Bai FW. Engineering *Zymomonas mobilis* for Robust Cellulosic Ethanol Production. Trends in Biotechnology 2019;37(9).

Xiao W, Duan X, Lin Y, Cao Q, Li S, Guo Y et al. Distinct Proteome Remodeling of Industrial *Saccharomyces cerevisiae* in Response to Prolonged Thermal Stress or Transient Heat Shock. J Proteome Res 2018;17:1812−1825.

Xu D, Cao J, Li Y, Howard A, Yu K. Effect of pyrolysis temperature on characteristics of biochars derived from different feedstocks: a case study on ammonium adsorption capacity. J Waste Manag 2019;87:652–660.

Xu FJ, Cai QJ, Li YL, Kang ET, Neoh KG. Covalent Immobilization of Glucose Oxidase on Well-Defined Poly(glycidyl methacrylate)−Si(111) Hybrids from Surface-Initiated Atom-Transfer Radical Polymerization. Biomacromolecules 2005;6(2)1012–1020.

Xu P, Jiang Y, Xu J, Li J, Sun X. Genomics in the common carp. Genomics in Aquaculture 2016;247-274.

Yan Z, Li J, Chang S, Cui T, Jiang Y, Yu M, et al. Lignin relocation contributed to the alkaline pretreatment efficiency of sweet sorghum bagasse. Fuel 2018;158:152–8.

Yan Z, Zhang J, Bao J. Increasing cellulosic ethanol production by enhancing phenolic tolerance of *Zymomonas mobilis* in adaptive evolution. Bioresour Technol 2021;329:124926.

Yang S, Fei Q, Zhang Y, Contreras LM, Utturkar SM, Brown SD, Himmel ME, Zhang M. *Zymomonas mobilis* as a model system for production of biofuels and biochemicals. Microb Biotechnol 2016;9(6):699–717.

Yaqoob H, Heng Teoh Y. Sher F, Jamil MA, Murtaza D, Qubeissi M, Hussan MU, Mujtaba MA. Current Status and Potential of Tire Pyrolysis Oil Production as an Alternative Fuel in Developing Countries. Sustainability 2021;13:3214.

Yeom SH, Jung KY. Recycling wasted scallop shell as an adsorbent for the removal of phosphate. J Ind Eng Chem 2009;15:40–44.

Yousuf A, Pirozzi D, Sannino F. Lignocellulosic Biomass to Liquid Biofuels. 2019. Academic Press.

Yu J, Zhang X, Tan T. A novel immobilization method of *Saccharomyces cerevisiae* to sorghum bagasse for ethanol production. J Biotechnol 2007;129:415–20.

Yuan H, Lu T, Huang H, Zhao D. Influence of pyrolysis temperature on physical and chemical properties of biochar made from sewage sludge. J Anal Appl Pyrolysis 2015;112:284–289.

Yuan JH, Xu RK, Zhang H. The forms of alkalis in the biochar produced from crop residues at different temperatures. Bioresour Technol 2011;102:3488–97.

Yuan WJ, Chang BL, Ren JG, Liu JP, Bai FW, Li YY. Consolidated bioprocessing strategy for ethanol production from Jerusalem artichoke tubers by *Kluyveromyces marxianus* under high gravity conditions. J Appl Microbiol 2011;112:38−44.

Zabet H, Sahu JN. Boyce AN, Faruq G. Bioethanol production from renewable sources: Current perspectives and technological progress. Renew Sust Energ Rev 2017;71:475–501.

Zafar S, Owais M. Ethanol production from crude whey by *Kluyveromyces marxianus*. Biochem Eng J 2006;27:295–298.

Zhang H, Tang J, Wang L, Liu J, Gurav RG, Sun K. A novel bioremediation strategy for petroleum hydrocarbon pollutants using salt tolerant *Corynebacterium variabile* HRJ4 and biochar. J Environ Sci 2016;47:7–13

Zhao F, Du Y, Bai P, Liu J, Lu W, Yuan Y. Enhancing *Saccharomyces cerevisiae* reactive oxygen species and ethanol stress tolerance for high level production protopanoxadiol. Bioresour Technol 2017;227:308-316.

Zhao F, Du Y, Bai P, Liu J, Lu W, Yuan Y. Enhancing *Saccharomyces cerevisiae* reactive oxygen species and ethanol stress tolerance for high-level production of protopanoxadiol. Bioresour Technol 2017;227:308–316.

Zhao H, Li J, Han B, Li X, Chen J. Improvement of oxidative stress tolerance in *Saccharomyces cerevisiae* through global transcription machinery engineering. J Ind Microbiol Biotechnol 2014;41:869–878.

Zhao J, Xia L. Ethanol production from corn stover hemicellulosic hydrolysate using immobilized recombinant yeast cells. Biochem Eng J 2010;49(1):28–32.

Zheng C, Sun X, Li L, Guan N. Scaling up of ethanol production from sugar molasses using yeast immobilized with alginate-based MCM-41 mesoporous zeolite composite carrier. Bioresour Technol 2012;115:208–14.

Zhu H, Shen F, Luo W, Zhu S, Zhao M, Natarajan B, et al. Low temperature carbonization of cellulose nanocrystals for high performance carbon anode of sodium ion batteries. Nano Energy 2017;33:37–44.

Zhuang S, Smart K, Powell C. Impact of extracellular osmolality on *Saccharomyces* yeast populations during brewing fermentations. J Am Soc Brew Chem 2017;75:244–254.

Zichová M, Stratilová E, Omelková J, Vadkertiová R, Babák L, Rosenberg M. Production of ethanol from waste paper using immobilized yeasts. Chem Pap 2017;71:553–561.

Zoghlami A, Paes G. Lignocellulosic Biomass: Understanding Recalcitrance and Predicting Hydrolysis. Front Chem 2019;7:874.

Zou D, Wu Y, Peng Y, Lei J, Wang G, Wang J, Pan Y, Yan W, Chen X. Characterization and application of Fe-modified biochar alleviating Cr(VI) stress in pak choi seedling cultivated in Cr-polluted hydroponics. Chemosphere 2023;340:139793.

APPENDIX I

Table 2.3.4: Oligonucleotide primers used in quantitative real-time RT-qPCR.

Gene	Pair of primers	Sequence	Source
HSF1	Forward	5´-AGAACCCAACAGCAAGCC-3´	Yamamoto et al., 2007
	Reverse	3´-CCCAGCCCGTCCATAATCA-5´	Yamamoto et al., 2007
tps	Forward	5´-TGTCTTCCGTGCAAAGAGTG-3´	Nuanpeng et al., 2016
	Reverse	3´-CTTGTGGATGAAATGGATGG-5´	Nuanpeng et al., 2016
HSP104	Forward	5´-CATATGGAACGTGACTTATCATCTGA-3´	Nuanpeng et al., 2016
	Reverse	3´-ACGGCATTGGAAACAGCTTT-5´	Nuanpeng et al., 2016
HSP12	Forward	5´-TAGGATCCATGTCTGACGCAGGTGA-3´	Welker et al., 2010
	Reverse	3´-ATGCGGCCGCTTACTTCTTGGTTGGGTC-5´	Welker et al., 2010
Msn2	Forward	5´-AGTGGCTCTGGGGCAAATC-3´	Yamamoto et al., 2007
	Reverse	3´-CCGATGAAGGTGACGGTGA-5´	Yamamoto et al., 2007
Msn4	Forward	5´-AGCAGTAGCACCACAAGGC-3´	Yamamoto et al., 2007
	Reverse	3´-CGCACCAAAAGCATCGTCTT-5´	Yamamoto et al., 2007
RDN18	Forward	5´-TCACCAGGTCCAGACACAAT-3´	Ye et al., 2009
	Reverse	3´-AGCAGACAAATCACTCCACC-5´	Ye et al., 2009